DOCTOR OF PHILOSOPHY

An investigation into Cdc28 phosphorylation of Ipl1 and the role of Haspin-like kinases in yeast cell cycle control

Corbishley, Stephen J.

Award date:
2013

Awarding institution:
University of Dundee

DOCTOR OF PHILOSOPHY

An investigation into Cdc28 phosphorylation of Ipl1 and the role of Haspin-like kinases in yeast cell cycle control

Stephen J. Corbishley

2013

University of Dundee

An investigation into Cdc28 phosphorylation of Ipl1 and the role of Haspin-like kinases in yeast cell cycle control

Stephen J. Corbishley

Submitted for the degree of
Doctor of Philosophy

University of Dundee

September 2013

TABLE OF CONTENTS

List of Tables

List of Figures

Abbreviations

ANOVA	Analysis of variance
APC/C	Anaphase promoting complex/cyclosome
CDK	Cyclin-dependent kinase
CPC	Chromosome passenger complex
DAmP	Decreased abundance by mRNA perturbation
D-box	Destruction box
EYFP	Enhanced yellow fluorescent protein
GAP	GTPase-activating protein
GEF	Guanine nucleotide exchange factor
GFP	Green fluorescent protein
GO	Gene ontology
GTPase	Guanosine 5'-triphosphatase
H3-T3	Threonine 3 of histone H3
H3-T3ph	Histone H3 phosphorylated at threonine 3
H3(T3A) cells	Yeast cells in which the sole source of histone H3 is a *hht2* allele encoding a T3A substitution
KEN-box	Lysine-glutamate-asparagine-box
MCC	Mitotic checkpoint complex
MRC	Medical Research Council
MTOC	Microtubule organising centre
ORF	Open reading frame
preRC	Pre-replicative complex
RNAi	Ribonucleic acid interference
RNase	Ribonuclease
SAC	Spindle assembly checkpoint

siRNA	Small interfering ribonucleic acid
SPB	Spindle pole body
SPoC	Spindle position checkpoint
SGD	*Saccharomyces* genome database
SMC	Structural maintenance of chromosomes
UPR	Unfolded protein response
WCE	Whole cell extract
WT	Wild-type
YFP	Yellow fluorescent protein

Acknowledgments

I would like to thank my supervisor Professor Mike Stark for giving me the opportunity to work in his lab, providing his support and imparting his scientific expertise. I would also like to thank my thesis committee, Professors Jason Swedlow and Tracy Palmer, for their time and support over the past four years and also Professor Kathryn Ayscough for agreeing to serve as my external examiner. I would also like to acknowledge the Medical Research Council for funding my studentship. I am grateful to Professors Noel Lowndes and Tomo Tanaka, and Dr. Kevin Hardwick for providing strains that have contributed to this study, to Dr. Jonathan Higgins for the H3-T3ph antibody, to Professor Steve Hubbard for help with the statistical analysis of data and also to Professor David Lydall and Dr. Peter Banks at Newcastle University for their collaboration and for providing training with SGA screening technologies.

It has been a privilege to work in such a fantastic department. I thank former Stark lab members Doctors Ashwin Bhat and Vasso Makrantoni for their mentoring, support and patience over the years and also my fellow PhD students Rachael Di Santo, Colin Hammond, Ross Fennessy, Oliver Anderson, Kevin Creavin and Alistair Davies for being excellent friends and colleagues. I am grateful to Dr. Etsushi Kitamura and other members of the Tanaka lab for their help with DeltaVision microscopy and to Dr. Ramasubramanian (Subbu) Sundaramoorthy and his colleagues in the Owen-Hughes lab for their help with protein biochemistry and sharing equipment and reagents. I would also like to thank the staff from the media preparation facility, stores and the wash-up facility for being so helpful and providing an excellent service and also the lab managers and divisional secretaries for their help and for keeping the department running smoothly.

Finally, I would like to thank those closest to me. My partner Debbie Matthews has had a rather boring summer while I have been writing and I hope to make it up to her soon. I thank her for all her support. My family have always provided their unwavering support and to them I am eternally grateful.

Declarations

I hereby declare that the following thesis is based on the results of work conducted by myself and that the thesis is of my own composition. Work other than my own is clearly indicated in the text by reference to the relevant researchers or their publications. This thesis has not in whole, or in part, been presented for a higher degree.

……

Stephen J. Corbishley

I certify that Stephen Corbishley has spent at least nine terms in research in the Centre for Gene Regulation and Expression, University of Dundee and that he has fulfilled the conditions of Ordinance General No. 39 of the University of Dundee and is qualified to submit the accompanying thesis in application for the degree of Doctor of Philosophy.

……

Prof. M. J. R Stark

Professor of Yeast Molecular Biology

University of Dundee

Abstract

The chromosomal passenger complex (CPC) is a conserved, essential protein complex in eukaryotes, consisting of Ipl1/Aurora B kinase and three regulatory subunits: Sli15/INCENP, Bir1/Survivin and Nbl1/Borealin. The CPC has numerous cell cycle roles, the best characterised of which is the regulation of kinetochore-microtubule attachments during metaphase to promote chromosome bi-orientation on the mitotic spindle. To efficiently perform these functions, the CPC must be properly regulated and localised. The original defining characteristic of 'chromosomal passenger' proteins was their dynamic localisation: associated with chromatin and centromeres during early mitosis followed by translocation to the spindle midzone during anaphase. However, exactly how the CPC is properly localised and regulated is not fully understood.

Recent studies demonstrated that phosphorylation of the CPC regulatory subunits by cyclin-dependent kinase (CDK) regulates localisation of the complex. For example, in budding yeast and human cells the dephosphorylation of CDK-phosphorylated sites in Sli15/INCENP is required for the efficient translocation of the CPC from centromeres in metaphase to the spindle in anaphase. Many Ipl1/Aurora B homologues also contain CDK phosphorylation motifs but whether modification of these sites is required for proper CPC localisation and function is not known – here this was investigated in budding yeast. Preventing phosphorylation of CDK consensus sites in the N-terminus of Ipl1 was found to result in its premature localisation to the spindle in metaphase; this was dependent on the yeast microtubule binding EB1 homologue Bim1. However, preventing or mimicking phosphorylation at these sites had no effect on cell viability or chromosome bi-orientation.

During the course of this study, several groups demonstrated that the conserved Haspin kinase in fission yeast, *Xenopus* and human cells contributes to CPC localisation at the centromere during metaphase by phosphorylating histone H3 on Threonine 3 (H3-T3). In light of these findings, two budding yeast Haspin kinase homologues (Alk1 and Alk2) were investigated. Although roles for Alk1 and Alk2 in histone H3 phosphorylation and CPC recruitment could not be conclusively determined, unusual phenotypes were observed in cells lacking both Alk1 and Alk2. In these cells, the spindle was frequently confined to the bud and incorrectly aligned. If these cells were arrested in metaphase, the bud became significantly larger than the mother cell. When anaphase was eventually triggered, the spindle elongated and then broke down entirely within the bud. These abnormalities were independent of histone H3-T3 phosphorylation, since mutation of H3-T3 to non-phosphorylatable alanine did not result in these phenotypes. Thus Alk1 and Alk2 share novel and redundant roles in spindle positioning, cell polarity and bud growth that are particularly important during a metaphase arrest.

CHAPTER 1

Introduction

1.1 General introduction

The ability to faithfully replicate the genetic and physical properties of the cell is fundamental for the proliferation of cellular life. This is achieved through a tightly ordered and regulated series of macromolecular events, collectively termed the cell cycle, that culminate in the production of two daughter cells each containing an identical genome. The regulation of these processes is especially critical for the normal development of higher eukaryotes where misregulation can result in cell death or aberrant cell proliferation, which in turn can lead to birth defects or the development of cancer. The unequal distribution of chromosomes during division leads to cells having an incorrect chromosome number: a state termed aneuploidy. Aneuploidy is the most common genetic alteration among solid tumours (reviewed in Weaver & Cleveland, 2006). However, there is a continuing debate as to whether aneuploidy is the cause or a consequence of cancer (Duesberg *et al*., 2001; Schvartzman *et al*., 2010; Gordon *et al*., 2012).

In 2010 in the UK alone around 325,000 people were diagnosed with cancer. Cancer is responsible for more than one in four of all deaths in the UK and more than one in three people in the UK will develop some form of cancer during their lifetime. There are more than 200 types of cancer each with different causes and symptoms and although cancer incidence rates have increased by a third since the 1970's, the survival rates have doubled and half of the people diagnosed now survive their disease for at least five years (Cancer Research UK, 2013). This is thanks in no small part to the extensive research that has been carried out during this time. While it is important to understand and educate people in how the risk of developing cancer can be minimized it is also important to understand what is happening at the genetic and cellular levels by developing our understanding of cell division, the processes involved and how they are

regulated. Targeting key components of the cell cycle presents unique opportunities for drug discovery to aid in the treatment and cure of cancers as well as many other diseases.

It became clear in the late 1980's that chromosome replication and segregation are essentially similar in all eukaryotic cells. This finding led to the use of a diverse array of organisms for research into these processes each with its own experimental advantages (and disadvantages) that have contributed to our current understanding of the cell cycle. A large proportion of our knowledge in this area comes from genetic studies with the budding yeast *Saccharomyces cerevisiae*, the organism that was first to have its entire genome sequenced (Goffeau *et al*., 1996) and is also the basis of this study. Simpler model organisms are often employed to study aspects of the cell cycle as they are more amenable to genetic manipulation and have shorter generation times than higher eukaryotes. Furthermore, many fundamental cellular processes are conserved from simple unicellular eukaryotes, such as *S. cerevisiae,* to more complex multicellular organisms, such as human and other mammals.

1.2 An overview of the cell cycle

The cell cycle is a complex series of events that involves a myriad of proteins and processes that regulate cell growth, DNA replication and segregation, and ultimately culminate in the production of two genetically identical daughter cells (for a comprehensive overview of the cell cycle, see Morgan, 2007) . This process can be divided into two morphologically distinct phases; interphase and M (mitotic) phase. Interphase can be further subdivided into G_1, S and G_2 phases. The G_1 and G_2 phases represent 'gaps' in the cell cycle between the two obvious landmarks of DNA replication in S phase and mitosis. During the complex and dramatic period of mitosis

the replicated DNA is equally segregated to opposite poles and the cell divides into two daughter cells.

In actively cycling somatic cells, RNAs and proteins are synthesised during the G_1 phase in preparation for DNA synthesis and chromosome replication during S phase. The process of chromosome replication is tightly regulated to ensure that the DNA is replicated accurately and only once per cell cycle. The replicated chromosomes are now referred to as sister chromatids and consist of two identical daughter DNA molecules (and their associated chromosomal proteins) bound together by the cohesin protein complex along their lengths. During the subsequent G_2 phase the cell prepares for mitosis. Mitosis can be subdivided into four cytologically distinguishable phases; prophase, metaphase, anaphase and telophase/cytokinesis. In prophase the nuclear membrane retracts into the endoplasmic reticulum in many higher eukaryotes and the Golgi apparatus breaks down into vesicles. Cellular microtubules start to form the mitotic spindle and the mass of replicated DNA begins to condense. In vertebrates, the cohesin complexes holding the sister chromatids together become confined to a discrete region on each chromosome called the centromere. During metaphase the multi-subunit kinetochore complex assembles at each centromere. The kinetochores of each sister chromatid pair associate with microtubules emanating from opposite poles of the mitotic spindle. The onset of anaphase is denoted by the loss of the remaining cohesin complexes and the separation of sister chromatids to opposite poles of the cell. Once this process is complete the cells enter telophase, when the mitotic spindle disassembles, the nuclear envelope reforms and the chromosomes decondense. Finally, the two daughter cells are physically separated from one another through the process of cytokinesis. At this point, cycling cells will re-enter G_1 and begin another cell cycle. Non-cycling cells will exit the cell cycle from early G_1 and enter a quiescent resting

phase known as G_0, where they may remain until death or until they are stimulated to re-enter the cell cycle (Morgan, 2007).

Progression through the cell cycle requires that a series of macromolecular events are executed in an ordered and timely fashion. Temporal control of the cell cycle is regulated by a small number of heterodimeric serine/threonine protein kinases that consist of a catalytic subunit (cyclin-dependent kinase, CDK) and a regulatory subunit (cyclin). Numerous cyclins are differentially expressed and degraded at different stages throughout the cell cycle. Association of a particular cyclin with a CDK results in the targeting of the kinase activity towards a particular set of substrates, which in turn trigger a series of downstream events. A number of surveillance mechanisms or 'checkpoints' exist that monitor key events, such as cell size, DNA replication and spindle assembly, and these checkpoints have the ability to prevent commitment into, or delay progression through, the cell cycle if conditions are unfavourable or the fidelity of the cycle is threatened (Morgan, 2007).

1.3 The budding yeast cell cycle

While many components, processes and principles are conserved between species, the budding yeast cell cycle differs in a number of ways to that of human cells. For example, in *S. cerevisiae* the cell cycle is coordinated by a single CDK, Cdc28 (Nasmyth, 1993), whereas there are four (Cdk1, 2, 4 and 6) that mediate these events in human cells. Cdk1 and Cdk2 operate primarily in M phase and S phase, respectively, while Cdk4 and Cdk6 are important in regulating entry into the cell cycle in response to extracellular factors (Malumbres & Barbacid, 2005). The duration also varies between these cell types. Human HeLa cells require approximately twenty four hours to complete a cell cycle whereas *S. cerevisiae* takes a mere ninety minutes under optimal

conditions. What follows is a summary of the key events during each stage of the budding yeast cell cycle (Fig. 1.1).

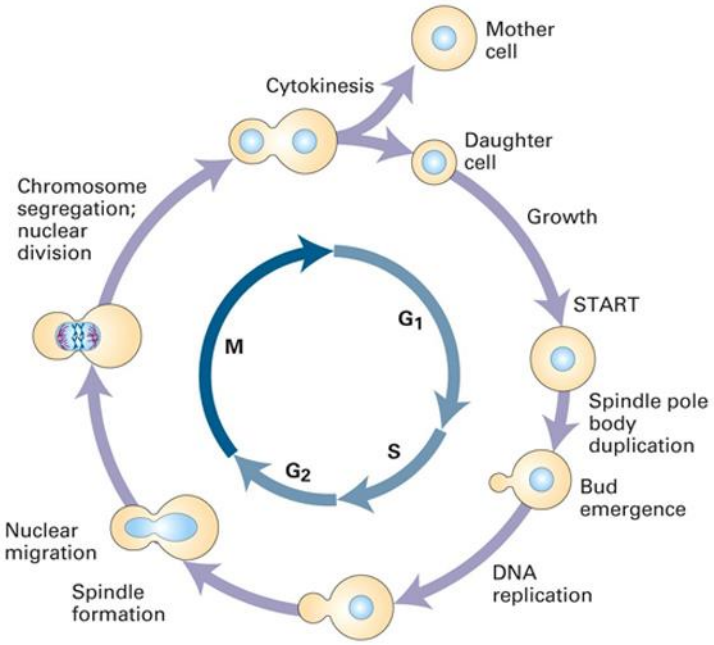

Figure 1.1. The budding yeast cell cycle. After the initial growth phase, G_1, the SPB is duplicated and the bud begins to emerge. DNA is replicated in S-phase and by M-phase, cells have established a bipolar spindle on which the chromosomes are bi-oriented and the nucleus migrates to the bud neck. Once all chromosomes are bi-oriented they are equally divided to opposite poles of the cell. The nucleus divides and the two cells are physically separated during cytokinesis. This figure is reproduced from Lodish *et al*. (2004).

1.3.1 *G_1*

Following cytokinesis at the end of the previous cycle the cell enters G_1. At this point the cell is unbudded with a single spindle pole body (SPB, the yeast microtubule organising centre, MTOC) and a single mass of DNA. Induction of mating or nutrient starvation at this point restricts cells in G_1 but if nutrients are plentiful and mating is not induced the cell enters the cell cycle. This transition is monitored by the START checkpoint, which coordinates the cell cycle with cell growth. Once cells reach a critical mass this checkpoint is satisfied and the cells pass this restriction point and become

irreversibly committed to progression through the cell cycle. This progression requires the association of the G_1 cyclin Cln3 with Cdc28 to activate the SBF and MBF transcription factors, which trigger a transcriptional programme needed for cell cycle progression (Dirick *et al*., 1995). SBF and MBF-regulated genes include those encoding the Cln1 and Cln2 G_1/S cyclins and the B-type Clb5 and Clb6 S-phase cyclins, which are required for DNA synthesis (Dirick *et al*., 1995). Pre-replicative complexes (pre-RCs) are also formed at DNA replication origins early in G_1 and this requires the absence of Cdc28 activity (reviewed in Diffley, 2004). The pre-RC consists of the origin recognition complex (ORC; Orc1-6), Cdc6, Cdt1 and Mcm2-7. As Cdc28 activity increases, further pre-RC assembly is inhibited (Diffley, 2004). A bud site is also selected after cell cycle commitment by the accumulation of cortical polarity determinants, which includes the polarisome protein complex. This requires Cln1/2-Cdc28 activity and subsequently leads to the polarisation of the actin cytoskeleton, which is important for numerous processes including bud growth, mitotic spindle orientation, protein trafficking and organelle inheritance (reviewed in Pruyne & Bretscher, 2000; Bi & Park, 2012). In late G_1 Cln1/2-Cdc28 complexes phosphorylate and inactivate Sic1, a potent inhibitor of Clb-Cdc28 complexes, and the cell enters S-phase (Schwob *et al*., 1994; Verma *et al*., 1997).

1.3.2 *S/G$_2$*

Clb5/6-Cdc28 and Cdc7-Dbf4 (Dbf4-dependent kinase or DDK) activity are required in S-phase for the initiation of DNA replication through activation of the pre-RCs. An active helicase is formed, double stranded DNA is unwound and DNA polymerases are loaded to initiate DNA synthesis. As well as being required for initiation, Clb-Cdc28 and DDK activity also inhibits the reassembly of pre-RCs thereby ensuring that origins initiate only once per cell cycle (reviewed in Toone *et al*., 1997;

Diffley, 2004). As the DNA is synthesised, the replicated chromosomes become physically linked by the cohesin complex, which is important for ensuring proper chromosome segregation in anaphase (Michaelis *et al*., 1997; reviewed in Nasmyth & Haering, 2009). A surveillance mechanism detects DNA damage and replication stress and can arrest cell cycle progression until these issues are dealt with (Baldo *et al*., 2012). The bud begins to emerge and Cln1/2-Cdc28 activity maintains actin polarisation and apical bud growth (reviewed in Pruyne & Bretscher, 2000; Bi & Park, 2012). SPBs are also duplicated and separated in S-phase and this requires phosphorylation of SPB components by Cdc28 and Mps1 (reviewed in Jaspersen & Winey, 2004). The SPB is a complex and dynamic organelle that is inserted in the nuclear membrane and, when replicated and divided, nucleates both nuclear and cytoplasmic microtubules to form the bipolar mitotic spindle (Jaspersen & Winey, 2004). Progression through S-phase also sees the expression of two additional B-type cyclins Clb3 and Clb4 (Richardson *et al*., 1992). When all chromosomes have been replicated, cells express proteins required for mitosis including the B-type cyclins Clb1 and Clb2 (Richardson *et al*., 1992) and the nucleus migrates towards the bud neck.

1.3.3 *Mitosis*

S. cerevisiae and other fungi undergo a ‘closed’ mitosis, in which the nuclear envelope remains intact throughout the cell cycle and mitosis occurs within the nucleus. The cells of higher eukaryotes on the other hand undergo ‘open’ mitosis where the nuclear envelope disassembles during the G_2/M transition and is not reassembled until after DNA segregation in telophase/G_1 (Morgan, 2007). In budding yeast, transition to M phase sees the random redistribution of actin patches around the bud cortex and a switch from apical to isotropic bud growth (reviewed in Pruyne & Bretscher, 2000; Bi & Park, 2012). At the onset of mitosis the condensin complex, which is closely related

to the cohesin complex, associates with the replicated DNA and facilitates the compaction of the amorphous mass of DNA into discrete sister chromatids (reviewed in Thadani *et al*., 2012). A protein complex known as the kinetochore assembles at the centromere of each chromosome and provides the attachment site for spindle microtubules (reviewed in Bloom & Joglekar, 2010). Most eukaryotes have vast regional centromeres that assemble large kinetochores and bind multiple microtubules. Budding yeast have discrete point centromeres that bind a single microtubule. For progression into anaphase each sister chromatid pair must be attached to a microtubule emanating from opposite poles of the bipolar spindle. This process is known as chromosome bi-orientation (reviewed in Tanaka *et al*., 2005). Once bi-orientation is established, tension is generated between sister chromatids as the cohesin complexes holding the sister chromatids together counteract the pulling forces generated by spindle microtubules (Tanaka *et al*., 2000). The spindle assembly checkpoint (SAC) delays progression into anaphase until all chromosomes are bi-oriented (reviewed in Musacchio & Salmon, 2007; Lara-Gonzalez *et al*., 2012). SAC components are recruited to unattached kinetochores and their signalling inhibits Cdc20, a co-factor and activator of the anaphase promoting complex/cyclosome (APC/C; reviewed in Peters, 2006; Barford, 2011), thereby delaying progression into anaphase. When all chromosomes are bi-oriented, SAC signalling ceases and Cdc20 is released. The APC/C^{Cdc20} subsequently ubiquitinates a number of proteins, targeting them for degradation by the proteasome (reviewed in Finley, 2009) and thus initiating anaphase. Such proteins include the key substrate Pds1, the yeast securin (Cohen-Fix *et al*., 1996). Pds1 binds to and inhibits the yeast separase Esp1. Upon Pds1 degradation, Esp1 is liberated and cleaves the Scc1 component of the cohesin complex allowing the separation of sister chromatids (Ciosk *et al*., 1998; Uhlmann *et al*., 2000). The mitotic spindle elongates and sister chromatids are pulled to opposite poles of the cell. A

cytokinetic actin ring assembles at the bud neck, the site of cell division. Esp1 is a member of the Cdc fourteen early anaphase release (FEAR) network and its activation also stimulates the partial release into the nucleus of the essential phosphatase Cdc14, which subsequently dephosphorylates Cdc28 substrates (reviewed in Rock & Amon, 2009). Cdc28 activity also declines rapidly in anaphase. This is brought about by APC/C-dependent targeting of mitotic cyclins for degradation (Peters, 2006) and expression of the Cdc28 inhibitor Sic1. In telophase the mitotic exit network (MEN) drives the full release of Cdc14 and consequently further dephosphorylation of Cdc28 substrates, including removing inhibitory phosphate groups from the APC/C co-factor Cdh1 (reviewed in Stegmeier & Amon, 2004). APC/C^{Cdh1} targets Cdc20 for degradation allowing the accumulation of G_1/S cyclins in the next cell cycle (Huang *et al*., 2001). Other proteins targeted for degradation include several involved in spindle integrity (Juang *et al*., 1997; Hildebrandt & Hoyt, 2001). Consequently, the mitotic spindle becomes unstable and disassembles. The cytokinetic ring contracts and actin patches repolarise to the bud neck to direct cell wall synthesis and physically separate the two cells (reviewed in Pruyne & Bretscher, 2000; Bi & Park, 2012). Cells enter G_1, origins of replication are reset through the formation of pre-RCs, Cdc28 activity is inhibited by Sic1 and the cell is primed to enter the next cell cycle.

Particular topics of interest with regard to this thesis are the events occurring during mitosis, particularly those surrounding the metaphase/anaphase transition that involve the conserved chromosomal passenger complex and Haspin kinases. These will be discussed in more detail in the following sections. The establishment of cell polarity and mechanisms of spindle positioning in budding yeast will also be discussed briefly to give context to certain experiments and observations made during the course of this study.

1.4 The actin cytoskeleton, cell polarity and bud growth

1.4.1 *An overview of actin*

A fundamental property of the cell is the ability to polarise and central to the establishment of cell polarity is actin. Actin is an essential protein that exists in monomeric globular (G-actin) and filamentous (F-actin) forms (reviewed in Dominguez & Holmes, 2011). F-actin and related proteins can assemble into discrete cortical actin patches and long actin cables to form a network known as the actin cytoskeleton (reviewed in Pruyne & Bretscher, 2000; Heng & Koh, 2010). F-actin has a structural and functional polarity. G-actin monomers within the F-actin filament are oriented towards the same end of the filament and therefore each end is distinct from one another. As these filaments have a defined polarity, the ends are referred to as the plus and minus ends. The dynamic assembly, disassembly and redistribution of these F-actin structures during the cell cycle or in response to other stimuli is considered to be central to actin function within the cell. These polarised actin networks play a key role in numerous processes including polarised growth, cell morphogenesis, cytokinesis, cell migration, vesicle trafficking and endocytosis (for example, see Pruyne & Bretscher, 2000; Heng & Koh, 2010; Jin, 2013). The actin cytoskeleton also influences mitotic spindle positioning and alignment, which is important during development in plants and animals to generate cell diversity (reviewed in Knoblich, 2010; De Smet & Beeckman, 2011; Morin & Bellaïche, 2011). These processes require the myosin family of proteins. Myosins have motor domains that track along the F-actin cables to facilitate the transport of the necessary factors to their required destinations within the cell (reviewed in Hartman & Spudich, 2012). Budding yeast undergoes highly polarised growth throughout the cell cycle and many of the genes that regulate cell polarity are conserved between yeast and more complex eukaryotic organisms (McCaffrey & Macara, 2009; Heng & Koh, 2010). Consequently, budding yeast has served as a powerful model

system for studying these fundamental processes (Pruyne & Bretscher, 2000; Moseley & Goode, 2006; Bi & Park, 2012).

1.4.2 *An overview of the budding yeast actin cytoskeleton in growth polarity*

The organisation of the actin cytoskeleton in *S. cerevisiae*, like other organisms, changes through the cell cycle (Fig. 1.2; Amberg, 1998; reviewed in Pruyne & Bretscher, 2000; Moseley & Goode, 2006; Heng & Koh, 2010). As cells commit to a new cell cycle in G_1 a bud site is selected. Cortical actin patches aggregate at this site and F-actin cables converge at this point (Amberg, 1998). Bud growth requires the transport of secretory vesicles along these actin cables to the bud site where they are tethered and fused with the plasma membrane (Pruyne *et al*., 1998). As the bud emerges in S-phase the actin patches cluster at its tip and actin cables extend from the mother into the bud. Bud growth at this point is apical (directed to the bud tip). Under certain conditions, such as nutrient starvation, some *S. cerevisiae* strains undergo an alternate filamentous growth state and prolong apical growth to generate highly elongated cells (reviewed in Dickinson, 2008; Cullen & Sprague, 2012). As cells progress into G_2/M-phase, actin patches and cables are redistributed around the bud cortex while cables from the mother still extend to the bud. Growth remains restricted to the bud and growth now proceeds isotropically and the bud expands into an ellipsoid shape (Tkacz & Lampen, 1973; Lew & Reed, 1993). When bud growth is complete the actin cytoskeleton is depolarised as actin filaments and cables are distributed randomly and a contractile F-actin ring forms at the bud neck, the site of cell division. As cells exit mitosis and progress through cytokinesis the F-actin ring contracts to force the ingression of the cell wall and plasma membrane (Bi *et al*., 1998). The actin ring disassembles and the cytoskeleton repolarises as actin patches and cables congregate at the former bud neck in both the mother and the bud to target membrane deposition at

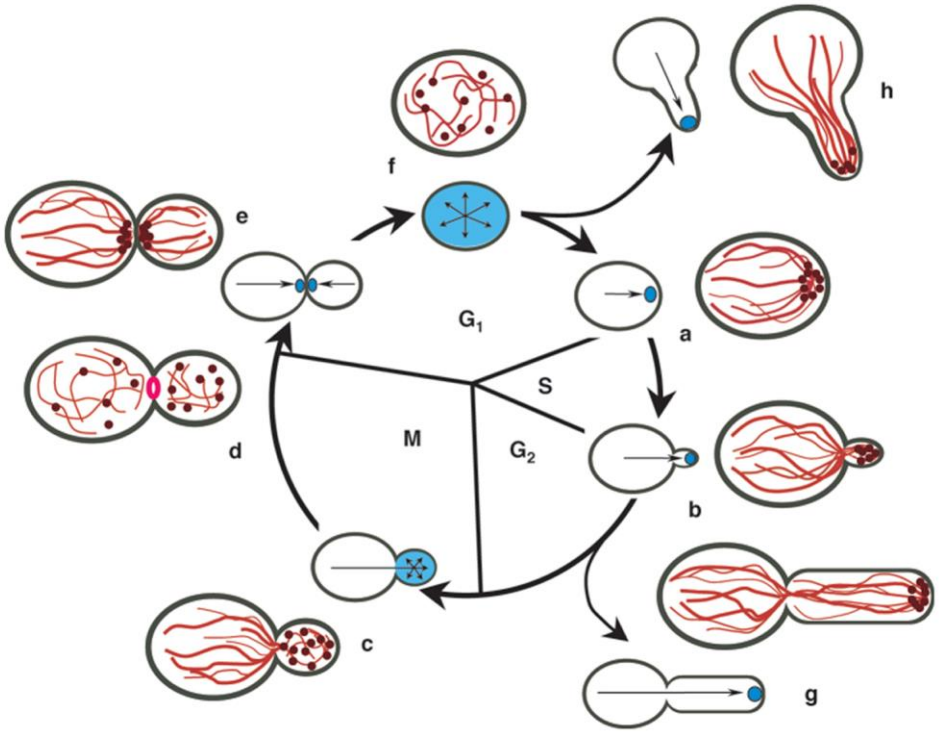

Fig. 1.2. Actin cytoskeleton organisation and polarised growth during the budding yeast cell cycle. (a) As cells commit to the cell cycle a bud site is established by the clustering of polarity determinants (such as Cdc42; blue) that orient the actin cytoskeleton to this position (brown, actin patch; red, actin cable). (b) Secretory vesicles are directed along the actin cytoskeleton to the bud site where they fuse, resulting in bud emergence and growth. (c) As cells enter G_2/M phase the polarity determinants are randomly distributed around the bud cortex and consequently bud growth proceeds isotropically. (d) When bud growth is complete the actin cytoskeleton is disorganised. A cytokinetic ring forms at the bud neck (pink), which contracts and disassembles after mitosis. (e) Polarity determinants cluster at the former bud neck, reorienting the actin cytoskeleton towards this point and thereby directing new cell wall growth to physically separate the two cells. The mother cell can re-enter another cell cycle immediately. (f) The daughter cell undergoes a phase of undirected growth. (g) Under certain conditions, some *S. cerevisiae* strains enter a filamentous growth state and prolong apical growth to form highly elongated cells. (h) Haploid yeast cells arrest in G_1 when exposed to mating pheromones and polarise growth towards mating partners to form a mating projection (shmoo). This figure is reproduced from Pruyne & Bretscher (2000).

this site and the synthesis of new cell walls between the cells (VerPlank & Li, 2005). Following cell division the actin cytoskeleton is depolarised.

Polarised growth is also stimulated during yeast mating. Haploid budding yeast cells exist as one of two mating types, *MAT***a** and *MATα.* Each mating type constitutively secretes a pheromone that triggers a mating response in cells of the opposite mating type. Exposure to a pheromone stimulates a signalling cascade that leads to cells becoming arrested in G_1 and initiates transcription of genes required for mating. Growth is oriented towards mating partners through polarisation of the actin cytoskeleton in the direction of the pheromone concentration gradient (Madden & Snyder, 1992; Arkowitz, 2009). This polarised growth forms a mating projection or shmoo. Shmoos from the two mating partners fuse and a diploid zygote is formed.

Throughout the cell cycle, growth is directed almost exclusively into the bud. Cells defective in proper polarised growth are often characterised by one of several unusual morphologies. Excessive apical growth results in the formation of highly elongated buds and excessive isotropic growth results in abnormally large and spherical buds (Watanabe *et al*., 2009). If growth is not directed to the bud at all, the mother cells grow into large unbudded cells.

1.4.3 *Establishment and reorganisation of actin polarity to direct bud growth and cell separation*

The process of establishing cell polarity and budding is controlled both spatially and temporally by a coordinated guanosine triphosphatase (GTPase) signalling cascade (reviewed in Bi & Park, 2012). A single specific bud site is selected to which polarised growth will be directed and this requires the Ras family GTPase Rsr1 and its regulators

(Cabib *et al*., 1998; Casamayor & Snyder, 2002). Proteins that are required for bud formation assemble and restrict growth to this position. Components of the polarisome complex and the Rho family GTPase Cdc42 and its regulators are central to this process. The core components of the polarisome complex include the scaffold protein Spa2, the actin-binding protein Bud6, the formin Bni1 and Pea2, a protein with an as yet unidentified function (Sheu *et al*., 1998). The polarisome and associated proteins regulate the downstream processes of Cdc42. Following the establishment of polarisation and the bud site, the exocytic deposition of secretory vesicles in the plasma membrane at this site leads to bud emergence and growth (Novick *et al*., 2006; Brennwald & Rossi, 2007). Remarkably, Cdc42 (and subsequently growth) can still effectively polarise at a single random site in the absence of any cortical landmarks, such as in *rsr1*Δ cells (Irazoqui *et al*., 2003). Exactly how polarisation occurs in the absence of spatial cues is not known but two distinct models have been proposed although these will not be discussed further here (Marco *et al*., 2007; Kozubowski *et al*., 2008; Smith *et al*., 2013).

Regardless of the mechanism, it is clear that Cdc42 plays a key role in the establishment of cell polarity, bud emergence and cell growth. Cdc42 was first discovered in yeast (Adams *et al*., 1990) and has since been shown to be highly conserved and required for cell polarisation in many, if not all, eukaryotic organisms (Etienne-Manneville, 2004). Cortical actin patches and actin cables still form in the absence of Cdc42 but they are completely disorganised (Adams *et al*., 1990). Cdc42, like other Rho GTPases, only signals to effectors in an active GTP-bound state. To bind GTP and become active, Cdc42 requires the guanine nucleotide exchange factor (GEF) Cdc24 (Zheng *et al*., 1994). Once active, Cdc42 signals to a number of effectors including: the formin Bni1 (Evangelista *et al*., 1997); the p21-activated kinases (PAKs)

Ste20 (Zhao *et al*., 1995), Cla4 (Cvrčková *et al*., 1995) and Skm1 (Martín *et al*., 1997); and the yeast-specific CRIB domain proteins Gic1 and Gic2 (Brown *et al.*, 1997). Through these effectors, Cdc42 signalling can differentially influence a wide range of processes including organisation of actin and septins (discussed later; Moseley & Goode, 2006; Oh & Bi, 2011; Okada *et al*., 2013), polarised secretion (Zhang *et al*., 2001), initiation of budding and response to mating pheromones (Simon *et al*., 1995). In addition to Cdc42, there are a number of other Rho GTPases that have roles in polarised growth as well as a myriad of other proteins that localise to sites of polarised growth (reviewed in Park & Bi, 2007; Bi & Park, 2012). For bud emergence and growth, these polarity determinants must remain concentrated at the bud tip. Although many of these proteins remain stably concentrated at the bud tip, studies measuring fluorescence recovery after photobleaching (FRAP) indicate that a number of these proteins, including Cdc42, reside at the bud tip for only a few seconds at a time (Wedlich-Soldner *et al*., 2004), indicating that the localisation of these proteins has to be dynamically maintained. It is believed that positive feedback loops, endocytic recycling and polarised secretion help to amplify and maintain this focussed localisation (Irazoqui *et al*., 2005; Slaughter *et al*., 2009; Okada *et al*., 2013). However, the mechanism is still not fully understood. The activity of Cdc28 in association with the G_1 cyclins Cln1 and Cln2 is also important for initiating and maintaining apical growth (Lew & Reed, 1993) as is Cdc42 signalling through Ste20 (Eby *et al*., 1998). As the bud grows the polarity determinants are randomly distributed around the bud cortex, which results in a switch from apical to isotropic bud growth (Pruyne & Bretscher, 2000). This switch is triggered by the activity of Cdc28 in association with the mitotic B-type cyclins Clb1 and Clb2 (Lew & Reed, 1993) and is also facilitated by Cdc42 signalling through Cla4 (Benton *et al*., 1997). Once bud growth is complete, the actin cytoskeleton is depolarised as the polarity determinants are randomly distributed in both the mother and

bud (Amberg, 1998; Pruyne & Bretscher, 2000). Septins at the bud neck function as a scaffold for the localisation of the actin-myosin ring in late anaphase/telophase, which subsequently contracts and disassembles (Oh & Bi, 2011). Cdc42 and other proteins become concentrated at the former neck in both the mother and bud and polarise the actin cytoskeleton to direct the synthesis of new cell walls to physically separate the two cells. Activation of the APC/C and the release of Cdc14 phosphatase are important for these processes in late mitosis (Tully *et al*., 2009; Sanchez-Diaz *et al*., 2012). The mechanisms involved in regulating the dynamic distribution of polarity determinants are both complex and numerous and will not be discussed further here.

1.5 Spindle positioning and orientation in budding yeast

1.5.1 *Microtubules and the mitotic spindle*

Like F-actin filaments, microtubules also have structural and functional polarity. Microtubules are hollow cylinders formed from heterodimeric subunits of α- and β-tubulin. These subunits join end to end in the same orientation to form protofilaments, which associate laterally to form a cylinder (Desai & Mitchison, 1997). This means that one end of the microtubule is capped with α-tubulin (minus end), while the other is capped with β-tubulin (plus end). The kinesin and dynein families of proteins have motor domains that can track along microtubules in a similar manner to myosin proteins on F-actin filaments. A third class of tubulin, known as γ-tubulin, is not incorporated into the microtubule but instead forms complexes with other proteins to regulate microtubule polymerisation (reviewed in Kollman *et al*., 2011). The most notable microtubule structure within eukaryotic cells is the mitotic spindle. Animals and many fungi also use microtubules as a cytoskeletal structure to polarise growth in a similar way to actin. However, budding yeast are divergent and only use microtubules to form the mitotic spindle.

The mitotic spindle is an essential structure in eukaryotic organisms that is required to accurately segregate replicated chromosomes between daughter cells during mitosis. In many eukaryotic organisms the mitotic spindle consists of microtubules that are nucleated by a pair of MTOCs (centrosomes in animals, SPBs in yeast). These structures define the spindle poles and nucleate microtubules that are organised into a bipolar spindle that consists of interpolar and kinetochore microtubules, which associate with one another and chromosomes respectively, and astral microtubules that extend away from the MTOCs towards the cell cortex. Many proteins are involved in the organisation and regulation of this highly dynamic structure and many of these will not be discussed here (for excellent reviews on the subject, see Walczak & Heald, 2008; Winey & Bloom, 2012).

1.5.2 *Spindle positioning and asymmetric cell division*

The actin cytoskeleton plays a role in the positioning and orientation of the mitotic spindle. In asymmetric cell divisions the spindle must be aligned with the cell polarity axis. This is accomplished through the targeting of astral microtubules originating from each spindle pole to the cortex of opposite cell compartments, which subsequently interact with the cytoskeleton to generate asymmetric pulling forces and position the spindle. Accurate spindle positioning is vital during cell division for proper development and cell diversity in multicellular organisms for a number of reasons. For example, the position of the spindle often determines the location at which the contractile ring is formed and therefore the division plane (reviewed in McNally, 2013). Symmetric and asymmetric cell divisions are also important for cell fate determination, tissue architecture and tissue morphogenesis in multicellular organisms (reviewed in Knoblich, 2010; De Smet & Beeckman, 2011; Morin & Bellaïche, 2011).

In budding yeast the site of cytokinesis (the bud neck) is predetermined and the spindle must be oriented relative to this division plane to ensure that the replicated chromosomes are equally distributed between both daughter cells (Fig. 1.3). This is achieved by two sequential and partially redundant pathways that are monitored by the budding yeast-specific spindle position checkpoint (SPoC; reviewed in Caydasi *et al*., 2010; Markus *et al*., 2012). The second pathway, which functions later in the cell cycle, requires the minus end-directed microtubule motor dynein to generate pulling forces at the cell cortex. This is a common and critical mechanism of spindle positioning in many organisms. However, budding yeast deficient in this pathway can still properly orient their spindle through the earlier acting 'Kar9 pathway'. Deletion of genes in either of these pathways results in a viable cell, whereas deletion of genes in both pathways is lethal (Miller & Rose, 1998).

1.5.3 *The Kar9 pathway*

Early experiments using latrunculin-A to disrupt F-actin indicated that spindle orientation early in the cell cycle requires actin cables, whereas orientation later in the cell cycle does not (Theesfeld *et al*., 1999). Actin perturbation prior to anaphase significantly reduced the number of cells exhibiting astral microtubules extending through the neck into the bud, resulting in misoriented spindles (Theesfeld *et al*., 1999). This suggested that actin cables play an important role early in the cell cycle to guide astral microtubules into the bud and/or anchor them with the bud cortex. This actin-dependent mechanism for early spindle alignment, now referred to as the Kar9 pathway, requires the yeast myosin V and microtubule binding EB1 homologues, Myo2 and Bim1, and the adaptor protein Kar9 (Korinek *et al*., 2000; Lee *et al*., 2000; Miller *et al*., 2000; Yin *et al*., 2000). Bim1 binds to the plus end of microtubules and to Kar9, which in turn binds Myo2. Through these interactions and through the motor activity of Myo2,

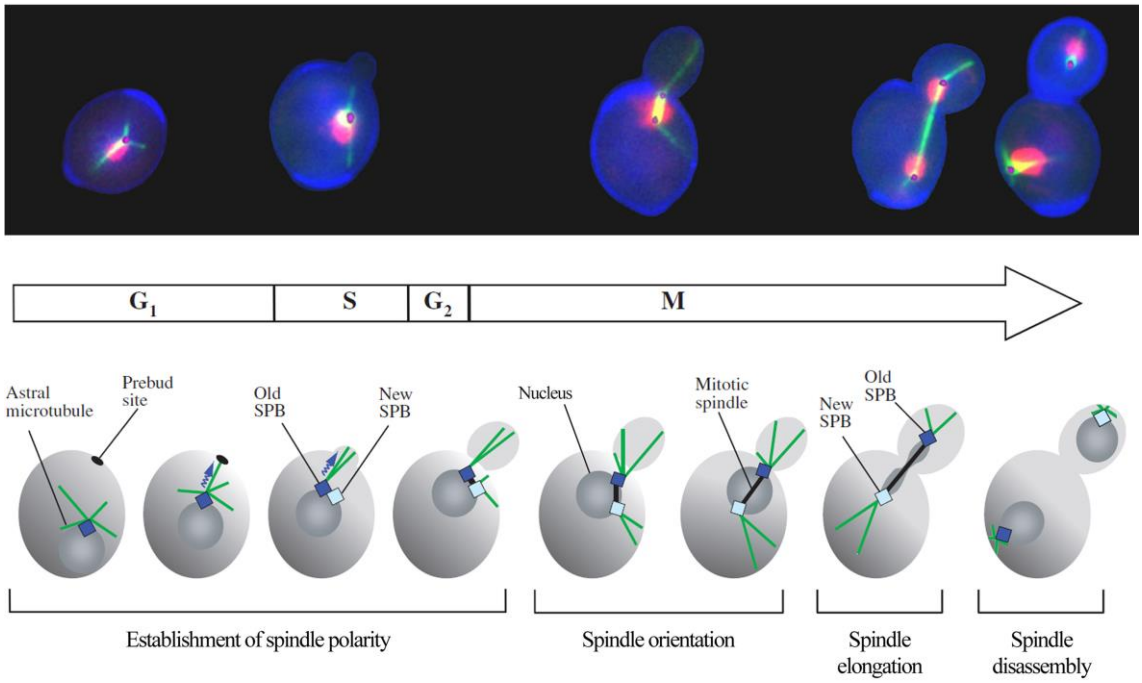

Fig. 1.3. Spindle positioning in budding yeast. Fluorescence microscopy images and a cartoon depicting mitotic spindle dynamics through the cell cycle. Astral microtubules are captured at the pre-bud site and pull the nucleus towards this position. After SPB duplication, CDK activity at the new SPB results in the differential recruitment of proteins to each SPB. As a result, the fate of each pole is specified (new SPB = mother-bound; old SPB = daughter-bound). This leads to the orientation of the spindle along the mother-bud axis. The spindle elongates during anaphase, segregating sister chromatids to opposite spindle poles. The spindle disassembles and the nucleus divides. Key to microscopy images: DNA, red; microtubules, green; SPB, magenta; cell outline, blue. This figure has been adapted from Hailey *et al*. (2001) and Huisman & Segal (2005).

astral microtubules are guided along actin cables towards the bud (Hwang *et al*., 2003). To ensure that only astral microtubules from one spindle pole body are directed towards the bud, Kar9 is asymmetrically localised to the daughter-bound SPB and not the mother-bound SPB. This asymmetry requires Cdc28-Clb4 activity. Cdc28-Clb4 preferentially localises to the mother-bound SPB where it phosphorylates Kar9 and inhibits its association with this SPB and Bim1 (Liakopoulos *et al*., 2003), thereby limiting the action of the Kar9 pathway to the daughter-bound SPB. Kar9-associated

microtubules are captured at the neck or bud cortex, possibly through the interaction of Bim1 with the cortical protein Bud6 (ten Hoopen *et al*., 2012). Subsequent attachment-dependent microtubule depolymerisation pulls the spindle towards the bud neck and aligns it along the mother-bud axis (Adames & Cooper, 2000). These microtubule 'capture-shrinkage' events are thought to be mediated by Kip3 (kinesin-8) and Kar3 (kinesin-14), both of which are microtubule minus end directed motors with plus end specific depolymerase activity (Gupta *et al*., 2006; Maddox *et al*., 2003; ten Hoopen *et al*., 2012).

1.5.4 *The dynein pathway*

The dynein pathway operates later in the cell cycle after the onset of anaphase. This pathway for spindle positioning requires that an astral microtubule is associated with cortically-anchored dynein. As the dynein motor tracks towards the minus end of the astral microtubule that is located at the SPB, the spindle is pulled towards the bud and aligned with the polarity axis. Localisation of cytoplasmic dynein to the bud cortex depends on its association with microtubule plus ends. This interaction is mediated by the plus end tracking protein Bik1 (Sheeman *et al*., 2003), the yeast homologue of CLIP-170. Bik1 (and therefore dynein) is transported to plus ends by a number of different mechanisms. One mechanism is through its association with plus end-directed kinesin Kip2 (Carvalho *et al*., 2004). Without Kip2, Bik1 and dynein can still localise to microtubule plus ends through mechanisms involving a C-terminal motif in α-tubulin and Bim1 (Caudron *et al*., 2008). When the plus end of a microtubule carrying dynein comes into contact with the cortical protein Num1, dynein is offloaded and becomes anchored to the cell cortex where its motor activity is stimulated to generate the force necessary to pull the spindle (Markus & Lee, 2011). How this pathway is regulated is not fully understood. For example, Num1 is distributed in cortical patches around both

the mother and bud cortex (Heil-Chapdelaine *et al*., 2000), yet dynein is preferentially offloaded at the bud cortex (Markus & Lee, 2011). This is possibly the result of asymmetric loading of dynein onto astral microtubules emanating from the daughter-bound SPB (Grava *et al*., 2006), similar to what is observed for Kar9 (Liakopoulos *et al*., 2003). It is also unclear how dynein remains associated with the plus ends of microtubules since it has minus end directed motor activity. Recent studies have shown that Pac1, the yeast homologue of LIS1 that binds dynein and is required for its plus end targeting, reduces the motility of dynein *in vitro* (Markus & Lee, 2011), suggesting that Pac1 may keep dynein in an inactive state. Additionally, dynein recruits its processivity factor and cargo adaptor dynactin at the plus end (Kardon *et al*., 2009). This has been proposed to trigger a conformational change that allows dynein to interact with Num1 at the cortex (Markus & Lee, 2011). The dynein pathway appears to be restricted to anaphase by the inhibitory action of She1, which seems to prevent the recruitment of dynactin to microtubules (Bergman *et al*., 2012) and inhibits dynein motility (Markus *et al*., 2012b). At the metaphase-anaphase transition, She1 is removed from astral microtubules, thereby activating the dynein pathway (Woodruff *et al*., 2009).

These pathways are required for proper positioning and orientation of the spindle relative to the division plane. As the spindle elongates in anaphase, the sister chromatids are pulled to opposite poles of the cell. This requires that the sister chromatids are attached to microtubules emanating from opposite spindle poles. The chromosomal passenger complex plays a key role in ensuring that these correct attachments are made prior to the onset of anaphase. The roles and regulation of this complex will be discussed in the following sections.

1.6 The Chromosomal Passenger Complex

1.6.1 *Discovery*

The term "chromosomal passenger" was first used by Earnshaw and Bernat as a means to classify a number of proteins that associated with chromosomes through mitosis and subsequently transferred to the spindle during anaphase (Fig. 1.4; Earnshaw & Bernat, 1991). Since their initial discovery, other chromosomal passengers have been identified and a subset of these associate to form what is now referred to as the chromosomal passenger complex (CPC; Adams *et al*., 2001; Gassmann *et al*., 2004). The CPC is an evolutionarily conserved four subunit complex consisting of Aurora B kinase and three non-enzymatic components, INCENP, Survivin and Borealin (Table 1.1; reviewed in Carmena *et al*., 2012).

The first member of this complex was identified in 1987 using a monoclonal antibody that was raised against a "mitotic chromosome scaffold" protein (Cooke *et al*., 1987). Staining with this antibody was concentrated at the centromere in metaphase and so this antigen was named INCENP (inner centromere protein). At the onset of anaphase, INCENP dissociated from the separating sister chromatids and localised to the spindle midzone and the equatorial cell cortex at the site of cleavage furrow formation (Cooke *et al*., 1987).

A number of years later it was shown that Aurora B interacts with INCENP (Adams *et al*., 2000). The Aurora kinases are a family of serine/threonine kinases that have essential roles in cell cycle regulation. The first Aurora kinase was identified in *S. cerevisiae* during a screen to identify mutants with altered chromosome copy number and was named Ipl1 (increase in ploidy 1; Chan & Botstein, 1993). Ipl1 was shown to associate with the budding yeast INCENP homologue Sli15 to promote proper

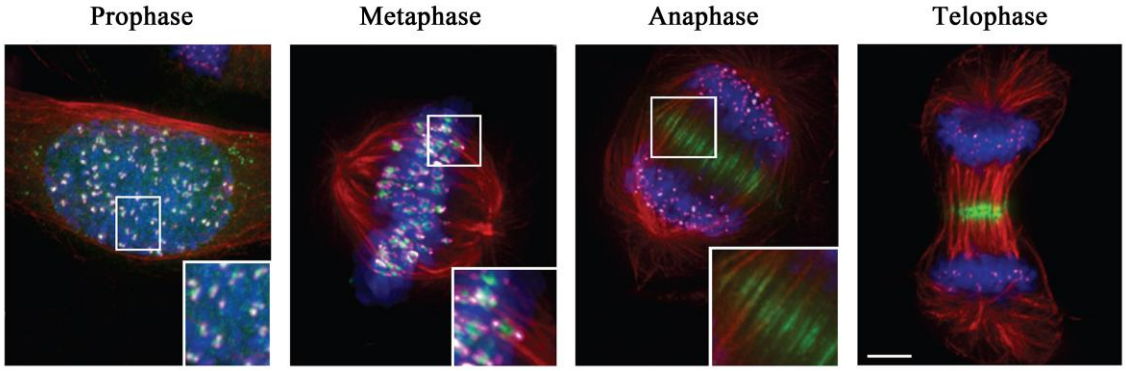

Fig. 1.4. Chromosomal passenger complex localisation during mitosis. Immunofluorescence in human HeLa cells shows the localisation of Aurora B (green) during mitosis with kinetochores (pink), microtubules (red) and DNA (blue). Aurora B is associated with chromosome arms and centromeres during prophase. In metaphase, chromosomes are aligned on the spindle. As cells progress into anaphase, Aurora B translocates to the spindle midzone. In telophase, Aurora B is concentrated at the equatorial cortex. Scale bar = 5 μm. Images are reproduced from Ruchaud *et al*. (2007).

Table 1.1 Chromosomal passenger complex components in various organisms

Organism	Aurora B	INCENP	Survivin	Borealin
S. cerevisiae	Ipl1	Sli15	Bir1	Nbl1
S. pombe	Ark1	Pic1	Cut17/Bir1	Nbl1
H. sapiens	Aurora B	INCENP	Survivin	Borealin
X. laevis	XAurora B	XINCENP	XSurvivn	Dasra A, Dasra B
C. elegans	AIR-2	ICP-1	BIR-1	CSC-1
D. melanogaster	Ial	Incenp	Deterin	Borealin

chromosome segregation (Kim *et al*., 1999). The first of the kinases to go by the name of Aurora was identified several years after Ipl1 during a screen designed to detect mutations that affect the structure and function of the mitotic spindle in *Drosophila melanogaster* (Glover *et al*., 1995). Since then Aurora kinases have been identified in the genomes of all eukaryotic organisms sequenced to date. *S. cerevisiae* has a single Aurora kinase whereas higher eukaryotes have up to three: Aurora A, B and C (Adams *et al*., 2001). Aurora A and Aurora B have different subcellular localisations and distinct

functions. Aurora A associates with spindle poles and functions in mitotic entry, centrosome maturation and bipolar spindle formation (Carmena *et al*., 2009). Ipl1/Aurora B follows the "chromosomal passenger" pattern of localisation and has numerous functions that will be discussed later. Our understanding of Aurora C is more limited. Aurora C is expressed primarily in the testis and may have a unique role in male meiosis (Dieterich *et al*., 2007), although it may also share similar functions with Aurora B as it has a similar pattern of localisation and can interact with other CPC components (Li *et al*., 2004; Yan *et al*., 2005; Slattery *et al*., 2009).

Survivin was the third component of the CPC to be identified. Survivin was thought to be linked with Aurora B and INCENP as it too was a chromosomal passenger protein and had similar mutant phenotypes (Uren *et al*., 2000; Adams *et al*., 2001). Later, Survivin was shown to interact with both Aurora B and INCENP (Wheatley *et al*., 2001). Survivin and its homologues are conserved members of the inhibitor of apoptosis protein (IAP) family and contain baculovirus IAP repeat (BIR) domains. Human Survivin contains a single BIR domain whereas the budding yeast homologue Bir1 contains two (Uren *et al*., 1999). Whether Bir1/Survivin is involved in the regulation of apoptosis is still actively debated. It has been suggested that cytoplasmic Survivin may inhibit cell death, while nuclear Survivin regulates mitosis either in complex with, or independently of, the CPC (Connell *et al*., 2008). However, analysis of Bir1/Survivin mutants in yeast and vertebrates has failed to identify any significant defects in cell death responses (Uren *et al*., 1999; Yue *et al*., 2008).

Borealin is the most recently identified member of the CPC and was first discovered in *Caenorhabditis elegans* and named CSC-1 (chromosome segregation and cytokinesis defective protein 1; Romano *et al*., 2003). Later, two independent studies

identified Borealin and Dasra B proteins in humans and *Xenopus laevis* respectively (Gassmann *et al*., 2004; Sampath *et al*., 2004). More recently the budding and fission yeast homologues of Borealin, Nbl1 (N-terminal borealin-like protein 1), were discovered (Nakajima *et al*., 2009; Bohnert *et al*., 2009). Like the other CPC subunits, Borealin was initially identified as a chromosomal passenger and subsequently found to interact with Aurora B, INCENP and Survivin (Gassmann *et al*., 2004; Sampath *et al*., 2004; Nakajima *et al*., 2009). *Xenopus* and a number of other vertebrates, excluding humans, have an additional distantly related protein, Dasra A, which may have similar functions (Sampath *et al*., 2004).

1.6.2 Functions of the CPC in mitosis

The CPC has many functions during mitosis (reviewed in Carmena *et al*., 2012). In early mitosis when the complex is associated with chromosomes, the CPC has roles in mitotic chromosome structure, spindle assembly, regulation of kinetochore-microtubule attachments and spindle checkpoint signalling. In late mitosis the CPC relocates to the spindle and has functions including anaphase chromatid compaction, spindle regulation and cytokinesis.

1.6.3 *Mitotic chromosome structure*

During mitosis the amorphous mass of replicated DNA becomes highly compacted into discrete sister chromatid pairs. The CPC has been suggested to aid in both the facilitation and maintenance of this compacted state. A well-recognised substrate of Ipl1/Aurora B is Serine 10 of histone H3 (H3-S10). The role of this modification is debated but it would appear to contribute to the release of HP1 (heterochromatin protein 1) in mammalian cells thereby contributing to chromosome condensation (Fischle *et al*., 2005; Hirota *et al*., 2005; Terada, 2006). Mutating H3-S10

in the ciliate protozoa *Tetrahymena thermophile* disrupts proper chromatin condensation and causes aberrant chromosome segregation (Wei *et al*., 1998). However, the equivalent mutation in *S. cerevisiae* has no such effect (Hsu *et al*., 2000), which could possibly be a reflection of the absence of HP1-like proteins and this pathway in budding yeast. Aurora B-dependent phosphorylation of H3-S10 has also been suggested to influence the binding of other proteins to chromatin (Maccallum *et al*., 2002; Loomis *et al*., 2009). The CPC has also been proposed to be involved in mitotic chromosome compaction through regulating the binding of condensin, a multi-subunit protein complex required for the establishment and maintenance of proper mitotic chromosome structure (Morishita *et al*., 2001; Petersen & Hagan, 2003; Tada *et al*., 2011; Thadani *et al*., 2012). Exactly how the CPC is involved in this process is also debated. There are two forms of condensin in most organisms, condensin I and II, whereas yeast have only one. The five-subunit condensin complex consists of two SMC (structural maintenance of chromosomes) proteins and three non-SMC regulatory proteins which include a member of the kleisin protein family (Thadani *et al*., 2012). Evidence from studies with fission yeast suggests that Ark1/Aurora B-dependent phosphorylation of the kleisin subunit of condensin promotes recruitment of condensin to chromosomes (Nakazawa *et al*., 2011). Similarly, phosphorylation of the human kleisin subunit by Aurora B promotes the efficient recruitment of condensin I, but not condensin II, to chromosomes in mitosis (Lipp *et al*., 2007). Ipl1 can also phosphorylate condensin but whether Ipl1 promotes chromosome condensation in early mitosis is unclear (Lavoie *et al*., 2004). However, Ipl1 activity and histone H3-S10 phosphorylation appear to contribute to maintenance of chromosome compaction during anaphase (Lavoie *et al*., 2004; Neurohr *et al*., 2011).

1.6.4 *Regulation of kinetochore-microtubule attachments*

To ensure that chromosomes are correctly segregated in anaphase it is essential that sister chromatids are attached to microtubules emanating from opposite spindle poles (bi-orientation; amphitelic attachment; Fig. 1.5 a). Sister chromatids can also be attached to microtubules from the same spindle pole (mono-orientation; syntelic attachment; Fig. 1.5 c) and these attachments must be corrected. Early studies in budding yeast first demonstrated that Ipl1 is required to disrupt kinetochore-microtubule interactions to promote bi-orientation (Biggins *et al*., 1999; Biggins & Murray, 2001; Tanaka *et al*., 2002a). Aurora B in higher eukaryotes was subsequently shown to perform the same function (Hauf *et al*., 2003; Lampson *et al*., 2004; Cimini *et al*., 2006). This function appears to involve the Ipl1/Aurora B-dependent phosphorylation of a number of substrates at the kinetochore-microtubule interface to destabilise mono-oriented attachments and allow for the correct bi-oriented attachments to be made. These substrates include MCAK (mitotic centromere-associated kinesin; kinesin-13) in metazoans, the Dam1 complex in yeast and components of the conserved outer kinetochore KMN (KNL1/Mis12 complex/Ndc80 complex) network. Phosphorylation of MCAK by Aurora B aids its recruitment to the centromere by facilitating its interaction with the centromeric protein Sgo2 (Andrews *et al*., 2004; Zhang *et al*., 2007; Tanno *et al*., 2010). Phosphorylation also simultaneously suppresses MCAK microtubule-depolymerising activity and its localisation to microtubule plus ends (Tanenbaum *et al*., 2011). Disruption of MCAK localisation to centromeres through mutation or depletion results in chromosome alignment defects similar to those seen when Aurora B function is disrupted (Andrews *et al*., 2004; Kline-Smith *et al*., 2004), suggesting MCAK plays a role in chromosome alignment. Exactly how MCAK contributes to this process is unclear, although it is possible that a balance of Aurora B and opposing phosphatase activity regulates MCAK microtubule depolymerisation

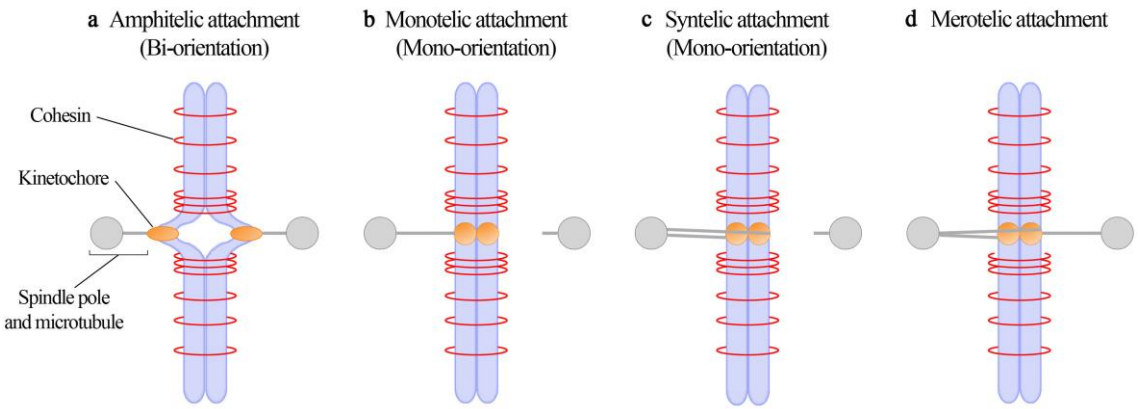

Fig. 1.5. Kinetochore-microtubule interactions on the mitotic spindle. (a) Amphitelic attachment. For proper chromosome segregation, sister chromatids must be bi-oriented. Each sister kinetochore is attached to microtubules emanating from opposite spindle poles. The opposing force generated through amphitelic attachment results in tension that stretches both centromeres and kinetochores. (b) Monotelic attachment. One sister kinetochore attaches to microtubules whereas the other does not. (c) Syntelic attachment. Microtubules from one spindle pole attach to both sister kinetochores. (d) Merotelic attachment. Microtubules from opposite spindle poles simultaneously attach to one sister kinetochore (reviewed in Tanaka *et al*., 2005).

activity at the centromere to control microtubule turnover at the kinetochore. There are no kinesin-13 family members in *S. cerevisiae* but it has been suggested that kinesin-8 and kinesin-13 family members may have overlapping or interdependent functions (Moore & Wordeman, 2004; Tanenbaum *et al*., 2011). Interestingly, deletion of *S. cerevisiae KIP3*, a gene which encodes the kinesin-8 family member Kip3, also results in chromosome alignment defects (Wargacki *et al*., 2010) and there are also several putative Ipl1/Aurora B consensus phosphorylation motifs in Kip3. It is possible that Kip3 performs an analogous function to MCAK in budding yeast.

Components of the fungi-specific Dam1 (or DASH) complex are phosphorylated by Ipl1 (Cheeseman *et al*., 2002). The Dam1 complex is a ten subunit complex that is

essential in budding yeast as deletion of any Dam1 complex component causes spindle abnormalities, chromosome segregation defects and cell death (Cheeseman *et al*., 2001; Janke *et al*., 2002; Li *et al*., 2005). *In vitro,* the Dam1 complex forms a ring that encircles the microtubule plus end like a collar, which allows the exchange of tubulin subunits while remaining tightly associated with the microtubule (Miranda *et al*., 2005; Westermann *et al*., 2005). *In vivo,* this complex localises to both the spindle and kinetochores, and the latter is dependent on the Ndc80 complex and tubulin (Nogales & Ramey 2009, Maure *et al*., 2011). The Dam1 complex is believed to contribute to maintaining the association between the kinetochore and microtubule through interaction with the Ndc80 complex and also couple microtubule depolymerisation with minus end-directed movement of chromosomes (Asbury *et al*., 2006; Westermann *et al*. 2006; Tanaka *et al*., 2007). Ipl1-dependent phosphorylation of Dam1 complex components, including Dam1, Ask1, Spc19 and Spc34 (Cheeseman *et al*., 2002), is believed to disrupt kinetochore-microtubule interactions and thereby promote bi-orientation. The ring formation is not necessary for the functions of the Dam1 complex (Gestaut *et al*., 2008), which raises the question of how the complex exists *in vivo*. Exactly how the Dam1 and Ndc80 complexes work in combination to contribute to proper kinetochore-microtubule interface formation and chromosome segregation is not fully understood (Lampert *et al*., 2010; Lampert *et al*., 2013). No proteins orthologous to Dam1 complex components are present in the genome of eukaryotes outside of fungi. However, recently the SKA (spindle and kinetochore-associated) complex has been discovered in human cells and this is proposed to be the functional analogue of the Dam1 complex in metazoans and is also negatively regulated by Aurora B phosphorylation (Welburn *et al*., 2009; Chan *et al*., 2012; Jeyaprakash *et al*., 2012).

Ndc80 (also known as Hec1 in humans) is a kinetochore protein that forms a four subunit complex with Nuf2, Spc24 and Spc25 (Janke *et al*., 2001) and is part of the KMN network, which is essential for generating stable load-bearing kinetochore-microtubule interactions (Kline-Smith *et al*., 2005; Cheeseman *et al*., 2006). Ipl1/Aurora B can phosphorylate the N-terminal globular head domain of Ndc80 *in vitro,* which reduces its affinity for microtubules (Cheeseman *et al*., 2002; Cheeseman *et al*., 2006). Human cells expressing a mutant of Ndc80 that cannot be phosphorylated by Aurora B, or cells injected with an antibody against the N-terminus of Ndc80 that also prevents Aurora B phosphorylation, have abnormally robust kinetochore-microtubule attachments and a high frequency of erroneous attachments (DeLuca *et al*., 2006). These observations suggest that Ipl1/Aurora B-dependent phosphorylation of Ndc80 is important for microtubule turnover and error correction to promote bi-orientation. More recent studies have identified other Aurora B substrates in the KMN network, namely the Dsn1 subunit of the Mis12 complex and KNL1/Spc105 (Emanuele *et al*., 2008; Yang *et al*., 2008; Welburn *et al*., 2010; Rosenberg *et al*., 2011; Akiyoshi *et al*., 2013). However, the functional significance of these modifications is debated. While one study has suggested that Aurora B phosphorylation of Dsn1 contributes to the destabilisation of erroneous kinetochore-microtubule attachments (Welburn *et al*., 2010), others have found that Dsn1 phosphorylation promotes kinetochore assembly in both yeast and human cells (Emanuele *et al*., 2008; Yang *et al*., 2008; Akiyoshi *et al*., 2013). KNL1/Spc105 has an N-terminal microtubule binding domain and through a conserved motif also recruits protein phosphatase 1 (PP1; Glc7 in yeast), the counteracting phosphatase of Aurora B, to the kinetochore. Aurora B phosphorylation at these sites has been suggested to lower the affinity of KNL1/Spc105 for microtubules (Welburn *et al*., 2010) and also disrupt the KNL1/Spc105-dependent recruitment of PP1/Glc7 to kinetochores (Liu *et al*., 2010; Rosenberg *et al*., 2011). Taken together, it

seems that dynamic regulation of Ipl1/Aurora B dependent phosphorylation and PP1/Glc7-dependent dephosphorylation of numerous substrates at the kinetochore/centromere is required for bi-orientation.

How is this dynamic regulation achieved and how does the CPC discriminate between bi-oriented and mono-oriented kinetochore-microtubule attachments? The fine details of the mechanism are still under investigation. However, it is clear that tension plays a role. Classic experiments performed in the late 1960's involving the micromanipulation of chromosomes in meiotic mantid spermatocytes revealed that kinetochore-microtubule attachments are stabilised when tension is applied (Nicklas & Koch, 1969). When sister chromatids are bi-oriented the pulling force generated by microtubules is opposed by the cohesin complex holding the sisters together. This results in the generation of tension that stretches both centromeres and kinetochores (Fig. 1.5 a). When sister chromatids are mono-oriented with either one or both sisters attached to a single spindle pole (monotelic and syntelic attachment respectively) no tension is generated (Fig. 1.5 b, c; Tanaka *et al*., 2005). It is this lack of tension that stimulates Ipl1/Aurora B activity towards its substrates at the kinetochore to disrupt improper kinetochore-microtubule interactions (Biggins & Murray, 2001; Tanaka *et al*., 2002a). The current models for how this tension-dependent mechanism operates are based on the proximity of Ipl1/Aurora B to its substrates. When sisters are syntelically attached there is no tension between sister chromatids such that the CPC, which is located at the inner centromere, is in close proximity to the kinetochore and so Ipl1/Aurora B can phosphorylate its substrates to induce microtubule turnover. When sisters are bi-oriented, the tension generated stretches the centromere and kinetochore, physically separating the CPC from its substrates and allowing the kinetochore-microtubule attachment to be stabilised (Liu *et al*., 2009; Welburn *et al*., 2010).

Consistent with this model, Ipl1 phosphorylation of Dam1 has been shown to be tension-dependent (Keating *et al*., 2009). Furthermore, experiments in human cells using targeted fluorescence resonance energy transfer (FRET) biosensors showed that an Aurora B substrate at the centromere was phosphorylated in both the presence and absence of tension, whereas a substrate at the kinetochore was only phosphorylated when in close proximity to the centromere in the absence of tension (Liu *et al*., 2009). In fission yeast and metazoan cells, where individual centromeres can accommodate multiple kinetochore-microtubule attachments, merotelic attachment can exist where a single centromere is attached to both spindle poles. While syntelic attachments generate no tension and amphitelic attachments generate maximum tension, merotelic attachments are intermediate between the two (Tanaka *et al*., 2005). Reduction of Aurora B activity or preventing phosphorylation of Hec1/Ndc80 increased the frequency of these attachments (Cimini *et al*., 2006; DeLuca *et al*., 2006) indicating that the CPC is required for their correction. So how does the correction of merotelic attachments fit into the tension model? It has been suggested that a gradient of Aurora B phosphorylation at the centromere can allow tension-dependent fine tuning of kinetochore-microtubule interactions through differential regulation of spatially distinct substrates within the kinetochore (Welburn *et al*., 2010).

1.6.5 *Spindle assembly checkpoint signalling*

Besides linking chromosomes to the mitotic spindle, kinetochores also host the spindle assembly checkpoint (SAC). The SAC, through its effector the mitotic checkpoint complex (MCC), prevents the activation of the APC/C, and consequently the onset of anaphase, until all chromosomes are properly bi-oriented (reviewed in Musacchio & Salmon, 2007; Lara-Gonzalez *et al*., 2012). The SAC was first discovered in budding yeast during genetic screens to identify mutants that were unable to halt cell

cycle progression in the presence of the microtubule destabilising drug benomyl (Hoyt *et al*., 1991; Li & Murray, 1991). These screens identified the majority of the key components including the *MAD* (mitotic arrest-deficient) genes *MAD1*, *MAD2* and *MAD3* (known as *BUBR1* in humans) and the *BUB* (budding uninhibited by benzimidazole) genes *BUB1* and *BUB3*. Later, other components were identified such as Mps1 (Weiss & Winey, 1996) and the SAC has since been found to be a conserved mechanism in eukaryotic cells. The MCC consists of Mad2, Mad3/BubR1 and Bub3 together with the APC/C activator Cdc20 (Hardwick *et al*., 2000; Fraschini *et al*., 2001; Sudakin *et al*., 2001). Both Mad2 and Mad3/BubR1 bind to Cdc20 directly and in doing so prevent the Cdc20-dependent activation of the APC/C and the onset of anaphase. A common method used in budding yeast to arrest cells in metaphase is through the depletion of Cdc20. This is often achieved by placing *CDC20* under the control of the methionine-repressible *MET3* promoter (Uhlmann *et al*., 2000). In addition to the MCC, other SAC components include Mad1 and the kinases Bub1, Mps1 and Ipl1/Aurora B. Mad1 serves as the kinetochore receptor for Mad2 and the kinases Bub1, Mps1 and Ipl1/Aurora B are important for recruiting SAC proteins to the kinetochore (Musacchio & Salmon, 2007; Lara-Gonzalez *et al*., 2012). Many other proteins have also been implicated in SAC function (Lara-Gonzalez *et al*., 2012). How all these components cooperate to regulate SAC signalling is complex and not fully understood and will not be discussed at length here.

It is believed that the SAC can respond to the presence of unattached kinetochores and to a lack of tension between sister chromatid pairs, although exactly how these signals integrate into an overall model for SAC activation is debated (tension vs. attachment; reviewed in Pinsky & Biggins, 2005; Maresca & Salmon, 2010). Studying the differential effects of tension and attachment on spindle checkpoint

activation is simplified in budding yeast due to the nature of their point centromeres. Each centromere binds a single kinetochore, which therefore exists in one of two states: attached or unattached. Higher eukaryotes have regional centromeres that assemble kinetochores that bind multiple microtubules and that can therefore exist in a third state of partial occupancy. Unlike point centromeres, regional centromeres bind multiple kinetochores and can therefore host merotelic attachments that result in varying levels of tension. Furthermore, the SAC is not essential in budding yeast during an unperturbed cell cycle, unlike in metazoans, which makes mutations or gene deletions that disrupt kinetochore-microtubule function or error correction relatively straightforward to study. In this model system there are also a number of ways to experimentally reduce tension without affecting attachment. For example, placing *SCC1* (which encodes a cohesin subunit) under the control of a glucose-repressible *GAL1* promoter allows depletion of Scc1, the loss of sister chromatid cohesion and therefore kinetochore-microtubule attachments that are not under tension (Indjeian *et al*., 2005; King *et al*., 2007a). Consequently, much of our understanding of the SAC is derived from studies using this model system.

A role for the CPC in the SAC was first implied in budding yeast where it was shown that Ipl1 was required when kinetochore-microtubule attachments were present but not under tension (Biggins & Murray, 2001). There are two models with regard to the involvement of the CPC in SAC signalling. The first model suggests that the SAC responds solely to unattached kinetochores and that the CPC functions indirectly in its activation by destabilising tensionless attachments, thereby generating unattached kinetochores (Tanaka *et al*., 2002a; Pinsky *et al*., 2006; Maresca & Salmon, 2010). The second more contested model suggests that, in addition to creating unattached kinetochores, the CPC has a direct role in SAC signalling that is independent of

generating unattached kinetochores, possibly through amplification of the checkpoint signal (Biggins & Murray, 2001; Hauf *et al*., 2003; King *et al*., 2007a; Vader *et al*., 2007; Maresca & Salmon, 2010; Santaguida *et al*., 2011).

The requirement of the CPC for generating a tension-dependent checkpoint response by destabilising incorrect kinetochore-microtubule attachments appears to be ubiquitous. Depletion or inhibition of Aurora B in human cells causes chromosome alignment defects that lead to improper chromosome segregation without activating the SAC (Ditchfield *et al*., 2003; Hauf *et al*., 2003; Lampson *et al*., 2004). Ipl1/Aurora B activity is required for the recruitment of checkpoint proteins to the kinetochore, but which proteins show CPC-dependent recruitment appears to vary by organism (reviewed in Musacchio & Salmon, 2007). These variations in the CPC-dependent recruitment of spindle checkpoint proteins to the kinetochore suggest that checkpoint signalling varies in different organisms. In support of this hypothesis, the requirement of the CPC for SAC signalling also appears to vary between organisms. In human cells and budding yeast, while the CPC is required for the tension checkpoint, it appears to be dispensable for checkpoint signalling in response to microtubule depolymerising drugs such as nocodazole (Biggins & Murray, 2001; Ditchfield *et al*., 2003; Hauf *et al*., 2003). This suggests that the CPC is not necessary to signal to the checkpoint when unattached kinetochores are present. However, in *Xenopus* and fission yeast, the CPC appears to be required for checkpoint signalling in response to both a lack of attachment and a lack of tension (Kallio *et al*., 2002; Petersen & Hagan, 2003). These findings, amongst many others, feed in to the hypothesis that the CPC has a role in checkpoint signalling that is independent of kinetochore-microtubule error correction (King *et al*., 2007a; Vader *et al*., 2007; Maresca & Salmon, 2010; Santaguida *et al*., 2011). However, the nature of this role remains elusive. In budding yeast, mutation of several consensus Ipl1

phosphorylation sites in Mad3 renders cells unable to mount a checkpoint response when there is a lack of tension between sister chromatids generated by Scc1 depletion (King *et al*., 2007a). However, the checkpoint is activated in response to unattached kinetochores generated by nocodazole treatment (King *et al*., 2007a). In human cells, BubR1 requires Aurora B for kinetochore localisation and is also phosphorylated by Aurora B (Ditchfield *et al*., 2003; Zachos *et al*., 2007). Whether this is important in human cells is unclear but it may contribute to sustaining the association between BubR1 with APC/C to maintain checkpoint signalling (Morrow *et al*., 2005). Trying to determine the contributions of tension and attachment in checkpoint signalling is made difficult by their intimate nature. Additionally, perturbation of Aurora B has pleiotropic effects, including defects in kinetochore assembly, which can have a detrimental effect on recruitment of checkpoint proteins to the kinetochore (Musacchio & Salmon, 2007). The severity of these defects could vary between different cell types or depend on the particular methodology employed to study CPC activity and spindle checkpoint signalling. Consequently, the debate still continues as to whether the CPC has a direct role in SAC signalling.

Once sister chromatids are properly bi-oriented, SAC signalling must cease to allow the activation of the APC/C. Spindle checkpoint silencing is achieved in a number of ways. Mad1 and other checkpoint proteins are removed from attached kinetochores. In metazoans, this process depends on the minus end-directed motor activity of dynein on microtubules (Howell *et al*., 2001). Checkpoint proteins are physically stripped from kinetochores and transported to the spindle poles (Howell *et al*., 2001). There is no nuclear dynein homologue in budding yeast and whether other minus end-directed motors perform a similar function in this organism is unknown. The activity of phosphatases to counteract the activity of mitotic kinases is also important for

checkpoint silencing since Mps1, Bub1 and Ipl1/Aurora B recruit checkpoint components to the kinetochore (reviewed in Lesage *et al*., 2011). As mentioned previously, tension and attachment appear to contribute to this process. The re-localisation of the CPC to the spindle in anaphase has also been shown to prevent checkpoint re-engagement as tension is lost when cohesin is cleaved (Mirchenko & Uhlmann, 2010; Vázquez-Novelle *et al*., 2010). Additionally, several mechanisms contribute to MCC disassembly (reviewed in Lesage *et al*., 2011). Once the SAC is silenced, the APC/C is activated and targets mitotic cyclins and securin for degradation allowing the separation of sister chromatids, elongation of the spindle and progression into anaphase.

1.6.6 *Formation of a stable spindle midzone*

The spindle midzone is formed from the bundled plus-ends of antiparallel microtubules and is the site of CPC localisation and function as cells progress through anaphase. The formation of this structure in human cells requires the microtubule bundling protein Prc1 (Mollinari *et al*., 2002), the kinesin Kif4 (Kurasawa *et al*., 2004) and centralspindlin, which is a complex that is formed by Mklp1 and the Rho family GTPase-activating protein (GAP) MgcRacGAP (Mishima *et al*., 2002). Aurora B has been shown to phosphorylate Mklp1, which promotes the clustering of centralspindlin, increases its microtubule-bundling activity and consequently stabilises the spindle midzone (Douglas *et al*., 2010). In budding yeast the formation of bipolar spindles and the bundling and stabilisation of interpolar microtubules is driven by the kinesins Cin8 and Kip1, and the Prc1 homologue Ase1 (de Gramont *et al*., 2007). Ipl1 phosphorylation of Ase1 is believed to be important for this process since an *ase1* mutant lacking Ipl1 consensus phosphorylation sites cannot assemble spindles in the absence of Cin8 (Kotwaliwale *et al*., 2007). Ipl1 mutants are also defective in spindle

disassembly (Buvelot *et al*., 2003; Woodruff *et al*., 2010). Recently, Ipl1 activity has also been reported to be required for maintaining the association of duplicated SPBs and preventing their over-duplication during meiosis (Shirk *et al*., 2011). Exactly how Ipl1 contributes to spindle function is unclear. In higher eukaryotes, Aurora A localises to centrosomes and has similar roles in bipolar spindle assembly and function that are distinct from those of Aurora B (Barr & Gergely, 2007; Carmena *et al*., 2009). The most well defined roles of Ipl1, the sole Aurora kinase in budding yeast, correspond to those of Aurora B. However, it would appear that Ipl1 can perform functions attributed to both Aurora A and Aurora B.

1.6.7 *Contractile ring formation and function*

The process of cytokinesis requires the assembly and constriction of an actin-myosin contractile ring at the site of cell division. Both the positioning and constriction of the ring are coordinated with chromosome segregation to ensure that the genome is accurately divided and two daughter cells are formed. The CPC has been shown to have an important role in the regulation of these processes (reviewed in Ruchaud *et al*., 2007, Waal *et al*., 2012).

In mammalian cells the CPC promotes cleavage furrow ingression at the equatorial cortex (reviewed in Waal *et al*., 2012). Exactly how the CPC is involved in this process is not fully understood, although it seems likely that it is mediated through CPC-dependent regulation of the centralspindlin complex. The CPC recruits centralspindlin to the spindle midzone, which in turn recruits the RhoA GEF Ect2 (Nishimura & Yonemura, 2006; Douglas *et al*., 2010). Aurora B phosphorylation of the centralspindlin component MgcRacGAP induces its Rho GAP activity (Minoshima *et al*., 2003). Properly regulated RhoA activity is required for proper assembly and

constriction of the actin-myosin ring (Piekny *et al*., 2005). In addition to this indirect regulation of RhoA, the CPC is thought to have a wider role in the regulation of the cytoskeleton during cytokinesis. It is widely believed that the interaction between actin filaments and myosin II provide the force required for constricting the actin-myosin ring thereby driving cleavage furrow ingression. Aurora B activity has been reported to modulate the binding of myosin II to the cytoskeleton (Ozlü *et al*., 2010). This may be via phosphorylation of myosin regulatory light chain II (Murata-Hori *et al*., 2000). However, this has not been confirmed in human cells (Ozlü *et al*., 2010). The CPC may also contribute to actin polymerisation at the cleavage furrow since it has been shown that Aurora B binds and phosphorylates the formin FHOD1, which interacts with Rac1 GTPase to regulate actin polymerisation (Ozlü *et al*., 2010).

Septins are also important for cytokinesis. Septins are GTP-binding cytoskeletal proteins and have a lipid-binding motif that allows them to bind to membranes (Casamayor & Snyder, 2003). They were first discovered in budding yeast during a screen to identify cell division cycle mutants (Hartwell, 1971) and have since been found to be highly conserved and required for cytokinesis in many organisms including humans (Kinoshita *et al*., 1997; Pan *et al*., 2007; DeMay *et al*., 2011). In *S. cerevisiae* septins form ordered rings at the bud neck where they act as a scaffold for the recruitment of other proteins required for actin-myosin ring function and membrane abscission, and also form a barrier that prevents the diffusion of cortical proteins between mother and daughter cells to maintain cell polarity (Gladfelter *et al*., 2001; Dobbelaere & Barral, 2004; Bertin & Nogales, 2012). In budding yeast, it has been suggested that a CPC sub-complex consisting of Sli15 and Bir1 regulates septin dynamics in late mitosis (Gillis *et al*., 2005; Thomas & Kaplan, 2007). Similarly, an interaction between the CPC and septins in *C. elegans* appears to be essential for

cytokinesis (Lewellyn *et al*., 2011) and human Aurora B has been shown to phosphorylate septin 1 (Qi *et al*., 2005). It remains to be demonstrated exactly how the CPC regulates cytokinesis.

1.6.8 *Regulation of abscission*

Abscission is required to complete cytokinesis and involves the fusion of cell membranes to physically separate the two cells. This process is monitored by the NoCut pathway, which delays abscission if chromatin is present in the cytoplasmic bridge between the two cells and thereby preventing chromosome damage. This pathway was first discovered in budding yeast (Norden *et al*., 2006; Mendoza *et al*., 2009) and has since been found to be conserved in human cells (also known as the abscission checkpoint; Steigemann *et al*., 2009). This mechanism is poorly understood but several studies have demonstrated that Ipl1/Aurora B is involved in its activation. In budding yeast, Ipl1 localisation and activity at the spindle midzone is required to activate the NoCut pathway by targeting Boi1 and Boi2, two anillin-like proteins implicated in polar growth and bud emergence, to the bud neck (Norden *et al*., 2006; Mendoza *et al*., 2009). Ahc1, a component of the ADA histone acetyltransferase complex, appears to act upstream of Ipl1 in NoCut activation and artificial targeting of Ipl1 to chromatin in anaphase is sufficient to trigger a NoCut response (Mendoza *et al*., 2009). These observations have led to the development of a model for the NoCut pathway. The current model states that Ipl1 at the spindle midzone becomes active through the interaction of chromatin-associated factors, which require Ahc1 and acetylated chromatin, and triggers the NoCut pathway. In the absence of chromatin in the cytoplasmic bridge, Ipl1 is inactive and NoCut signalling ceases (Mendoza *et al*., 2009). Aurora B localisation and activity at the spindle midzone is also required for the activation of the abscission pathway in human cells (Steigemann *et al*., 2009). Recent

studies have identified that Borealin binds to CHMP4C, a subunit of the ESCRT-III (endosomal sorting complex required for transport) complex (Capalbo *et al*., 2012; Carlton *et al*., 2012). ESCRT-III mediates membrane fission at the end of cytokinesis (Elia *et al*., 2011; Guizetti *et al*., 2011) and it has been suggested that Borealin binding may mediate phosphorylation of CHMP4C by Aurora B, inhibiting its involvement in this process and thereby delaying cytokinesis (reviewed in Carmena, 2012).

1.6.9 Activation and regulation of Ipl1/Aurora B

The activity of Ipl1/Aurora B is regulated in a number of ways through its protein interactions, post-translational modifications, localisation and degradation. The activation of its kinase activity is a complex process that is achieved in numerous steps. Ipl1/Aurora B first binds to a conserved region at the C-terminus of Sli15/INCENP known as the IN box (Kang *et al*., 2001; Honda *et al*., 2003), which stimulates a low level of kinase activity. This enables Ipl1/Aurora B to phosphorylate a conserved TSS (Thr-Ser-Ser) motif in the C-terminus of Sli15/INCENP (Bishop & Schumacher, 2002; Honda *et al*., 2003) and also auto-phosphorylate the threonine in the T-loop of its kinase domain (Thr-260 in budding yeast, Thr-232 in human cells; Yasui *et al*., 2004; Sessa *et al*., 2005), which results in the full activation of the Ipl1/Aurora B. Crystal structures of Aurora B with an INCENP fragment suggest that INCENP allosterically induces the extension of the activation loop to facilitate its modification and phosphorylation of the TSS motif mediates the opening of the catalytic cleft, both of which are required for full Aurora B activation (Sessa *et al*., 2005). These phosphorylation events are thought to occur in trans, suggesting that Aurora B activation is local concentration dependent (Sessa *et al*., 2005). This goes towards explaining why kinase activation is coupled with its enrichment at the centromere and spindle midzone. Aurora B can also be activated by microtubules (Rosasco-Nitcher *et al*., 2008; Tseng *et al*., 2010) and this requires TD-

60 (Rosasco-Nitcher *et al*., 2008), another chromosomal passenger protein. Since TD-60 is required for CPC localisation (Mollinari *et al*., 2003), it is possible that it stimulates Aurora B activation by increasing its local concentration.

Other kinases can also influence Aurora B activity. The checkpoint kinase Chk1 is required to delay entry into mitosis when cells have unreplicated or damaged DNA (Takai *et al*., 2000). However, it has also been implicated in proper spindle checkpoint function since Chk1-deficient cells have an increased resistance to the microtubule stabilising drug taxol, chromosome segregation defects and fail to recruit BubR1 to kinetochores (Zachos *et al*., 2007). In budding yeast, Chk1 has been shown to phosphorylate and stabilise the yeast securin Pds1 to prevent progression into anaphase (Wang *et al*., 2001). It has recently been demonstrated that Chk1 is localised to kinetochores and that full activation of human Aurora B requires phosphorylation of Ser-311 by Chk1 (Zachos *et al*., 2007; Petsalaki *et al*., 2011). Although Chk1 is conserved, it is unclear if this mechanism is conserved in budding yeast as Ipl1 does not contain a phosphorylatable amino acid at or around the equivalent position to Ser-311 in Aurora B.

Other post-translational modifications of Aurora B have also been reported to regulate its localisation and activity. Ubiquitination of Aurora B has been shown to promote the removal of the CPC from chromatin and its recruitment to the spindle in anaphase (Sumara *et al*., 2007; Maerki *et al*., 2009). Sumoylation of Aurora B is also required for proper mitotic progression since an Aurora B mutant that cannot be sumoylated at a single site in its kinase domain exhibits abnormal CPC localisation, chromosome segregation defects and fails to complete cytokinesis (Fernández-Miranda *et al*., 2010).

Modification of other CPC subunits has also been reported to contribute to its localisation and Aurora B activity. Ubiquitination of Survivin is required for its association with centromeres in metaphase and its deubiquitination is necessary for its targeting to the spindle in anaphase (Vong *et al*., 2005). The phosphorylation of Borealin by Mps1 appears to be required for optimal Aurora B activity at centromeres *in vivo* but is not required for CPC localisation (Jelluma *et al*., 2008). Phosphorylation of INCENP, Survivin and Borealin by CDK has been shown to modulate CPC localisation and function (Pereira & Schiebel, 2003; Hümmer & Mayer, 2009; Tsukahara *et al*., 2010), although these appear to vary between organisms. Prior to this current study, whether CDK phosphorylation of Ipl1 regulates its activity or localisation was unknown. Aurora B activity is ultimately terminated during mitotic exit when the CPC is targeted by the APC/C and degraded by the proteasome (Nguyen *et al*., 2005; Stewart & Fang, 2005).

For proper cell cycle progression it is essential that the phosphorylation of Ipl1/Aurora B substrates is regulated. This requires the antagonistic action of phosphatases to appropriately dephosphorylate these substrates. This regulatory relationship is complex and continues to be a highly active area of research. It is best understood in early mitosis during the process of kinetochore-microtubule error correction and bi-orientation. As mentioned previously, Glc7/PP1 is the major counteracting phosphatase for Ipl1/Aurora B and is recruited to the outer kinetochore during mitosis by Spc105/KNL1 (Hsu *et al*., 2000; Pinsky *et al*., 2006b; Rosenberg *et al*., 2011). A number of other proteins have also been suggested to facilitate recruitment of PP1 to kinetochores. These proteins include the PP1 regulatory subunit Sds22 (Posch *et al*., 2010) and the kinesin-7 CENP-E (Kim *et al*., 2010) in humans, the kinesin-8 Klp5/Klp6 in fission yeast (Meadows *et al*., 2011) and the Glc7 regulatory subunit Fin1

in budding yeast (Akiyoshi *et al*., 2009). The phosphatase PP2A has also been reported to oppose Aurora B activity (Sugiyama *et al*., 2002; Foley *et al*., 2011). In human cells, PP2A along with its B56 regulatory subunit, dephosphorylates Aurora B substrates to stabilise kinetochore-microtubule attachments (Foley *et al*., 2011). PP2A is enriched at centromeres without microtubule attachment and dissociates upon establishment of a proper bi-oriented attachment (Foley *et al*., 2011). Whether PP2A is required in budding yeast for the same function is unclear. However, it has been shown that Ipl1/Aurora B is required to maintain the centromeric localisation of PP2A at centromeres in meiosis to protect centromeric cohesin (Yu & Koshland, 2007; Tanno *et al*., 2010), suggesting that PP2A has conserved functions at the centromere. As discussed previously, it is believed that the tension-dependent stretching and relaxation of the centromere and kinetochore regulates whether an Ipl1/Aurora B substrate is in proximity of the kinase or phosphatase (Liu *et al*., 2009; Welburn *et al*., 2010). However, there are a number of other factors that can also influence Ipl1/Aurora B activity towards its substrates. For example, the acetylation and phosphorylation of histone H3 (Li *et al*., 2006; Rosasco-Nitcher *et al*., 2008) and methylation of Dam1 (Zhang *et al*., 2005) alters their affinity as substrates for Ipl1/Aurora B. It is possible that similar mechanisms may regulate Ipl1/Aurora B phosphorylation of other substrates.

1.6.10 Localisation of the CPC in early mitosis

While the distinct localisation pattern was the original defining characteristic of the CPC, how its localisation was regulated remained unclear until relatively recently. A number of studies have identified two histone modifications that are important for the recruitment of the CPC to the centromere: phosphorylation of histone H2A and histone H3 (Kawashima *et al*., 2010; Kelly *et al*., 2010; Yamagishi *et al*., 2010; Wang *et al*., 2010).

Studies have shown that Sgo2 (Shugoshin 2) regulates CPC localisation in fission yeast mitosis, likely through interaction with Bir1/Survivin (Vanoosthuyse *et al*., 2007; Kawashima *et al*., 2007) and that the conserved SAC protein kinase Bub1 is required for the centromeric localisation of Shugoshin (Kitajima *et al*., 2004; Fernius & Hardwick, 2007). Shugoshins are conserved and important chromatin-associated proteins that have a number of roles in chromosome segregation during both mitosis and meiosis (reviewed in Gutiérrez-Caballero *et al*., 2012). While fission yeast Sgo2 is essential for CPC recruitment (Vanoosthuyse *et al*., 2007), Sgo1 is required for the protection of centromeric cohesion (Kitajima *et al*., 2004). This separation in function is not reflected in human cells as depletion of both Sgo1 and Sgo2 are required to disrupt the localisation of the CPC (Tsukahara *et al*., 2010). A later study by Kawashima *et al*. (2010) uncovered the link between Bub1 and Shugoshin by demonstrating that Bub1 phosphorylates the conserved Ser-121 residue of histone H2A in *S. pombe*, which provides a mark for the direct binding of Shugoshin. This also appears to be a conserved mechanism in budding yeast and mammalian cells (Kawashima *et al*., 2010). Bub1 siRNA treatment or injection of an antibody that recognises histone H2A phosphorylated at the equivalent Thr-120 position (H2A-T120ph) in human cells interferes with the centromeric localisation of Sgo1 (Kawashima *et al*., 2010). However, in human cells it appears that the Borealin subunit of the CPC interacts with Shugoshin as opposed to Bir1 in fission yeast (Tsukahara *et al*., 2010; Vader & Lens, 2010). Additionally, it also appears that Cdk1 phosphorylation of Borealin in human cells and Bir1 in fission yeast is required for their interaction with Shugoshin since mutation of these sites abolishes centromere localisation and function of the CPC (Tsukahara *et al*., 2010). Mutation of Ser-121 in *S. cerevisiae* histone H2A or deletion of *BUB1* abolishes Sgo1 localisation (Kawashima *et al*., 2010). However, in budding yeast, neither Bub1 nor the sole Shugoshin Sgo1 are required for CPC localisation or Ipl1 activity

(Storchová *et al*., 2011). Localisation of the CPC in budding yeast may be achieved by the direct binding of Bir1 with the Ndc10 component of the CBF3 complex (Yoon & Carbon, 1999; Bouck & Bloom, 2005; Gillis *et al*., 2005), which is the DNA sequence-specific scaffold of the kinetochore at the yeast centromere.

Phosphorylation of histone H3 on the conserved Thr-3 residue (H3-T3ph) has also been shown to contribute to the centromeric localisation of the CPC in fission yeast, *Xenopus* and human cells (Kelly *et al*., 2010; Yamagishi *et al*., 2010; Wang *et al*., 2010). This modification is performed by the evolutionarily conserved Haspin kinase (Higgins, 2003; discussed in more detail later) and appears to provide a mark for the direct binding of Survivin via its conserved BIR domain (Kelly *et al*., 2010; Yamagishi *et al*., 2010; Wang *et al*., 2010). Whether Haspin kinases in budding yeast phosphorylate histone H3 on Thr-3 or contribute to CPC localisation is unknown.

Phosphorylation of the kinetochore protein Spc105/KNL1 by Mps1 recruits Bub1 to kinetochores (London *et al*., 2012; Yamagishi *et al*., 2012) and consequently phosphorylated histone H2A-S121 is most abundant at the centromere (Kawashima *et al*., 2010). Haspin and histone H3-T3ph are found along the length of chromosomes and become particularly concentrated at the centromere as cells progress into metaphase (Dai *et al*. 2005; Yamagishi *et al*. 2010). In fission yeast, the activity of Hrk1 (Haspin-related kinase 1) requires the cohesin regulator Pds5 and the HP1 homologue Swi6 (Yamagishi *et al*., 2010). The CPC is most highly enriched in the region where these two histone modifications overlap (Fig. 1.6; Yamagishi *et al*., 2010). Perturbation of either of these pathways by Haspin or Bub1 RNAi in human cells disrupts Aurora B localisation (Wang *et al*., 2010; Yamagishi *et al*., 2010). Similarly, deletion of components from these pathways or mutation of histone H3-T3 or histone H2A-S121 in

fission yeast has the same effect and results in chromosome bi-orientation and segregation defects (Yamagishi *et al*., 2010). Disruption of both pathways simultaneously significantly increases the severity of these phenotypes and results in a strong growth defect (Yamagishi *et al*., 2010).

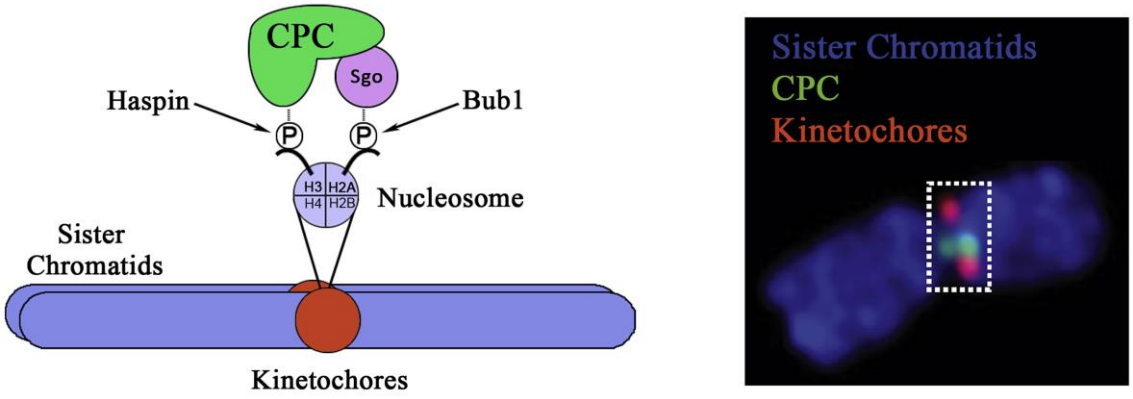

Fig. 1.6. Chromosomal passenger complex recruitment to the centromere in early mitosis. Phosphorylation of histone H2A by Bub1 and histone H3 by Haspin has been reported to recruit the CPC to centromeres in fission yeast and human cells. This figure is adapted from Vader & Lens (2010).

Together, these studies show that Haspin, Bub1 and Shugoshin are required for the enrichment of the CPC at the centromere in fission yeast and higher eukaryotes. However, the localisation of Bub1 and Shugoshin and the accumulation of H3-T3ph at the centromere require Aurora B activity (Hauf *et al*., 2003; Dai *et al*., 2006; Wang *et al*., 2011), suggesting the existence of a positive feedback loop that is required for the association of the CPC with the centromere. In support of this hypothesis, Wang *et al*. (2011) have demonstrated that Haspin is phosphorylated by Aurora B and that preventing this modification by mutating these sites or inhibiting Aurora B prevents full

Haspin activity in mitosis, reducing the level of centromeric CPC. Additionally, they were able to show that mutations in the Survivin BIR domain that disrupt the association with H3-T3ph results in the diffuse distribution of the CPC on chromatin and reduced H3-T3ph at the centromere. The Bub1-Shugoshin pathway also contributes to this feedback mechanism at least in part by localising the CPC to centromeres (Wang *et al*., 2011). It is also well established that Mps1 localisation to the kinetochore, and consequently Bub1, is Aurora B-dependent (Jelluma *et al*., 2010; Santaguida *et al*., 2010). Therefore, this intricate feedback loop ensures the rapid enrichment of the CPC to centromeres during mitosis.

1.6.11 Re-localisation of the CPC during anaphase

As cells progress into anaphase the CPC is transferred from the inner centromere to the spindle midzone and a decrease in Cyclin B-CDK activity is important for this translocation. In budding yeast the Cdc14-dependent dephosphorylation of a number of CDK phosphorylation sites in Sli15 facilitates this transition (Pereira & Schiebel, 2003). Mutation of these residues to prevent CDK phosphorylation results in the premature localisation of Sli15 to the spindle in metaphase (Ser-335 mediates much of this phenotype; Pereira & Schiebel, 2003). In human cells, CPC translocation to the spindle requires the dephosphorylation of a single CDK site in INCENP (Thr-59; Hümmer & Mayer, 2009), presumably by Cdc14 (Gruneberg *et al*., 2004), and a phospho-mimetic mutant of INCENP (T59E) fails to localise to the spindle midzone in anaphase (Hümmer & Mayer, 2009). In budding yeast the Sli15 CDK sites lie within the domain required for the direct binding of microtubules (Kang *et al*., 2001), which suggests that the dephosphorylation of these sites is necessary for this interaction and translocation to the spindle. In human cells, the dephosphorylation of Thr-59 promotes the interaction of INCENP with the kinesin-6 MKlp2, which binds to microtubules at the spindle midzone

(Hümmer & Mayer, 2009). Aurora B can also directly bind MKlp2 (Gruneberg *et al*., 2004). Budding yeast lack MKlp2 and it was unclear how the CPC was targeted to the spindle midzone in this organism prior to this current study.

CPC recruitment to centromeres in human cells is suppressed by the dephosphorylation of histone H3-T3 as cells enter anaphase (Kelly *et al*., 2010; Qian *et al*., 2011), which likely contributes to its translocation. Additionally, active removal of the CPC from mitotic chromosomes may also facilitate this process. Aurora B is ubiquitylated by two spindle midzone-associated Cullin3-based E3 ubiquitin ligase complexes (Sumara *et al*. 2007; Maerki *et al*. 2009). Ubiquitinated Aurora B is then removed from chromosomes by Cdc48 and its adaptor proteins (Ramadan *et al*., 2007; Dobrynin *et al*., 2011). Ubiquitination of Aurora B may also promote its retention at the midzone (Maerki *et al*., 2009).

Recently, in budding yeast, the phosphorylation of Sli15 by Ipl1 has also been shown to regulate binding to microtubules. Mutation of a number of serine and threonine residues that exist within Ipl1 consensus phosphorylation sites in Sli15 results in the premature localisation of Sli15 to the spindle in metaphase (Nakajima *et al*., 2011; Makrantoni *et al*., unpublished) and to the midzone in anaphase (Nakajima *et al*., 2011). Additionally, inhibition of Ipl1 activity with the use of an ATP analogue-sensitive *IPL1* allele (*ipl1-as6*) also resulted in the same premature spindle localisation. These observations suggest that Ipl1 phosphorylation of Sli15 is also important for regulating the localisation of the CPC. Whether Aurora B phosphorylation of INCENP is important for a similar mechanism is not known. Loss of Ipl1 activity results in the premature localisation of the CPC to the spindle (Nakajima *et al*., 2011). In contrast to this, Aurora B activity is required for CPC localisation to the spindle in chicken DT40

cells and rat NRK cells (Murata-Hori *et al*., 2002; Xu *et al*., 2009). This may suggest that this mechanism is not conserved.

1.7 Haspin kinases

1.7.1 *Discovery and overview*

Haspin (haploid germ cell-specific nuclear protein kinase; reviewed in Higgins, 2010) was first identified in mice and was believed to be a testis-specific gene (Tanaka *et al*., 1994; Tanaka *et al*., 1999). It was shown to localise to the nuclei of round spermatids and possess intrinsic serine/threonine kinase activity. Several years later the human Haspin gene was discovered and it was also shown to be highly abundant in the testis, although it was also found at lower levels in other somatic tissues that have high numbers of dividing cells and in all proliferating cell lines that were tested (Higgins, 2001). Since then, genes encoding Haspin homologues have been identified in every eukaryotic genome sequenced to date, which includes numerous vertebrates, arthropods, nematodes, amoebozoa, fungi and plants. Most species have a single Haspin homologue, although *S. cerevisiae* has two and *C. elegans* has at least three together with approximately sixteen Haspin-related genes (Higgins, 2003). A Haspin homologue can even be found in the microsporidium *Encephalitozoon cuniculi*, which contains less than 2000 potential protein-encoding genes and has a genome size of around 2.9 megabases that is smaller than many bacterial genomes (Katinka *et al*., 2001). This suggests that Haspins have an important and conserved role to play in the biology of eukaryotic organisms. All Haspin genes encode proteins containing a distinctive atypical kinase domain at their C-terminus that lack a number of the conserved motifs found in canonical protein kinases (Higgins, 2003). Despite this, yeast, plant, *Xenopus* and human Haspins have all been shown to be active kinases (Dai *et al*., 2005; Nespoli *et al*., 2006; Kelly *et al*., 2010; Yamagishi *et al*., 2010; Ashtiyani *et al*., 2011). The N-

termini of the Haspin proteins are much less conserved, having no clear homology with any known domains or other proteins.

Several years after its discovery, the localisation of human Haspin was more accurately defined. Dai *et al*. (2005) observed that Haspin was associated predominantly with condensed chromosomes throughout mitosis and was particularly concentrated at centromeric regions. They also found that Haspin co-purifies with histone H3 and phosphorylates it at Thr-3 (H3-T3ph). Haspin homologues in fission yeast and plants have also been shown to have similar patterns of localisation and phosphorylate histone H3 at the same position during mitosis (Yamagishi *et al*., 2010; Ashtiyani *et al*., 2011). To date, histone H3 remains the only known substrate of the Haspin kinases (other than themselves). Histone H3 is heavily and differentially modified throughout the cell cycle. These modifications include phosphorylation, methylation, acetylation and ubiquitinylation (reviewed in Oliver & Denu, 2010). In mitosis, histone H3 is phosphorylated at a number of sites in the densely modified N-terminal tail, including Thr-3, Thr-6, Ser-10, Thr-11 and Ser-28 (Dai *et al*., 2005). Histone H3 Ser-10 is phosphorylated by Ipl1/Aurora B and is the best characterised of these modifications (Hsu *et al*., 2000; Giet & Glover, 2001; Crosio *et al*., 2002). The role of H3-T3ph and Haspin was unclear. However, it was noticed that depletion of Haspin by RNAi resulted in aberrant metaphase chromosome alignment and that Haspin overexpression delayed progression through early mitosis (Dai *et al*., 2005). Recently, Haspin and histone H3-T3ph were shown to be required for the efficient recruitment of the CPC to centromeres in fission yeast, *Xenopus* and human cells as discussed above (Kelly *et al*., 2010; Yamagishi *et al*., 2010; Wang *et al*., 2010).

1.7.2 *Haspin-like kinases in budding yeast*

Two Haspin homologues have been identified in budding yeast: Alk1 and Alk2 (Haspin-like kinase; Higgins, 2001a). However, the function of these kinases is yet to be determined and it is not known whether they perform the same role as described in fission yeast and higher eukaryotes. To date, there has only been a single publication where Alk1 and Alk2 have been the subject of investigation (Nespoli *et al*., 2006).

Nespoli *et al*. (2006) became interested in the budding yeast Haspins when they identified *ALK1* as the top hit in a 2-hybrid screen using the DNA damage checkpoint protein Ddc1 as bait. This was curious since an annotation for *ALK1* in the GenBank database stated that it was a novel DNA-damage response gene although it is not clear how this was established. Nespoli *et al*. (2006) found that knockouts of either or both *ALK1* and *ALK2* were viable but they were not sensitive to the DNA damage induced by ultraviolet irradiation, hydroxyurea (HU) or methyl methanesulphonate (MMS). They did find that both Alk1 and Alk2 were hyperphosphorylated in response to DNA damage but it is still unclear if either have a role in the DNA-damage response.

By comparing the expression of HA tagged Alk1 and Alk2 with the progression of nuclear division, spindle length and the DNA content of synchronously cycling cells they were able to determine that both Alk1 and Alk2 levels fluctuate throughout the cell cycle. Both proteins were absent in cells arrested in G_1 with α-factor and Alk1 and Alk2 levels peaked in G_2/M and late S/early G_2 respectively before being degraded as cells exited mitosis. Both proteins contain KEN- and D-box sequences. These are recognised by activators of the APC/C, which subsequently targets these proteins for degradation (Glotzer *et al*., 1991; Pfleger & Kirschner, 2000). Nespoli *et al*. (2006) demonstrated that mutation of these sequences stabilised the levels of both proteins, although Alk1

was stabilised to a lesser extent. This suggests that both proteins are degraded in an APC/C-dependent manner.

Although Alk1 and Alk2 are Haspin homologues, they are somewhat divergent and lack a number of conserved motifs that are normally associated with kinase activity (Higgins, 2001a), suggesting that they may not be active kinases. However, Nespoli *et al*., (2006) demonstrated that both are in fact active kinases as Alk1 and Alk2 immunoprecipitated from yeast or bacteria were able to auto-phosphorylate when subjected to *in vitro* kinase assays. Furthermore, they were able to demonstrate that mutagenesis of one of the conserved kinase motifs significantly reduced this activity. While attempting to purify the Haspin-like kinases from yeast they found that overexpression of Alk2, but not Alk1, from multi-copy plasmids resulted in the accumulation of cells with replicated DNA and short bipolar spindles, suggestive of an early mitotic block. This block was found to be dependent on the kinase activity of Alk2 since the overexpression of the kinase deficient mutant attenuated this delay (Nespoli *et al*., 2006). Interestingly, overexpression of Haspin in human cells also resulted in a delay during mitosis (Dai *et al*., 2005). Although Haspin was known to phosphorylate histone H3 at Thr-3 (Dai *et al*., 2005), Nespoli *et al*. (2006) were unable to identify histone H3 as an *in vitro* substrate of either Alk1 and Alk2 although this experiment was not presented in their publication.

Collectively, these observations suggest that Alk1 and Alk2 are active kinases and that they most likely have roles in mitosis. Whether they also phosphorylate histone H3 and contribute to CPC localisation at centromeres like their counterparts in other species is not known.

1.8 Aims of the thesis

The CPC is an essential and conserved protein complex with numerous roles during mitosis. Although the CPC has been studied extensively there are still many aspects of its function and regulation that are still not fully understood. In this study, several lines of investigation were followed using the yeast *Saccharomyces cerevisiae* in the hope of further developing our understanding of how this complex is regulated.

The initial aim of this work was to investigate whether the regulated phosphorylation of consensus CDK motifs in the budding yeast Aurora B homologue Ipl1 was necessary for its proper function as a regulator of the cell division cycle. However, following the recent discovery that Haspin kinase contributes to the localisation and function of the CPC in fission yeast and human cells, a second major goal was to establish whether the largely uncharacterised budding yeast Haspin-like kinases Alk1 and Alk2 played a similar role. This led to the unexpected discovery that rather than being important as regulators of Ipl1 function, the budding yeast Haspin-like kinases are required to ensure proper spindle orientation and regulate bud growth during mitosis.

CHAPTER 2

Material and Methods

2.1 Strains, media and growth conditions

2.1.1 *Strains*

All yeast (*S. cerevisiae*, *S. pombe*) and bacteria (*E. coli*) strains used in this study are listed in Tables 2.1 and 2.2 respectively. All strains were saved as 20% glycerol stocks that were snap frozen and stored at -80°C.

Table 2.1. Yeast strains used in this study ¶

Figure	Strain	Genotype	Source
3.2 A	K699	*MAT***a** *ade2-1 his3-11,15 leu2-3,112 trp1-1 ura3-1 can1-100 ssd1-d2*	K. Nasmyth
	NRY38a	*MAT***a** *ipl1-321::HIS3MX6*	Lab collection
	SJC175	*MAT***a** *sgo1Δ::HIS3MX6*	This study
	YABD302	*MAT***a** *mad2Δ::HIS3MX6*	Lab collection
	SJC13	*MAT***a** *ipl1(S15A)::HIS3MX6*	This study
	SJC15	*MAT***a** *ipl1(S50A)::HIS3MX6*	This study
	SJC17	*MAT***a** *ipl1(S76A)::HIS3MX6*	This study
	SJC30	*MAT***a** *ipl1(S15A,S50A)::HIS3MX6*	This study
	SJC32	*MAT***a** *ipl1(S15A,S76A)::HISMX6*	This study
	SJC34	*MAT***a** *ipl1(S50A,S76A)::HIS3MX6*	This study
	SJC42	*MAT***a** *ipl1(S15A,S50A,S76A)::HIS3MX6*	This study
	SJC114	*MAT***a** *ipl1(S38A,S50A,S76A)::HIS3MX6*	This study
	SJC115	*MAT***a** *ipl1(S15A,S38A,S50A,S76A)::HIS3MX6*	This study
	SJC202	*MAT***a** *ipl1(S269A)::HIS3MX6*	This study
	SJC19	*MAT***a** *ipl1(S15E)::HIS3MX6*	This study
	SJC21	*MAT***a** *ipl1(S50E)::HIS3MX6*	This study
	SJC23	*MAT***a** *ipl1(S76E)::HIS3MX6*	This study
	SJC36	*MAT***a** *ipl1(S15E,S50E)::HIS3MX6*	This study
	SJC38	*MAT***a** *ipl1(S15E,S76E)::HIS3MX6*	This study
	SJC40	*MAT***a** *ipl1(S50E,S76E)::HIS3MX6*	This study
	SJC44	*MAT***a** *ipl1(S15E,S50E,S76E)::HIS3MX6*	This study
	SJC213	*MAT***a** *ipl1(S38E,S50E,S76E)::HIS3MX6*	This study
	SJC214	*MAT***a** *ipl1(S15E,S38E,S50E,S76E)::HIS3MX6*	This study
3.2 B	SJC206	*MAT***a***/MATα IPL1/ipl1(S269E)::HIS3MX6*	This study
	SJC207	*MAT***a***/MATα IPL1/ipl1(S269E)::HIS3MX6*	This study
	SJC208	*MAT***a***/MATα IPL1/ipl1(S269E)::HIS3MX6*	This study
	SJC209	*MAT***a***/MATα IPL1/ipl1(S269E)::HIS3MX6*	This study
3.3 B	SJC79	*MATα TRP1 CFIII(CEN3.L.YPH278) URA3 SUP11*	This study
	SJC133	*MATα ipl1(4SA)::HIS3MX6 TRP1 CFIII(CEN3.L.YPH278) URA3 SUP11*	This study
	SJC449	*MATα ipl1(4SE)::HIS3MX6 TRP1 CFIII(CEN3.L.YPH278) URA3 SUP11*	This study
	SJC447	*MATα ipl1(S269A)::HIS3MX6 TRP1 CFIII(CEN3.L.YPH278) URA3 SUP11*	This study

(Table continues)

Table 2.1. continued…

Figure	Strain	Genotype	Source
	VMY113	*MATα bir1-17::NATMX4 TRP1 CFIII(CEN3.L.YPH278) URA3 SUP11*	Lab collection
3.3 D	SJC90	*MAT***a** *CEN3-tetO$_{336}$::URA3 tetR-GFP::LEU2 YFP-TUB1::TRP1* p*MET-CDC20::TRP1*	This study
	SJC132	*MAT***a** *ipl1(4SA)::HIS3MX6 CEN3-tetO$_{336}$::URA3 tetR-GFP::LEU2 YFP-TUB1::TRP1* p*MET-CDC20::TRP1*	This study
	SJC318	*MAT***a** *ipl1(4SE)::HIS3MX6 CEN3-tetO$_{336}$::URA3 tetR-GFP::LEU2 YFP-TUB1::TRP1* p*MET-CDC20::TRP1*	This study
	SJC259	*MAT***a** *ipl1(S269A)::HIS3MX6 CEN3-tetO$_{336}$::URA3 tetR-GFP::LEU2 YFP-TUB1::TRP1* p*MET-CDC20::TRP1*	This study
3.4	YABD352	*MAT***a** *PDS1-myc$_{18}$::LEU2 kanMX6*-p*GAL1-SCC1 bar1Δ::HPHMX4*	Lab collection
	SJC660	*MAT***a** *ipl1(4SA)::HIS3MX6 PDS1-myc$_{18}$::LEU2 KANMX6*-p*GAL1-SCC1 bar1Δ::HPHMX4*	This study
	SJC664	*MAT***a** *ipl1(4SE)::HIS3MX6 PDS1-myc$_{18}$::LEU2 KANMX6*-p*GAL1-SCC1 bar1Δ::HPHMX4*	This study
3.5	SJC606	*MAT***a** *IPL1-EGFP::KANMX6 YFP-TUB1::TRP1* p*MET-CDC20::TRP1*	This study
	SJC607	*MAT***a** *ipl1(4SA)-EGFP::KANMX6 YFP-TUB1::TRP1* p*MET-CDC20::TRP1*	This study
	SJC609	*MAT***a** *ipl1(4SE)-EGFP::KANMX6 YFP-TUB1::TRP1* p*MET-CDC20::TRP1*	This study
	SJC815	*MAT***a** *bim1Δ::NATMX6 ipl1(4SA)-EGFP::KANMX6 YFP-TUB1::TRP1* p*MET-CDC20::TRP1*	This study
3.6 A	VMY30	*MAT***a** *sli15Δ::KANMX6 his3::SLI15::HIS3*	Lab collection
	SJC641	*MAT***a** *ipl1(2SA)::HIS3MX6 sli15Δ::KANMX6 his3::SLI15::HIS3*	This study
	VMY363	*MAT***a** *sli15Δ::KANMX6 his3::sli15(S335A)::HIS3*	Lab collection
	SJC594	*MAT***a** *ipl1(2SA)::HIS3MX6 sli15Δ::KANMX6 his3::sli15(S335A)::HIS3*	This study
	SJC644	*MAT***a** *ipl1(2SE)::HIS3MX6 sli15Δ::KANMX6 his3::SLI15::HIS3*	This study
	VMY361	*MAT***a** *sli15Δ::KANMX6 his3::sli15(S335D)::HIS3*	Lab collection
	SJC600	*MAT***a** *ipl1(2SE)::HIS3MX6 sli15Δ::KANMX6 his3::sli15(S335D)::HIS3*	This study
3.6 B	VMY148	*MAT***a** *sli15Δ::KANMX6 his3::sli15(20A)::HIS3*	Lab collection
	SJC597	*MAT***a** *ipl1(2SA)::HIS3MX6 sli15Δ::KANMX6 his3::sli15(20A)::HIS3*	This study
	VMY365	*MAT***a** *sli15Δ::KANMX6 his3::sli15(20A,S335A)::HIS3*	Lab collection
	SJC649	*MAT***a** *ipl1(2SA)::HIS3MX6 sli15Δ::KANMX6 his3::sli15(20A,335A)::HIS3*	This study
	VMY187	*MAT***a** *sli15Δ::KANMX6 his3::sli15(20D)::HIS3*	Lab collection
	SJC603	*MAT***a** *ipl1(2SE)::HIS3MX6 sli15Δ::KANMX6 his3::sli15(20D)::HIS3*	This study
	VMY367	*MAT***a** *sli15Δ::KANMX6 his3::sli15(20D,S335D)::HIS3*	Lab collection
	SJC655	*MAT***a** *ipl1(2SE)::HIS3MX6 sli15Δ::KANMX6 his3::sli15(20D,S335D)::HIS3*	This study
4.1 A i	K699	*MAT***a**	Lab collection
	NRY38a	*MAT***a** *ipl1-321::HIS3MX6*	Lab collection
	YABD377	*MAT***a** *mad3Δ::NATMX4*	Lab collection
	SJC125	*MAT***a** *alk1Δ::NATMX4*	This study
	SJC127	*MAT***a** *alk2Δ::NATMX4*	This study

(Table continues)

Table 2.1. continued…

Figure	Strain	Genotype	Source
	SJC123	*MAT***a** *alk1Δ::NATMX4 alk2Δ::NATMX4*	This study
4.1 A ii	SJC711	*MAT***a** [YCplac111]	J. Smith; this study
	SJC696	*MAT***a** *alk1Δ::NATMX4 alk2Δ::KANMX6* [YCplac111]	J. Smith; this study
	SJC699	*MAT***a** *alk1Δ::NATMX4 alk2Δ::KANMX6* [YCplac111-ALK1]	J. Smith; this study
	SJC702	*MAT***a** *alk1Δ::NATMX4 alk2Δ::KANMX6* [YCplac111-ALK2]	J. Smith; this study
4.1 B	K699	*MAT***a**	Lab collection
	SJC125	*MAT***a** *alk1Δ::NATMX4*	This study
	SJC399	*MATα alk2Δ::KANMX6*	This study
	SJC423	*MAT***a** *alk1Δ::NATMX4 alk2Δ::KANMX6*	This study
	YABD302	*MAT***a** *mad2Δ::HIS3MX6*	Lab collection
4.3	SJC56	*MAT***a** *PDS1-myc$_{18}$::LEU2 bar1Δ::HPHMX4*	This study
	SJC754	*MAT***a** *mad3Δ::KANMX6 PDS1-myc$_{18}$::LEU2 bar1Δ::HPHMX4*	This study
	SJC753	*MAT***a** *alk1Δ::NATMX4 alk2Δ::KANMX6 PDS1-myc$_{18}$::LEU2 bar1Δ::HPHMX4*	This study
4.4	SJC403	*MAT***a** *ALK1-3HA::HIS3MX6 PDS1-myc$_{18}$::LEU2 bar1Δ::HPHMX4*	This study
	SJC409	*MAT***a** *ALK2-3HA::HIS3MX6 PDS1-myc$_{18}$::LEU2 bar1Δ::HPHMX4*	This study
4.5 A i	SJC435	*MAT***a** *hht1-hhf1Δ::KANMX3 HHT2-HHF2::URA3*	This study
	SJC441	*MAT***a** *hht1-hhf1Δ::KANMX3 hht2(T3A)-HHF2::URA3*	This study
	SJC483	*MAT***a** *hht1-hhf1Δ::KANMX3 HHT2-HHF2::URA3 alk1Δ::NATMX4*	This study
	SJC487	*MATα hht1-hhf1Δ::KANMX3 HHT2-HHF2::URA3 alk2Δ::NATMX4*	This study
	SJC491	*MATα hht1-hhf1Δ::KANMX3 HHT2-HHF2::URA3 alk1Δ::NATMX4 alk2Δ::NATMX4*	This study
4.5 A ii	SJC435	*MAT***a** *hht1-hhf1Δ::KANMX3 HHT2-HHF2::URA3*	This study
	SJC441	*MAT***a** *hht1-hhf1Δ::KANMX3 hht2(T3A)-HHF2::URA3*	This study
	SJC770	*MAT***a** *bub1Δ::HIS3 hht1-hhf1Δ::KANMX3 HHT2-HHF2::URA3*	This study
	SJC773	*MAT***a** *bub1Δ::HIS3 hht1-hhf1Δ::KANMX3 hht2(T3A)-HHF2::URA3*	This study
	SJC475	*MAT***a** *hht1-hhf1Δ::KANMX3 HHT2-HHF2::URA sgo1Δ::HIS3MX6*	This study
	SJC480	*MAT***a** *hht1-hhf1Δ::KANMX3 hht2(T3A)-HHF2::URA sgo1Δ::HIS3MX6*	This study
4.5 B	K699	*MAT***a**	Lab collection
	SJC125	*MAT***a** *alk1Δ::NATMX4*	This study
	SJC399	*MAT***a** *alk2Δ::KANMX6*	This study
	SJC423	*MAT***a** *alk1Δ::NATMX4 alk2Δ::KANMX6*	This study
	K7508	*MATα bub1Δ::HIS3*	K. Nasmyth
	SJC175	*MAT***a** *sgo1Δ::HIS3MX6*	This study
	SJC776	*MAT***a** *bub1Δ::HIS3 alk1Δ::NATMX4*	This study
	SJC779	*MAT***a** *bub1Δ::HIS3 alk2Δ::KANMX6*	This study
	SJC782	*MAT***a** *bub1Δ::HIS3 alk1Δ::NATMX4 alk2Δ::KANMX6*	This study
	SJC451	*MAT***a** *sgo1Δ::HIS3MX6 alk1Δ::NATMX4*	This study
	SJC455	*MAT***a** *sgo1Δ::HIS3MX6 alk2Δ::KANMX6*	This study

(Table continues)

Table 2.1. continued…

Figure	Strain	Genotype	Source
	SJC459	*MAT***a** *sgo1Δ::HIS3MX6 alk1Δ::NATMX4 alk2Δ::KANMX6*	This study
4.6 B	SJC90	*MAT***a** *CEN3-tetO$_{336}$::URA3 tetR-GFP::LEU2 YFP-TUB1::TRP1* p*MET-CDC20::TRP1*	This study
	SJC144	*MAT***a** *alk1Δ::NATMX4 alk2Δ::NATMX4 CEN3-tetO$_{336}$::URA3 tetR-GFP::LEU2 YFP-TUB1::TRP1* p*MET3-CDC20::TRP1*	This study
	SJC970	*MAT***a** *sgo1Δ::HIS3MX6 CEN3-tetO$_{336}$::URA3 tetR-GFP::LEU2 YFP-TUB1::TRP1* p*MET3-CDC20::TRP1*	This study
	SJC974	*MAT***a** *sgo1Δ::HIS3MX6 alk1Δ::NATMX4 alk2Δ::NATMX4 CEN3-tetO$_{336}$::URA3 tetR-GFP::LEU2 YFP-TUB1::TRP1* p*MET3-CDC20::TRP1*	This study
	SJC587	*MAT***a** *hht1-hhf1Δ::KANMX3 HHT2-HHF2::URA3 trp1::YFP-TUB1::TRP1* p*MET-CDC20::TRP1 his3::LacI-NLS-GFP::HIS3 CEN15-LacOs::URA3*	This study
	SJC589	*MAT***a** *hht1-hhf1Δ::KANMX3 hht2(T3A)-HHF2::URA3 trp1::YFP-TUB1::TRP1* p*MET-CDC20::TRP1 his3::LacI-NLS-GFP::HIS3 CEN15-LacOs::URA3*	This study
4.7 B, C	SJC79	*MATα TRP1 CFIII(CEN3.L.YPH278) URA3 SUP11*	This study
	SJC149	*MATα alk1Δ::NATMX4 alk2Δ::NATMX4 TRP1 CFIII(CEN3.L.YPH278) URA3 SUP11*	This study
	SJC949	*MAT***a** *sgo1Δ::HIS3MX6 TRP1 CFIII(CEN3.L.YPH278) URA3 SUP11*	This study
	SJC952	*MAT***a** *sgo1Δ::HIS3MX6 alk1Δ::NATMX4 alk2Δ::NATMX4 TRP1 CFIII(CEN3.L.YPH278) URA3 SUP11*	This study
4.8 A	SJC910	*MAT***a** *trp1::pTEF1-mCherry-TUB1::TRP1 pMET-CDC20::TRP1 bar1Δ::HPHMX4*	This study
	SJC906	*MAT***a** *alk1Δ::NatMX4 alk2Δ::KanMX6 trp1::pTEF1-mCherry-TUB1::TRP1 pMET-CDC20::TRP1 bar1Δ::HPHMX4*	This study
4.8 B	SJC587	*MAT***a** *hht1-hhf1Δ::KANMX3 HHT2-HHF2::URA3 trp1::YFP-TUB1::TRP1* p*MET-CDC20::TRP1 his3::LacI-NLS-GFP::HIS3 CEN15-LacOs::URA3*	This study
	SJC589	*MAT***a** *hht1-hhf1Δ::KANMX3 hht2(T3A)-HHF2::URA3 trp1::YFP-TUB1::TRP1* p*MET-CDC20::TRP1 his3::LacI-NLS-GFP::HIS3 CEN15-LacOs::URA3*	This study
4.9	SJC910	*MAT***a** *trp1::pTEF1-mCherry-TUB1::TRP1 pMET-CDC20::TRP1 bar1Δ::HPHMX4*	This study
	SJC906	*MAT***a** *alk1Δ::NatMX4 alk2Δ::KanMX6 trp1::pTEF1-mCherry-TUB1::TRP1 pMET-CDC20::TRP1 bar1Δ::HPHMX4*	This study
4.10 A	SJC395	*MAT***a** *kar9Δ::TRP1*	This study
	SJC263	*MATα dyn1Δ::HIS3MX6*	This study
4.10 B	SJC429	*MAT***a** *kar9Δ::TRP1 dyn1Δ::HIS3MX6*	This study
	SJC426	*MATα alk1Δ::NATMX4 alk2Δ::KANMX6*	This study
4.10 C	SJC250	*MAT***a** *bim1Δ::HIS3MX6*	This study
	SJC426	*MATα alk1Δ::NATMX4 alk2Δ::KANMX6*	This study
4.10 D	SJC256	*MAT***a** *jnm1Δ::HIS3MX6*	This study
	SJC426	*MATα alk1Δ::NATMX4 alk2Δ::KANMX6*	This study
4.10 E	K699	*MAT***a**	Lab collection
	SJC395	*MAT***a** *kar9Δ::TRP1*	This study
	SJC244	*MAT***a** *dyn1Δ::HIS3MX6*	This study
	SJC429	*MAT***a** *kar9Δ::TRP1 dyn1Δ::HIS3MX6*	This study
4.10 F	K699	*MAT***a**	Lab collection

(Table continues)

Table 2.1. continued…

Figure	Strain	Genotype	Source
	SJC125	*MAT***a** *alk1Δ::NATMX4*	This study
	SJC127	*MAT***a** *alk2Δ::NATMX4*	This study
	SJC123	*MAT***a** *alk1Δ::NATMX4 alk2Δ::NATMX4*	This study
	SJC241	*MAT***a** *kar9Δ::HIS3MX6*	This study
	SJC273	*MAT***a** *kar9Δ::HIS3MX6 alk1Δ::NATMX4*	This study
	SJC275	*MAT***a** *kar9Δ::HIS3MX6 alk2Δ::NATMX4*	This study
	SJC277	*MAT***a** *kar9Δ::HIS3MX6 alk1Δ::NATMX4 alk2Δ::NATMX4*	This study
	SJC250	*MATα bim1Δ::HIS3MX6*	This study
	SJC290	*MAT***a** *bim1Δ::HIS3MX6 alk1Δ::NATMX4*	This study
	SJC292	*MAT***a** *bim1Δ::HIS3MX6 alk2Δ::NATMX4*	This study
	SJC294	*MAT***a** *bim1Δ::HIS3MX6 alk1Δ::NATMX4 alk2Δ::NATMX4*	This study
	SJC244	*MAT***a** *dyn1Δ::HIS3MX6*	This study
	SJC279	*MAT***a** *dyn1Δ::HIS3MX6 alk1Δ::NATMX4*	This study
	SJC281	*MAT***a** *dyn1Δ::HIS3MX6 alk2Δ::NATMX4*	This study
	SJC283	*MAT***a** *dyn1Δ::HIS3MX6 alk1Δ::NATMX4 alk2Δ::NATMX4*	This study
	SJC256	*MAT***a** *jnm1Δ::HIS3MX6*	This study
	SJC302	*MAT***a** *jnm1Δ::HIS3MX6 alk1Δ::NATMX4*	This study
	SJC304	*MAT***a** *jnm1Δ::HIS3MX6 alk2Δ::NATMX4*	This study
	SJC305	*MAT***a** *jnm1Δ::HIS3MX6 alk1Δ::NATMX4 alk2Δ::NATMX4*	This study
4.11	SJC581	*MAT***a** *ALK1-EYFP::NATMX4 bar1Δ::HPHMX4* p*MET-CDC20::TRP1*	This study
	SJC584	*MAT***a** *ALK2-EYFP::NATMX4 bar1Δ::HPHMX4* p*MET-CDC20::TRP1*	This study
4.13 A	SJC785	*MAT***a** *zrt1Δ::HIS3MX6*	This study
	SJC426	*MATα alk1Δ::NATMX4 alk2Δ::KANMX6*	This study
4.13 B	K699	*MAT***a**	Lab collection
	SJC125	*MAT***a** *alk1Δ::NATMX4*	This study
	SJC399	*MAT***a** *alk2Δ::KANMX6*	This study
	SJC423	*MAT***a** *alk1Δ::NATMX4 alk2Δ::KANMX6*	This study
	SJC785	*MAT***a** *zrt1Δ::HIS3MX6*	This study
	SJC796	*MAT***a** *zrt1Δ::HIS3MX6 alk1Δ::NATMX4*	This study
	SJC799	*MAT***a** *zrt1Δ::HIS3MX6 alk2Δ::KANMX6*	This study
	SJC802	*MAT***a** *zrt1Δ::HIS3MX6 alk1Δ::NATMX4 alk2Δ::KANMX6*	This study
4.13 C	SJC831	*MAT***a** *hac1Δ::HIS3MX6*	This study
	SJC426	*MATα alk1Δ::NATMX4 alk2Δ::KANMX6*	This study
4.13 D	SJC834	*MAT***a** *ire1Δ::HIS3MX6*	This study
	SJC426	*MATα alk1Δ::NATMX4 alk2Δ::KANMX6*	This study
4.13 E	SJC837	*MAT***a** *spt3Δ::HIS3MX6*	This study
	SJC426	*MATα alk1Δ::NATMX4 alk2Δ::KANMX6*	This study
A2	K699	*MAT***a**	Lab collection
	SJC423	*MAT***a** *alk1Δ::NATMX4 alk2Δ::KANMX6*	This study
	SJC175	*MAT***a** *sgo1Δ::HIS3MX6*	This study
	SJC459	*MAT***a** *sgo1Δ::HIS3MX6 alk1Δ::NATMX4 alk2Δ::KANMX6*	This study
	YABD302	*MAT***a** *mad2Δ::HIS3MX6*	Lab collection

(Table continues)

Table 2.1. continued…

Figure	Strain	Genotype	Source
A3	SJC679	*MAT***a** *IPL1-EGFP::KANMX6 trp1::pTEF1-mCherry-TUB1::TRP1* p*MET-CDC20::TRP1*	This study
	SJC750	*MAT***a** *alk1Δ::NATMX4 alk2Δ::NATMX4 IPL1-EGFP::KANMX6 trp1::pTEF1-mCherry-TUB1::TRP1* p*MET-CDC20::TRP1*	This study
A4	SJC587	*MAT***a** *hht1-hhf1Δ::KANMX3 HHT2-HHF2::URA3 trp1::YFP-TUB1::TRP1* p*MET-CDC20::TRP1 his3::LacI-NLS-GFP::HIS3 CEN15-LacOs::URA3*	This study
	SJC589	*MAT***a** *hht1-hhf1Δ::KANMX3 hht2(T3A)-HHF2::URA3 trp1::YFP-TUB1::TRP1* p*MET-CDC20::TRP1 his3::LacI-NLS-GFP::HIS3 CEN15-LacOs::URA3*	This study
	KP340	*nda3-KM311 h⁻ (S. pombe)*	K. Hardwick
N/A	AYS927	*MAT***a***/MATα ade2-1 his3-11,15 leu2-3,112 trp1-1 ura3-1 can1-100 ssd1-d2*	Lab collection
	SJC614	*MATα alk1Δ::NATMX4 lyp1::HPH::LEU2 can1Δ::STE2pr-Sphis5 his3Δ1 leu2Δ0 ura3Δ0 met15Δ0 (S288C background)*	This study
	SJC617	*MATα alk2Δ::NATMX4 lyp1::HPH::LEU2 can1Δ::STE2pr-Sphis5 his3Δ1 leu2Δ0 ura3Δ0 met15Δ0 (S288C background)*	This study
	SJC620-1	*MATα alk1Δ::NATMX4 alk2Δ::HPHMX4 can1Δ::STE2pr-Sphis5 lyp1Δ::LEU2 his3Δ1 leu2Δ0 ura3Δ0 met15Δ0 (S288C background)*	This study

¶ Unless stated otherwise, all strains are *S. cerevisiae* and are derived from the W303 background, containing the alleles listed under the K699 genotype in addition to those shown for each strain.

Table 2.2. *E. coli* strains used in this study

Strain	Genotype	Source
DH5α	*F– Φ80lacZΔM15 Δ(lacZYA-argF) U169 recA1 endA1 hsdR17 (r_K^-, m_K^+) phoA supE44 λ^- thi-1 gyrA96 relA1*	Invitrogen

2.1.2 *Media and growth conditions*

All solid and liquid media for the propagation of yeast and bacteria were prepared by the Media Service within the College of Life Sciences. Yeast strains were cultured in or grown on various media (see Table 2.3) and at various temperatures depending on the genotype of the strain and the purpose of the experiment. Strains were typically grown at 26°C unless otherwise stated. *E. coli* strains were cultured in or grown on lysogeny broth (LB) medium (see Table 2.4) and incubated at 37°C. To maintain selection for plasmids the medium was supplemented with ampicillin (AMP). *E. coli* strain DH5α was used in all cloning and transformation procedures.

2.2 Yeast strain construction

2.2.1 *Crossing, diploid selection, zygotes and tetrad dissection*

Yeast strains were crossed by taking a small scoop of cells of opposite mating type and resuspending thoroughly in 20 µl of sterile water. This cell suspension was then spread onto an appropriate agar plate and incubated at 26°C overnight. Diploids were selected by streaking a sample of the crossed strains onto the appropriate selective medium. Where diploid selection by this method was not possible (i.e. if the two strains being crossed had no unique auxotrophic or drug selection markers) zygotes were picked. Yeast strains were crossed as above but after incubation for 5 – 8 hours zygotes were identified as described in Stansfield & Stark (2007) and picked using a Singer "Sporeplay" micromanipulator. Once the diploids had formed colonies they were patched onto YPAD and grown overnight before being patched onto VB sporulation medium and incubated at 26°C. Tetrads (four-spored asci) typically developed after 2 days. Tetrad dissection was performed by resuspending sporulated cells in 200 µl sterile water and adding 40 µg of Zymolyase 100T. The digestion was carried out at room temperature for 5 minutes. Once digested, 1 ml sterile water was gently added and the

Table 2.3. Yeast growth medium and supplements	
YPA	**% (w/v)**
yeast extract	1
peptone	2
adenine hydrochloride	0.01
glucose (YPA**D**)	2
raffinose/galactose (YPA**RG**)	2 (each)
agar (for plates)	2
SD (synthetic drop-out)	**% (w/v)**
yeast nitrogen base (w/o amino acids)	0.0067
amino acids (omit as appropriate)	varied
glucose	2
VB (sporulation medium)	**% (w/v)**
sodium acetate	0.82
potassium chloride	0.19
sodium chloride	0.12
magnesium sulphate	0.035
agar (for plates)	1.5
YES (for *S. pombe*)	**% (w/v)**
yeast extract	0.5
arginine, histidine, leucine, lysine, uracil, adenine	0.0002 (each)
glucose	2
agar (for plates)	2
Drugs and working concentrations	**µg/ml**
Geneticin (G418)	200
Nourseothricin (clonNAT)	100
Hygromycin B (HygB)	200
For detailed recipes of yeast media, see (Amberg *et al*., 2005)	

Table 2.4. *E. coli* growth medium and supplements	
LB medium	**% (w/v)**
tryptone	1
yeast extract	0.5
sodium chloride	1
agar (for plates)	1.2
Drugs and working concentrations	**µg/ml**
ampicillin (AMP)	100

cell suspension was pipetted onto the search area of an angled plate. Tetrad dissection was performed using a Singer "Sporeplay" micromanipulator.

2.2.2 *Yeast transformation*

Yeast strains were transformed following the lithium acetate method described previously (Gietz & Woods, 2002). Cells from 25 ml of an exponentially growing culture were collected by centrifugation at 3,000 rpm for 2 minutes at room temperature, washed once with distilled water and finally resuspended in 1 ml distilled water. For each transformation, 200 µl of the cell suspension was centrifuged and the following mix was added to the pellet: 360 µl PEG 3350 33% (w/v), 100 mM lithium acetate, 100 µg sheared herring sperm DNA and a suitable amount of plasmid or PCR product (typically a few µg of PCR product or 50 – 100 ng of plasmid DNA). The pellet was resuspended by thorough vortexing before heat-shock incubation at 42°C for 40 minutes. Finally the cells were washed and inoculated onto the appropriate selective plates. When using drug selection (G418, clonNAT, Hygromycin), cells were resuspended in 1 ml YPAD and incubated at 26°C for 3 hours following the heat shock before being inoculated onto selective plates. Correct transformants were identified by colony PCR.

2.2.3 *Colony PCR*

A small amount of yeast cells was resuspended in 10 µl of SPZ solution [1.2 M sorbitol, 100 mM sodium phosphate (pH 7.5) and 2.5 mg/ml Zymolyase 100T] and subsequently incubated at 37°C for 30 minutes and then 95°C for a further 5 minutes to digest the cell wall and liberate the genomic DNA. This suspension was then diluted 10-fold with distilled water and 2.5 µl used as a template in a 25 µl PCR reaction (See 2.3.2 PCR and primers).

2.2.4 *Generation of IPL1 mutant alleles*

IPL1 mutant alleles were generated at the genomic *IPL1* locus following the methodology described by Toulmay & Schneiter (2006). Briefly, a *HIS3MX6* cassette was inserted downstream of the *IPL1* genomic locus. Using this DNA as a template (see genomic DNA preparation), one of the forward primers listed in Table 2.5 and a reverse primer downstream of the *HIS3MX6*, a PCR product was generated using Phusion® High Fidelity DNA Polymerase (NEB Inc.) that incorporated the codon mutation and cassette. This was subsequently transformed into a wild-type diploid W303 strain (AYS927) to generate heterozygous diploids to avoid problems associated with sickness or lethality caused by the mutations. Correct transformants were identified with a combination of PCR, restriction digest and sequencing. These diploid strains were then sporulated and dissected to obtain haploid strains containing the *IPL1* mutant allele. Tetrad analysis identified the lethality associated with the *ipl1-S269E* allele. Four independent transformants (verified by sequencing) were dissected to confirm the lethality associated with this mutant allele.

Table 2.5. Primers used for *IPL1* mutagenesis

Primer	Sequence
IPL1_S15A_F	GAAGTAAAAAGGGAATGCAACGCAATAGTTTAGTAAATATCAAACTAAACGCTAATGCACCATCGAAAAAGACCAC
IPL1_S50A_F	CCATGGAGAATATCCCATTCGCCGCAGCAAAGAAACCCGAATTCAAAAATACCTGCACCTGTAAGAGAAAAATTGAAC
IPL1_S76A_F	GATTACCTGTAAACAATAAGAAGTTTTTGGATATGGAAAGCTCCAAAATTCCAGCACCTATAAGGAAAGCGAC
IPL1_S15E_F	GAAGTAAAAAGGGAATGCAACGCAATAGTTTAGTAAATATCAAACTAAACGCTAATGAACCATCGAAAAAGACCAC
IPL1_S50E_F	CCATGGAGAATATCCCATTCGCCGCAGCAAAGAAACCCGAATTCAAAAATACCTGAACCTGTAAGAGAAAAATTGAAC
IPL1_S76E_F	GATTACCTGTAAACAATAAGAAGTTTTTGGATATGGAAAGCTCCAAAATTCCAGAACCTATAAGGAAAGCGAC
IPL1_S38A_F	CGTCCAGGATCAATAAACCATGGAGAATATCCCATGCACCGCAGCAAAGAAACCC
IPL1_S38E_S50E_F	CAATAAACCATGGAGAATATCCCATGAACCGCAGCAAAGAAACCCGAATTCAAAAATACCTGAACCTGTAAGAGAAAAATTGAAC

Optimized codon mutations are highlighted in red. All primers were synthesized by Sigma Aldrich, UK

2.2.5 *Generation of histone H3 mutant strains*

The *S. cerevisiae* genome contains two genes that encode histone H3 (*HHT1* and *HHT2*) and each are expressed at different loci from a bi-directional promoter that is shared with one of two copies of histone H4 (*HHF1* and *HHF2*). To generate H3(T3A) and the corresponding H3 control cells, a strain was acquired in which both loci were deleted (*hht1-hhf1*Δ::*KANMX3 hht2-hhf2*Δ::*HIS3*) and viability was maintained through the expression of *HHT2-HHF2* from a *URA3*-marked plasmid (*YCpURA3[HHT2-HHF2]*; a gift from N. Lowndes, NUI Galway). These two knockout loci were separated into different strains by backcrossing with a wild-type strain. As these resulting haploid strains now had the respective wild-type and knockout loci, the covering plasmid was removed by several round of selection on 5-FOA plates. Two plasmids were sourced that carried a synthetic locus of *HHT2-HHF2* with either wild-type *HHT2* or mutant *hht2(T3A)* that were marked with *URA3* and had flanking sequence homology with the *HHT2-HHF2* genomic locus (Thermo Scientific Open Biosystems Histone H3 and H4 Mutant Collection; Dai *et al*., 2008). A *TRP1* marker was also present on these plasmids at a position not linked to the synthetic *HHT2-HHF2* locus. These plasmids were linearised at their unique *Swa*I restriction site and transformed into the strain carrying *hht2-hhf2*Δ::*HIS3* so as to replace *hht2-hhf2*Δ*::HIS3* with *HHT2-HHF2::URA3* or *hht2(T3A)-HHF2::URA3*. Transformants were struck out onto selective plates to check that the synthetic locus had integrated correctly and replaced the knockout locus (correct integration = Trp^-, His^-, Ura^+). These *HHT2-HHF2* and *hht2(T3A)-HHF2* strains were then crossed with the strain carrying *hht1*Δ-*hhf1*Δ to generate haploid strains where the sole source of histone H3 was either *HHT2* or *hht2(T3A).*

2.3 Molecular biology techniques

2.3.1 *Yeast genomic DNA preparation*

A 10 ml overnight yeast culture was harvested by centrifugation at 3,000 rpm for 2 minutes. The pellet was resuspended in 0.5 ml of a 1 M sorbitol, 0.1 M EDTA (pH 7.5) buffer to which 100 µg of Lyticase was added before incubation at 37°C for 60 minutes. A pellet was collected by centrifugation at 13,200 rpm for 1 minute and subsequently resuspended in 0.5 ml 50 mM Tris-HCl (pH 7.4), 20 mM Na_2EDTA to which 25 µl of SDS 20% (w/v) was added. The suspension was mixed thoroughly and incubated on ice for 60 minutes. A large white pellet was collected by centrifugation at 13,200 rpm for 5 minutes and the supernatant transferred to a new tube. One volume of 100% isopropanol was added to the supernatant, mixed thoroughly by inversion and left to stand for 5 minutes. Following centrifugation at 13,200 rpm for 10 seconds, the supernatant was discarded and the pellet air-dried for 15 minutes. The pellet was resuspended in 0.3 ml TE buffer [10 mM Tris-HCl (pH 7.4), 1 mM EDTA (pH 8.0)] and 15 µg of RNase A was added before incubation for 30 minutes at 37°C. 30 µl of 3 M NaOAc was added and mixed followed by 200 µl of 100% isopropanol to precipitate the DNA. After several inversions of the tube the DNA was pelleted by centrifugation at 13,200 rpm for 10 seconds. The pellet was air-dried and resuspended in 50 µl of distilled water.

2.3.2 *PCR and primers*

A typical PCR reaction contained 50 – 200 ng template DNA, 1× PCR buffer, 200 µM dNTPs, 0.2 µM each of forward and reverse primers, 1 – 5 U DNA polymerase and made up to 50 µl with sterile water. A typical PCR program consisted of an initial denaturation step of 2 minutes 94°C followed by 30 cycles of 1 minute 94°C (denaturation), 30 seconds 55°C (annealing) and 1 minute per kb DNA 72°C

(elongation). A final elongation step for 10 minutes 72°C concluded the program. All primers used in this study were synthesised by Sigma Aldrich UK. The annealing temperature was adjusted if required based on the temperatures specified by the manufacturer. Recombinant Taq polymerase (purified in-house) was used for diagnostic PCR and followed the conditions listed above. The Expand Long Template PCR System (Roche) was used as a higher fidelity option for generating PCR fragments for transformation. For instances where the DNA sequence needed to be correct after amplification, Phusion® High Fidelity DNA Polymerase (NEB) was used. Reaction constituents and conditions were adjusted when using these enzymes based on the manufacturers' specifications.

2.3.3 *Plasmid isolation, restriction digests and ligations*

A single colony of an *E. coli* strain carrying the plasmid of interest was inoculated into LB medium supplemented with the relevant drug to maintain selection for the plasmid and incubated at 37°C for 16 – 24 hours. Plasmid DNA was isolated using a miniprep kit (Bioline Reagents). Typically 0.5 – 5 μg (depending on the application) of isolated plasmid DNA was incubated with 10 U of the relevant restriction enzyme(s) (NEB) in the appropriate buffer and at the applicable temperature for one to three hours. Digests were analysed by running the samples on an agarose gel (1 - 2% (w/v) agarose, 1× TAE [40 mM Tris, 20 mM acetic acid, 1 mM EDTA]) containing 5 μl SafeView nucleic acid stain (NBS Biologicals Ltd.) per 100 ml agarose. For ligation reactions the vector and insert bands of interest were excised from the gel and the DNA extracted using a gel extraction kit (Qiagen). Vector DNA was dephosphorylated using Antarctic phosphatase (NEB) before the ligation reaction was performed using a rapid ligation kit (Roche). Ligations were subsequently transformed

into an appropriate *E. coli* strain, typically DH5α. Positive clones were identified by restriction digest and sequencing.

2.3.4 *E. coli competent cell preparation and transformation*

Competent cell preparation and transformation were carried out following the improved methodology described in Tu *et al*. (2005). Briefly, for transformation, approximately 0.5 µg of plasmid DNA and 1 µl DMSO was added to 100 µl of competent cells, mixed thoroughly and incubated on ice for 30 minutes. Cells were then heat shocked at 42°C for 90 seconds and placed on ice for 2 minutes. Following a one hour recovery period in 1 ml LB medium at 37°C (with shaking), cells were plated onto the appropriate selective medium.

2.3.5 *Plasmid and PCR fragment sequencing*

All plasmid and PCR fragment sequencing was carried out by the DNA Sequencing & Services facility within the College of Life Sciences. DNA samples were prepared following the facilities guidelines available at www.dnaseq.co.uk

2.3.6 *Generation of ALK1 and ALK2 containing vectors for complementation studies*

ALK1 and *ALK2* (including approximately 500 bp of upstream and downstream DNA) were amplified from a genomic DNA preparation of a wild-type W303 background strain (K699) using the primers listed in Table 2.6 and Phusion® High Fidelity DNA Polymerase (NEB Inc.). These fragments were then gel purified and inserted into the pJET1.2 blunt cloning vector (Fermentas) using the Rapid DNA Ligation Kit (Roche) as per the manufacturer's instructions and transformed into the DH5α *E. coli* strain. Correct clones were identified by restriction digest and sequencing. The cloned *ALK1* and *ALK2* sequences were then excised from the pJET1.2 vector, gel

purified and inserted into the yeast centromere containing YCplac111 plasmid (*LEU2 CEN4 ARS1* amp^R; Gietz & Sugino, 1998). *ALK1* was excised using *Swa*I and *Bgl*II and cloned into the *Bam*HI site of YCplac111. *ALK2* was excised using *Xho*I and *Mfe*I and cloned between the *Eco*RI and *Sal*I of YCplac111. Following transformation into *E. coli* strain DH5α, correct clones were identified by restriction digest and DNA sequencing.

Table 2.6. Primers used in *ALK1* and *ALK2* vector construction

Primer	Sequence
ALK1_F	ATGTCCTACAAAGATTTCCC
ALK1_R	CACAAACTCAGGTTATTGGC
ALK2_F	TGTTCATAAATGACATGGGG
ALK2_R	CAACCTTTTCCCATCGTGGC

All primers were synthesized by Sigma Aldrich, UK

2.4 Yeast protein extraction and analysis

2.4.1 *NaOH/TCA method for total protein extraction*

Cells were harvested and thoroughly resuspended in 4 volumes of NaOH buffer [1.8 M NaOH, 7% β-mercaptoethanol] and chilled on ice for 10 minutes. TCA was added (10% final) and mixed by inversion followed by a further 10 minute incubation on ice. Samples were centrifuged at 13,200 rpm for 2 minutes and the supernatant discarded. 1 volume of cold acetone was added to the pellet, vortexed and centrifuged at 13,200 rpm for 2 minutes. The supernatant was discarded and the pellets left to air-dry briefly. The pellet was dispersed in 4 volumes of 2× Laemmli buffer [0.125 M Tris-HCl (pH 6.8), 4% SDS (w/v), 20% glycerol, 0.01% bromophenol blue, 5% β-mercaptoethanol] and heated to 75°C for 15 minutes. The sample was then vortexed thoroughly and centrifuged at 13,200 rpm for 2 minutes to collect the insoluble cell debris. Typically, 5 µl of the supernatant was used for SDS-PAGE analysis.

2.4.2 *Nuclei preparation and histone acid extraction*

Histones were extracted from yeast nuclei using a standard acid extraction method adapted from Gardner *et al*. (2011). Briefly, 250 ml cultures were grown to 1.5 OD_{600} /ml at 26°C. Cells were harvested by centrifugation at 3000 × g for 5 minutes and washed once with STOP buffer [154 mM NaCl, 1 mM NaN_3, 50 mM NaF, 1 mM Na_3VO_4, 10 mM EDTA], once with water and then resuspended in 7.5 ml Buffer 1 [0.1 mM Tris-Cl (pH 9.4), 10 mM DTT] and incubated at 30°C with shaking at 150 rpm for 15 minutes. Cells were collected by centrifugation for 3 minutes at 3000 × g and washed once with 15 ml Buffer 2 [1.2 M sorbitol, 20 mM HEPES (pH 7.4)]. Cells were harvested as before and resuspended in 15 ml Buffer 2 containing 0.2 mg/ml Zymolyase 100T and incubated at 30°C with shaking at 150 rpm until at least 90% of cells were spheroplasted. Spheroplasting typically took 40 – 50 minutes and was monitored by mixing 4 µl of the cell suspension with 4 µl 1% SDS on a glass slide and visually inspecting the ratio of intact and ghosted cells. Once adequately spheroplasted, 15 ml ice-cold buffer 3 [1.2 M sorbitol, 20 mM PIPES (pH 6.8), 1 mM $MgCl_2$] was added. Cells were collected by centrifugation at 1300 × g for 5 minutes at 4°C, gently resuspended in 7.5 ml ice-cold Buffer 4 [0.25 M sucrose, 60 mM KCl, 14 mM NaCl, 5 mM $MgCl_2$, 1 mM $CaCl_2$, 15 mM MES (pH 6.6), 1 mM PMSF, 0.8% TritonX-100], incubated on ice for 20 minutes and collected by centrifugation at 1700 × g for 5 minutes. Nuclei isolation in Buffer 4 was completed three times in total. Nuclei were washed three times in 12.5 ml Wash Buffer 1 [10 mM Tris-Cl (pH 8.0), 0.5% NP-40, 75 mM NaCl, 1 mM PMSF] for 15 minutes on ice for the first two washes and 5 minutes on the third wash, followed by two washes in Wash Buffer 2 [10 mM Tris-Cl (pH 8.0), 400 mM NaCl, 1 mM PMSF] for 10 minutes on the first wash and then centrifuged immediately after the second resuspension. Histones were extracted by resuspending nuclei in 1.5 ml 0.4 N H_2SO_4 and incubating on ice for 30 minutes with occasional

vortexing. Debris was pelleted by centrifugation at 10,000 × g and histones were precipitated from the supernatant by addition of 100% (w/v) TCA to a final concentration of 20% with incubation on ice for 30 minutes. Histones were pelleted by centrifugation at 15,000 × g for 30 minutes, washed once with cold acetone containing 1% (v/v) HCl and once with cold acetone. Following removal of acetone and air-drying, the pellet was resuspended in 200 µl 10 mM Tris-Cl (pH 8.0).

2.4.3 *SDS-PAGE*

Protein samples were analysed by SDS-PAGE using NuPAGE® 4-12% and 10% Bis-Tris precast gels (Invitrogen). Around 20 µg of protein was loaded per lane alongside 3.5 µl of SeeBlue® Plus2 pre-stained standard (Invitrogen). Gels were run in NuPAGE® MOPS SDS running buffer at 200 V for 50 minutes. Direct visualisation of protein bands in SDS-PAGE gels was achieved by InstantBlue Coomassie (Novexin) or silver staining.

2.4.4 *Western blotting*

Following SDS-PAGE proteins were transferred to Immobilon-P PVDF membrane (Millipore) using Towbin buffer [25 mM Tris base, 192 mM glycine, 20% methanol (v/v)] in a Bio-Rad transfer tank at 100 V for 60 minutes. Following transfer the membrane was stained with Ponceau S [0.1% (w/v) Ponceau S, 5% (v/v) acetic acid] to check the efficiency of the transfer and then washed in TBST [50 mM Tris-Cl (pH 7.5), 150 mM NaCl, 0.2% (v/v) Tween-20]. Membranes were blocked for 60 minutes in TBST with 5% (w/v) of milk or BSA. Membranes were then incubated with a primary antibody overnight at 4°C. The membrane was subsequently washed three times for 10 minutes each in TBST on a rocking platform before being incubated with an appropriate HRP conjugated secondary antibody for 60 minutes. The membrane was washed as

before and incubated with ECL reagent (Millipore) according to the manufacturers' guidelines and chemiluminescence was detected using a Fujifilm LAS-4000 system and Image Reader software.

2.4.5 Antibodies

Each of the antibodies used in this study are listed in Table 2.7.

Table 2.7. Antibodies used in this study

Target	Source	Cat. #/ID	Dilution used
Cdc28 (C-term)	Santa Cruz Biotechnology	sc-6709	1 in 10,000
GFP	Roche	11814460001	1 in 1000
HA	Santa Cruz Biotechnology	sc-7392	1 in 3000
H3 (C-term)	Abcam	ab1791	1 in 5000
H3-T3ph	Upstate/Millipore	07-424	1 in 2000
H3-T3ph	J. Higgins (Dai *et al*. 2005)	B8634	1 in 2000
H3-T3phK4me3	Abcam	ab3738	1 in 5000
Myc	Santa Cruz Biotechnology	sc-789	1 in 10,000
TAP	Pierce/Thermo Scientific	CAB1001	1 in 5000

2.5 Yeast experimental procedures

2.5.1 *Spot assays*

Spot assays were used to assess sensitivity of yeast strains to various temperatures or drugs. Exponentially growing cultures were diluted in YPAD to 1.0 OD_{600} /ml and four subsequent 10-fold dilutions were spotted onto appropriate agar plates. After two days incubation the plates were imaged to compare growth. To test thermosensitivity, several identical plates would be spotted and incubated at a range of temperatures (typically 26°C, 30°C and 37°C). To test sensitivity to a particular drug, cells were spotted onto several agar plates, each containing varying concentrations of the drug. Typically, three independently isolated strains of the same genotype were tested.

2.5.2 *Generating synchronous yeast cultures using alpha-factor*

An appropriate volume of a mid-log phase culture was harvested and the resulting pellet was washed thoroughly in pre-warmed media to remove traces of the extracellular Bar1 protease (the protease which degrades alpha-factor). The cells were then diluted to 0.18 OD_{600} /ml in media containing 1.25 μg/ml of alpha-factor (0.5 μg/ml for *bar1*Δ cells) to arrest cells in G_1. Alpha-factor was then added at the same concentration after the first 60 minutes and then every 30 minutes thereafter. Synchronisation was generally achieved after 2 hours. Cell cultures had arrested efficiently if 95% of cells displayed shmoo morphology.

2.5.3 *Metaphase arrest through Cdc20 depletion*

Cells containing *CDC20* under the control of the *MET3* methionine-repressible promoter (p*MET3-CDC20*) were arrested with α-factor as previously described in medium lacking methionine to deplete Cdc20. These cells were released from G_1 by thoroughly washing the cells and then resuspending them in YPAD supplemented with 5 mM methionine to repress the expression of Cdc20. Efficient metaphase arrest was usually achieved after 2.5 hours and was confirmed by the accumulation of either large budded cells or cells with short bipolar spindles.

2.5.4 *Metaphase arrest using benomyl or nocodazole*

Cells were arrested in metaphase by the addition of 30 μg/ml benomyl or 15 μg/ml nocodazole. Media due to receive either of these drugs were supplemented with 1% DMSO to maintain solubility of the drugs. Efficient metaphase arrest was confirmed by the accumulation of either large budded cells or the persistence of Pds1/Securin (assessed by western blotting).

2.5.5 *Monitoring spindle checkpoint signalling through the kinetics of Pds1 destruction in synchronous cultures*

Cell cycle progression and spindle checkpoint signalling can be observed by monitoring the cell cycle regulated expression and degradation of the yeast securin Pds1. Pds1 is rapidly degraded upon entry into anaphase, but persists when cells arrest in metaphase. Briefly, cells expressing Pds1-myc$_{18}$ were harvested from a mid-log phase culture and diluted to 1.8 OD_{600} /ml in 20 ml medium and α-factor was added to synchronise cells in G_1. Cells were then washed thoroughly with 100 ml medium to remove the α-factor and then resuspended in 200 ml medium to synchronously release cells from G_1. For the first time-point a 25 ml sample was taken immediately and centrifuged at 3,000 rpm to collect the cells. The pellet was then resuspended in 1 ml sterile water and transferred to a 1.5 ml microcentrifuge tube and centrifuged at 10,000 rpm for 30 seconds. The supernatant was discarded and the pellet was frozen on dry ice. This process was repeated usually every 20 minutes for each time-point. Protein extraction from the cell pellets was performed using the NaOH/TCA method. Pds1-myc$_{18}$ levels were monitored by SDS-PAGE and western blotting.

2.5.6 *Assessing tension-dependent checkpoint signalling – depletion of Scc1*

A p*GAL-SCC1* construct was used to conditionally deplete cells of Scc1, a subunit of the cohesin complex, and thereby prevent proper cohesin loading onto replicated DNA. This results in the loss of tension at centromeric regions of sister chromatids and triggers a checkpoint response in wild-type cells. The same time-course approach to monitor Pds1 kinetics was used but varied in several ways. Cells were initially cultured in medium containing galactose (YPARG) to maintain expression of Scc1. G_1 synchronisation using α-factor was then performed in medium containing

glucose (YPAD) to deplete cells of Scc1 and cells were also released in YPAD medium to maintain the depletion.

2.5.7 *Assessing chromosome bi-orientation and segregation using 'CEN-dot' strains*

Strains were constructed to enable the visualisation of both the microtubules (*YFP-TUB1*) and sister centromeres of chromosome III by way of *tetR-GFP* binding to an array of *tetO* repeats inserted close to the centromere of chromosome III (*CEN3*). These strains also carried p*MET3-CDC20* so that cells could be efficiently arrested in metaphase (strain SJC90). Cells from mid-log phase cultures were arrested in G_1 with α-factor and released to a metaphase block in rich medium as described above. Time-lapse images were taken over a 5 minute period for each field of cells (see 2.6 Microscopy Techniques). In these "*CEN*-dot" strains, bi-oriented chromosomes are characterised by the dynamic separation and convergence of the two sister *CEN*-dots in metaphase, whereas mono-oriented chromosomes appear as a single, unresolved *CEN*-dot that is localised towards a single spindle pole (Tanaka *et al*. 2000). Only large budded cells were scored with spindles that were visible and remained on the plane of view for the duration of the time-course. When these cells are released from metaphase into anaphase, the spindle elongates and proper chromosome segregation is deduced from observing two separate dots at opposite ends of the spindle. Unsuccessful segregation results in a single GFP dot being visible at one spindle pole. Fisher's exact test was used for the statistical analysis to compare results from different strains and all *P*-values are two tailed.

2.5.8 *Chromosome loss assay*

The rate of chromosome loss was assayed as previously described (Spencer & Hieter, 1992) by monitoring the loss of a supernumerary chromosome III fragment (CFIII) carrying *URA3* and *SUP11* in a colony sectoring assay. Loss of CFIII (and consequently *SUP11*) results in a red colony colour due to the inability to suppress the *ade2-1* mutation. The wild-type assay strain (SJC79) and mutant derivatives were grown in SD medium lacking uracil to mid-log phase at 26°C and then washed and resuspended in YPD medium which lacks additional adenine. Following brief sonication to separate cells, suitable dilutions were made and cells were plated onto YPD agar and incubated at 26°C for 6 days. The loss of CFIII was monitored visually by the production of red sectored colonies and the loss rate per cell division was calculated by dividing the number of half-sectored red colonies (50% or more red) by the total number of colonies (excluding completely red colonies that were derived from cells that lost CFIII before plating).

2.5.9 Viability assays

The viability of yeast strains was evaluated by using a number of different assays. Methylene blue staining was performed by mixing equal parts of a briefly sonicated mid-log phase culture growing in SC (synthetic complete) medium with 0.1 % (w/v) methylene blue solution and leaving for 5 minutes to stain. Viable cells are able to metabolise methylene blue and remain unstained whereas dead cells are not metabolically active and are stained blue. Averages of over 900 cells were counted on a haemocytometer per strain and the percent viability was calculated by dividing the number of unstained cells by the total number of cells counted.

An alternative method employed to determine viability was to assess the ability of cells to form colonies. Sample of cells were taken from mid-log phase cultures and sonicated. Cell number per millilitre was determined by haemocytometer counts and an appropriate volume of culture containing approximately 200 cells was plated onto each of four YPAD plates per strain. Viability was calculated as a percentage of colonies formed versus the number of cells plated.

To assess the relative viability of strains after exposure to benomyl, cultures were grown to mid-log phase and diluted to an appropriate cell density. Samples were taken, briefly sonicated and plated onto three YPAD medium per strain at a density of approximately 200 cells per plate. An equal volume of medium containing 60 μg/ml benomyl was added to the cultures (final concentration of 30 μg/ml) and equivalent samples (taking the dilution factor into account) were taken every 2 hours, sonicated and plated out as before. Over 500 colonies were present at time zero for each strain. In each case, this value was set at 100% and viability at subsequent time points was plotted by expressing colony forming units as a percentage of the time zero value.

2.6 Microscopy techniques and image analysis

2.6.1 *Microscopy equipment*

Visualisation of proteins with a fluorescent tag was achieved using a DeltaVision RT microscope (Applied Precision), a 100× UplanSApo 1.4 numerical aperture oil immersion objective lens (Olympus), SoftWoRx image acquisition software (Applied Precision) and a CoolSnap HQ charge-coupled device camera (Photometrics). GFP, YFP and mCherry were visualised with an ET filter set or a JP3 filter set was used to distinguish between GFP and YFP when expressed in the same yeast strain.

2.6.2 *Image acquisition*

Image acquisition was performed following the methodology described in Tanaka *et al*. (2010). Typically, cells expressing a fluorescent protein were immobilised on an agarose pad and ten z-section images spaced 0.5 μm apart were taken at ambient temperature (23°C). For time-lapse imaging a series of z-sections were collected every 15 seconds for 5 minutes. An exposure time to excitation light was typically 0.1 seconds but this varied depending on the signal intensity of target samples.

2.6.3 *Image analysis*

Acquired images were deconvolved using the Spinlock Cluster Deconvolution server (College of Life Sciences) and z-sections were typically projected with maximum intensity signals to 2D images with Volocity image analysis software (Perkin Elmer). Statistical analysis of data obtained from microscopy experiments was performed as described in the legend of the relevant figures.

2.7 SGA screening and data analysis

2.7.1 *Query strain construction*

The *alk1*Δ and *alk2*Δ single mutant query strains were generated by transforming DLY7325 with an *NATMX4* cassette amplified using primers with gene specific flanking sequences to delete the genes of interest (SJC614, SJC617). The *alk1*Δ *alk2*Δ double mutant query strain was generated by sequential transformation of strain Y7092 with *NATMX4* and *HPHMX4* cassettes to delete *ALK1* and *ALK2* respectively. The resulting strain was then crossed by Dr. Peter Banks to generate a strain with the same complement of drug resistance and auxotrophic markers as the single mutant query strains (SJC620-1).

2.7.2 *SGA screening*

The SGA screens were funded by an MRC Centenary Award and performed in collaboration with Prof. David Lydall at the University of Newcastle. The screens themselves were carried out by Dr. Peter Banks (High Throughput Screening Facility Manager) following previously described methodology (Tong and Boone, 2006). Briefly, the query strains generated in this study were crossed with a collection of around 5000 viable gene deletion mutants (Winzeler *et al*. 1999, Giaever *et al*. 2002) and approximately 800 compromised alleles of essential genes (Breslow *et al*. 2008). Funds were also allocated to allow me to spend 3 days at the facility to work alongside Dr. Banks which allowed me to be involved in several key steps in the screening process and gain experience using the equipment.

2.7.3 *Data analysis*

The raw interaction data was analysed and filtered as described in Chapter 4. Gene ontology (GO) enrichment analysis was performed with the BiNGO plug-in (v2.44; Maere *et al*. 2005) for the open-source network visualisation software Cytoscape (v2.82; Smoot *et al*. 2011; www.cytoscape.org). The latest ontology and annotation files were used in the analysis (www.geneontology.org). For details of the parameters and output, see Appendix Table A4.

CHAPTER 3

CDK-dependent phosphorylation of Ipl1 prevents premature localisation of Ipl1 to the mitotic spindle in metaphase

3.1 Introduction

Temporally regulated phosphorylation of a wide range of proteins by cyclin-dependent kinases (CDKs) is critical for timely and coordinated progression through the cell cycle. Association of stage-specific cyclins with CDKs differentially targets the kinase activity towards specific substrates. Amongst this plethora of confirmed and putative CDK substrates are the components of the CPC. Consensus CDK phosphorylation motifs can be found in each of the *S. cerevisiae* CPC proteins (Ipl1, Sli15, Bir1, Nbl1; see Appendix Fig. A1). Some of these motifs have been confirmed as targets for phosphorylation by CDK and shown to have functional significance. For example, dephosphorylation of residues targeted by CDK in Sli15/INCENP has been shown to be required for efficient translocation of the CPC from the centromere/kinetochore in metaphase to the central spindle in anaphase in budding yeast and human cells (Pereira & Schiebel, 2003; Parry *et al*., 2003; Gruneberg *et al*., 2004; Hümmer & Mayer, 2009). This change in the localisation of the CPC has been proposed to be required to prevent checkpoint reactivation when tension between sister chromatids is lost upon entry into anaphase (Mirchenko & Uhlmann, 2010; Vázquez-Novelle & Petronczki, 2010), and also for other functions such as the regulation of septin dynamics at the bud neck (Thomas & Kaplan, 2007).

Aurora B homologues in a variety of different species contain putative CDK phosphorylation sites. Many of these sites are found within the less well conserved N-terminal domains, although in some species, such as *S. cerevisiae* and *D. melanogaster*, there are sites within the C-terminal kinase domain (Fig. 3.1 A). Previous studies have demonstrated that the budding yeast Aurora B homologue Ipl1 is phosphorylated by the yeast CDK Cdc28 (see next section for references), although the functional significance of these post-translational modifications were unknown prior to this study (Fig. 3.1 B).

Are these modifications required to regulate Ipl1 kinase activity, localisation or binding to other proteins? In this chapter a potential functional role for Cdc28-dependent phosphorylation of Ipl1 was investigated.

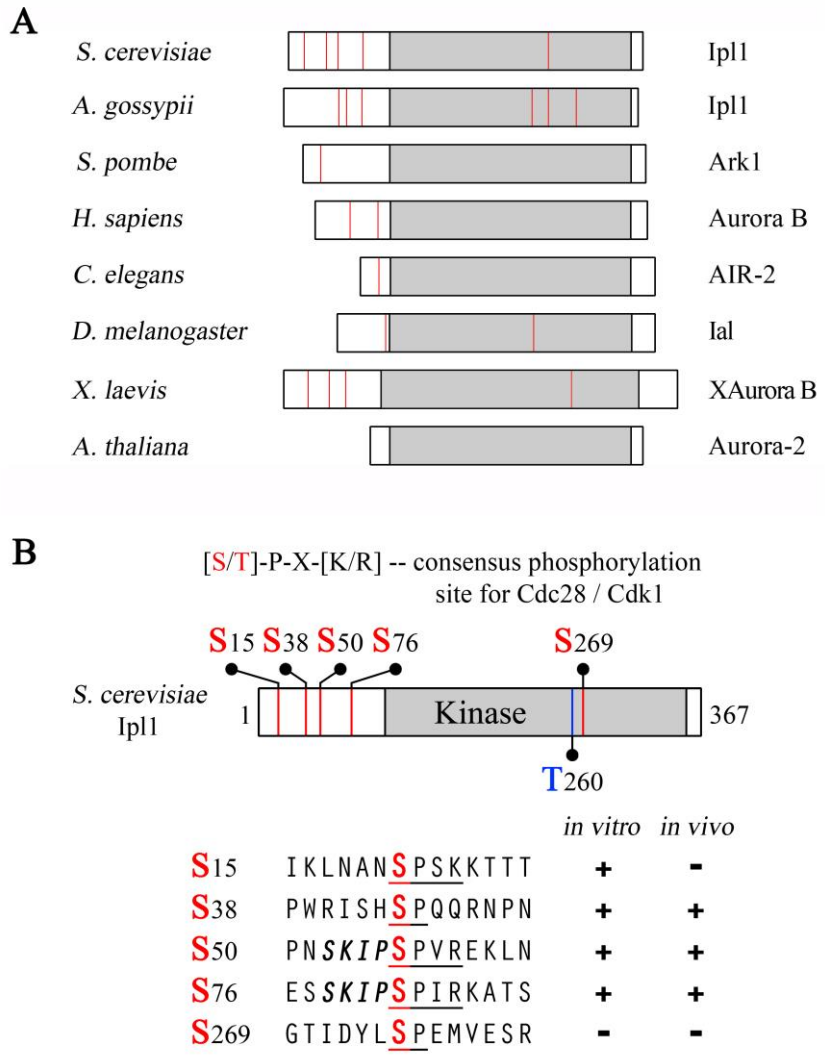

Figure 3.1. Cdc28/Cdk1 phosphorylation motifs in Ipl1 and other Aurora B homologues. (A) Aurora B homologues from a number of different species contain Cdk1 phosphorylation motifs (red). A large proportion of these Cdk1 consensus sites are found within the N-terminal non-kinase domain of the protein (white), although in some species they can also be found in the kinase domain (grey). Database entries searched for CDK consensus sites were: *S. cerevisiae* (P38991); *A. gossypii* (Q755C4); *S. pombe* (O59790); *H. sapiens* (Q96GD4); *C. elegans* (O01427); *D. melanogaster* (Q9VKN7); *X. laevis* (Q6GPL3); *A. thaliana* (Q683C9). (B) Ipl1 has five consensus Cdc28 sites in total (red). Four are located within the non-kinase N-terminus and a fifth site that is located in the kinase domain close to the canonical threonine residue of the activation loop ('T-loop'; blue). All four of the N-terminal sites have been mapped following phosphorylation *in vitro* but only three have been identified *in vivo* (see main text for references).

3.2 Mutation of confirmed and putative CDK phosphorylation motifs in Ipl1

Cdc28 is the major CDK responsible for coordinating passage through the cell cycle in budding yeast. Previous studies have demonstrated that the N-terminus of Ipl1 is phosphorylated by Cdc28 both *in vitro* and *in vivo*. Analysis of the full length peptide sequence of Ipl1 (367 amino acids; Appendix Fig. A1) reveals a total of three sites that conform to the full consensus CDK phosphorylation motif [$^{S}/_{T}$-P-X-$^{K}/_{R}$] (S15, S50, S76) and a further two sites (S38, S269) that have the minimal CDK phosphorylation motif [$^{S}/_{T}$-P] (Fig. 3.1 B). Although all of the N-terminal sites have been shown to be phosphorylated by Cdc28 *in vitro* (Chang *et al*., 2004; Zimniak *et al*., 2012) only three (S38, S50, S76) have been confirmed *in vivo* (S38: Chi *et al*., 2007; Smolka *et al*., 2007; Huber *et al*., 2009; S50: Gnad *et al*., 2009; Soufi *et al*., 2009; Soulard *et al*., 2010; Zimniak *et al*., 2012; S76: Cheeseman *et al*., 2002; Holt *et al*., 2009; Zimniak *et al*., 2012). The functional relevance of these post-translational modifications was unclear. Four of these consensus sites are located in the non-kinase N-terminus of the protein within the first 80 amino acids. The S76 site is conserved in many fungi and in *S. cerevisiae*, the motif is embedded in a repeated sequence (-SKIPSP[$^{I}/_{V}$]R-) shared with the S50 site (Fig. 3.1 B).

To investigate whether or not phosphorylation of these residues play a role in the regulation of Ipl1, the serine residues within these motifs were mutated to alanine residues, individually and in combination, to create a series of non-phosphorylatable mutants. This was achieved by using a two-step method to introduce single and multiple mutations at a single *IPL1* genomic locus in a wild-type diploid strain, followed by tetrad dissection to isolate haploid mutants (see Methods; Toulmay & Schneiter, 2006). This approach was used for several reasons. Firstly, expression from the *IPL1* genomic locus ensures defined copy number, homogenous expression across the cell population

and expression of the protein at endogenous levels. Secondly, generating haploid mutants from heterozygous diploid strains makes no assumptions about whether particular substitutions might be lethal or drive selection of suppressor mutations and is therefore an unbiased method for determining associated phenotypes. Once generated these mutants were assayed for any robust growth defects, including altered growth rate, temperature sensitivity and hypersensitivity to the microtubule destabilising drug benomyl. No obvious growth defects were observed when comparing the wild-type and mutant strains (Fig. 3.2 A). A previous study had reported that mutation at the S76 position resulted in a temperature sensitive phenotype (Francisco & Chan, 1994), but this finding could not be replicated in the current study. A series of phospho-mimetic mutants were also generated, in which each serine residue within the CDK motif was replaced with glutamic acid residues to mimic constitutive phosphorylation at these sites. This series of mutants was also tested for robust growth phenotypes but again none were observed (Fig. 3.2 A), with the sole exception that viable haploid strains carrying the *ipl1-S269E* mutation could not be isolated. Tetrad analysis was performed on four independently verified diploid strains heterozygous for the *ipl1-S269E* mutation and each displayed the same 2:2 segregation pattern (Fig. 3.2 B). Additionally, mutants could not be isolated by transforming the *ipl1-S269E* mutant allele directly into a wild-type haploid strain. Intriguingly, S269 is positioned nine amino acids downstream of the canonical threonine residue of the activation loop ('T-loop') in the heart of the kinase domain. However, alignment of Ipl1 homologues from several different species indicates that this residue is most often a proline residue and only appears to be a serine residue in several species within the *Saccharomycetaceae* family including *Kluyveromyces lactis*, *Candida glabrata* and *Ashbya gossypii* (Fig. 3.2 C).

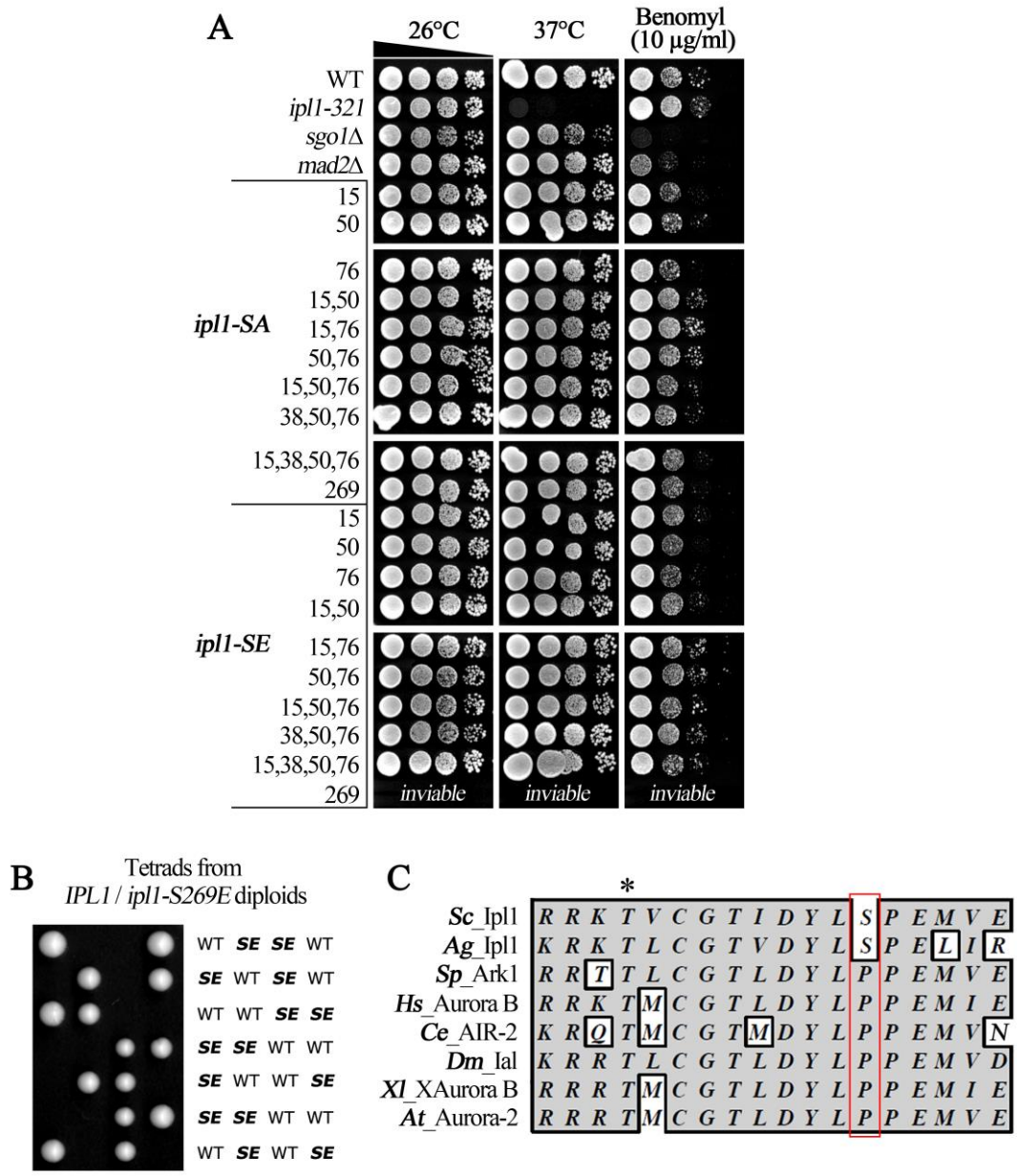

Figure 3.2. Mutation of CDK phosphorylation motifs in Ipl1. (A) The single and multiple Ipl1 CDK site mutants were spotted in 10-fold serial dilutions onto YPAD medium to test for any growth defect, temperature sensitivity or hypersensitivity to benomyl. All the generated mutant combinations displayed no obvious growth phenotype and behaved as wild-type except for the *ipl1-S269E* mutation, which was lethal. (B) Tetrad dissection of a diploid *IPL1*/*ipl1-S269E* strain highlights the lethality associated with this mutation. This tetrad analysis is representative of four independent diploid strains tested. (C) Sequence alignment of the region surrounding the S269 position in Ipl1 and other Aurora B homologues. S269 and the equivalent positions in other species are indicated by the red box. This residue is only a serine in several yeasts and is in close proximity to the canonical threonine residue of the activation loop/T-loop (*). Key to sequence database entries: *S. cerevisiae* (P38991), *A. gossypii* (Q755C4), *S. pombe* (O59790), *H. sapiens* (Q96GD4), *C. elegans* (O01427), *D. melanogaster* (Q9VKN7), *X. laevis* (Q6GPL3), *A. thaliana* (Q683C9).

3.3 Chromosome bi-orientation and segregation are not affected in Ipl1 CDK site mutants

Although no strong growth defects were apparent in the initial set of assays (excluding *ipl1-S269E*), the Ipl1 CDK site mutants could confer more subtle phenotypes not revealed by the previous assays. Ipl1 has been shown to be required for the destabilisation of syntelic microtubule attachments to allow the correct bi-oriented kinetochore-microtubule attachments to be made (reviewed in Lampson & Cheeseman, 2010; Musacchio, 2011; Carmena *et al*., 2012). Without properly regulated Ipl1 kinase activity and localisation, these syntelic attachments may persist, resulting in an increased frequency of mono-oriented chromosomes and aberrant chromosome segregation as cells progress into anaphase. Two different methods were used to test whether chromosome bi-orientation or segregation were perturbed in strains carrying the Ipl1 CDK site mutations. The first approach involved the generation of a series of strains where the loss of a supernumerary chromosome fragment could be visualised in a colony sectoring assay. Loss of the chromosome fragment carrying the *SUP11* gene results in the formation of a red colony colour due to the inability to supress the *ade2-1* mutation present in the genetic background of the strains being used (Fig. 3.3 A). The number of half sectored colonies in relation to the total number of colonies can then be used to calculate the chromosome loss rate per cell division (see Methods). Each of the Ipl1 CDK site mutants tested behaved in a comparable manner to a wild-type strain and showed no significant increase in chromosome loss rate, whereas the temperature sensitive *bir1-17* mutant, used here as a positive control and described previously by Makrantoni & Stark (2009), displayed a greater than 20-fold increase in loss rate even when grown at the 26°C permissive temperature (Fig. 3.3 B).

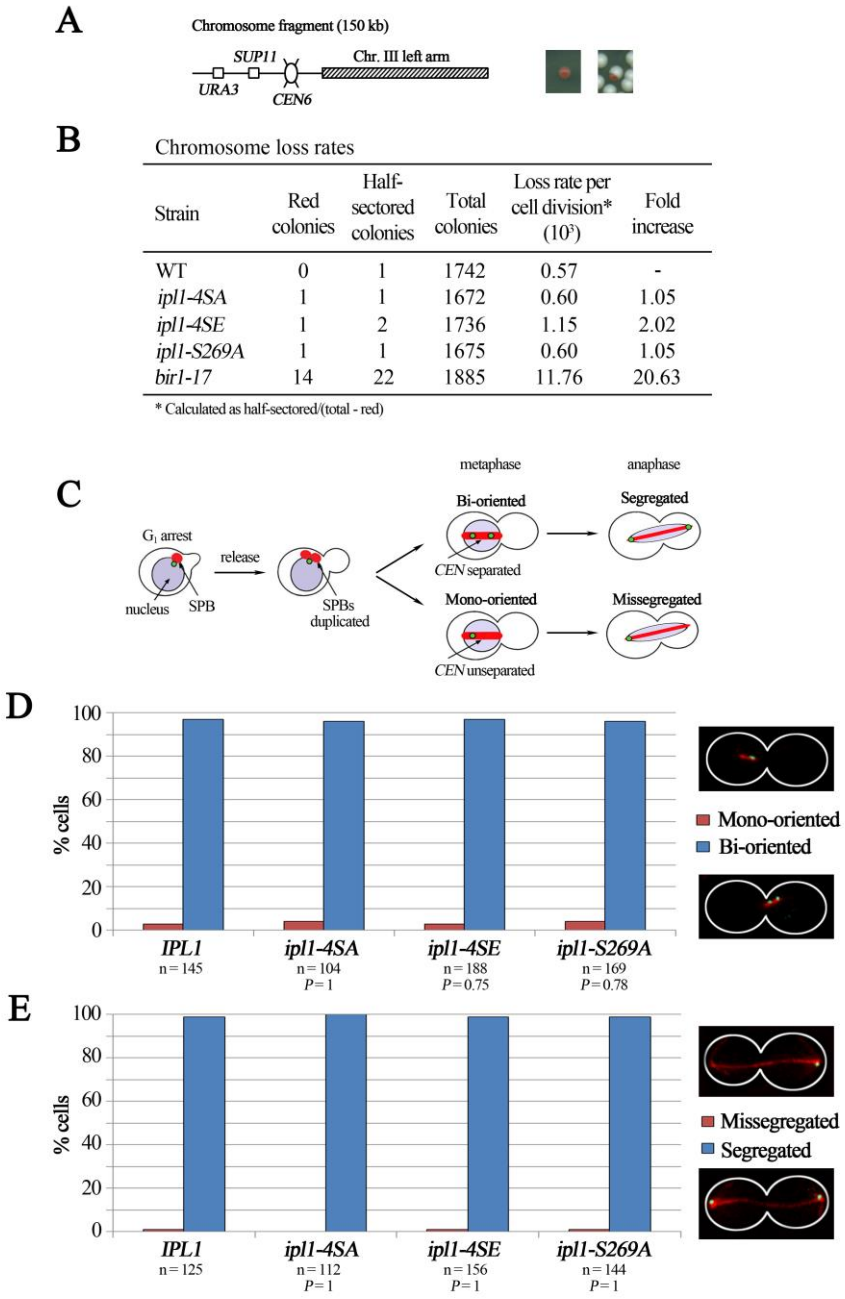

Strain	Red colonies	Half-sectored colonies	Total colonies	Loss rate per cell division* (10^{-5})	Fold increase
WT	0	1	1742	0.57	-
ipl1-4SA	1	1	1672	0.60	1.05
ipl1-4SE	1	2	1736	1.15	2.02
ipl1-S269A	1	1	1675	0.60	1.05
bir1-17	14	22	1885	11.76	20.63

* Calculated as half-sectored/(total - red)

Figure 3.3. *IPL1* mutant cells show no chromosome bi-orientation or segregation defects. (A) Loss of the indicated chromosome fragment was monitored in a colony sectoring assay by the formation of a red colony colour. Representative images of red and half-sectored colonies are shown. (B) Quantification of chromosome loss rates for wild-type (WT) and *ipl1* mutant strains. *bir1-17* was used as a positive control. (C) Wild-type (WT) and *ipl1* mutant cells containing *CEN3-(tetO)*$_{336}$, *tetR-GFP*, *YFP-TUB1* and p*MET3-CDC20* were arrested in G_1 with α-factor and released to a metaphase block in rich medium supplemented with 5 mM methionine (to deplete Cdc20) to assess bi-orientation, and then subsequently released into anaphase (in medium lacking methionine) to assess segregation. Quantification of (D) chromosome bi-orientation and (E) segregation. Representative images from the respective image sequences are shown. n = total number of cells scored for each strain. *P*-values are two-tailed and were calculated using Fisher's exact test comparing mutants with the wild-type.

The second approach involved the generation of control and *ipl1* mutant strains in which bi-orientation and chromosome segregation could be monitored microscopically and in real-time. Microtubules were visualised through fluorescently tagged tubulin (YFP-Tub1) and sister centromeres on chromosome III were visualised by tetR-GFP binding to an array of *tet* operators inserted in the pericentromeric region of *CEN3*. In metaphase arrested cells, bi-oriented chromosomes were scored where there was a dynamic splitting and reassociation of '*CEN*-dots', whereas mono-oriented chromosomes were scored in instances where there was only a single unresolved *CEN*-dot visible (Tanaka *et al*., 2000). Chromosome segregation can also be monitored in these cells by allowing them to progress into anaphase. Proper chromosome segregation can be inferred when two separate dots are visible at opposite ends of the elongated anaphase spindle (Fig. 3.3 C). Five minute time-lapse image sequences were taken for multiple fields and over 100 metaphase arrested cells were scored for bi-orientation or persistent mono-orientation (Fig. 3.3 D). Cells were then released from metaphase and over 100 cells were also scored for proper segregation (Fig. 3.3 E). The data obtained from these experiments showed that there was no statistically significant difference in the incidence of chromosome mono-orientation or missegregation in the *ipl1* mutants compared to wild-type.

3.4 Spindle assembly checkpoint signalling is not defective in *ipl1-4SA* and *ipl1-4SE* cells

Ipl1 has previously been shown to be required for spindle checkpoint activation in response to a lack of tension between sister chromatids. Biggins & Murray (2001) demonstrated that the temperature sensitive *ipl1-321* mutant can still activate the spindle checkpoint in response to microtubule depolymerisation induced by nocodazole but cannot in response to a lack of tension in a *mcd1-1* (*scc1*) cohesin mutant. If Ipl1 is

incorrectly localised or regulated then it is reasonable to hypothesise that checkpoint signalling in response to a lack of tension may be compromised. To address this possibility, a series of strains were generated in which spindle checkpoint signalling under several conditions could be visualised by monitoring the levels of the yeast securin Pds1. Wild-type, *ipl1-4SA* and *ipl1-4SE* cells expressing Pds1-myc$_{18}$ were arrested in G_1 with α-factor and released into three different media. These cells also expressed Scc1, a subunit of the cohesin complex, under control of the *GAL* promoter (p*GAL-SCC1*) to allow the conditional depletion of Scc1 and consequently the generation of tensionless sister chromatid pairs. Cells were released into medium containing galactose (to maintain *SCC1* expression) with or without benomyl and into medium containing glucose to deplete Scc1. Cells were harvested at the indicated times after release and Pds1 levels were determined by western blot. The *ipl1-4SA* and *ipl1-4SE* cells behaved similarly to wild-type under each condition. Pds1 levels rose and fell when the cell cycle was not perturbed and levels persisted when treated with benomyl and when Scc1 was depleted (Fig. 3.4). These results suggest that the *ipl1-4SA* and *ipl1-4SE* mutants are not defective in spindle checkpoint signalling in response to microtubule depolymerisation or lack of sister chromatid tension.

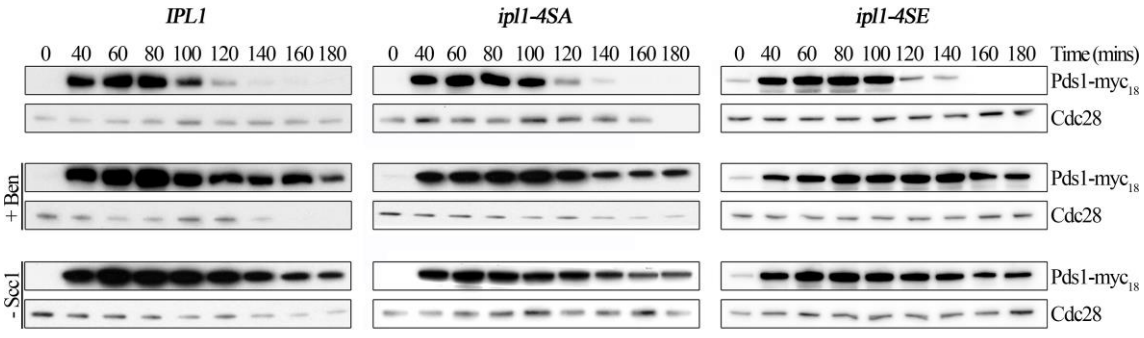

Figure 3.4. Spindle checkpoint signalling is not defective in *ipl1-4SA* and *ipl1-4SE* cells. Wild-type, *ipl1-4SA* and *ipl1-4SE* cells expressing Pds1-myc$_{18}$ and Scc1 under control of the *GAL* promoter were synchronised in G_1 with α-factor and released into medium with or without benomyl or with glucose to repress the expression of *SCC1*. Samples were taken at the indicated times and analysed by western blotting. Cdc28 detected by an anti-Cdc28 antibody was used as a loading control.

3.5 Ipl1-4SA is prematurely loaded onto spindle microtubules in metaphase

Previous studies have demonstrated that Cdc14-dependent dephosphorylation of CDK phosphorylated sites in Sli15/INCENP is required for the translocation of the CPC from centromeres in metaphase to the central spindle in anaphase (Pereira & Schiebel, 2003; Parry *et al*., 2003; Gruneberg *et al*., 2004; Hümmer & Mayer, 2009). It stands to reason that the same may apply to phosphorylated sites on Ipl1. A series of strains were generated to test whether Ipl1 localisation was affected in cells carrying the Ipl1 N-terminal mutants. This was achieved by fusing an in-frame *EGFP* cassette immediately prior to the *IPL1* stop codon of the wild-type and mutant sequences at the *IPL1* locus. Expression of Ipl1-EGFP in these strains was confirmed by microscopy. These cells were synchronised in G_1 with α-factor and released to a metaphase block through Cdc20 depletion (p*MET3-CDC20*). Five minute time-lapse image sequences were taken and over 100 cells were analysed for each strain. *IPL1* wild-type and *ipl1-4SE* mutants displayed a diffuse localisation in the majority of cells. In contrast to this, the *ipl1-4SA* mutants displayed a strong localisation to the metaphase spindle ($P < 0.0001$, Fig. 3.5 A, B). This would suggest that the loss of CDK phosphorylation in the Ipl1-4SA mutant allows either direct or indirect association with spindle microtubules. Ipl1 has previously been shown to bind to the yeast microtubule plus end-tracking EB1 homologue Bim1 (Zimniak *et al*., 2009) and EB1 has been shown to interact with other proteins through a conserved SxIP motif (Honnappa *et al*., 2009). Two of the four phosphorylatable serine residues that form part of the N-terminal CDK phosphorylation motifs in Ipl1 (S50, S76) lie immediately downstream of a SKIP motif (Fig. 3.1 B). Could the loss of the adjacent CDK phosphorylatable serine residue result in premature binding of Ipl1-4SA to Bim1 and subsequently the metaphase spindle? To begin to address this, *BIM1* was knocked out in the *ipl1-4SA* strain. In these cells the premature spindle localisation of Ipl1-4SA was absent and appeared similar to wild-type (Fig. 3.5

A, B). Together these results suggest that the loss of CDK regulated phosphorylation of Ipl1 results in the premature association of Ipl1 with the metaphase spindle, and that this interaction is dependent on Bim1.

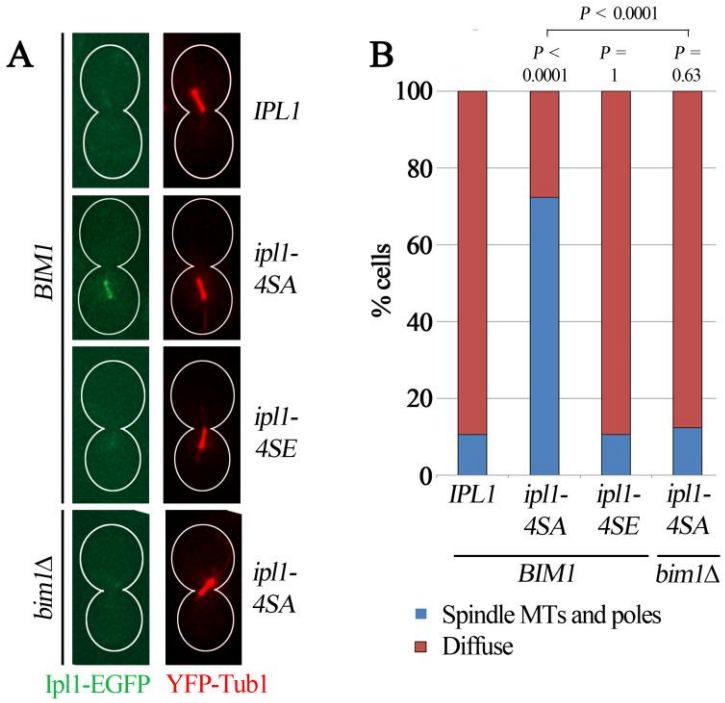

Figure 3.5. Ipl1-4SA is prematurely loaded onto spindle microtubules in metaphase. (A) Cells expressing YFP-Tub1 and either wild-type or mutant Ipl1-EGFP were synchronised in G_1 with α-factor and released to a metaphase block through depletion of Cdc20. (B) Localisation was scored in over 100 cells for each strain. n is the number of cells scored for each strain: *IPL1*, n = 190; *ipl1-4SA*, n = 145; *ipl1-4SE*, n = 190; *ipl1-4SA*, n = 179. *P*-values are two-tailed and were calculated using Fisher's exact comparing mutants with the wild-type unless otherwise indicated.

3.6 Genetic interaction of *IPL1* and *SLI15* mutants

Serine 335 of Sli15 is one of a number of serine residues that lies within a consensus CDK phosphorylation motif (Appendix Fig. A1). Mutating this residue to alanine (*sli15-S335A*) has previously been shown to result in the premature localisation of Sli15 to the metaphase spindle (Pereira & Schiebel, 2003). A concurrent study

published by Zimniak *et al*. (2012) shows that a *ipl1-2SA* (S50A, S76A) mutant also binds prematurely to the spindle in metaphase. These observations suggest that a degree of redundancy may exist between Ipl1 and Sli15 for localisation of the CPC to the spindle. Preventing or mimicking phosphorylation at these sites in both proteins may result in an additive phenotype. To begin to investigate this possibility, the *ipl1-2A* and *ipl1-2E* mutants generated in this study were crossed with *sli15-S335A* and *sli15-S335D* mutants respectively. All mutant combinations were viable and their fitness was assessed by spotting onto the appropriate medium. Interestingly, no additive growth phenotype was observed when these mutations were combined and grown at either 26°C or 37°C to test for thermosensitivity or in the presence of the microtubule destabilising drug benomyl (Fig. 3.6 A). A concurrent study in the Stark laboratory (Makrantoni *et al*., unpublished) and another by Nakajima *et al*. (2011) found that Ipl1-dependent phosphorylation of Sli15 also influences CPC localisation. They showed that alanine substitution mutations at a number of phosphorylatable residues within Ipl1 consensus sites resulted in the premature localisation of Sli15 to the spindle in metaphase. This provides evidence for an additional mode for regulating CPC localisation and suggests that a further level of redundancy may exist. Additional strains were generated that combined the *ipl1* CDK site mutants with *sli15* alleles mutated at CDK and/or Ipl1 consensus sites. All mutant combinations were viable and were spotted onto the appropriate medium to compare growth (Fig. 3.6 B). Combinations of alleles with mutations to alanine residues that would be expected to localise prematurely and strongly to the metaphase spindle showed no growth defect, thermosensitivity or sensitivity to benomyl. Conversely, all strains carrying phospho-mimetic mutations of the Ipl1 consensus sites in Sli15 showed a marked sensitivity to benomyl compared to all the other strains tested. The *sli15-20D* strain exhibited mild thermosensitivity and a marked sensitivity to benomyl. The combination of *ipl1-2SE* and *sli15-20D* intensified

this thermosensitivity and also resulted in a mild growth defect when grown 26°C, indicated by the smaller colony size. Interestingly, this growth defect was not observed in *ipl1-2SE sli15-20D, S335D* strains and the thermosensitivity was recovered somewhat although both strains carrying the *sli15-20D, S335D* allele displayed the same intermediate level of thermosensitivity compared with *sli15-20D* and *ipl1-2SE sli15-20D* mutants. These results suggest that premature localisation of the CPC to the spindle does not interfere with progression through mitosis. On the other hand, it would appear that preventing proper spindle localisation of the CPC in the case of the phospho-mimetic alleles is more of an issue when mitosis is stressed due to increased temperature or microtubule depolymerisation.

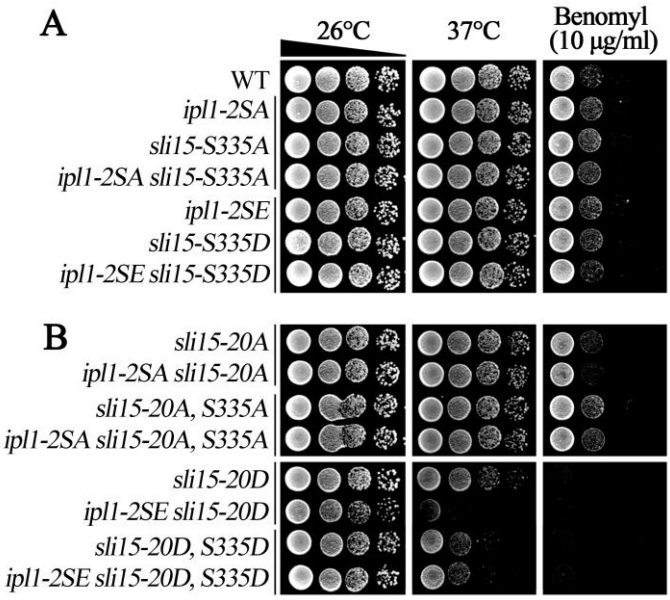

Figure 3.6. Combinations of *ipl1* and *sli15* alleles defective in proper CPC localisation. The indicated strains were spotted in 10-fold serial dilutions onto YPAD medium to test for any additive growth defect, temperature sensitivity or hypersensitivity to benomyl. (A) Combinations of *ipl1* and *sli15* CDK site mutants. (B) Combinations of *ipl1* CDK site mutants and *sli15* alleles mutated at both CDK-dependent and Ipl1-dependent sites.

3.7 Discussion

The localisation and function of many proteins can be influenced by discrete post-translational modifications. Phosphorylation of proteins is a common regulatory modification and the Sli15 and Bir1 components of the budding yeast CPC have all been shown to be phosphorylated at CDK consensus sequences *in vivo*. While the phosphorylation of Bir1 is required for proper anaphase spindle elongation and localisation of Ndc10 (Bouck & Bloom, 2005; Widlund *et al*., 2006) and Cdc14-depenedent dephosphorylation of Sli15 is required for translocation of the CPC from centromeres to the spindle in anaphase (Pereira & Schiebel, 2003), it was unclear whether the regulated modification of CDK sites in Ipl1 is important for its function prior to this study.

To begin to investigate whether modification at these sites in Ipl1 has any functional significance, the phosphorylatable serine residues contained within the CDK consensus motifs were mutated individually and in combination to either non-phosphorylatable alanine residues or phospho-mimetic glutamic acid residues. All single and multiple mutants of the N-terminal cluster of sites behaved like wild-type when assayed for growth defects, thermosensitivity or hypersensitivity to benomyl. A previous study had suggested that mutation of S76 to alanine resulted in a temperature sensitive phenotype (Francisco & Chan, 1994), although this was not found in the current study. The reason for this discrepancy is unclear although it may be explained, at least in part, by the fact that the previous study used a plasmid based system to harbour the mutations and support growth of an *IPL1* knockout strain, whereas the mutations were introduced directly into the genomic locus in this study. Mutation of the C-terminal CDK site located within the highly conserved kinase domain close to the T-loop produced a different result. While the *ipl1-S269A* mutant was viable and behaved

like wild-type, the *ipl1-S269E* mutation was lethal. Tetrad dissection of four independent heterozygous diploid strains yielded no viable haploid *ipl1-S269E* strains. Additionally, mutants could not be isolated by direct transformation into a haploid strain, which suggests that the inability to isolate the mutant from the tetrad dissection was not a result of issues in meiosis. While these data may suggest that phosphorylation of S269 could play a significant role in the regulation of Ipl1 there are a number of things to consider. Firstly, S269 is the only phosphorylatable CDK site residue in Ipl1 that has not been identified as being phosphorylated either *in vitro* or *in vivo*. Additionally, the residue equivalent to S269 is only conserved amongst a subset of yeast species, so any regulatory mechanism related to this residue is unlikely to be widely conserved. Also, while mutation to alanine absolutely prevents phosphorylation, mutation to glutamic acid does not necessarily mimic phosphorylation. It is possible that S269 is not phosphorylated *in vivo* and that replacing it with an amino acid that has a large, negatively charged side chain disrupts the structure and function of the T-loop and kinase domain, resulting in lethality. More research will be required to ascertain whether S269 is phosphorylated by Cdc28, and whether the finding that the *ipl1-S269E* mutation is lethal provides information that is useful for understanding Ipl1 function.

Subsequent experiments were performed to characterise the Ipl1 CDK site mutants further. Ipl1 activity has been shown to be required to promote bi-orientation of sister chromatids (Biggins & Murray, 2001; Kang *et al*., 2001; Tanaka *et al*., 2002). If the *ipl1* mutants are incorrectly localised or regulated then it would be reasonable to hypothesise that an increase in mono-oriented and missegregated chromosomes may be observed. However, no defects in chromosome bi-orientation or segregation were identified. Previous studies have also demonstrated that an *ipl1-321* mutant is unable to activate the spindle checkpoint in response to a lack of tension between sister

chromatids but can in response to microtubule depolymerisation (Biggins & Murray, 2001). However, the *ipl1-4SA* and *ipl1-4SE* mutants generated in this study can respond to both reduced tension and microtubule depolymerisation. Taken together, these results suggest that the bi-orientation and tension-dependent checkpoint signalling functions of Ipl1 are not affected when the CDK sites are mutated.

In contrast, what does appear to be affected is the localisation of Ipl1. In metaphase-arrested cells Ipl1-4SA prematurely localised to the spindle whereas wild-type and Ipl1-4SE displayed a diffuse localisation. This premature localisation was similar to that described for Sli15 CDK site mutants (Pereira & Schiebel, 2003). Recombinant Ipl1 has been shown to bind directly to microtubules using *in vitro* co-sedimentation assays (Kang *et al*., 2001) so it is possible that without CDK phosphorylation, Ipl1-4SA can bind directly to microtubules in metaphase. However, both S50 and S76 lie immediately downstream of SKIP motifs, which are consensus sequences for Bim1/EB1 binding (Honnappa *et al*., 2009). Ipl1 and Bim1 have previously been shown to form a stable complex (Zimniak *et al*., 2009) so the possibility that Ipl1-4SA may be binding to microtubules indirectly through interaction with Bim1 was considered. Indeed, when *BIM1* was deleted, Ipl1-4SA exhibited a diffuse localisation in metaphase similar to wild-type, suggesting that the premature spindle localisation of Ipl1-4SA was due to interaction with Bim1. This is supported by a concurrent study that was recently published. Zimniak *et al*. (2012) demonstrated that Ipl1 interacts with Bim1 through the SKIP motifs and that CDK-dependent phosphorylation of the adjacent serine residues (S50, S76) inhibits this interaction.

It seemed curious that such a striking change of localisation in the *ipl1-4SA* mutant did not affect the viability of the cells or cause defects in bi-orientation or

chromosome segregation. Since previous studies have identified that Sli15/INCENP binding to microtubules is also regulated by CDK phosphorylation (Pereira & Schiebel, 2003; Hümmer & Mayer, 2009) it was hypothesised that combining *ipl1* and *sli15* CDK site mutant alleles may result in a synergistic defect and decreased viability. However, *ipl1-2SA sli15-S335A* and *ipl1-2SE sli15-S335D* double mutants were viable, with no additive growth defect compared to the single mutants and wild-type. While Ipl1-2SA and Sli15-S335A proteins have been shown to localise prematurely to the spindle in metaphase (Pereira & Schiebel, 2003; Zimniak *et al*., 2012), there are additional CDK sites in Sli15 that may contribute to the regulation of microtubule binding. Zimniak *et al*. (2012) were unable to isolate *ipl1-2A sli15-6A* double mutants by crossing, but by using a conditional system to express *ipl1* mutants in *sli15-6A* strains they were able to show that viability is dramatically decreased, suggesting that CDK regulation of both Ipl1 and Sli15 is important for viability. Other studies from the Stark laboratory (Makrantoni *et al*., unpublished) and by Nakajima *et al*. (2011) demonstrated that Ipl1-dependent phosphorylation of Sli15 also inhibits CPC binding to pre-anaphase spindles. Alleles of *sli15* with mutated Ipl1 consensus phosphorylation sites were also combined with Ipl1 and Sli15 CDK site mutants. All combinations of the non-phosphorylatable alleles grew similarly to wild-type whereas the phospho-mimetic alleles displayed growth defects. While the *sli15-20D* mutant was mildly sensitive to temperature and hypersensitive to benomyl, the combination of *ipl1-2E sli15-20D* was significantly temperature-sensitive and even displayed a growth defect when grown at 26°C. This may suggest that preventing proper spindle localisation of the CPC in anaphase is more detrimental than premature localisation to the spindle in metaphase, although further experiments would be required to demonstrate this.

The picture emerging from the data collected during this study and the others mentioned above is that CDK-dependent phosphorylation of Ipl1 and Sli15 and the Ipl1-dependent phosphorylation of Sli15 are important for regulating CPC localisation to the spindle in budding yeast. An important question is whether these mechanisms for CPC localisation are conserved in other organisms. While there is evidence to suggest that CDK phosphorylation of INCENP regulates microtubule binding in human cells (Hümmer & Mayer, 2009), it is unclear whether Aurora B phosphorylation of INCENP has a similar role. Inhibition of Ipl1 in yeast results in the premature localisation of the CPC to the central spindle (Nakajima *et al*., 2011) whereas Aurora B activity is required for central spindle targeting in chicken DT40 cells and rat NRK cells (Murata-Hori *et al*., 2002; Xu *et al*., 2009), suggesting this may not be a conserved mechanism. It is also not clear whether the interaction between Ipl1 and Bim1 observed in *S. cerevisiae* is evolutionarily conserved. The Ipl1/Aurora B homologue in the closely related filamentous fungus *A. gossypii* has CDK phosphorylation motifs at the equivalent positions to S50 and S76. However, these are not preceded by SxIP motifs nor are there any SxIP motifs present in the entire amino acid sequence. The Ipl1/Aurora B homologue in the budding yeast *K. lactis* has neither SxIP motifs nor N-terminal CDK consensus sequences. Based on these observations it seems unlikely that this interaction and mode of microtubule binding is conserved even in closely related fungi. However, while human Aurora B also does not have any SxIP motifs, physical interactions have been reported between Aurora B and EB1 (Sun *et al*., 2008). It is therefore possible that the Aurora B/EB1 interaction is conserved but that the mode of interaction may differ. Alternatively, other proteins may perform a similar role in higher eukaryotes. For example MKlp2, a kinesin-6 motor protein absent in yeast, binds the CPC and is required for its translocation to the spindle midzone and equatorial cortex, where Aurora B activity is essential for cleavage furrow ingression and cytokinesis (Gruneberg *et al*.,

2004; Hümmer & Mayer, 2009; Kitagawa *et al*., 2013). This interaction between MKlp2 and the CPC is negatively regulated by Cdk1 phosphorylation (Hümmer & Mayer, 2009) similarly to the Ipl1-Bim1 interaction (Zimniak *et al*., 2012).

Based on these observations it appears that the mechanisms involved in the targeting of the CPC to the spindle midzone vary in different organisms. Additionally, it would seem that pre-anaphase targeting of the CPC to centromeric chromatin also varies. In budding yeast it appears that the CPC is targeted to the centromere by a single Bir1-dependent interaction. Bir1 binds directly to the Ndc10 subunit of the centromeric DNA-binding budding yeast-specific CBF3 complex, an interaction that requires CDK phosphorylation of Bir1 (Widlund *et al*., 2006; Cho & Harrison, 2011). In fission yeast, Bir1 binds to Sgo2 (Shugoshin), which recognises and binds to histone H2A phosphorylated at a conserved residue by the kinetochore-associated Bub1 kinase (Kawashima *et al*., 2010). This mechanism is conserved in human cells although the interaction between Shugoshin and the CPC is mediated by Borealin rather than Bir1/Survivin (Vader & Lens, 2010). These interactions also require CDK phosphorylation of the respective CPC component (Tsukahara *et al*., 2010). While the recruitment of Shugoshin to centromeres through Bub1 phosphorylation of histone H2A appears to be conserved in budding yeast (Kawashima *et al*., 2010), Bub1 and Sgo1 are not required for CPC localisation or Ipl1 activity (Storchová *et al*., 2011), unlike in fission yeast and human cells (Vanoosthuyse *et al*., 2007; Tsukahara *et al*., 2010). This may suggest that this mechanism for CPC recruitment is not conserved in budding yeast although this remains to be tested. In fission yeast and higher eukaryotes, the phosphorylation of histone H3 on Thr-3 by Haspin kinase also contributes to the centromeric targeting of the CPC (Kelly *et al*., 2010; Yamagishi *et al*., 2010; Wang *et al*., 2010). However, while several Haspin-like kinases have been identified in *S.*

cerevisiae, it is not known whether this function is shared and this will be the subject of the next chapter. While these mechanisms vary between species, it would seem that the regulation of CPC localisation by Cdk1 is an evolutionarily conserved principle.

These differences between *S. cerevisiae* and other organisms may be explained by the fact that budding yeast has a single Aurora kinase whereas vertebrates have Aurora A and Aurora B, each with distinct functions and patterns of localisation (Carmena *et al*., 2009). Although the most well defined roles of Ipl1 correspond to the known functions of Aurora B, Ipl1 has also been implicated in proper bipolar spindle assembly (Kotwaliwale *et al*., 2007), which is an Aurora A-dependent function in higher eukaryotes (Barr & Gergely, 2007; Carmena *et al*., 2009). It is therefore reasonable to hypothesise that Ipl1 carries out the functions of both Aurora A and Aurora B and as a result requires different regulatory patterns. Consistent with this idea, non-phosphorylatable *ipl1* and *sli15* mutants accumulate at spindle poles and microtubules, which resembles Aurora A localisation (Barr & Gergely, 2007; Carmena *et al*., 2009). Differential patterns of phosphorylation of CPC subunits could specifically target the complex to discrete locations at specific times to perform the combined roles of Aurora A and B.

In this study, evidence has been provided suggesting that phosphorylation of Ipl1 by CDK prevents the association of Ipl1 with the mitotic spindle in metaphase. Mimicking or preventing CDK phosphorylation of Ipl1 has no effect on chromosome bi-orientation or cell viability. The premature spindle localisation of Ipl1-4SA appears to be mediated through interaction with the yeast EB1 homologue Bim1, although it is not clear whether this interaction is conserved in other species.

CHAPTER 4

A role for the budding yeast Haspin-like kinases Alk1 and Alk2 in regulating isotropic bud growth and spindle orientation

4.1 Introduction

Haspin kinases are a family of atypical protein kinases that are conserved in many eukaryotic organisms including fission yeast, plants and mammals (Higgins, 2003). Haspin in these organisms has been shown to localise predominantly to chromosomes and phosphorylate histone H3 at Thr-3 (H3-T3ph) during mitosis (Dai *et al*., 2005; Yamagishi *et al*., 2010; Ashtiyani *et al*., 2011). This modification along with Bub1 mediated phosphorylation of histone H2A have recently been identified as being required for the efficient localisation of the CPC to centromeres (Kelly *et al*., 2010; Yamagishi *et al*., 2010; Wang *et al*., 2010). Interest in the Haspin kinases has intensified since this discovery and there is still much to learn with regard to their regulation and any additional functions they may perform.

Two Haspin homologues (Alk1, Alk2) have been identified in the budding yeast *S. cerevisiae* (Higgins, 2001a) although very little is known about them and it is not clear whether they perform the same role as reported for Haspins in other organisms. At the time this work was undertaken, there had only been one publication where Alk1 and Alk2 have been investigated directly. Nespoli *et al*. (2006) identified *ALK1* in a two-hybrid screen using the DNA damage checkpoint protein Ddc1 as bait. They proceeded by attempting to characterise Alk1 and Alk2 and showed that their expression is cell cycle regulated and that the stability of both proteins is regulated by KEN- and D-boxes. Interestingly, they found that both proteins are hyperphosphorylated in response to DNA damage but that neither single nor double knockouts of *ALK1* and *ALK2* are sensitive to DNA damaging agents. Although they were able to show that both have weak autophosphorylation activity, they were unable to detect phosphorylation of histone H3 in *in vitro* kinase assays using recombinant proteins expressed and purified from *E. coli*. In their initial attempts to overexpress and purify the Haspin-like kinases

directly from budding yeast they found that overexpression of Alk2 but not Alk1 blocks progression through mitosis. This phenotype was linked to the kinase activity of Alk2, since overexpression of a hypomorphic kinase-deficient mutant greatly reduced the mitotic delay.

Together, these observations indicate a role for the budding yeast Haspin-like kinases in mitosis although it was still unclear what this role may be. In this chapter the Haspin-like kinases Alk1 and Alk2 were investigated in an attempt to characterise their role in budding yeast mitosis.

4.2 Deletion of *ALK1* and *ALK2* results in a hypersensitivity to the microtubule destabilising drug benomyl

To gain insight into the function of the Haspin-like kinases in budding yeast it was necessary first to knockout both *ALK1* and *ALK2*. Nespoli *et al*. (2006) had previously confirmed that cells remain viable when both of the Haspin-like kinases were knocked out and this finding was replicated in this study. The single and double knockouts showed no obvious growth defect or thermosensitivity (Fig. 4.1 A i) and the double knockout showed no significant loss of viability compared to wild-type cells as determined by two independent assays (Fig. A2). However, when these strains were spotted onto medium containing benomyl it was noticed that the double knockout strain displayed benomyl hypersensitivity (Fig. 4.1 A i). This phenotype can be rescued by complementing the double knockout with plasmid-borne copies of either *ALK1* or *ALK2* (Fig. 4.1 A ii; see 2.3.6 Methods). This confirms that the benomyl hypersensitivity is a result of the loss of both *ALK1* and *ALK2* and not due to the disruption of adjacent genes and also suggests complementary or overlapping functions of these Haspin-like kinases. Deletion of genes encoding spindle checkpoint proteins, such as Mad3, also

results in a hypersensitivity to the microtubule poison benomyl. These cells are unable to activate the spindle assembly checkpoint in response to tensionless or unattached kinetochores and prematurely enter anaphase without properly bi-oriented chromosomes, resulting in aberrant chromosome segregation and ultimately cell death (King *et al*., 2007a; Musacchio & Salmon, 2007). Interestingly, in this spotting assay the *alk1*Δ *alk2*Δ strain appeared to be more sensitive to benomyl than a *mad3*Δ strain (Fig. 4.1 A i).

4.3 Spindle assembly checkpoint signalling is not disrupted in *alk1*Δ *alk2*Δ cells

Hypersensitivity to spindle poisons such as benomyl is a classic hallmark of mutants defective in spindle checkpoint signalling (Straight *et al*., 1996). It was therefore reasonable to hypothesise that Alk1 and Alk2 may have redundant roles in promoting proper checkpoint signalling. Several experiments were designed to address this possibility. Spindle checkpoint mutants die rapidly in liquid cultures supplemented with spindle poisons such as benomyl and nocodazole (Straight *et al*., 1996). Having identified that *alk1*Δ *alk2*Δ cells appeared more sensitive than *mad3*Δ cells when grown on solid medium containing benomyl (Fig. 4.1 A i), it was decided to test how long *alk1*Δ *alk2*Δ cells maintained viability when exposed to benomyl in liquid culture. Cells were grown to mid-log phase and transferred to medium containing 30 μg/ml benomyl. Cells were harvested from these cultures at two hour intervals, washed to remove traces of the drug and plated onto solid rich medium. Viability was scored as the percentage of cells able to form colonies with the number of colonies formed at time zero for each strain normalised to 100%. *ALK1* and *ALK2* single knockouts maintained a similar level of viability to the wild-type control strain whereas the checkpoint deficient *mad2*Δ cells died rapidly (Fig. 4.1 B). Interestingly, *alk1*Δ *alk2*Δ cells retained a level of viability similar to that of wild-type cells after the initial 2 hour exposure to benomyl but then

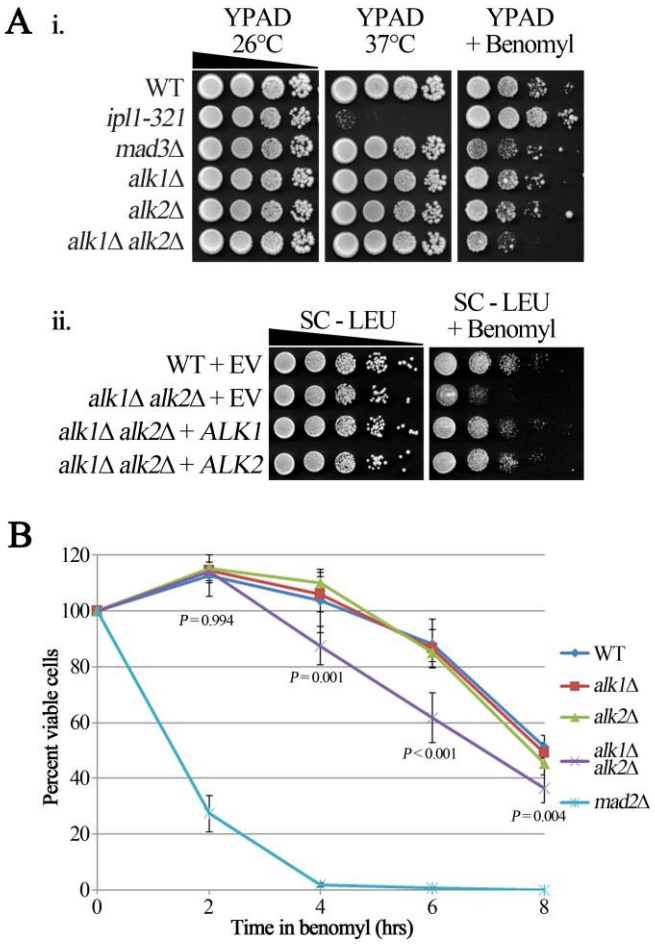

Figure 4.1. Deletion of *ALK1* and *ALK2* results in a hypersensitivity to benomyl. (A) (i) The indicated strains were spotted in 10-fold serial dilutions onto YPAD medium and grown at 26°C, 37°C or at 26°C in the presence of 10 μg/ml benomyl. (ii) Wild-type (WT) or *alk1*Δ *alk2*Δ strains carrying either an empty vector (EV) or a vector containing *ALK1* or *ALK2* as indicated were spotted on SC-LEU medium (to maintain selection for the plasmids) and grown at 26°C in the absence or presence of 10 μg/ml benomyl. (B) The indicated strains were grown in liquid YPAD medium to mid-log phase and transferred to YPAD medium supplemented with 30 μg/ml benomyl. Samples were taken from these cultures at the indicated time-points and plated onto solid YPAD medium lacking benomyl. The viability of these cells was measured as a percentage of cells able to form colonies with the number of colonies formed at time zero for each strain normalised to 100%. Over 500 colonies were present at time zero for each strain and the experiment was performed in triplicate. Error bars represent the standard deviation. Data were subjected to a two way ANOVA test which showed a significant effect of genotype [$F(4, 50) = 461.5$, $P < 0.001$] and time in benomyl [$F(4, 50) = 392.6$, $P < 0.001$] on viability. The interaction between genotype and time was also significant [$F(16, 50) = 40.4$, $P < 0.001$]. Subsequent pairwise comparisons were performed using the Holm-Sidak method to analyse the significance of the variation in the viability of each strain at individual time-points. *P*-values shown are those calculated between WT and *alk1*Δ *alk2*Δ. No statistically significant difference in viability exists between the WT control strain and single *alk1*Δ and *alk2*Δ mutant strains at any time-point.

displayed a marked reduction in viability after this point. However, this loss of viability was nowhere near as dramatic as that of the *mad2*Δ cells (Fig. 4.1 B). These results would suggest that the spindle checkpoint is not absent in *alk1*Δ *alk2*Δ cells although it may be partially compromised. A visual inspection of these cells throughout the experiment also highlighted a curious morphological phenotype associated with *alk1*Δ *alk2*Δ cells. In wild-type cells, exposure to benomyl resulted in a prolonged metaphase arrest evident by the formation of large budded cells with both compartments remaining of approximately equal proportions between 4 and 8 hours, although the overall size of the budded cells was larger after 8 hours. In *alk1*Δ *alk2*Δ cultures supplemented with benomyl, large budded cells were initially formed but rather than both compartments remaining a similar size, one compartment became much larger than the other after

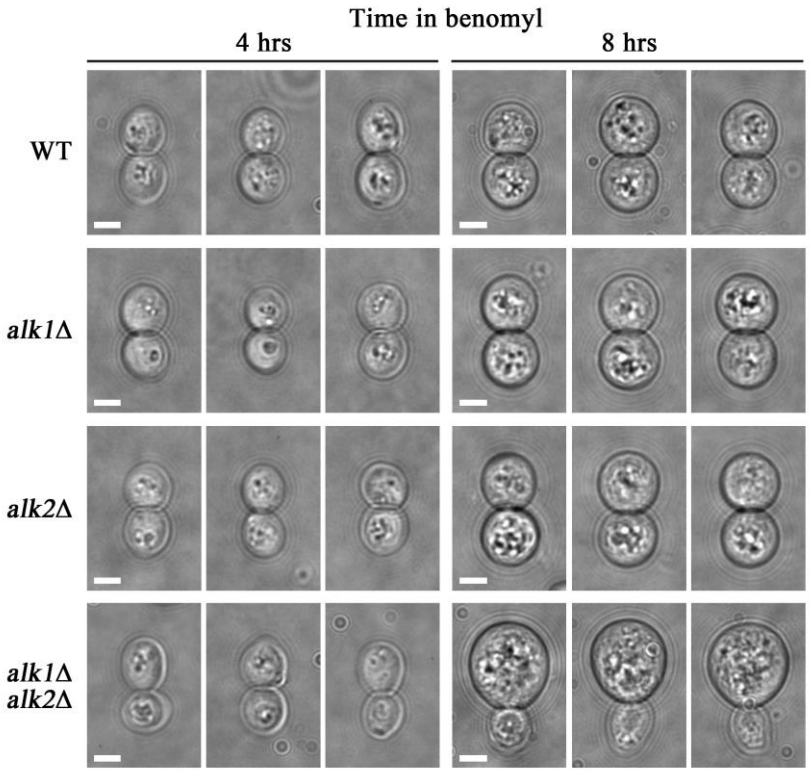

Figure 4.2. Morphology of wild-type and Haspin-like kinase knockout cells when treated with benomyl. Cells of the indicated genotypes were grown to mid-log phase and then transferred to medium containing benomyl. Representative images of different cells after 4 and 8 hours exposure to benomyl. Scale bar represent 3 μm.

8 hours (Fig. 4.2). While it was not possible to quantitate this phenomenon accurately, estimates from the images taken suggested a 6 – 17-fold disparity in the volume of the two compartments after 8 hours.

To gauge more accurately the checkpoint response in *alk1*Δ *alk2*Δ cells, a series of strains were generated in which the progression of the cell cycle and the onset of anaphase could be observed by monitoring the cell cycle regulated expression and degradation of the yeast securin Pds1. Wild-type, *mad3*Δ and *alk1*Δ *alk2*Δ cells expressing Pds1-myc$_{18}$ were arrested in G_1 with α-factor and released into rich medium including or excluding benomyl. Cells were harvested at the indicated time-points after release and Pds1 levels were analysed by western blotting (Fig. 4.3). Pds1 is expressed as cells enter S-phase and levels peak during mitosis. At the onset of anaphase Pds1 is targeted for degradation by the APC/C thus liberating the yeast separase Esp1, which then cleaves cohesin and initiates chromosome segregation. This pattern of expression and degradation can be seen during unperturbed cell cycles in wild-type, *mad3*Δ and *alk1*Δ *alk2*Δ cells (Fig. 4.3). In *mad3*Δ cells, proper checkpoint signalling is absent and in the presence of benomyl these cells are unable to delay cell cycle progression. This is apparent as the Pds1 expression profile observed for *mad3*Δ cells in benomyl medium was similar to that of an unperturbed cell cycle (Fig. 4.3 B). *alk1*Δ *alk2*Δ cells on the other hand behaved like wild-type cells in that Pds1 persisted in the presence of benomyl (Fig. 4.3 A,C).

Taken together, these results suggest that spindle checkpoint signalling is not compromised in *alk1*Δ *alk2*Δ cells and that the hypersensitivity to the spindle poison benomyl is a consequence of some other effect on these cells caused by the loss of Alk1 and Alk2.

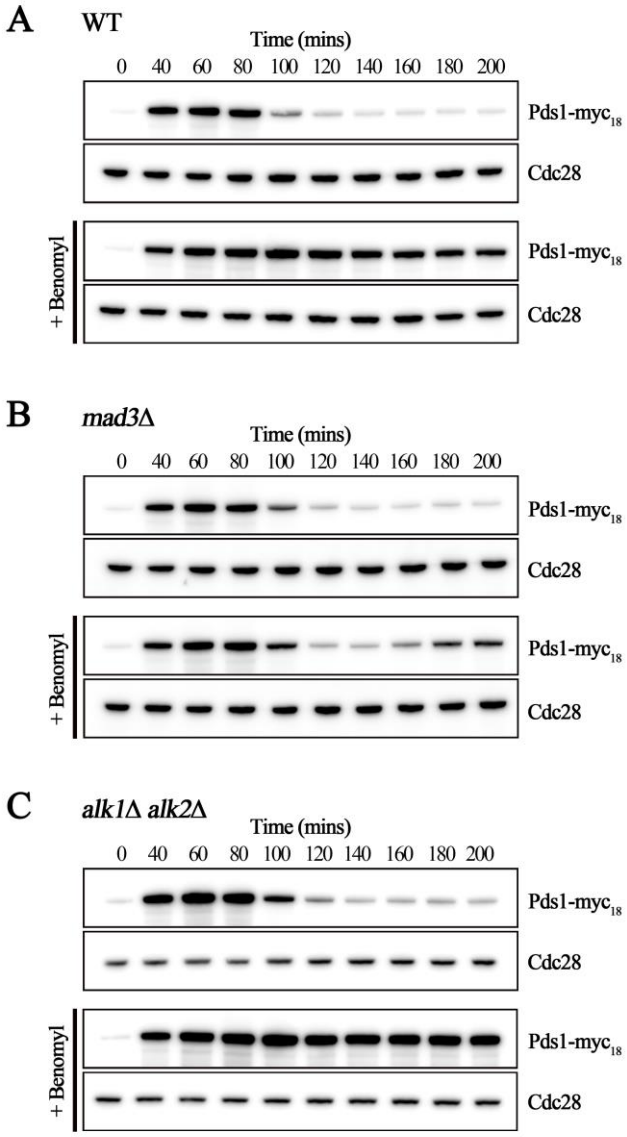

Figure 4.3. Benomyl hypersensitivity of *alk1*Δ *alk2*Δ cells is not a consequence of defective spindle assembly checkpoint signalling. (A) WT, (B) *mad3*Δ (C) *alk1*Δ *alk2*Δ cells expressing Pds1-myc$_{18}$ were synchronised with α-factor and released into YPAD medium with or without benomyl. Samples were taken at the indicated times and analysed by western blotting. Cdc28 detected by an anti-Cdc28 antibody was used as a loading control.

4.4 Alk1 and Alk2 levels peak around the metaphase to anaphase transition and persist when the spindle checkpoint is activated

The levels of human Haspin remain near constant throughout the cell cycle (Dai *et al*., 2005). In contrast to this, the levels of Alk1 and Alk2 have been reported to be cell cycle regulated, peaking in mitosis and late G_2 respectively (Sullivan *et al*., 2004; Nespoli *et al*., 2006). This is consistent with potential mitotic roles for Alk1 and Alk2. Having identified the benomyl hypersensitivity of *alk1*Δ *alk2*Δ cells it was decided to look at how Alk1 and Alk2 levels correspond to the kinetics of Pds1 expression and degradation and whether the two kinases persist in response to spindle checkpoint activation. Strains were constructed that contained C-terminally 3HA-tagged versions of either Alk1 or Alk2 and also expressed Pds1-myc_{18}. These cells were synchronised in G_1 with α-factor and released into rich medium with or without benomyl. Cells were harvested at the indicated time-points after release and protein levels were analysed by western blotting (Fig. 4.4). Alk1 expression peaked after anaphase was triggered at around 100 minutes (Fig. 4.4 A), whereas Alk2 levels were highest immediately prior to anaphase initiation at 80 minutes (Fig. 4.4 B). In contrast to unperturbed cultures in which both Alk1 and Alk2 had largely disappeared by 40 minutes after the respective peaks, Alk1 and Alk2 were still detectable after 200 minutes when the spindle checkpoint was activated in the presence of benomyl. These results indicate that both Alk1 and Alk2 are present at the metaphase/anaphase transition and suggest that their activities are required in metaphase and during a metaphase block as their levels persist during a spindle checkpoint arrest. Additionally, the signal intensity of Alk2-3HA was much lower than Alk1-3HA. As the amount of whole cell lysate loaded from both strains was approximately equal and both blots were exposed for the same time, this suggests that the abundance of Alk2 is significantly lower than Alk1.

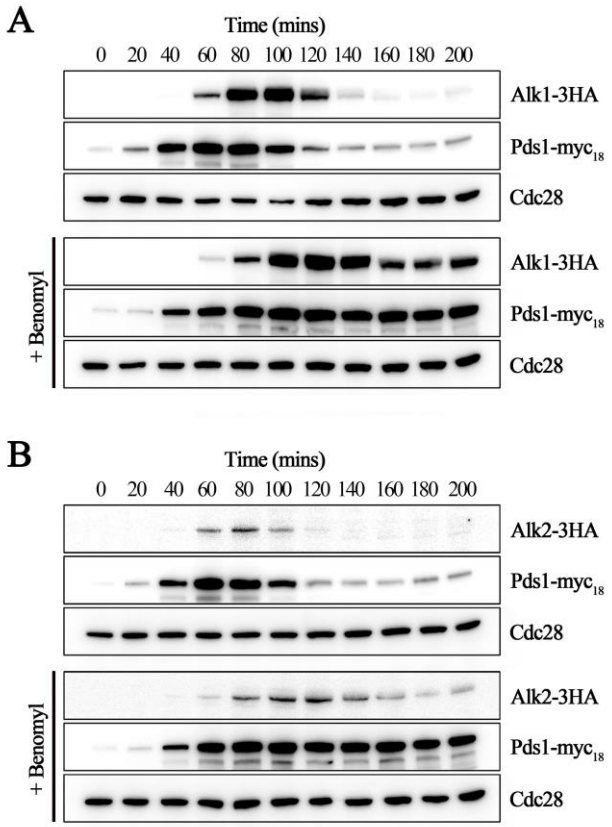

Figure 4.4. Alk1 and Alk2 levels peak around the metaphase to anaphase transition and persist when the spindle checkpoint is activated. Cells expressing Pds1-myc$_{18}$ and either (A) Alk1-3HA or (B) Alk2-3HA were synchronised in G_1 with α-factor and released into YPAD medium with or without benomyl. Cells were harvested at the indicated time-points after release and protein levels were analysed by western blotting. Cdc28 detected by an anti-Cdc28 antibody was used as a loading control.

4.5 *bub1*Δ and *sgo1*Δ do not interact genetically with H3(T3A) or *alk1*Δ *alk2*Δ

Previous studies have demonstrated that the phosphorylation of a conserved residue in histone H2A (Ser-121 in fission yeast, Thr-120 in human cells) by Bub1 is required for the centromeric localisation of Shugoshin and subsequently recruitment of the CPC (Vanoosthuyse *et al*., 2007; Kawashima *et al*., 2007; Kawashima *et al*., 2010). This conserved residue is also phosphorylated by Bub1 in *S. cerevisiae* and is required for Shugoshin localisation (Kawashima *et al*., 2010). The recent discovery that Haspin-mediated phosphorylation of histone H3 at the conserved Thr-3 position also contributes

to centromeric CPC localisation has provided a better understanding of how the CPC is recruited to the inner centromere during early mitosis (Kelly *et al*., 2010; Yamagishi *et al*., 2010; Wang *et al*., 2010). Yamagishi *et al*. (2010) highlighted a partial redundancy that exists between these two pathways of CPC recruitment. They were able to show that knocking out Hrk1/Haspin or mutating histone H3 at the Thr-3 position [H3(T3A)] in fission yeast resulted in a reduction in the level of Ark1/Aurora B at centromeres, but the cells remained viable with only a minor growth defect. Likewise, they showed that disrupting the Bub1-mediated pathway by knocking out Sgo2 had a similar effect. However, disruption of both pathways in H3(T3A) *sgo2*Δ or *hrk1*Δ *sgo2*Δ cells resulted in a severe growth defect. It was therefore reasonable to hypothesise that if Alk1 and Alk2 have a similar role in CPC recruitment that these genetic interactions would be replicated in *S. cerevisiae*. To address this, a series of mutants were generated (Fig. 4.5).

The *S. cerevisiae* genome contains two genes that encode histone H3 (*HHT1* and *HHT2*) and each are expressed at different loci from a bi-directional promoter that is shared with one of two copies of histone H4 (*HHF1* and *HHF2*). To generate cells expressing either histone H3(T3A) or the corresponding wild-type histone H3, strains lacking the *HHT1-HHF1* locus but with either a wild-type or T3A mutant *HHT2-HHF2* locus were constructed (see 2.2.5 Methods). Both the H3 wild-type and T3A mutant strains were viable and the T3A mutant showed no hypersensitivity to high temperature or benomyl compared to the wild-type strain (Fig. 4.5 A). *ALK1* and *ALK2* knockouts were also generated in the context of the wild-type histone H3 genotype and, in line with previous observations, the *alk1*Δ *alk2*Δ double mutant is hypersensitive to benomyl (Fig. 4.5 A i). The histone strains were also crossed with *BUB1* and *SGO1* knockout strains and sporulated to generate haploid mutants. All the required combinations of

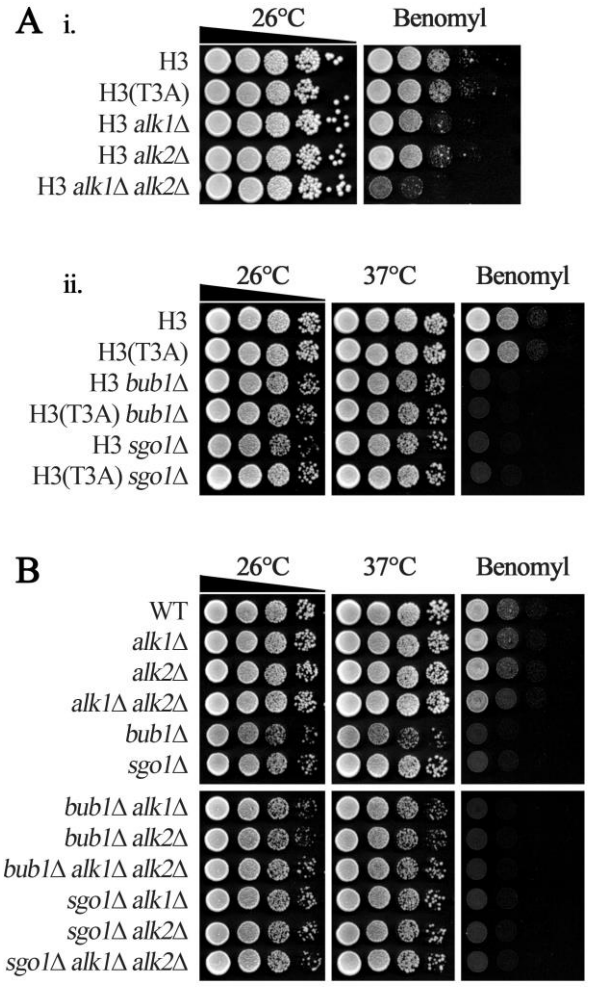

Figure 4.5. *bub1*Δ and *sgo1*Δ do not interact genetically with H3(T3A) or *alk1*Δ *alk2*Δ. Mutants were generated in *S. cerevisiae* to identify whether any genetic interactions analogous to those observed in *S. pombe* could be replicated. The indicated strains were spotted in 10-fold serial dilutions onto YPAD medium and incubated at 26°C, 37°C or in the presence of benomyl. (A) Combinations of histone H3 mutants with (i) *ALK1*/*ALK2* knockouts or (ii) *BUB1* and *SGO1* knockouts. These cells contained only wild-type or mutant versions of the *HHT2-HHF2* locus as their source of histones H3 and H4 (see text). (B) Combinations of *ALK1*, *ALK2*, *BUB1* and *SGO1* mutants.

mutants were recovered from the crosses. H3(T3A) *sgo1*Δ and H3(T3A) *bub1*Δ strains were viable with no negative genetic interactions apparent (Fig. 4.5 A ii), unlike the equivalent interactions described in fission yeast (Yamagishi *et al*., 2010). Strains were also generated to test for negative genetic interactions between Haspin-like kinase knockouts and *BUB1* or *SGO1* knockouts. Again, no interaction was observed for the phenotypes tested (Fig. 4.5 B). The relative viability of several of these mutants was also assessed. No significant difference in methylene blue staining of wild-type, *alk1*Δ *alk2*Δ, *sgo1*Δ and *sgo1*Δ *alk1*Δ *alk2*Δ mutants was observed suggesting that there was no difference in viability of these cells (Fig. A2 A). However, this method for determining cell viability can be unreliable and inaccurate due to a potentially high false positive detection rate (Smart *et al*., 1999). Old or stressed cells that cannot divide may not stain. An alternate method is to determine the number of colonies formed on agar plates compared to the total number of cells inoculated. This method indicated that the viability of *sgo1*Δ mutants was significantly reduced compared to wild-type and *alk1*Δ *alk2*Δ cells. However, the combination of *sgo1*Δ with *alk1*Δ *alk2*Δ did not significantly reduce viability further (Fig. A2 B).

Collectively, these data suggest that phosphorylation of histone H3 at Thr-3 is not essential for growth and that if the Haspin/H3/CPC pathway exists in budding yeast, mutations that would disrupt its function do not interact with mutations in the Bub1/Shugoshin/CPC pathway, unlike the analogous mutant combinations in fission yeast (Yamagishi *et al*., 2010).

4.6 *alk1*Δ *alk2*Δ cells do not exhibit defects in chromosome bi-orientation or chromosome maintenance

Previous studies have demonstrated that the kinase activity of Ipl1/Aurora B is required during mitosis to phosphorylate substrates present at the kinetochore-microtubule interface to destabilise improper microtubule attachments and allow for re-orientation and the establishment of bi-orientation (Cheeseman *et al*., 2006; Welburn *et al*., 2010). Without properly localised Ipl1/Aurora B these syntelic attachments may persist, resulting in an increased frequency of mono-orientation and aberrant chromosome segregation. Yamagishi *et al*. (2010) have shown that fission yeast cells lacking Haspin or phosphorylatable H3-T3 have decreased levels of centromeric Ark1/Aurora B and exhibit defects in chromosome bi-orientation and segregation. To test whether this is the case in budding yeast, a series of strains were generated to assess chromosome bi-orientation and chromosome maintenance in *alk1*Δ *alk2*Δ and H3(T3A) cells.

Chromosome bi-orientation in *alk1*Δ *alk2*Δ cells was monitored by incorporating *YFP-TUB1* to visualise microtubules and sister centromeres on chromosome III were visualised by tetR-GFP binding to an array of *tet* operators that were inserted at a position close to *CEN3*. Cultures of these '*CEN*-dot' strains were synchronised in G_1 with α-factor and released to a metaphase block through Cdc20 depletion by virtue of the methionine repressible p*MET3-CDC20* construct (Tanaka *et al*., 2000). Bi-oriented chromosomes in metaphase-arrested cells were scored by the dynamic splitting and reassociation of GFP dots whereas mono-orientation was scored when a persistent unresolved *CEN*-dot was observed (Fig. 4.6 A). Five minute time-lapse image sequences were taken for multiple fields. There was no significant increase in the occurrence of mono-oriented chromosomes in *alk1*Δ *alk2*Δ cells ($P = 1$; Fig. 4.6 B).

Due to the proposed redundancy that is reported to exist between the Haspin and Bub1/Shugoshin pathways in other organisms (Yamagishi *et al*., 2010), it was hypothesised that combining knockouts of these pathways in budding yeast may result in chromosome bi-orientation defects. However, although *sgo1*Δ cells displayed a significant increase in the persistence of mono-orientation compared to wild-type and *alk1*Δ *alk2*Δ cells ($P < 0.001$), the combination of *sgo1*Δ *alk1*Δ and *alk2*Δ mutations did not result in a significant synergistic defect ($P = 0.255$; Fig. 4.6 B). A similar method was employed to monitor bi-orientation in H3 and H3(T3A) cells. These cells differed in that the '*CEN*-dot' system functioned through lacI-GFP binding to *lac* operators inserted in the pericentromeric region of *CEN15* (Kitamura *et al*., 2007) and that both contained the necessary knockouts and synthetic histone loci to express either solely wild-type or T3A versions of histone H3 (see 2.2.5 Methods). No significant variation in the frequency of mono-oriented chromosomes was detected between these strains ($P = 0.731$; Fig. 4.6 B).

To assess chromosome maintenance in cells lacking the Haspin-like kinases, a series of strains were generated in which the loss of a previously described supernumerary chromosome fragment could be visualised in a colony sectoring assay (Spencer & Hieter, 1992). Loss of the chromosome fragment, and consequently the *SUP11* gene, results in the formation of a red colony colour due to the inability to supress the *ade2-1* mutation present in the genetic background of the strains used in this study (Fig. 4.7 A). The chromosome loss rate per cell division can then be calculated from the number of half-sectored colonies in relation to the total number of colonies (see 2.5.8 Methods). Cells lacking both of the Haspin-like kinases showed no significant increase in chromosome loss rate compared to wild-type control cells ($P = 1$; Fig. 4.7 B). In contrast, *sgo1*Δ cells that have previously been demonstrated to be defective in

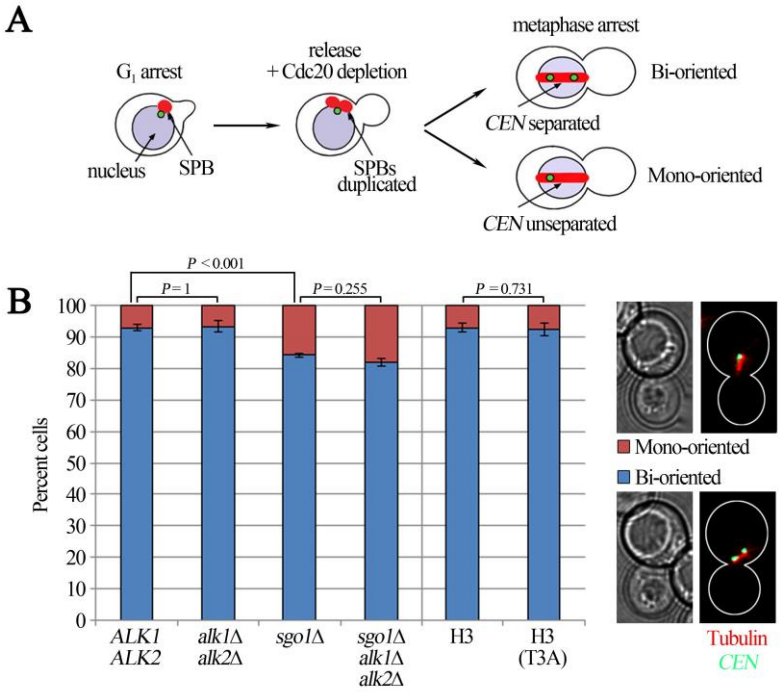

Figure 4.6. *alk1*Δ *alk2*Δ cells do not show defects in chromosome bi-orientation. (A) Cartoon depicting the experimental design to assess chromosome bi-orientation. Cells containing a '*CEN*-dot' system were synchronised in G_1 with α-factor and released to a metaphase block in medium supplemented with 5 mM methionine to deplete Cdc20. Bi-oriented chromosomes display a dynamic separation and reassociation of sister *CEN*s. (B) Chromosome bi-orientation was scored in over 125 cells for each strain per experiment and each experiment was performed in triplicate. Error bars represent the standard deviation. Representative images of mono-oriented and bi-oriented chromosomes from time-lapse image sequences are also shown. Data for *ALK1 ALK2*, *alk1*Δ *alk2*Δ, *sgo1*Δ and *sgo1*Δ *alk1*Δ *alk2*Δ passed normality and equal variance tests and were subjected to a one way ANOVA test [$F(3, 8) = 67.2$, $P < 0.001$]. Subsequent pairwise comparisons were performed using the Bonferroni t-test. WT vs. *alk1*Δ *alk2*Δ $P = 1$; *sgo1*Δ vs. *sgo1*Δ *alk1*Δ *alk2*Δ $P = 0.255$; all other pairwise comparisons $P < 0.001$. Data for H3 and H3(T3A) also passed normality and equal variance tests and were subjected to a one way ANOVA test [$F(1, 4) = 0.136$, $P = 0.731$].

proper chromosome bi-orientation (Fig. 4.6 B; Fernius & Hardwick, 2007) showed a substantial increase in the chromosome loss rate per cell division (approximately 140 fold; $P < 0.001$; Fig. 4.7 B,C). Cells with the combination of *sgo1*Δ *alk1*Δ and *alk2*Δ mutations displayed a chromosome loss rate similar to that of *sgo1*Δ cells indicating no synergistic effect of Haspin and Shugoshin knockouts ($P = 1$; Fig. 4.7 B,C).

Together, these results suggest that the sole budding yeast Shugoshin (Sgo1) is very important for the promotion of chromosome bi-orientation and correct chromosome segregation whereas the potential phosphorylation of histone H3 at Thr-3 and the Haspin-like kinases (Alk1, Alk2) appear to be dispensable for these processes.

A

B

Chromosome loss rates

Strain	Total red colonies	Total half-sectored colonies	Total colonies	Average loss rate per cell division* (10^3) ± SD
WT	36	11	32183	0.34 ± 0.15
alk1Δ alk2Δ	11	7	33820	0.20 ± 0.11
sgo1Δ	1515	898	20412	47.69 ± 3.79
sgo1Δ alk1Δ alk2Δ	1279	810	18110	48.34 ± 5.76

* Calculated as half-sectored/(total - red)

C

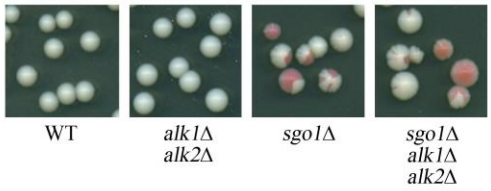

Figure 4.7. *alk1*Δ *alk2*Δ cells do not show an increase in the frequency of chromosome loss. (A) Cartoon depicting the synthetic chromosome III fragment (CFIII) used to assess chromosome maintenance in a colony sectoring assay and examples of white, red and half-sectored colonies. (B) Chromosome loss rates of CFIII were determined in wild-type (WT), *alk1*Δ *alk2*Δ, *sgo1*Δ and *sgo1*Δ *alk1*Δ *alk2*Δ cells. The experiment was performed in triplicate and the total numbers of colonies are shown along with the average loss rate per cell division. Square root transformed values of the chromosome loss rates passed normality and equal variance tests and were subjected to a one way ANOVA test [$F(3, 8) = 572.2$, $P<0.001$]. Subsequent pairwise comparisons were performed using the Bonferroni t-test. WT vs. *alk1*Δ *alk2*Δ $P = 1$; *sgo1*Δ vs. *sgo1*Δ *alk1*Δ *alk2*Δ $P = 1$; all other pairwise comparisons $P < 0.001$. (C) Representative images of colonies from the strains of the indicated genotypes.

4.7 *alk1*Δ *alk2*Δ cells exhibit cell morphology and spindle positioning defects

During the analysis of the time-lapse images taken for the assessment of bi-orientation, very prominent cell morphology and spindle positioning defects were observed in *alk1*Δ *alk2*Δ cells. When these cells were arrested in metaphase through Cdc20 depletion (p*MET3-CDC20*), it was noticed that one compartment of the cell became larger than the other while wild-type cells remained homogenously large budded. This phenotype was similar to that observed when *alk1*Δ *alk2*Δ cells were treated with benomyl (Fig. 4.2). However, it was not possible to determine which compartment of the cell (mother or bud) was enlarging in these previous experiments. To make this distinction, a series of strains were generated in which the gene encoding the α-factor degrading Bar1 protease was knocked out. These *bar1*Δ cells form a very distinct mating projection or shmoo when treated with α-factor in addition to becoming synchronised in G_1. Upon removal of the pheromone from the growth medium the cells abandon the mating response, re-enter the cell cycle and select a bud site at a position away from the shmoo. Therefore, the shmoo defines which compartment of the cell is the mother. This procedure was performed using wild-type and *alk1*Δ *alk2*Δ cells which were then arrested in metaphase through benomyl treatment or Cdc20 depletion. Analysis of cells from these cultures indicated that it was the bud that became abnormally large when *alk1*Δ *alk2*Δ cells were arrested in metaphase (Fig. 4.8 A). H3 and H3(T3A) strains were tested in a similar manner to examine the possibility that this phenotype is caused by the loss of H3-T3ph. Although these cells were not *bar1*Δ mutants, and therefore the identity of the cell compartments could not be distinguished, it was apparent that both cell compartments remained of similar proportions during an extended metaphase arrest (Fig. 4.8 B).

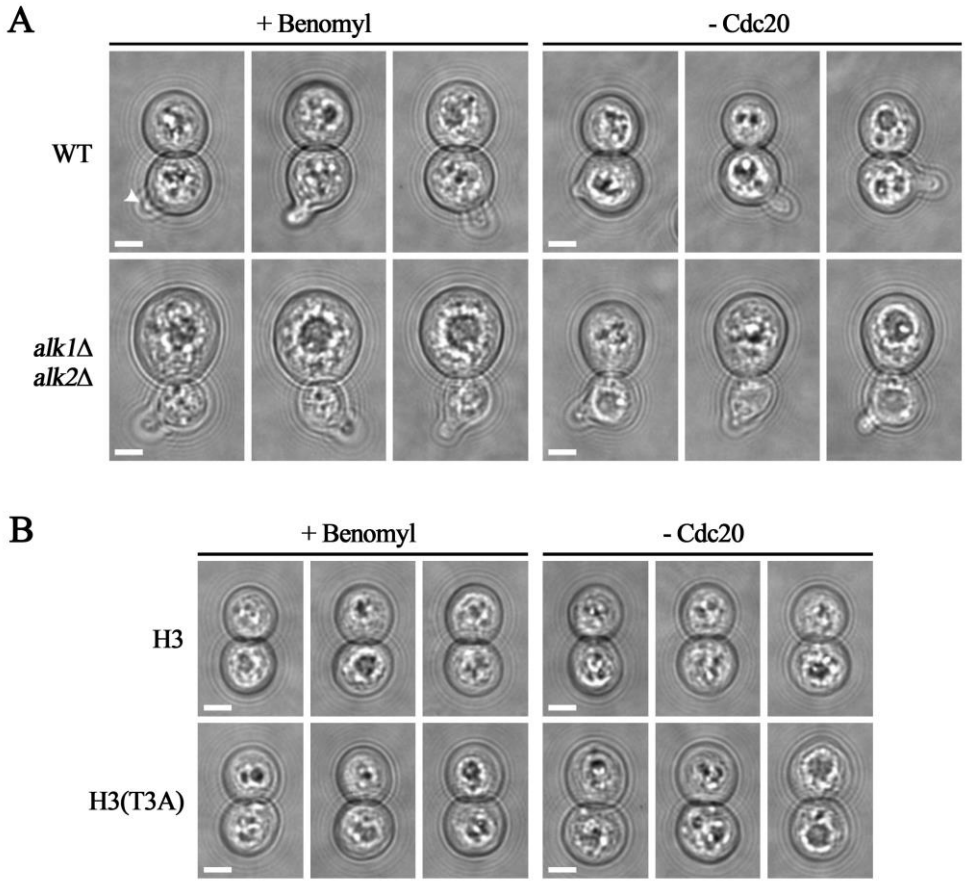

Figure 4.8. The bud of *alk1*Δ *alk2*Δ cells becomes abnormally large during an extended metaphase arrest. (A) Wild-type (WT) and *alk1*Δ *alk2*Δ cells with *bar1*Δ and p*MET3-CDC20* mutations were synchronised in G_1 with α-factor and released to a metaphase block by transferring the cells into medium containing benomyl or methionine. Images were taken 8 hours after release from α-factor arrest. The mating projection or shmoo that defines the mother cell is clearly visible (arrow). (B) H3 and H3(T3A) cells containing p*MET3-CDC20* were grown to mid-log phase and transferred into medium containing benomyl or methionine to block cells in metaphase. Images were taken 8 hours after release from α-factor arrest. Scale bars represent 3 μm.

In the original bi-orientation experiments it was also noticed that the mitotic spindle was often mispositioned in *alk1*Δ *alk2*Δ cells. In metaphase-arrested wild-type cells the mitotic spindle was normally positioned in close proximity to the bud neck and aligned along the mother-bud axis as expected. Conversely, in *alk1*Δ *alk2*Δ cells the spindle was frequently positioned away from the bud neck and misaligned. However,

once again it was not possible to determine which compartment of the cell the spindle was located from this previous experiment. To address this, control and *alk1*Δ *alk2*Δ cells expressing mCherry-Tub1 with the *bar1*Δ mutation were generated. These cells were synchronised in G_1 with α-factor and released to a metaphase block by Cdc20 depletion (p*MET3-CDC20*). Three hours after release from G_1, a series of five minute time-lapse image sequences were taken. Examples of cells from these image sequences are shown in Figure 4.9 A. In total, twenty one images were taken over each five minute time-lapse series and spindle position was scored in cells as being in one of four positions relative to the bud neck in each image: Bud (Distal); Bud (Proximal); Mother (Proximal); Mother (Distal). In instances where the spindle spanned two zones, the spindle was scored as being in the position where the largest proportion of the spindle was present. These data from a number of cells (n) were pooled and the relative spindle position is represented as a percentage (Fig. 4.9 B). Although spindles in metaphase-arrested wild-type and *alk1*Δ *alk2*Δ cells were most frequently positioned in the bud (WT 72.9%; *alk1*Δ *alk2*Δ 98.8%), wild-type cell spindles spent the majority of the time at the neck in the bud (WT 72.6%; *alk1*Δ *alk2*Δ 42.2%; $P < 0.001$) while *alk1*Δ *alk2*Δ cell spindles were most commonly positioned in the bud away from the neck (*alk1*Δ *alk2*Δ 56.6%; WT 0.3%; $P < 0.001$; Fig. 4.9 A, B). In contrast to wild-type cells, when *alk1*Δ *alk2*Δ cells were released from the metaphase block into anaphase many elongating spindles did not properly align and were unable to penetrate the bud neck and elongated within the bud where they remained and broke down (Fig. 4.9 C).

These results suggest that Alk1 and Alk2 are required during metaphase to promote or maintain proper spindle positioning and to regulate bud growth.

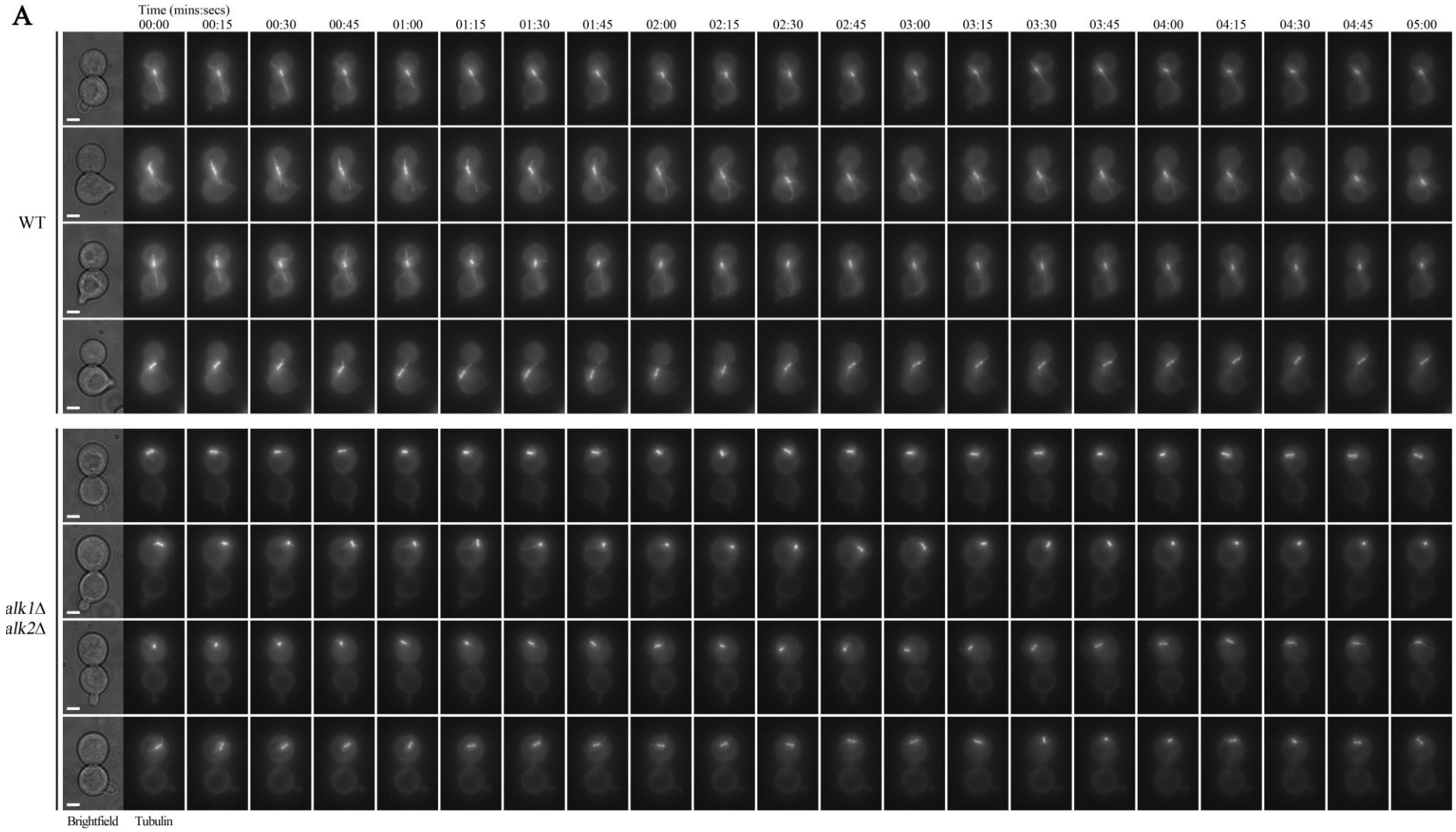
A
Time (mins:secs)
00:00
00:15
00:30
00:45
01:00
01:15
01:30
01:45
02:00
02:15
02:30
02:45
03:00
03:15
03:30
03:45
04:00
04:15
04:30
04:45
05:00
WT
alk1Δ
alk2Δ
Brightfield
Tubulin

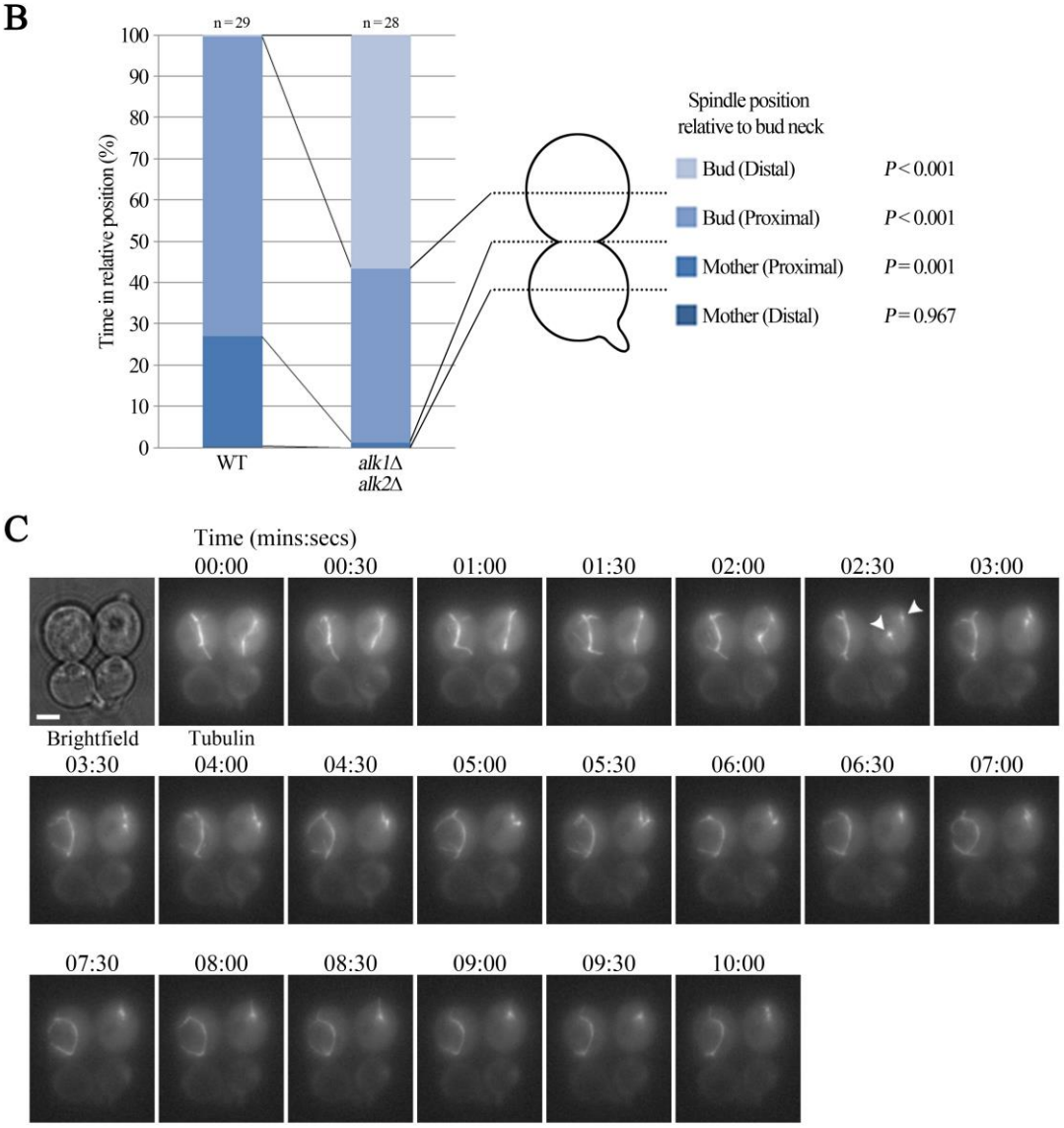

Figure 4.9. Metaphase-arrested *alk1*Δ *alk2*Δ cells exhibit spindle positioning defects. (A) Cells expressing mCherry-Tub1 were synchronised in G_1 with α-factor and released to a metaphase block through Cdc20 depletion. A series of 5 minute time-lapse image sequences to assess mitotic spindle positioning. (B) Quantification of spindle position in metaphase-arrested cells. Data were subjected to a two way ANOVA test which showed that genotype has a significant effect on spindle position [$F(3, 220) = 25.5$, $P < 0.001$]. Subsequent pairwise comparisons of relative spindle position between the wild-type control and *alk1*Δ *alk2*Δ cells were calculated using the Holm-Sidak method. n = number of cells in which spindle positioned was scored in 21 time-lapse images taken over 5 minutes. (C) Examples of spindle elongation and breakdown within the bud of *alk1*Δ *alk2*Δ cells released from a metaphase block into anaphase. Arrows highlight separate spindle poles in the bud after spindle break down. Scale bars represent 3 μm.

4.8 Alk1 and Alk2 do not function directly in either the Kar9 or the Dyn1 mediated pathways of spindle positioning

The striking defect in spindle positioning observed in the experiments with metaphase-arrested *alk1*Δ *alk2*Δ cells suggested that the Haspin-like kinases may have a role in orienting and aligning the mitotic spindle through one of two sequential and partially redundant pathways that are already known to position the spindle relative to the bud neck. The first pathway, which functions early in the cell cycle, involves the yeast EB1 and myosin V homologues, Bim1 and Myo2 respectively, and the yeast specific adaptor protein Kar9. The microtubule plus end tracking protein Bim1 binds to Kar9 which, in turn, binds to Myo2. Myo2 subsequently directs the growing microtubule plus ends along polarised actin cables towards the bud tip. The second pathway, which functions later in the cell cycle, involves dynein and the yeast CLIP-170 homologue Bik1. At the metaphase to anaphase transition the yeast-specific dynein inhibitor She1 is removed from cytoplasmic microtubules. This allows the targeting of cytoplasmic dynein to microtubule plus ends through interaction with Bik1. When a microtubule carrying dynein interacts with the yeast-specific cortical protein Num1, dynein becomes anchored to the cortex and subsequently pulls the spindle through the action of its minus end-directed motor activity (for review, see Huisman & Segal, 2005; McNally 2013). Deletion of genes involved in either of these pathways results in a viable cell, although the spindle is frequently mispositioned, whereas deletions of genes involved in both pathways has been reported to result in synthetic lethality (Eshel *et al*., 1993; Miller & Rose, 1998; Hwang *et al*., 2003).

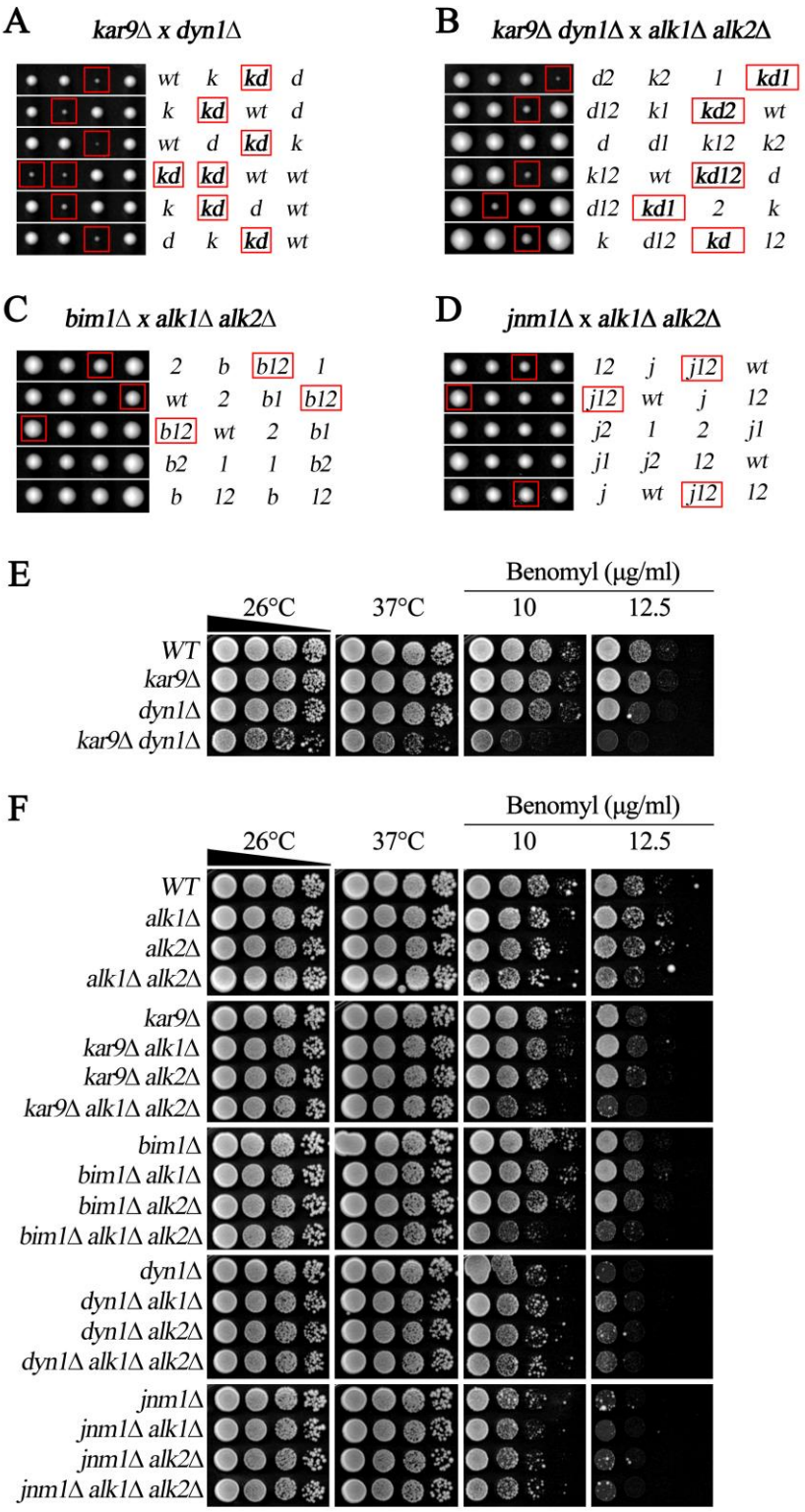

Figure 4.10. Alk1 and Alk2 do not appear to function directly in the Kar9 or the dynein mediated pathways of spindle positioning. (A-D) Diploid strains heterozygous for deletions of *ALK1*, *ALK2* and known components of spindle positioning pathways were sporulated to generate haploid progeny and subjected to genotypic analysis. Genotypes of spores are denoted as follows: *wt*, wild-type; *1*, *alk1*Δ; *2*, *alk2*Δ; *k*, *kar9*Δ; *d*, *dyn1*Δ; *b*, *bim1*Δ; *j*, *jnm1*Δ. Colonies with genotypes of interest are highlighted with red boxes. (E, F) The indicated strains were spotted in 10-fold serial dilutions and grown at 26°C, 37°C or at 26°C in the presence of benomyl.

As it would appear that Alk1 and Alk2 are functioning redundantly with regard to their contribution to spindle positioning it is possible that their involvement in either of these pathways has remained undetected in previous analyses. To ascertain whether Alk1 and Alk2 are involved in either of these pathways, a series of mutants were generated to assess whether any synergistic interaction exists between the Haspin-like kinases and components of the two partially redundant spindle positioning pathways. As a control it was first necessary to replicate the reported interaction between *kar9*Δ and *dyn1*Δ mutations for comparison. This was achieved by crossing haploid *kar9*Δ and *dyn1*Δ strains to generate a *kar9*Δ *dyn1*Δ heterozygous diploid. This diploid strain was then sporulated to form haploid meiotic progeny and subjected to tetrad analysis. Although viable *kar9*Δ *dyn1*Δ double mutants were isolated from this cross they were severely compromised for proliferation (Fig. 4.10 A, highlighted with red boxes). Next an *alk1*Δ *alk2*Δ *kar9*Δ *dyn1*Δ heterozygous diploid strain was generated and the same analysis was performed. Again, any strains bearing both *kar9*Δ and *dyn1*Δ knockouts were severely compromised (Fig. 4.10 B, highlighted with red boxes), although no synergistic interactions associated with combinations of *alk1*Δ and *alk2*Δ with either *kar9*Δ or *dyn1*Δ were observed in this analysis (Fig. 4.10 B). Additional knockouts of another component from each pathway were also tested, namely *bim1*Δ and *jnm1*Δ. Interestingly, a synthetic lethal interaction between *jnm1*Δ and *alk1*Δ had been described previously (Schöner *et al*., 2008). However, this could not be replicated in this study and no synergistic negative interaction was identified following tetrad analysis with combinations of *alk1*Δ and *alk2*Δ with either *bim1*Δ or *jnm1*Δ (Fig. 4.10 C, D; triple knockouts highlighted by red boxes). However, further analysis of the Kar9 and dynein pathway mutants revealed that *kar9*Δ *dyn1*Δ double mutants were hypersensitive to benomyl (Fig. 4.10 E). Triple mutant strains containing *alk1*Δ *alk2*Δ in combination with either *kar9*Δ or *bim1*Δ also showed an increased sensitivity to

benomyl compared to the relevant single and double mutant combinations whereas *alk1*Δ *alk2*Δ in combination with *dyn1*Δ or *jnm1*Δ did not (Fig. 4.10 F).

These data suggest that Alk1 and Alk2 do not function directly in the early Kar9 or late dynein spindle positioning pathways as there is no strong genetic interaction with regards to unperturbed growth between *ALK1* and *ALK2* knockouts in combination with spindle positioning pathway knockouts. However, the synthetic benomyl sensitivity shown by *alk1*Δ *alk2*Δ with the loss of the Kar9 pathway may indicate that Alk1 and Alk2 have a function within the dynein pathway when mitosis is delayed that is not evident during unperturbed proliferation.

4.9 Alk1 is localised to the cell cortex in metaphase-arrested cells

Haspin in HeLa cells appears to be localised exclusively in the nucleus and associates strongly with condensed chromosomes throughout mitosis (Dai *et al*., 2005). The Haspin homologue in *A. thaliana* also shares a similar localisation pattern during mitosis but differs during interphase, where it is predominantly visible in the cytoplasm (Kurihara *et al*., 2011). This raised the question of whether the budding yeast Haspin-like kinases share a similar localisation pattern. There are no existing data describing the localisation of Alk2. However, the localisation of Alk1-GFP was examined as part of two separate studies investigating the localisation of proteins using systematic genome-wide approaches, although the images obtained are ambiguous (Huh *et al*., 2003; Tkach *et al*., 2012). To investigate the localisation of Alk1 and Alk2, a series of strains were generated expressing enhanced yellow fluorescent protein (EYFP) fusion proteins (Alk1-EYFP, Alk2-EYFP) from endogenous promoters by in-frame insertion of the EYFP coding sequence immediately preceding the stop codon of *ALK1* and *ALK2*. The brighter EYFP variant was used as the previous studies hinted at potential difficulties in

assessing Alk1 localisation with GFP. Additionally, since both Alk1 and Alk2 are cell cycle regulated with their levels peaking around metaphase (Fig. 4.4), p*MET3-CDC20* was also incorporated into these strains so that cells could be synchronously arrested in metaphase through Cdc20 depletion to increase the likelihood of detecting a signal. Expression of the fusion proteins was confirmed by western blot analysis (Fig. 4.11 A). Alk1-EYFP was found to localise to the cell cortex in metaphase-arrested cells (Fig 4.11 B). Unfortunately, a full cell cycle analysis of Alk1-EYFP localisation was impeded by poor fluorescence and a signal above background could not be detected in cells expressing Alk2-EYFP. Detection of Alk1-EYFP at the cell cortex supports the hypothesis of a role for Alk1 in the regulation of cell polarity.

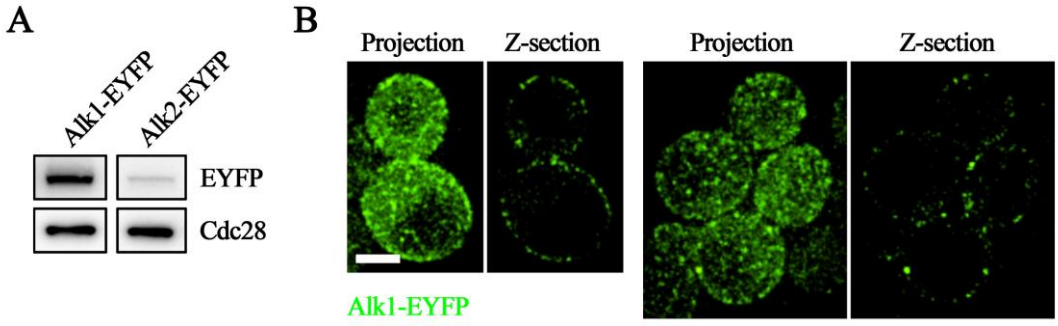

Figure 4.11. Alk1 is localised to the cell cortex in metaphase. (A) Expression of Alk1-EYFP and Alk2-EYFP fusion proteins in the respective strains was confirmed by western blotting. EYFP was detected using an anti-GFP antibody. Cdc28 detected by an anti-Cdc28 antibody was used as a loading control. (B) Cells expressing Alk1-EYFP were synchronised in G_1 with α-factor, released to a metaphase block through Cdc20 depletion and imaged. Projections are series of Z-sections merged. Scale bar represents 3 μm. A signal above background could not be detected in Alk2-EYFP cells.

4.10 Synthetic genetic array analysis to identify genes interacting with *ALK1* and *ALK2*

Genetic analysis is an important and powerful tool for evaluating the roles of genes *in vivo* and for identifying novel components of specific pathways. A common approach is to test whether a combination of mutations in two genes results in reduced fitness or cell death. These are termed 'synthetic sick' and 'synthetic lethal' interactions respectively. This approach has been used extensively in a number of different organisms to aid in the identification and characterisation of genes. For *S. cerevisiae* a collection of approximately 5000 viable gene deletion mutants were generated by an international consortium of laboratories (Winzeler *et al*., 1999; Giaever *et al*., 2002). Using this collection, a query strain and a method termed Synthetic Genetic Array (SGA) analysis developed by Tong & Boone (2006) it is possible to construct double mutants systematically and score for growth defects thus allowing large-scale mapping of synthetic genetic interactions.

With funds granted from an MRC Centenary Award, a series of SGA screens were performed in collaboration with Prof. David Lydall at the University of Newcastle. Having identified a functional redundancy between *ALK1* and *ALK2* it was decided that three screens would be performed in parallel, using each of the single deletions and the double deletion as query strains. In addition to the array of approximately 5000 viable deletion mutants, the three query strains were also crossed with an array of compromised alleles of essential genes. These alleles were generated by Breslow *et al*. (2008) by utilising the Decreased Abundance by mRNA Perturbation (DAmP) approach, which involved inserting a kanamycin resistance cassette immediately downstream of the stop codon of essential genes. This has been shown to destabilise the corresponding transcript and can reduce mRNA levels four to ten-fold. By incorporating

this collection, an additional ≈ 800 essential genes not present in the standard knockout collection were screened, thus providing a more comprehensive genetic analysis.

The query strains were crossed with each strain from the collection in quadruplicate and following sporulation and several rounds of selection the resulting haploid progeny, if viable, were given a fitness score based on colony size (Lawless *et al*., 2010). The raw interaction data obtained from these screens identified a range of negative genetic interactions. These data were subsequently filtered using several criteria to improve the quality and focus. For each interaction a *P*-value was calculated from the fitness scores of each replicate to determine whether the replicates were consistent and if the interactions were significant. To reduce false positives and allow for a direct comparison between the three screens, genes that were located within 10 kb of *ALK1* and *ALK2* were removed from all three datasets to account for linkage effects and only interactions with a *P*-value less than 0.05 were considered (Fig. 4.12 A i). To enrich for strong and biologically relevant interactions the data were further filtered based on the genetic interaction score (GIS). The GIS gives a measure of the fitness of the mutant combination compared against the average fitness of all strains in the experiment. Interactions with a GIS of -15,000 or less were considered for further analysis (Fig. 4.12 A ii). Filtered data for the three screens that conform to the above criteria can be found in Appendix Tables A1, A2 and A3. Interactions with a *P*-value less than 0.05 and a GIS less than -15,000 were deemed to be synthetic lethal if the mutant combination had a fitness score of 10,000 or less. Synthetic lethal interactions are represented in Figure 4.12 B and brief descriptions of the interacting gene functions are summarised in Tables 4.1, 4.2 and 4.3. The fitness scores from the control SGA screen are included for comparison.

Next, the filtered data was evaluated using gene ontology enrichment analysis software. Gene ontology (GO) is a major public bioinformatics initiative that aims to provide descriptions of molecular functions, biological processes, and sub-cellular locations associated with gene products in a range of different organisms using a controlled vocabulary. By analysing high-throughput datasets in this manner it is possible to assess whether groups of strong interactors are enriched for particular GO terms, therefore providing an insight into processes and pathways in which query genes of interest may be involved. The analysis generated a list of enriched GO terms along with the genes from the query data associated with these particular terms and a *P*-value indicating the statistical significance. A summary of these results can be found in Appendix Table A4. This full GO analysis consists of many thousands of GO terms, many of which are highly specific, nested and related terms that may apply to multiple species. This makes visualisation of the enrichment network problematic due to its complexity. To address this, a more focussed analysis was carried out using Yeast GO-slim terms. GO-slims are tailored to particular organisms and contain only a subset of the terms from the full ontologies to give a broad overview of the GO content. These are particularly useful for the annotation of genes in genome wide or microarray studies where a broad classification of gene product function is required. The Yeast GO-slim analysis for the negative interactors from each screen highlighted a number of enriched GO-slim terms (Fig. 4.13). Genes involved in processes which include endosomal transport, vesicle organisation and mitochondrion organisation were enriched in single knockout screens (Fig. 4.13 A, B). Mitochondrion organisation was also a term that was enriched in the double knockout screen. However, this screen also had a number of additional enriched terms including chromatin organisation, cellular response to DNA damage stimulus and DNA repair (Fig. 4.13 C). To further visualise the relationship between the three screens the synthetic sick and lethal interactors that were shared with

Table 4.1. *alk1*Δ synthetic lethal interactions

ORF	Gene	Essential ?	*P*	GIS	Query Fitness	Control Fitness	Description
YBR144C	*YBR144C*	n	3.87E-04	-60063	3634	93327	Dubious ORF. Mutants defective in endocytosis and have abnormal vacuolar morphology
YDR319C	*YFT2*	n	6.80E-12	-57474	78	84323	Required for normal ER membrane biogenesis. Interacts with Sst2, a GTPase activating protein required to prevent receptor-independent signalling of the mating pathway
YDR213W	*UPC2*	n	3.81E-16	-53560	77	78586	Sterol regulatory element, induces transcription of sterol biosynthetic genes
YDR107C	*TMN2*	n	9.88E-03	-48168	9185	84031	Transmembrane protein with a role in cellular adhesion and filamentous growth
YGL255W	*ZRT1*	n	6.02E-05	-48112	6619	80190	High-affinity zinc transporter of the plasma membrane.
YDR111C	*ALT2*	n	1.84E-02	-46183	9895	82164	Catalytically inactive alanine transaminase. Mutants have abnormal vacuole morphology.
YDR150W	*NUM1*	n	7.36E-04	-38307	4396	62567	Required for nuclear migration and mitochondria distribution. Component of mitochondria-ER-cortex-anchor (MECA). Localises to mother cell cortex and bud tip.
YBL094C	*YBL094C*	n	2.55E-03	-34983	0	51255	Dubious ORF. Overlaps uncharacterised YBL095W. Mutants have increased cell size and abnormal bud morphology
YDL143W	*CCT4*	y	7.37E-04	-30844	4813	52243	Subunit of the cytosolic chaperonin Cct ring complex required for assembly of actin and tubulins.
YHL025W	*SNF6*	n	9.41E-13	-25919	5383	45862	Subunit of SWI/SNF chromatin remodelling complex involved in transcriptional regulation
YBR200W	*BEM1*	n	1.00E-02	-25749	7130	48173	Involved in establishing cell polarity and morphogenesis. Functions as a scaffold for complexes that include Cdc24, Cdc42 and Cla4.
YIL076W	*SEC28*	n	4.23E-04	-24610	4384	42481	Subunit of coatomer, regulates retrograde Golgi-to-ER protein traffic.
YLR066W	*SPC3*	y	3.37E-02	-22915	9930	48122	Subunit of signal peptidase complex which catalyses cleavage of N-terminal signal sequences of proteins targeted to secretory pathway
YBR289W	*SNF5*	n	2.35E-03	-18058	1503	28661	Subunit of SWI/SNF chromatin remodelling complex involved in transcriptional regulation

Table 4.2. *alk2*Δ synthetic lethal interactions

ORF	Gene	Essential ?	*P*	GIS	Query Fitness	Control Fitness	Description
YGL255W	*ZRT1*	n	8.04E-06	-63583	3125	80190	High-affinity zinc transporter of the plasma membrane.
YFL032W	*YFL032W*	n	6.50E-05	-59359	7149	79950	Overlaps HAC1, which is a transcription factor that regulates unfolded protein response. Also induces transcription of genes involved in membrane biogenesis
YBR036C	*CSG2*	n	1.54E-05	-56487	1226	69376	Endoplasmic reticulum membrane protein, required for mannosylation of inositolphosphorylceramide and growth at high calcium concentrations
YMR205C	*PFK2*	n	8.67E-05	-56394	8991	78599	Subunit of phosphofructokinase involved in glycolysis. Mutation inhibits glucose induction of cell cycle regulated genes
YKL212W	*SAC1*	n	3.32E-07	-49952	247	60344	Phosphatidylinositol phosphate phosphatase. Involved in protein trafficking and processing, secretion and cell wall maintenance
YNL315C	*ATP11*	n	3.80E-05	-35633	8872	53500	Molecular chaperone required for assembly of mitochondrial ATP synthase
YGL092W	*NUP145*	y	7.32E-03	-29129	4960	40978	Nuclear pore protein with roles in nuclear pore complex biogenesis, localisation of genes to nuclear periphery and nucleocytoplasmic transport
YIL076W	*SEC28*	n	5.62E-04	-28896	6443	42481	Subunit of coatomer, regulates retrograde Golgi-to-ER protein traffic.
YBR289W	*SNF5*	n	1.94E-03	-23285	557	28661	Subunit of SWI/SNF chromatin remodelling complex involved in transcriptional regulation

Table 4.3. *alk1*Δ *alk2*Δ synthetic lethal interactions

ORF	Gene	Essential ?	*P*	GIS	Query Fitness	Control Fitness	Description
YGL116W	*CDC20*	y	3.42E-16	-62826	46	88386	Activator of anaphase promoting complex required for metaphase/anaphase transition by directing ubiquitination of mitotic cyclins and anaphase inhibitors
YGL255W	*ZRT1*	n	2.55E-14	-56623	418	80190	High-affinity zinc transporter of the plasma membrane.
YLR166C	*SEC10*	y	3.59E-13	-55975	0	78691	Subunit of exocyst complex, mediates polarised targeting and tethering of post-Golgi secretory vesicles to active sites of exocytosis at the plasma membrane
YBR011C	*IPP1*	y	7.05E-11	-54345	0	76400	Cytoplasmic inorganic pyrophosphatase that catalyses the rapid exchange of oxygens from Pi with water
YLR339C	*YLR339C*	y	9.42E-07	-51609	0	72553	Dubious ORF. Overlaps with RPP0 that encodes a conserved ribosomal protein involved in interaction between translational elongation factors and the ribosome
YML031W	*NDC1*	y	6.39E-05	-41486	2264	61504	Subunit of transmembrane ring of nuclear pore complex (NPC). Contributes to nucleocytoplasmic transport, NPC biogenesis and spindle pole body duplication
YFL031W	*HAC1*	n	4.51E-08	-41210	8783	70281	Transcription factor that regulates unfolded protein response. Also induces transcription of genes involved in membrane biogenesis
YPL063W	*TIM50*	y	4.49E-03	-40320	6859	66325	Component of translocase of the inner mitochondrial membrane
YOR224C	*RPB8*	y	1.15E-02	-28038	154	39633	RNA polymerase subunit ABC14.5; common to RNA polymerases I, II, and III
YLR198C	*YLR198C*	y	6.14E-03	-25411	2303	38961	Dubious ORF. Overlaps SIK1 that encodes essential nucleolar protein component of box C/D snoRNP complexes, overexpression causes spindle orientation defects.
YOL078W	*AVO1*	y	2.58E-03	-24476	0	34409	Component of membrane-bound complex containing Tor2 and other proteins which may have a role in regulation of cell growth
YMR309C	*NIP1*	y	2.04E-02	-23953	3315	38334	eIF3c subunit of the eukaryotic translation initiation factor 3 (eIF3); involved in the assembly of preinitiation complex and start codon selection
YDR123C	*INO2*	n	5.02E-03	-20315	7471	39062	Component of complex that binds inositol/choline-responsive elements, required for derepression of phospholipid biosynthetic genes in response to inositol depletion
YGL136C	*MRM2*	n	2.43E-02	-19410	9659	40866	Mitochondrial methyltransferase. Deletion confers loss of mitochondrial DNA and abnormal vacuolar and lipid particle morphology.
YBR109C	*CMD1*	y	4.53E-02	-18689	6857	35914	Calmodulin, regulates processes such as mitosis, bud growth, actin organisation, endocytosis and stress-activated pathways.
YBR289W	*SNF5*	n	3.38E-03	-18161	2227	28661	Subunit of SWI/SNF chromatin remodelling complex involved in transcriptional regulation

Table 4.4. Genes identified as viable in query SGA screens that were inviable in the control screen

Screen	ORF	Gene	Essential ?	P	GIS	Query Fitness	Control Fitness	Description
***alk1*Δ**	YLR088W	*GAA1*	y	8.41E-04	30076	30112	53	Subunit of GPI protein transamidase complex. Removes GPI anchoring signal and attaches GPI to proteins in ER. Reduction of function decreases shmoo formation
	YDR103W	*STE5*	n	1.05E-05	48618	48618	0	Pheromone-responsive MAPK scaffold protein
	YDR410C	*STE14*	n	6.09E-05	49930	49930	0	Farnesyl cysteine-carboxyl methyltransferase, mediates a step during processing of a-factor and RAS proteins in ER. Localises to ER
	YHR193C	*EGD2*	n	1.03E-03	50178	50189	17	Subunit of NAC complex involved in protein sorting and translocation
	YIL054W	*YIL054W*	n	2.41E-04	62264	62264	0	Uncharacterised. Mutants have increased cell size and abnormal vacuolar morphology.
	YDR461W	*MFA1*	n	4.37E-04	63502	63502	0	Mating pheromone a-factor.
	YDR227W	*SIR4*	n	3.03E-04	63916	63916	0	Silent information regulator, involved in assembly of silent chromatin domains at telomeres and silent mating-type loci.
***alk2*Δ**	YDL090C	*RAM1*	n	1.15E-03	25034	25034	0	Subunit of CAAX farensyltransferase that prenylates a-factor mating pheromone and Ras proteins and is required for their membrane localisation
	YLR088W	*GAA1*	y	2.14E-03	34085	34130	53	Subunit of GPI protein transamidase complex. Removes GPI anchoring signal and attaches GPI to proteins in ER. Reduction of function decreases shmoo formation
	YDL042C	*SIR2*	n	6.60E-03	42031	42031	0	NAD+ dependent histone deacetylase with role in silencing mating type loci and telomeres
***alk1*Δ *alk2*Δ**	YLR088W	*GAA1*	y	3.73E-04	32942	32980	53	Subunit of GPI protein transamidase complex. Removes GPI anchoring signal and attaches GPI to proteins in ER. Reduction of function decreases shmoo formation
	YHL007C	*STE20*	n	3.84E-04	37520	37520	0	Cdc42-activated signal transducing kinase of the PAK family. Involved in pheromone response, invasive growth, vacuole inheritance and down-regulation of sterol uptake
	YHR059W	*FYV4*	n	9.61E-03	45796	45796	0	Unknown function, required for survival upon exposure to K1 killer toxin
	YDR461W	*MFA1*	n	4.87E-02	52939	52939	0	Mating pheromone a-factor.
	YHR193C	*EGD2*	n	3.20E-04	67388	67400	17	Subunit of NAC complex involved in protein sorting and translocation

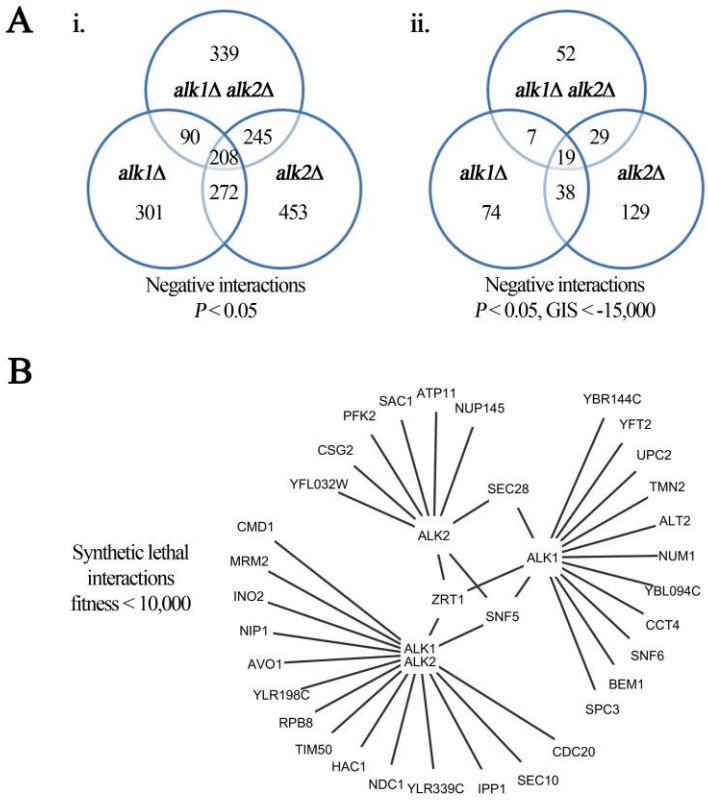

Figure 4.12. Synthetic genetic array (SGA) analysis to identify genes interacting with *ALK1* and *ALK2*. (A) (i) The raw interaction data from the *alk1*Δ, *alk2*Δ and *alk1*Δ *alk2*Δ screens was initially filtered to remove genes linked to either *ALK1* or *ALK2* and interactions with a *P*-value greater than 0.05 to reduce false positives. (ii) For further analysis, only genes with a genetic interaction score (GIS) less than -15,000 were considered likely to be enriched for biologically relevant interactions. (B) Interactions with fitness of less than 10,000 were scored as synthetic lethal.

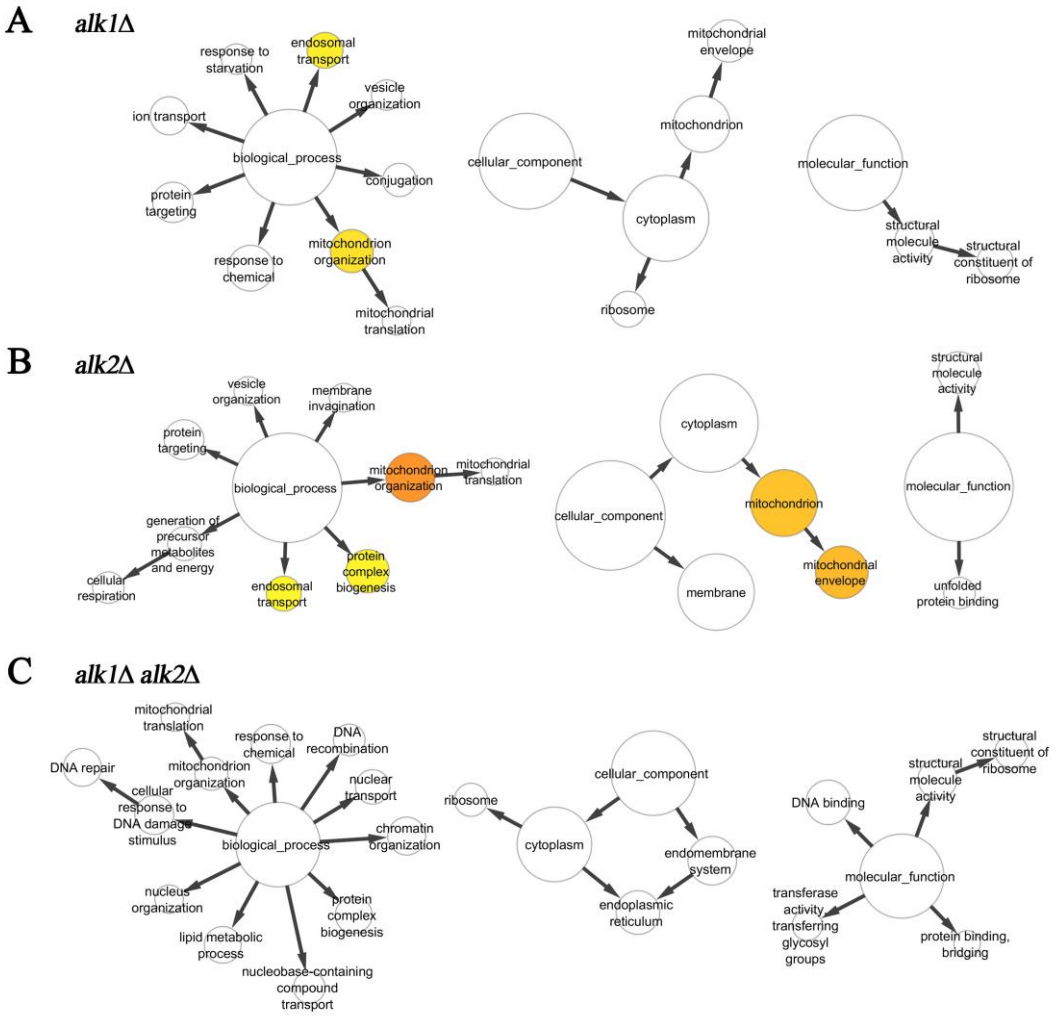

Figure 4.13. Gene ontology (GO) analysis for negative interactions. The filtered interaction data were subjected to Yeast GO-slim enrichment analysis that identified a number of GO-slim terms that were enriched in the negative interactors ($P < 0.05$, GIS < -15,000) for the (A) *alk1*Δ, (B) *alk2*Δ and (C) *alk1*Δ *alk2*Δ screens. All nodes represent a significant enrichment of that particular Yeast GO-slim term. White nodes were identified as significant in the initial analysis and coloured nodes indicate significant enrichments after *P*-value correction to account for false discovery rates. Yellow through orange represents an improvement in the associated *P*-value for the enrichment of that particular GO-slim term following *P*-value correction. Node size is representative of the number of genes in each category.

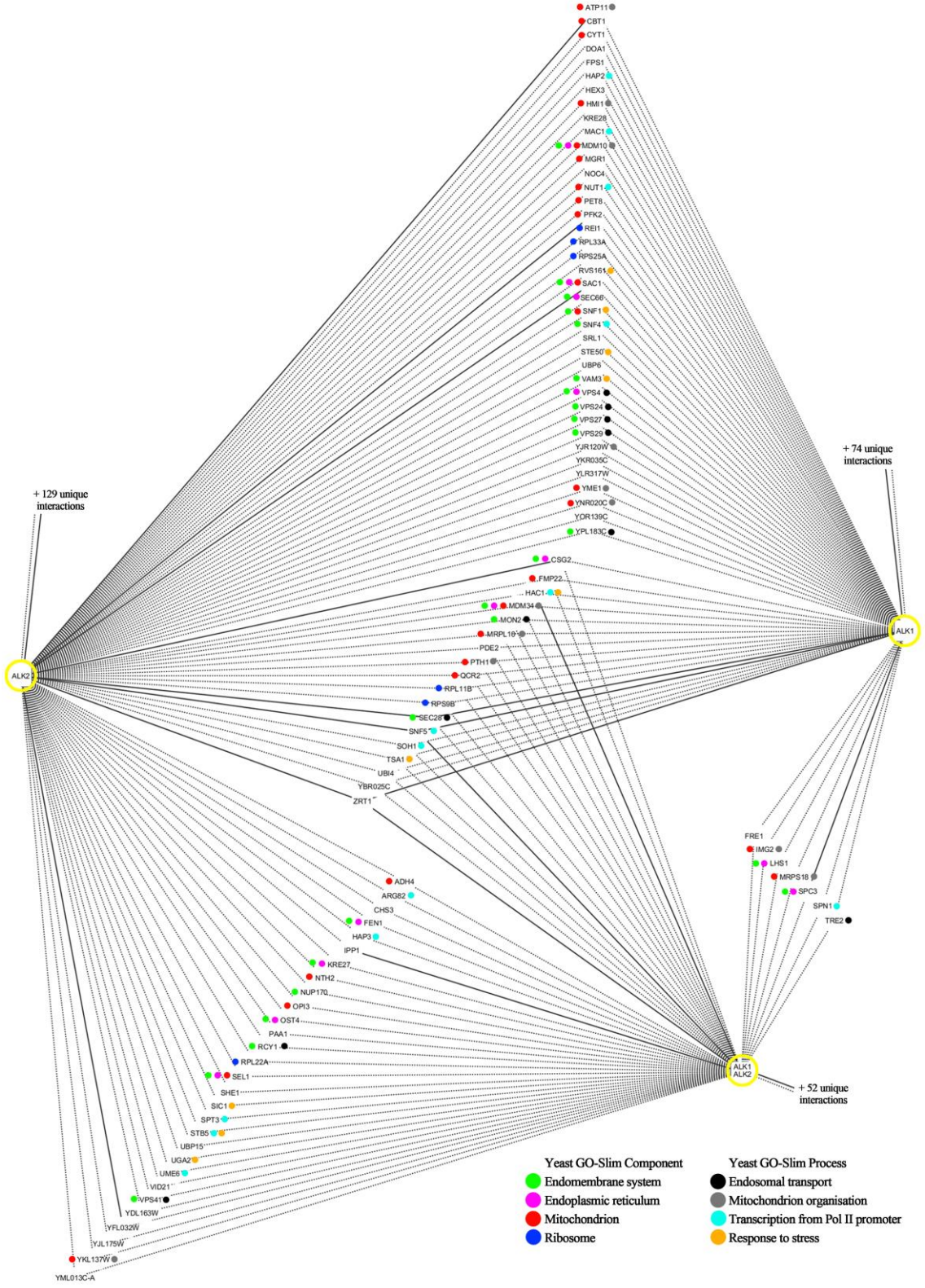

Figure 4.14. Common synthetic sick and synthetic lethal interactions. Negative genetic interactions shared between two or all screens are shown. Solid lines represent synthetic lethal interactions and dotted lines represent negative genetic interactions. Colour-coding indicates that the particular gene is annotated with the corresponding GO term.

two or all of the screens were plotted. A number of GO terms that were enriched within this data set are also indicated (Fig. 4.14). A large number of these genes are associated with the mitochondrion and the endomembrane system.

The equivalent GO analysis was performed for positive interactions from the three screens although no GO term enrichment was identified. However, some interesting positive genetic interactions were observed. A number of viable deletion mutants that usually do not come through SGA screens, such as those defective in mating or meiosis, have produced viable mutants in the Haspin-like kinase SGA screens. An example from the *alk1*Δ *alk2*Δ screen is *ste20*Δ, which is defective in mating and annotated as sterile. Mutants that had fitness scores of less than 10,000 in the control screen and a significant recovery of fitness in the query screens are listed in Table 4.4.

Large scale SGA screens such as these often generate a number of false positives and while the initial statistical analysis can help to reduce the numbers, it is also important to independently validate genetic interactions of interest. Accordingly, attempts were made to validate a number of the synthetic lethal and synthetic sick interactions identified in the screens. The first to be tested was *zrt1*Δ, which was synthetic lethal in all three query screens (Fig. 4.12 B). However, when a *zrt1*Δ strain was crossed with an *alk1*Δ *alk2*Δ strain and tetrad analysis was performed it was discovered that viable haploid strains with all mutant combinations could be isolated (Fig. 4.13 A). Zrt1 is a high-affinity transporter of the plasma membrane required for zinc uptake (Zhao & Eide, 1996). Accordingly, it was hypothesised that the Haspin-like kinases may have some role in the regulation of zinc uptake or the induction of a response to the stress of zinc deficiency. To address this, a series of mutants were

spotted onto medium containing EDTA to limit the availability of zinc. Strains with single and double deletions of *ALK1* and *ALK2* showed growth comparable to wild-type strains on media with limited zinc whereas all strains with *zrt1*Δ displayed an equivalent level of sensitivity. *zrt1*Δ strains also showed no synergistic effects in terms of growth at 37°C or in the presence of benomyl (Fig. 4.15 B). Next, several genes were examined that are involved in the unfolded protein response (UPR; reviewed in Ron & Walter, 2007) and were strong negative genetic interactors in the screens, namely *HAC1*, *IRE1* and *SPT3*. *HAC1* encodes a transcription factor that increases the transcription of genes involved in the UPR. Transcription of these genes involves the SAGA histone acetyltransferase complex of which Spt3 is a member and this complex, along with Ire1, is required for *HAC1* mRNA splicing *in vivo* (Welihinda *et al*., 2000). As well as responding to endoplasmic reticulum stress due to accumulation of unfolded proteins, there is increasing evidence to suggest that the UPR is involved in lipid homeostasis (Raychaudhuri *et al*., 2012). Additionally, zinc depletion has also been shown to strongly activate Ire1 and stimulate the UPR (North *et al*., 2012; Nguyen *et al*., 2013). An *alk1*Δ *alk2*Δ strain was crossed with *hac1*Δ, *ire1*Δ and *spt3*Δ strains and tetrad analysis was performed. Again, viable haploid strains with all mutant combinations were isolated (Fig. 4.15 C, D, E). The colony sizes of mutants isolated from the *hac1*Δ and *ire1*Δ tetrad analysis showed a degree of variability. For example, some of the single *hac1*Δ and *ire1*Δ mutants formed colonies of a size comparable to wild-type while others only formed micro-colonies. The same was also true for double and triple mutant combinations (Fig. 4.15 C, D). *spt3*Δ tetrad analysis was more consistent although no obvious synergistic interaction was observed with the various mutant combinations (Fig. 4.15 E). A particularly interesting synthetic lethal interaction in the *alk1*Δ *alk2*Δ double mutant screen that was not replicated in either of the single mutant screens was with the DAmP allele of *CDC20*. Presumably, strains carrying this allele

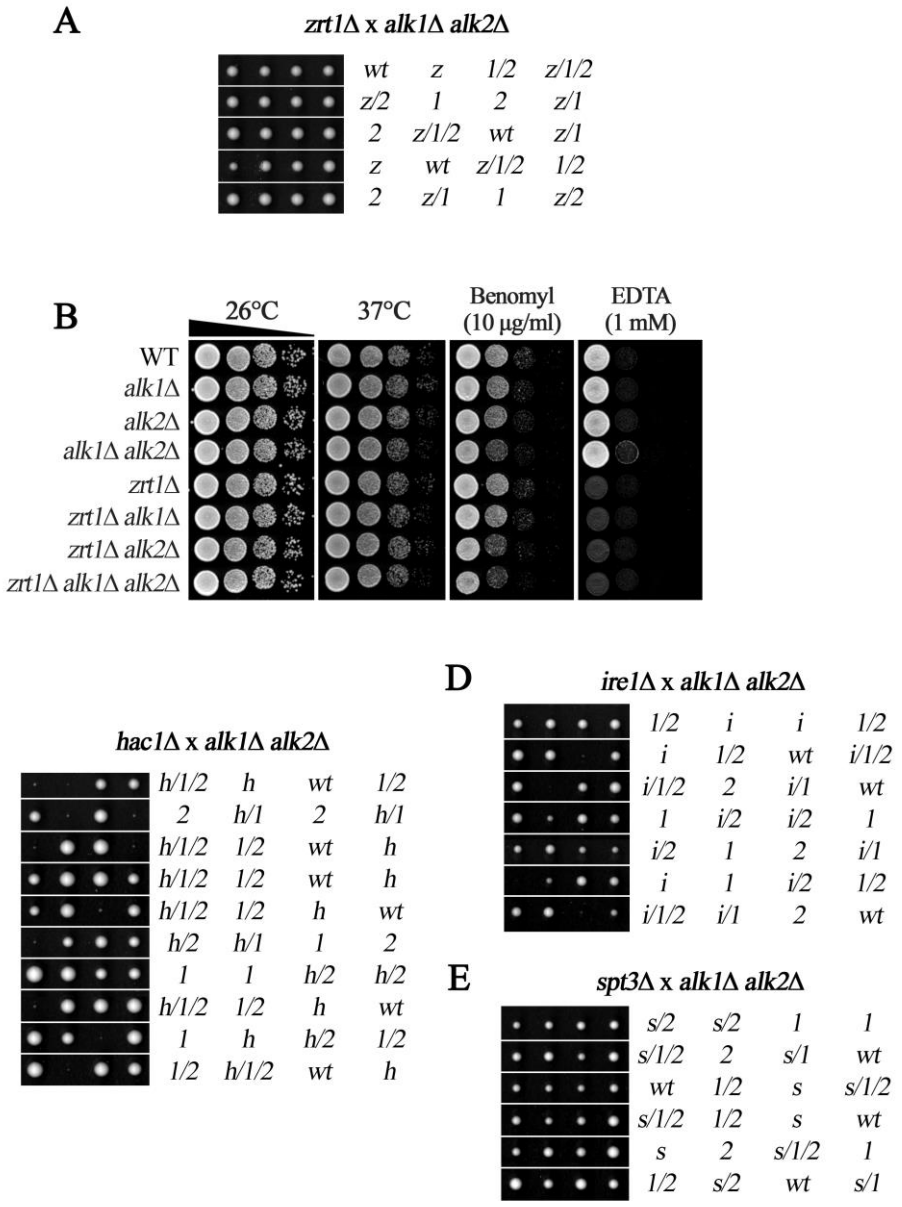

Figure 4.15. Verifying hits from the SGA screens. (A) Diploid strains heterozygous for *alk1*Δ, *alk2*Δ and *zrt1*Δ mutations were sporulated to generate haploid progeny and the genotypes were determined through tetrad analysis. (B) The indicated strains were spotted in 10-fold serial dilutions and grown at the indicated temperatures or at 26°C in the presence of benomyl and EDTA. (C, D, E) Tetrad analysis from the indicated crosses. Genotypes of spores are denoted as follows: *wt*, wild-type; *1*, *alk1*Δ; *2*, *alk2*Δ; z, *zrt1*Δ; h, *hac1*Δ; i, *ire1*Δ; s, *spt3*Δ.

will express lower than normal levels of Cdc20 resulting in a prolonged metaphase. Although this interaction has not been independently verified it is consistent with the hypothesis that *alk1*Δ *alk2*Δ cells lose viability when arrested in metaphase. Unfortunately, further investigation into these interactions and others identified in the screens could not be pursued due to time constraints.

4.11 Discussion

Haspins are atypical serine/threonine protein kinases that were originally identified in mice (Tanaka *et al*., 1994). Homologues have since been discovered in the genomes of many other eukaryotic organisms including the genome of the microsporidian *E. cuniculi*, which is predicted to contain less than 2000 protein-encoding genes (Katinka *et al*., 2001), suggesting an important and conserved role for Haspins. Two Haspin homologues, Alk1 and Alk2 are encoded by the *S. cerevisiae* genome, although they are largely uncharacterised. Recently, a number of studies have demonstrated that Haspins in fission yeast and higher eukaryotes contribute to localising the CPC to the centromere during mitosis (Kelly *et al*., 2010; Yamagishi *et al*., 2010; Wang *et al*., 2010). In the light of this information an attempt was made to characterise the two budding yeast Haspin-like kinases.

4.11.1 Haspin-like kinases, H3-T3ph and the CPC

Although the data contained herein does not conclusively demonstrate whether or not the Haspin-like kinases contribute to CPC localisation in budding yeast, evidence has been provided to suggest that deletion of *ALK1* and *ALK2* or mutation of histone H3-T3 does not interfere with the function of the CPC at the centromere. In *alk1*Δ *alk2*Δ and H3(T3A) cells there was no significant defect in chromosome bi-orientation or maintenance, unlike what was observed for Haspin and histone mutants in fission yeast

(Yamagishi *et al*., 2010). Kawashima *et al*. (2010) have demonstrated that phosphorylation of histone H2A at a conserved residue by Bub1 is required for Shugoshin localisation and function in humans and both fission and budding yeasts, suggesting that the Bub1/H2A/Shugoshin pathway is likely to be conserved. However, the negative genetic interactions observed in fission yeast between components of the Haspin/H3 and Bub1/H2A/Shugoshin pathways of CPC recruitment were not replicated using the equivalent mutants in budding yeast. Furthermore, while *sgo1*Δ cells displayed significant defects in chromosome bi-orientation and chromosome maintenance, the combination of *sgo1*Δ *alk1*Δ *alk2*Δ did not result in an additive phenotype. An additional experiment would be to examine whether CPC localisation is disrupted in these cells. Strains were generated to look at Ipl1-EGFP localisation in *alk1*Δ *alk2*Δ cells although there was not time to carry out a comprehensive analysis. Preliminary inspection of Ipl1-EGFP localisation in these cells appears to suggest that Ipl1 localisation is not disrupted in *alk1*Δ *alk2*Δ cells (Fig. A3). However, it would be necessary to quantify this signal and include mutants such as *sgo1*Δ and *sgo1*Δ *alk1*Δ *alk2*Δ in the analysis to determine whether these partially redundant pathways for CPC recruitment that exist in other organisms are shared with *S. cerevisiae*. It has been reported that Ipl1 association with the centromere is not disrupted in *alk1*Δ *alk2*Δ cells as determined by chromatin immunoprecipitation (Adele Marston, unpublished) and another study has shown that Ipl1 localisation is not disrupted in Bub1 or Sgo1 knockouts (Storchová *et al*., 2011). However, this does not rule out a potential redundancy between the two proposed pathways and would require further testing.

The localisation of Alk1 also differs compared to Haspins in other organisms. While strong localisation of Haspin to mitotic chromosomes is observed in the likes of human and fission yeast cells (Dai *et al*., 2005; Yamagishi *et al*., 2010), here it was

found that Alk1 localises to the cell cortex in metaphase, with no discernible signal that would suggest the presence of a nuclear pool. Unfortunately, the subcellular localisation of Alk2 could not be determined as an Alk2-EYFP signal could not be detected above the background signal. This is likely a reflection of the lower abundance of Alk2 compared to Alk1, as determined by western blotting. Of course it is possible that Alk2 localises to the nucleus and this will need to be investigated further and it will also be of interest to determine whether the localisation of these kinases is dynamic. Several annotations in the *Saccharomyces* Genome Database (SGD) suggest that Alk1 may be associated with the centromere and chromatin. Ranjitkar *et al*. (2010) detected Alk1 by mass spectrometry analysis of fractions eluted from an immunoprecipitation of the centromeric histone H3 variant Cse4 and Gilmore *et al*. (2012) detected Alk1 associated with affinity purified histone H3 and histone H4 through the same analysis. However, closer inspection of the data from these studies indicates that these interactions may not be significant, since very few Alk1 peptides were detected. An interesting experiment for the future would be to investigate whether the reciprocal interactions are observed when immunoprecipitating Alk1 and Alk2 from whole cell lysates.

A key observation that is yet to be made in budding yeast is whether histone H3 is phosphorylated at Thr-3 and if the Haspin-like kinases perform this modification. Although Nespoli *et al*. (2006) were able to show that Alk1 and Alk2 have weak autophosphorylation activity, they were unable to detect any activity towards histone H3 in *in vitro* kinase assays. However, this may have been due to technical issues as they state that the purification of both endogenous and recombinant Alk1 and Alk2 was problematic. Attempts were made during the course of this study to identify H3-T3ph by western blotting of whole cell extracts from asynchronous and metaphase arrested wild-type and *alk1*Δ *alk2*Δ cells, using extracts from H3(T3A) cells as a negative

control and lysates from metaphase-arrested *S. pombe nda3-KM311* mutant cells as a positive control (Yamagishi *et al*., 2010). Western blots were probed with a commercially available H3-T3ph antibody (Millipore) and one that was generously gifted by Dr. J. Higgins (Dai *et al*., 2005) although a signal could not be detected with either antibody even in the control samples. However, a signal was detected using an antibody against the dual modification of histone H3 Thr-3 phosphorylation and Lys-4 trimethylation (H3-T3phK4me3) in whole cell extracts from asynchronous and metaphase-arrested wild-type *S. cerevisiae* strains and a *S. pombe* strain. This signal was not detectable in a whole cell extract from an H3(T3A) budding yeast strain (Appendix Fig. A4 A). While this may hint at the presence of H3-T3ph in budding yeast, it is important that these experiments are repeated to include an *alk1*Δ *alk2*Δ strain and the other antibodies. It has been reported that H3-T3ph in *S. pombe* was only detected in extracts from metaphase-arrested cells (Yamagishi *et al*., 2010). However, probing with an H3-T3phK4me3 antibody showed a detectable signal in extracts from both asynchronous and metaphase-arrested cultures (Appendix Fig. A4 A). This raises the question of specificity regarding antibodies for detection of histone modifications. For example, the N-terminal tail of histone H3 is heavily modified post-translation and these modifications can exist in a multitude of different combinations that can differentially influence adjacent modifications, chromatin structure or protein binding (Oliver & Denu, 2010). Karimi-Ashtiyani & Houben (2013) have shown that the *in vitro* phosphorylation of histone H3 at Thr-3 by the *Arabidopsis thaliana* Haspin homologue is strongly influenced by the post-translational modifications of the adjacent amino acids. The particular combination of modifications is also likely to affect antibody recognition. An antibody that recognises H3-T3ph may not bind to H3-T3phK4me3 for example. Therefore, it is important that any observations regarding the distribution of histone modifications made with antibodies is interpreted with caution. It

may be necessary to test the antibodies used in this study against a panel of histone H3 N-terminal peptides with a variety of known modifications to determine the specificity. Alternatively, a different method of detection could be used such as mass spectrometry. This may also go towards explaining the poor signal observed in the western blots although this could be due to numerous factors, including low antibody avidity or modification abundance. In an attempt to address these potential issues preliminary experiments were carried out to isolate nuclei from yeast and extract proteins associated with chromatin. This significantly enriched the amount of histones in the protein extract and dramatically depleted non-nuclear proteins compared to whole cell extracts (Appendix Fig. A4 B). It will be necessary to continue to pursue these experiments in the future and determine whether histone H3 is phosphorylated at Thr-3 in budding yeast and, if so, whether Alk1 and/or Alk2 are responsible for the modification.

Another interesting observation from this study was that the deletion of both *ALK1* and *ALK2* results in a hypersensitivity to the microtubule destabilising drug benomyl. Hypersensitivity to microtubule poisons is a hallmark of mutants defective in spindle checkpoint signalling so it was hypothesised that the spindle checkpoint might be perturbed in *alk1*Δ *alk2*Δ cells. However, western blot analysis to monitor Pds1 levels indicated that these cells were able to mount a checkpoint response and arrest in metaphase when treated with benomyl. Additionally, these cells did not rapidly lose viability during benomyl treatment, unlike *bona fide* checkpoint mutants. If this phenotype was caused by the loss of H3-T3ph in these cells it stood to reason that H3(T3A) cells may also be benomyl sensitive; however, this was not the case. These observations therefore point towards a function for the Haspin-like kinases which is not related to the phosphorylation of histone H3 at Thr-3.

4.11.2 A role for the budding yeast Haspin-like kinases in the regulation of isotropic bud growth and cell polarity

Spindle positioning and cell morphology

Evidence has been provided to suggest that the Haspin-like kinases Alk1 and Alk2 have a role in the regulation of cell polarity and bud growth that is not linked to H3-T3ph. Initial experiments indicated that the mitotic spindle was frequently misaligned in *alk1*Δ *alk2*Δ cells arrested in metaphase and it was presumed that the spindle was in the mother cell and unable to orient towards the bud. This phenotype was not observed in wild-type or H3(T3A) cells. This led to the hypothesis that Alk1 and Alk2 may have some role in spindle orientation through the early or late microtubule delivery pathways, since mutants affecting these pathways displayed similar phenotypes (reviewed in Huisman & Segal, 2005) and the combination of knockouts of *ALK1* and *JNM1*, a component of the late pathway, was reported to be lethal (Schöner *et al*., 2008). By generating a series of mutant strains with combinations of Haspin-like kinase deletions and early/late pathway deletions it has been shown that it is unlikely that Alk1 or Alk2 have a direct role in either pathway and the reported synthetic lethal interaction between *alk1*Δ and *jnm1*Δ could also not be replicated. However, it remains possible that the Haspin-like kinases may have an indirect or lesser influence on these pathways that would not be highlighted in this analysis.

Subsequent experiments highlighted that the bud became abnormally large when *alk1*Δ *alk2*Δ cells were metaphase-arrested for a prolonged period of time, either through benomyl treatment or Cdc20 depletion, whereas wild-type and H3(T3A) cells remained homogenously large budded. Additionally, in metaphase-arrested cells it was noticed that the mitotic spindle became restricted to the enlarged bud in the majority of *alk1*Δ *alk2*Δ cells and eventually elongated in this compartment. This would result in

the formation of anucleate mother cells and binucleate daughters and have a severely negative effect on cell viability and subsequent mitosis. These observations suggest that both Alk1 and Alk2 are required to prevent continued isotropic bud growth in metaphase-arrested cells (Fig. 4.16). Normally, when bud growth is complete, cortical actin patches and cables are redistributed randomly thus preventing further bud growth (Fig. 4.16 b). Could the actin cytoskeleton remain polarised towards the bud in *alk1*Δ *alk2*Δ cells (Fig. 4.16 d)? This would provide an explanation for the abnormal morphology observed in metaphase-arrested *alk1*Δ *alk2*Δ cells and also why the DAmP allele of *CDC20* is synthetic lethal with *alk1*Δ *alk2*Δ but not with the individual deletions. This would also explain why the viability of *alk1*Δ *alk2*Δ cells was maintained if the metaphase block was lifted after a short arrest. If cells are only arrested in metaphase for a short period of time before being allowed to progress into anaphase and complete the cell cycle then presumably isotropic bud growth and polarisation does not become excessive and interfere with the proper anaphase spindle dynamics.

Many genes identified in the SGA screens also have roles in the regulation of the actin cytoskeleton and processes such as endocytosis that require actin. Potentially interesting genes that were lethal include *bem1*Δ and *num1*Δ. Bem1 (Bud EMergence 1) is involved in establishing cell polarity and morphogenesis and functions as a scaffold for complexes that include Cdc24, Rsr1 and Ste20 (Kozubowski *et al*., 2008; for review see Bi & Park, 2012). Num1 (NUclear Migration 1) is required for nuclear migration and localises to the mother and bud cell cortices (in a very similar pattern to Alk1) where it mediates interactions of dynein and cytoplasmic microtubules preferentially with the bud cell cortex (Heil-Chapdelaine *et al*., 2000; Markus & Lee, 2011). Misregulation of either of these proteins may go towards explaining the phenotypes

associated with *alk1*Δ *alk2*Δ cells. However, *bem1*Δ and *num1*Δ were only synthetically lethal with *alk1*Δ and neither was even synthetically sick with *alk2*Δ or *alk1*Δ *alk2*Δ. Similarly, *rvs161*Δ and *rvs167*Δ, knockouts of genes encoding proteins involved in the regulation of the actin cytoskeleton, endocytosis and cell polarity were severely synthetically sick with *alk2*Δ and may also be of interest. However, while *rvs161*Δ was synthetically sick, albeit to a much lesser degree, with *alk1*Δ, *rvs167*Δ was not and neither was found to interact with *alk1*Δ *alk2*Δ. This apparent lack of overlap in the top hits between the three screens is curious and will require further investigation.

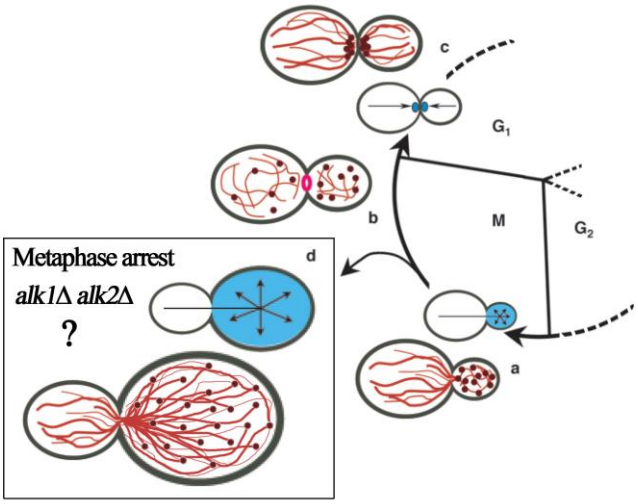

Figure 4.16. Model for excessive bud growth seen in metaphase-arrested *alk1*Δ *alk2*Δ cells. (a) In G_2/M there is a switch from bud-tip directed growth to isotropic growth resulting in the formation of an ellipsoidal shaped bud. (b) When bud growth is complete, polarity determinants (blue) are removed from the cell cortex, actin cables (red) and patches (brown) become disorganised and a cytokinetic ring forms, which contracts and disassembles after mitosis. (c) Actin and growth is repolarised between the mother and daughter cells to generate new cells walls. (d) In *alk1*Δ *alk2*Δ cells it would appear that isotropic growth in the bud persists during a metaphase arrest, resulting in the formation of an abnormally large bud. Adapted from Pruyne & Bretscher (2000).

If Alk1 and Alk2 are functionally redundant, then it would be reasonable to hypothesise that a number of unique or synergistic interactions would be observed in the *alk1*Δ *alk2*Δ double knockout screen that were not present in the single knockout screens. Examples of potentially interesting genes to which this applies include *AVO1*, *CMD1* and *SEC10*. *AVO1* encodes an essential component of the TORC2 complex and is required for TORC2 binding to the plasma membrane (Berchtold & Walther 2009). TORC2 is involved in the regulation of the actin cytoskeleton during polarised growth and cell wall integrity (Loewith *et al*., 2002) and localises to the cell cortex in a similar pattern to Alk1 (Berchtold & Walther 2009). Interestingly, *avo1* and *tor2* mutants are sensitive to benomyl like *alk1*Δ *alk2*Δ mutants (van Pel *et al*., 2013). *CMD1* encodes the essential calcium binding protein Calmodulin which is known to be involved in a vast number of different processes including spindle pole body (SPB) formation, organisation of the actin cytoskeleton, polarised growth, endocytosis, and mating and stress responses (Cyert, 2001; Okano & Ohya, 2003; Schaerer-Brodbeck & Riezman, 2003; Muller *et al*., 2005; Grötsch *et al*., 2010). *SEC10* encodes an essential subunit of the exocyst complex that is required for the polarised targeting of secretory vesicles to sites of exocytosis at the plasma membrane (e.g. the bud site; Hsu *et al*., 2004). The relevance of these interactions is unclear but some potentially interesting relationships between these genes and the yeast Haspin-like kinases can be inferred based on the literature and the phenotypes associated with *alk1*Δ *alk2*Δ mutants. For example, a recent study has shown that plasma membrane stress induced by either inhibition of sphingolipid metabolism or by mechanical stretching the membrane leads to the activation of the TORC2 complex (Berchtold *et al*., 2012), which in turn triggers a signalling cascade resulting in the upregulation of sphingolipid biosynthesis (Aronova *et al*., 2008). The excessive bud growth observed in *alk1*Δ *alk2*Δ suggests that bud growth is not being properly regulated and therefore lipid homeostasis may be

disrupted. If this is true, then there would be a significant requirement for sphingolipid biosynthesis in these cells and this may explain why the perturbation of proper TORC2 function would lead to such a detrimental effect on cell viability. A number of other negative interactors identified in the screens are also involved in lipid or membrane biosynthesis such as *INO2*, *FEN1*, *SAC1* and *ARG82*. Components of the unfolded protein response also regulate membrane biogenesis (Raychaudhuri *et al*., 2012) and many other genes identified in the screens are related to the endomembrane system in some way. Another recent study has shown that Cdc28-Clb2 dependent phosphorylation of the exocyst component Exo84 (which binds directly to Sec10) in mitosis disrupts exocyst assembly and thereby inhibits bud growth prior to the metaphase-anaphase transition (Luo *et al*., 2013). Could Alk1 and Alk2 be involved in this pathway? How the synthetic lethality of *sec10-DAmP alk1*Δ *alk2*Δ would fit into this hypothesis is unclear. We also know that mitotic delay reduces the viability of *alk1*Δ *alk2*Δ cells so any mutation that causes a delay in mitosis is likely to be synthetically sick or lethal in combination with *alk1*Δ *alk2*Δ. Calmodulin is required for SPB organisation (Muller *et al*., 2005) so it is possible that the *cmd1-DAmP* allele causes a delay in mitosis due to defective spindle formation which would explain the observed synthetic lethality. Many more inferences can be made based on the results of the screen but without further investigation they are speculative. Consequently, extended discussion of the screen will remain limited to the examples given above.

The cortical localisation of Alk1 in metaphase-arrested cells also suggests that Alk1 is ideally positioned to regulate actin dynamics or the cortical localisation/function of other proteins during this time. It will be important to investigate this further by comparing the arrangement of the actin cytoskeleton and by looking at the localisation of cortical polarity determinants, such as the Rho-like GTPase Cdc42, in metaphase-

arrested wild-type and *alk1*Δ *alk2*Δ cells. It will also be of interest to fully characterise the localisation pattern of Alk1 and Alk2 and determine whether the localisation of these kinases changes during different phases of the cell cycle. This analysis was hindered during this study due to the poor signal provided by the EYFP fusion proteins. Possible ways to overcome this would be to generate strains expressing fusion proteins with brighter fluorophores or to overexpress the fusion proteins. While this latter option would almost certainly aid in the visualisation of both kinases, the expression would no longer be cell cycle regulated and the localisation pattern observed may not be representative of the endogenous proteins. There is also the issue of the reported metaphase block induced by the overexpression of Alk2 to consider (Nespoli *et al*., 2006). Therefore, it would seem appropriate to proceed by generating strains expressing Alk1 and Alk2 fusion proteins with brighter fluorophores.

Identifying substrates and other proteins physically interacting with Alk1 and Alk2

An important direction for future work will be to uncover how the Haspin-like kinases function and dissect their individual or shared contributions to these functions by identifying substrates and physical interactors. A genome-wide phosphoproteomic analysis carried out by Bodenmiller *et al*. (2010) with *Saccharomyces cerevisiae* has provided some insight into what some of the substrates may be. By systematically deleting or mutating kinases and phosphatases and analysing phosphopeptides isolated from each mutant strain by mass spectrometry, they were able to identify 8814 regulated phosphorylation events and generate a system-wide protein phosphorylation network. Amongst the kinases analysed in their study were the Haspin-like kinases Alk1 and Alk2. They identified significant variations in the levels of phosphopeptides mapping to 19 proteins in *alk1*Δ cells and 9 proteins in *alk2*Δ cells. Hits from this phosphoproteomic screen are summarised in Table 4.5. These hits represent both

increases and decreases in the abundance of particular phosphopeptides. While a reduction or loss of a particular phosphopeptide may indicate that the associated protein is a substrate of either Alk1 or Alk2, it is also possible that the relative abundance is changing due to misregulation of other associated proteins resulting from the loss of the Haspin-like kinase activity. The hits representing increases in the abundance of a particular phosphopeptide could also be the result of misregulated proteins in *alk1*Δ and *alk2*Δ cells. Interestingly, many of the proteins identified in this phosphoproteomic screen are annotated as being involved in cytoskeletal organisation, endocytosis, stress responses and regulation of the pheromone response pathway, which correlates with the cell polarity phenotype observed in *alk1*Δ *alk2*Δ cells and the annotated functions of many of the positive and negative interactors identified in the SGA screens performed for this study.

A marked reduction in the phosphorylation of Akr1 was seen in *alk1*Δ cells (Bodenmiller *et al*., 2010) and this protein is annotated as being required for the endocytosis of pheromone receptors and control of cell shape. Null mutants of *AKR1* display abnormal bud morphology and increased cell size (Watanabe *et al*., 2009) as well as a hypersensitivity to benomyl (Parsons *et al*., 2004), similar to *alk1*Δ *alk2*Δ cells. Phosphorylation of Dig1 is reduced in both *alk1*Δ and *alk2*Δ cells (Bodenmiller *et al*., 2010). Dig1 is a MAP kinase-responsive inhibitor of the Ste12 transcription factor which is involved in the regulation of mating-specific genes and the invasive growth pathway (Olson *et al*., 2000). Phosphorylation of Bbc1, a protein involved in the assembly of actin patches and endocytosis, is reduced in *alk2*Δ cells (Bodenmiller *et al*., 2010). Intriguingly, *bbc1* null mutants suppress the abnormally large cell morphology and endocytosis defects seen in *vrp1*Δ cells (Mochida *et al*., 2002) and phosphorylation

Table 4.5. Changes detected in the phosphoproteome of *alk1*Δ and *alk2*Δ cells (Bodenmiller *et al*., 2010)

Kinase	Target	Type	logFC (log2)	Description of target
ALK1	*SKG1*	FC	2.5	Transmembrane protein with a role in cell wall polymer composition; localizes on inner surface of plasma membrane at bud and daughter cell
	EDE1	FC	2.4, 1.9	Endocytic protein; involved in a network of interactions with other endocytic proteins, binds membranes
	STB1	FC	2.3	Protein with role in regulation of MBF-specific transcription during G1/S transition, binds Swi6.
	IRS4	FC	1.8	Involved in regulating phosphatidylinositol 4,5-bisphosphate levels and autophagy; Irs4p and Tax4p bind and activate the PtdIns phosphatase Inp51p
	NUP2	FC	1.8	Nucleoporin involved in nucleocytoplasmic transport, binds to either the nucleoplasmic or cytoplasmic faces of the nuclear pore complex depending on Ran-GTP levels; also has a role in chromatin organization
	VRP1	FC	1.7	Proline-rich actin-associated protein involved in cytoskeletal organization and cytokinesis
	HRB1	FC	1.6	Poly(A+) RNA-binding protein; involved in the export of mRNAs from the nucleus to the cytoplasm
	RCK2	FC	1.6	Protein kinase involved in response to oxidative and osmotic stress
	MCK1	FC	1.6	Dual-specificity ser/thr and tyrosine protein kinase; roles in chromosome segregation, meiotic entry, genome stability, phosphorylation-dependent protein degradation (Rcn1p and Cdc6p), inhibition of protein kinase A, transcriptional regulation, inhibition of RNA pol III, calcium stress and inhibition of Clb2p-Cdc28p after nuclear division
	STE20	FC	1.5	Cdc42p-activated signal transducing kinase of the PAK (p21-activated kinase) family; involved in pheromone response, pseudohyphal/invasive growth, vacuole inheritance, down-regulation of sterol uptake
	YBL005W-B	FC	-1.5	Transposable element
	BCY1	FC	-1.5	Regulatory subunit of the cyclic AMP-dependent protein kinase (PKA), a component of a signaling pathway that controls a variety of cellular processes, including metabolism, cell cycle, stress response, stationary phase, and sporulation
	STF2	FC	-1.6	Protein involved in resistance to dessication stress, exhibits antioxidant properties, binds to F0 sector of mitochondrial F1F0 ATPase
	ITR1	FC	-1.8	Myo-inositol transporter; member of the sugar transporter superfamily; expression is repressed by inositol and choline via Opi1p and derepressed via Ino2p and Ino4p
	YAR009C	FC	-1.8	Transposable element
	AKR1	FC	-1.9	Palmitoyl transferase involved in protein palmitoylation; acts as a negative regulator of pheromone response pathway; required for endocytosis of pheromone receptors; involved in cell shape control
	DIG1	FC	-2.4, -1.6	MAP kinase-responsive inhibitor of the Ste12p transcription factor; involved in the regulation of mating-specific genes and the invasive growth pathway
	TPO2	V	-8.6	Polyamine transporter of the major facilitator superfamily; member of the 12-spanner drug:H(+) antiporter DHA1 family; specific for spermine; localizes to the plasma membrane
	YMR045C	V	-11.6	Transposable element
ALK2	*SPO12*	FC	2.9	Nucleolar protein of unknown function; positive regulator of mitotic exit; involved in regulating release of Cdc14p from the nucleolus in early anaphase
	PCT1	FC	1.8	Cholinephosphate cytidylyltransferase; a rate-determining enzyme of the CDP-choline pathway for phosphatidylcholine synthesis, inhibited by Sec14p, activated upon lipid-binding
	ZEO1	FC	-1.6	Peripheral membrane protein of the plasma membrane that interacts with Mid2p; regulates the cell integrity pathway mediated by Pkc1p and Slt2p; the authentic protein is detected in a phosphorylated state in highly purified mitochondria
	DIG1	FC	-1.8	MAP kinase-responsive inhibitor of the Ste12p transcription factor; involved in the regulation of mating-specific genes and the invasive growth pathway
	SOD1	FC	-1.9	Cytosolic copper-zinc superoxide dismutase; detoxifies superoxide and is involved in repressing respiration in the presence of glucose, via stabilization of Yck1p and Yck2p kinases
	IGD1	FC	-2	Cytoplasmic protein that inhibits Gdb1p glycogen debranching activity; required for normal intracellular accumulation of glycogen
	BBC1	FC	-2.2	Protein possibly involved in assembly of actin patches; interacts with an actin assembly factor Las17p and with the SH3 domains of Type I myosins Myo3p and Myo5p; localized predominantly to cortical actin patches
	SPC29	V	-6	Inner plaque spindle pole body (SPB) component, links the central plaque component Spc42p to the inner plaque component Spc110p; required for SPB duplication
	NUP2	V	-6	Nucleoporin involved in nucleocytoplasmic transport, binds to either the nucleoplasmic or cytoplasmic faces of the nuclear pore complex depending on Ran-GTP levels; also has a role in chromatin organization

FC = Fold change, V = Vanished. Gene descriptions sourced from SGD.

of Vrp1, a homologue Wiskott-Aldrich Syndrome Protein (WASP)-Interacting Protein (WIP), has been shown to increase in *alk1*Δ cells (Bodenmiller *et al*., 2010).

Phosphorylation of particular residues in the nucleoporin Nup2 and the spindle pole body component Spc29 disappear completely in *alk2*Δ cells hinting at a possible relationship between Alk2, the nucleus and the mitotic spindle. This could be potentially significant as Haspin in HeLa cells has also been shown to localise to spindle microtubules and spindle poles (Dai *et al*., 2005). There are many other potentially interesting hits identified in the phosphoproteomic screens carried out by Bodenmiller *et al*. (2010) and it would be interesting to see if any of these proteins are in fact substrates of Alk1 and Alk2. It is also worth considering that if Alk1 and Alk2 are functioning redundantly they may have activity towards common substrates, so phosphorylation events that are reduced in both *alk1*Δ and *alk2*Δ knockouts, such as those observed for Dig1, may disappear altogether in the double knockout for example. Likewise, substrates for which both Alk1 and Alk2 have a similar affinity may not even be identified in this screen. To address this and gain more insight into the role of the Haspin-like kinases it may be worthwhile to apply this phosphoproteomic approach in a more comprehensive and focused study directly comparing the phosphoproteome of wild-type, *alk1*Δ, *alk2*Δ and *alk1*Δ *alk2*Δ cells. As Alk1 and Alk2 are cell cycle regulated it may be of additional benefit to perform this analysis in metaphase-arrested cells to enrich for changes in the phosphoproteome at the stage in the cell cycle when the Haspin-like kinases are normally expressed.

Immunoprecipitation and mass spectrometry analysis would also facilitate the identification of potential substrates and also interacting partners. During this study, strains were generated expressing Alk1 and Alk2 with in-frame tandem affinity

purification (TAP) tag fused to their C-termini (Alk1-TAP, Alk2-TAP). Attempts were made to isolate Alk1 and Alk2 along with any other associated proteins from whole cell lysates. Unfortunately, progress was hampered by technical issues. Preliminary data (not shown) identifies a number of potentially interesting proteins although it would be essential to repeat these experiments before any conclusions were made as the peptide counts were very low. A potentially interesting hit with Alk1-TAP is the yeast homologue of protein kinase C, Pkc1. Pkc1 regulates a highly-conserved cell wall integrity pathway that is essential for cell wall remodelling in proliferating cells and localises to the bud neck and sites of polarised growth (Andrews & Stark, 2000). Intriguingly, Pkc1 also has nuclear localisation and mitotic spindle binding domains, which may provide a molecular explanation for observations that suggest an additional role for Pkc1 in regulating microtubule dynamics (Denis & Cyert, 2005).

Could Alk1 and Alk2 regulate cell polarity by promoting the displacement or inactivation of cortical determinants of cell polarity through direct phosphorylation of substrates at the cell cortex and transcriptional regulation? Without further investigation this is only speculation, although collectively the data provided here from this study and those gathered from other sources certainly support this hypothesis. It will be a priority in the future to unravel the mechanism behind this novel role for the Haspin-like kinases in the regulation of cell polarity.

Is the role for the budding yeast Haspin-like kinases in the regulation of cell polarity conserved?

A key question is whether this role for Alk1 and Alk2 in the regulation of cell polarity is shared with Haspin homologues in other organisms. Evidence gathered from research into the *Arabidopsis thaliana* homologue of Haspin (AtHaspin) hints that this

may be the case. Complete loss of function of AtHaspin results in embryonic lethality, but a striking effect on plant development was observed in AtHaspin mutant zygotes. After fertilisation, wild-type zygotes first elongate approximately three-fold before the first cell division, which is asymmetric and results in the production of a large basal cell and a small apical cell. The basal cell subsequently divides longitudinally to produce a file of cells and the apical cell divides twice longitudinally and once laterally to form an eight cell proembryo (Zhang & Laux, 2011). In AtHaspin mutant zygotes the plane of this first cell division is skewed. Abnormal arrangements of apical cell progeny are observed and extra cell divisions are seen in the basal cell progeny resulting in clusters of cells rather than a single file of longitudinal cells (Kurihara *et al*., 2011; Ashtiyani *et al*., 2011). AtHaspin RNAi also results in a range of pleiotropic growth phenotypes such as adventitious shoot formation, defects in vascular tissue patterning and lateral organ outgrowth (Ashtiyani *et al*., 2011). These phenotypes resemble those seen in mutants with defective auxin transduction pathway signalling and polar auxin transport in plants is a key process for guiding plant polarity and morphogenesis (Yoshida *et al*., 2013). Additionally, AtHaspin is expressed in actively dividing tissues such as those found at root and shoot tips and is absent or at very low levels in differentiated tissues except the vasculature, a pattern shared with proteins involved in the auxin pathway and similar to Haspin homologues in other cell types (Higgins, 2001). Many of the auxin pathway proteins are highly polar in localisation and are involved in signal transduction, endosomal protein recycling and vesicle trafficking. Interestingly, the expression of a number of these genes is also significantly reduced in AtHaspin mutant plants (Ashtiyani *et al*., 2011). Data gathered from the budding yeast SGA screens showed that many of the genes interacting negatively with *alk1*Δ and *alk2*Δ are involved in endocytosis, cell and organelle membranes and regulation of transcription. A number of studies have also identified that MAPK signalling pathways can influence auxin signal

transduction pathways (Lee *et al*., 2009; Zhao *et al*., 2013). Could AtHaspin have some effect on the regulation of these pathways to influence cell polarity?

Interestingly, Haspin in HeLa cells also appears to localise to spindle microtubules and spindle poles as well as mitotic chromosomes (Dai *et al*., 2005), and Haspin RNAi leads to the development of multiple extra centrosome-like foci that nucleate microtubules (Dai *et al*., 2009). Plants have no centrosomes, but microtubules polymerise around the nuclear envelope during prophase and this is where AtHaspin is localised at this time (Kurihara *et al*., 2011). These microtubules become sorted into two poles that are perpendicular to the cell division plane that is predetermined by a cortical ring of microtubules (Ambrose & Cyr, 2008). Could the abnormal symmetry of cell divisions observed by Ashtiyani *et al*. (2011) in AtHapsin mutants and the appearance of extra centrosome-like foci in HeLa cells after Haspin RNAi treatment described by Dai *et al*. (2005) be the result of misregulation of these spindle or cortical microtubules?

These observations suggest additional roles for Haspin kinases. However, further investigation will be required before these roles can be accurately defined.

CHAPTER 5

Final discussion and perspectives

5.1 *Ipl1, Bim1 and microtubule binding*

Data has been provided within this study suggesting that preventing phosphorylation of several serine residues in CDK phosphorylation motifs present in the N-terminal non-kinase domain of Ipl1 results in its premature localisation to the spindle in metaphase. Furthermore, this interaction between Ipl1 and microtubules appears to be mediated by the yeast microtubule binding EB1 homologue Bim1. These observations were supported by a concurrent study that also showed that the phosphorylation status of the CDK motifs regulates the direct binding of Ipl1 to Bim1 through the adjacent EB1 binding motifs (SxIP; Zimniak *et al*., 2012). Dephosphorylation of these CDK sites as cells progress into anaphase allows the binding of Ipl1 to Bim1 and contributes to the spindle localisation of the CPC. Whether this is a conserved mechanism for Ipl1/Aurora B localisation in other organisms is not clear. Ipl1 homologues in the closely related yeasts *K. lactis* and *A. gossypii* do not contain SxIP motifs and neither does human Aurora B. However, a physical interaction has been reported between human Aurora B and EB1 (Sun *et al*., 2008), suggesting that the interaction is conserved but the mode of interaction may differ. Whether this interaction is regulated by CDK phosphorylation or contributes to CPC localisation is not known and would require further investigation. Indeed, it is also not known whether CDK directly phosphorylates Aurora B.

5.2 *How is the budding yeast CPC localised to centromeres?*

Recent studies have demonstrated that the conserved Haspin and Bub1 kinases phosphorylate histone H3 and histone H2A respectively to mediate the recruitment of the CPC to centromeres in fission yeast and human cells (Tsukahara *et al*., 2010; Yamagishi *et al*., 2010; Wang *et al*., 2010). While phosphorylated histone H3 binds Bir1/Survivin directly, phosphorylated histone H2A recruits Shugoshin, which acts as an adaptor protein for the CPC. Perturbation of either or both of these CPC recruitment

pathways disrupts CPC localisation to the centromere (Wang *et al*., 2010; Yamagishi *et al*., 2010) and causes defects in chromosome bi-orientation and reduced viability in fission yeast (Yamagishi *et al*., 2010).

Is this mechanism for the centromeric recruitment of the CPC conserved in budding yeast? The data presented here and from other studies appear to suggest that it is not. Firstly, while the recruitment of Shugoshin through Bub1-mediated phosphorylation of histone H2A appears to be conserved (Yamagishi *et al*., 2010), neither Bub1 nor Shugoshin are required for CPC localisation in budding yeast (Storchová *et al*., 2011). Furthermore, Ipl1 localisation at centromeric regions as determined by chromatin precipitation (Adele Marston, unpublished) and microscopy (this study) is not disrupted by loss of Alk1 and Alk2. Additionally, Alk1, Alk2 or H3-T3ph was not required for proper functioning of the CPC at centromeres or for viability when either Shugoshin or Bub1 were absent (this study), suggesting that the CPC was correctly localised in these cells although this still needs to be confirmed.

So how is the CPC localised to centromeres in budding yeast? This is still unclear and will require further investigation. Previous studies have demonstrated that Bir1 can bind directly to the Ndc10 subunit of the CBF3 complex (Yoon & Carbon, 1999; Widlund *et al*., 2006). This complex is budding yeast-specific and binds to centromere-specific DNA sequences to provide a platform for kinetochore formation. This interaction could be sufficient to localise the CPC to centromeres in budding yeast although it is possible that other as yet unknown interactions also contribute to this process. A recent study has demonstrated that deleting the N-terminus of Sli15 prevents the association of Ipl1-Sli15 with Bir1-Nbl1, yet chromosome bi-orientation and segregation occur normally (Campbell & Desai, 2013). This Sli15 mutant was found to

localise strongly and prematurely to the spindle in metaphase-arrested cells similarly to the Ipl1 and Sli15 CDK site mutants (this study; Pereira & Schiebel, 2003; Zimniak *et al*., 2012), suggesting that the localisation of Ipl1-Sli15 on microtubules is sufficient for bi-orientation in the absence of Bir1-dependent targeting to kinetochores. This discovery has intriguing implications for how Ipl1/Aurora B discriminates between correct and incorrect kinetochore-microtubule attachments. Current models state that the tension generated by bi-oriented attachments stretches the centromere and kinetochore, physically separating Ipl1/Aurora B at the inner centromere from its substrates in the kinetochore. This separation and subsequent dephosphorylation of Ipl1/Aurora B substrates by outer-kinetochore-localised phosphatase activity has been suggested to stabilise this attachment (Liu *et al*., 2009; Welburn *et al*., 2010; Lampson & Cheeseman, 2011). However, if bi-orientation proceeds normally when Ipl1 is localised to the spindle then this suggests that proximity between Ipl1 and its substrates is not the factor used to discriminate between correct and incorrect attachments in budding yeast. Since it is clear from numerous studies that tension is central to this error correction mechanism, one possible explanation is that conformational changes induced when the kinetochore complex is under tension prevents Ipl1 gaining access to its substrates (Campbell & Desai, 2013). In support of this hypothesis, studies using super-resolution imaging has identified structural changes in kinetochores that are attached and under tension compared to those that are not (Joglekar *et al*., 2009; Wan *et al*., 2009; reviewed in DeLuca & Musacchio, 2011). These findings warrant further investigation to uncover how Ipl1/Aurora B discriminates between microtubule attachments and also contribute an additional factor to be considered in current models of microtubule error correction and bi-orientation. Furthermore, the Sli15 N-terminal mutant also suppressed the lethality of *BIR1* and *NBL1* deletion (Campbell & Desai, 2013). The ability to create viable yeast strains with deletions of these seemingly essential proteins provides a

method to investigate the individual contributions of Bir1 and Nbl1 in CPC function and may also lead to the identification of CPC-independent roles of these proteins.

5.3 *A novel role for Alk1 and Alk2 in the regulation of cell polarity and spindle positioning*

Two weeks prior to the submission of this thesis, a paper was published online ahead of print regarding Alk1 and Alk2 (Panigada *et al*., 2013; from the same lab that published Nespoli *et al*., 2006). In this paper they presented many observations that concur with those made during this current study. They too show that *alk1*Δ *alk2*Δ cells are hypersensitive to benomyl and that this is not a result of defective spindle checkpoint signalling by analysing the degradation kinetics of Pds1. They also observed spindle mispositioning, elongation and disassembly in the bud of *alk1*Δ *alk2*Δ cells after mitotic arrest (through nocodazole treatment and Cdc20 depletion) in addition to continued bud growth. They too investigated whether Alk1 and Alk2 were directly involved with Kar9 and Dyn1 mechanisms of spindle positioning and came to the same conclusion that they are not.

Panigada *et al*. (2013) have also presented a number of additional observations that are of interest. A hypothesis that was described in the discussion of Chapter 4 is that Haspin-like kinases may function by regulating the displacement or inactivation of cortical determinants of cell polarity to depolarise the actin cytoskeleton. This would provide an explanation as to why the bud continues to grow in metaphase-arrested *alk1*Δ *alk2*Δ cells. In support of this hypothesis, Panigada *et al*. (2013) have shown that the actin cytoskeleton remained polarised towards the bud in metaphase-arrested *alk1*Δ *alk2*Δ cells (Fig. 4.14 b). In contrast to this, metaphase-arrested wild-type cells evenly redistributed actin between mother and bud (Fig. 4.14 d). Additionally, they found that a

number of polarity determinants were mislocalised in *alk1*Δ *alk2*Δ cells. The formin Bnr1, which nucleates actin filaments, and the polarisome component Spa2, which functions in actin organisation, remained asymmetrically distributed to the bud in metaphase-arrested *alk1*Δ *alk2*Δ cells but not in wild-type cells (Panigada *et al*., 2013). Bud6, another polarisome component that interacts with formins and actin, was also mislocalised in *alk1*Δ *alk2*Δ cells. Bud6 is important for astral microtubule interaction at the bud neck and bud cortex to align and position the spindle. In *alk1*Δ *alk2*Δ cells, Bud6 was absent from the bud neck and enriched at the bud cortex (Panigada *et al*., 2013). This could provide an explanation as to why the spindle becomes restricted to the bud in these cells. The cortical localisation of Alk1 (this study) suggests that it is ideally positioned to regulate the dynamics of these proteins during the period surrounding the metaphase to anaphase transition. It will be interesting to see whether Alk2 shares a similar localisation pattern and whether the localisation of both kinases is dynamic. Together, these observations and the data gathered from the *alk1*Δ *alk2*Δ phosphoproteomic (Bodenmiller *et al*., 2010) and SGA (this study) screens all suggest a novel role for the budding yeast Haspin-like kinases in regulating cell polarity.

The data presented here also shows that these phenotypes are not related to H3-T3 phosphorylation. Panigada *et al*. (2013) found that cells expressing kinase-deficient alleles of *ALK1* and *ALK2* also displayed similar phenotypes to *alk1*Δ *alk2*Δ cells. Together, this shows that the kinase activity of Alk1 and Alk2 is required for their function but that their function is mediated through substrates other than H3-T3. However, no substrates of either kinase have been identified to date. As discussed at the end of the Chapter 4, it will be important in the future to identify the substrates and interacting partners of Alk1 and Alk2 to dissect their mode of action and understand how they contribute to spindle positioning and cell polarity.

5.4 *A conserved role for Haspin kinases in regulating cell polarity?*

As discussed in Chapter 4, the strongest evidence for a conserved role for Haspin kinases in the regulation of cell polarity comes from studies with *Arabidopsis thaliana,* since AtHaspin mutant zygotes divide along abnormal division planes leading to defects in tissue patterning and development (Kurihara *et al*., 2011; Ashtiyani *et al*., 2011). However, until the mechanisms are investigated further this suggestion of conservation is relatively speculative. On this subject, one of the most intriguing results presented by Panigada *et al*. (2013) was that expression of AtHaspin in *alk1*Δ *alk2*Δ cells suppressed their benomyl hypersensitivity and significantly rescued the numbers of cells with binucleate buds (Panigada *et al*., 2013). This provides further evidence to suggest that the role for Haspin kinases in the regulation of cell polarity is evolutionarily conserved. Asymmetric cell divisions are critical during embryogenesis for cell differentiation and for tissue maintenance in adult organisms. It will be interesting to investigate whether this role for the budding yeast Haspin-like kinases in the regulation of cell polarity is shared with Haspin homologues in mammalian cells and other model organisms used to study development such as *D. melanogaster* or *C. elegans*.

REFERENCES

Adames, N.R., Cooper, J.A., (2000). Microtubule interactions with the cell cortex causing nuclear movements in Saccharomyces cerevisiae. *J. Cell Biol.* **149**, 863–874.

Adams, A.E.M., Johnson, D.I., Longnecker, R.M., Sloat, B.F., Pringle, J.R., (1990). CDC42 and CDC43. Two Additional Genes Involved in Budding and the Establishment of Cell Polarity in the Yeast Saccharomyces cerevisiae. *J. Cell Biol.* **111**, 131–142.

Adams, R.R., Carmena, M., Earnshaw, W.C., (2001). Chromosomal passengers and the (aurora) ABCs of mitosis. *TRENDS Cell Biol*. **11**, 49–54.

Adams, R.R., Wheatley, S.P., Gouldsworthy, A.M., Kandels-Lewis, S.E., Carmena, M., Smythe, C., Gerloff, D.L., Earnshaw, W.C., (2000). INCENP binds the Aurora-related kinase AIRK2 and is required to target it to chromosomes, the central spindle and cleavage furrow. *Curr. Biol.* **10**, 1075–1078.

Akiyoshi, B., Nelson, C.R., Biggins, S., (2013). The aurora B kinase promotes inner and outer kinetochore interactions in budding yeast. *Genetics* **194**, 785–789.

Akiyoshi, B., Nelson, C.R., Ranish, J.A., Biggins, S., (2009). Quantitative proteomic analysis of purified yeast kinetochores identifies a PP1 regulatory subunit. *Genes Dev.* **23**, 2887–2899.

Amberg, D.C., (1998) Three-dimensional imaging of the yeast actin cytoskeleton through the budding cell cycle. *Mol. Biol. Cell* **9**, 3259-3262

Amberg, D.C., Burke, D.J., Strathern, J.N., (2005). *Methods in Yeast Genetics: A Cold Spring Harbor Laboratory Manual*. Cold Spring Harbor Laboratory Press, New York.

Ambrose, J.C., Cyr, R., (2008). Mitotic spindle organization by the preprophase band. *Mol. Plant* **1**, 950–960.

Andrews, P.D., Ovechkina, Y., Morrice, N., Wagenbach, M., Duncan, K., Wordeman, L., Swedlow, J.R., (2004). Aurora B regulates MCAK at the mitotic centromere. *Dev. Cell* **6**, 253–268.

Andrews, P.D., Stark, M.J.R., (2000). Dynamic, Rho1p-dependent localization of Pkc1p to sites of polarized growth. *J. Cell Sci.* **113**, 2685–2693.

Arkowitz, R.A., (2009). Chemical gradients and chemotropism in yeast. *Cold Spring Harb. Perspect. Biol*. **1**, a001958

Aronova, S., Wedaman, K., Aronov, P.A., Fontes, K., Ramos, K., Hammock, B.D., Powers, T., (2008). Regulation of ceramide biosynthesis by TOR complex 2. *Cell Metab.* **7**, 148-158.

Asbury, C.L., Gestaut, D.R., Powers, A.F., Franck, A.D., Davis, T.N., (2006). The Dam1 kinetochore complex harnesses microtubule dynamics to produce force and movement. *PNAS* **103**, 9873–9878.

Ashtiyani, R.K., Moghaddam, A.M.B., Schubert, V., Rutten, T., Fuchs, J., Demidov, D., Blattner, F.R., Houben, A., (2011). AtHaspin phosphorylates histone H3 at threonine 3 during mitosis and contributes to embryonic patterning in Arabidopsis. *The Plant Journal* **68**, 443–454.

Baldo, V., Liang, J., Wang, G., Zhou, H., (2012). Preserving Yeast Genetic Heritage through DNA Damage Checkpoint Regulation and Telomere Maintenance. *Biomolecules* **2**, 505–523.

Barford, D., (2011). Structure, function and mechanism of the anaphase promoting complex (APC/C). *Quart. Rev. Biophys.* **44**, 153–190.

Barr, A.R., Gergely, F., (2007). Aurora-A: the maker and breaker of spindle poles. *J. Cell Sci.* **120**, 2987–2996.

Benton, B.K., Tinkelenberg, A., Gonzalez, I., Cross, F.R., (1997). Cla4p, a Saccharomyces cerevisiae Cdc42p-Activated Kinase Involved in Cytokinesis, Is Activated at Mitosis. *Mol. Cell. Biol.* **17**, 5067–5076.

Berchtold, D., Piccolis, M., Chiaruttini, N., Riezman, I., Riezman, H., Roux, A., Walther, T.C., Loewith, R., (2012). Plasma membrane stress induces relocalization of Slm proteins and activation of TORC2 to promote sphingolipid synthesis. *Nat. Cell Biol.* **14**, 542-547.

Berchtold, D., Walther, T.C., (2009). TORC2 plasma membrane localization is essential for cell viability and restricted to a distinct domain. *Mol. Biol. Cell* **20**, 1565-1575.

Bergman, Z.J., Xia, X., Amaro, I.A., Huffaker, T.C., (2012). Constitutive dynein activity in She1 mutants reveals differences in microtubule attachment at the yeast spindle pole body. *Mol. Biol. Cell* **23**, 2319–2326.

Bertin, A., Nogales, E., (2012). Septin filament organization in Saccharomyces cerevisiae. *Comm. Int. Biol.* **5**, 503–505.

Bi, E., Maddox, P., Lew, D.J., Salmon, E.D., McMillan, J.N., Yeh, E., Pringle, J.R., (1998). Involvement of an actomyosin contractile ring in Saccharomyces cerevisiae cytokinesis. *J. Cell Biol.* **142**, 1301-1312

Bi, E., Park, H.-O., (2012). Cell polarization and cytokinesis in budding yeast. *Genetics* **191**, 347–387.

Biggins, S., Murray, A.W., (2001). The budding yeast protein kinase Ipl1/Aurora allows the absence of tension to activate the spindle checkpoint. *Genes Dev.* **15**, 3118–3129.

Biggins, S., Severin, F.F., Bhalla, N., Sassoon, I., Hyman, A.A., Murray, A.W., (1999). The conserved protein kinase Ipl1 regulates microtubule binding to kinetochores in budding yeast. *Genes Dev.* **13**, 532–544.

Bishop, J.D., Schumacher, J.M., (2002). Phosphorylation of the carboxyl terminus of inner centromere protein (INCENP) by the Aurora B Kinase stimulates Aurora B kinase activity. *J. Biol. Chem.* **277**, 27577–27580.

Bloom, K., Joglekar, A.P., (2010). Towards building a chromosome segregation machine. *Nature* **463**, 446–456.

Bodenmiller, B., Wanka, S., Kraft, C., Urban, J., Campbell, D., Pedrioli, P.G., Gerrits, B., Picotti, P., Lam, H., Vitek, O., Brusniak, M.-Y., Roschitzki, B., Zhang, C., Shokat, K.M., Schlapbach, R., Colman-Lerner, A., Nolan, G.P., Nesvizhskii, A.I., Peter, M., Loewith, R., von Mering, C., Aebersold, R., (2010). Phosphoproteomic analysis reveals interconnected system-wide responses to perturbations of kinases and phosphatases in yeast. *Sci. Sig*. **3**, rs4.

Bohnert, K.A., Chen, J., Clifford, D.M., Kooi, C.W. Vander, Gould, K.L., (2009). A Link between Aurora Kinase and Clp1/Cdc14 Regulation Uncovered by the Identification of a Fission Yeast Borealin-Like Protein. *Mol. Biol. Cell* **20**, 3646–3659.

Bouck, D.C., Bloom, K.S., (2005). The kinetochore protein Ndc10p is required for spindle stability and cytokinesis in yeast. *PNAS* **102**, 5408–5413.

Brennwald, P., Rossi, G., (2007). Spatial regulation of exocytosis and cell polarity: yeast as a model for animal cells. *FEBS Letters* **581**, 2119-2124.

Breslow, D.K., Cameron, D.M., Collins, S.R., Stewart-Ornstein, J., Newman, H.W., Braun, S., Madhani, D., Krogan, N.J., Weissman, J.S., (2008). A comprehensive strategy enabling high-resolution functional analysis of the yeast genome. *Nat. Methods* **5**, 711–718.

Brown, J.L., Jaquenoud, M., Gulli, M-P., Chant, J., Peter, M., (1997). Novel Cdc42-binding proteins Gic1 and Gic2 control cell polarity in yeast. *Genes Dev.* **11**, 2972-2982.

Buvelot, S., Tatsutani, S.Y., Vermaak, D., Biggins, S., (2003). The budding yeast Ipl1/Aurora protein kinase regulates mitotic spindle disassembly. *J. Cell Biol.* **160**, 329–339.

Cabib, E., Drgonova, J., Drgon, T., (1998). Role of small G proteins in yeast cell polarization and wall biosynthesis. *Annu. Rev. Biochem.* **67**, 307–333.

Campbell, C.S., Desai, A., (2013). Tension sensing by Aurora B kinase is independent of survivin-based centromere localization. *Nature* **497**, 118–121.

Cancer Research UK, (2013). All Cancers: Combined Key Facts [WWW Document]. URL http://www.cancerresearchuk.org/cancer-info/cancerstats/keyfacts/Allcancerscombined/

Capalbo, L., Montembault, E., Takeda, T., Bassi, Z.I., Glover, D.M., D'Avino, P.P., (2012). The chromosomal passenger complex controls the function of endosomal

sorting complex required for transport-III Snf7 proteins during cytokinesis. *Open Biol.* **2**, 120070.

Carlton, J.G., Caballe, A., Agromayor, M., Kloc, M., Martin-Serrano, J., (2012). ESCRT-III governs the Aurora B-mediated abscission checkpoint through CHMP4C. *Science* **336**, 220–225.

Carmena, M., (2012). Abscission checkpoint control: stuck in the middle with Aurora B. *Open Biol.* **2**, 120095.

Carmena, M., Ruchaud, S., Earnshaw, W.C., (2009). Making the Auroras glow: regulation of Aurora A and B kinase function by interacting proteins. *Curr. Opin. Cell Biol.* **21**, 796–805.

Carmena, M., Wheelock, M., Funabiki, H., Earnshaw, W.C., (2012). The chromosomal passenger complex (CPC): from easy rider to the godfather of mitosis. *Nat. Rev. Mol. Cell Biol.* **13**, 789–803.

Carvalho, P., Gupta, M.L., Hoyt, M.A., Pellman, D., (2004). Cell cycle control of kinesin-mediated transport of Bik1 (CLIP-170) regulates microtubule stability and dynein activation. *Dev. Cell* **6**, 815–829.

Casamayor, A., Snyder, M., (2002). Bud-site selection and cell polarity in budding yeast. *Curr. Op. Microbiol.* **5**, 179-186

Casamayor, A., Snyder, M., (2003). Molecular Dissection of a Yeast Septin: Distinct Domains Are Required for Septin Interaction, Localization, and Function. *Mol. Cell Biol.* **23**, 2762–2777.

Caudron, F., Andrieux, A., Job, D., Boscheron, C., (2008). A new role for kinesin-directed transport of Bik1p (CLIP-170) in Saccharomyces cerevisiae. *J. Cell Sci.* **121**, 1506–1513.

Caydasi, A.K., Ibrahim, B., Pereira, G., (2010). Monitoring spindle orientation: Spindle position checkpoint in charge. *Cell Div.* **5**, 1–15.

Chan, C.S., Botstein, D., (1993). Isolation and characterization of chromosome-gain and increase-in-ploidy mutants in yeast. *Genetics* **135**, 677–691.

Chan, Y.W., Jeyaprakash, A.A., Nigg, E.A., Santamaria, A., (2012). Aurora B controls kinetochore-microtubule attachments by inhibiting Ska complex-KMN network interaction. *J. Cell Biol.* **196**, 563–571.

Chang, E.J., Archambault, V., McLachlin, D.T., Krutchinsky, A.N., Chait, B.T., (2004). Analysis of Protein Phosphorylation by Hypothesis-Driven Multiple-Stage Mass Spectrometry. *Anal. Chem.* **76**, 4472–4483.

Cheeseman, I.M., Anderson, S., Jwa, M., Green, E.M., Kang, J.-S., Yates, J.R., Chan, C.S.M., Drubin, D.G., Barnes, G., (2002). Phospho-regulation of kinetochore-microtubule attachments by the Aurora kinase Ipl1p. *Cell* **111**, 163–172.

Cheeseman, I.M., Brew, C., Wolyniak, M., Desai, A., Anderson, S., Muster, N., Yates, J.R., Huffaker, T.C., Drubin, D.G., Barnes, G., (2001). Implication of a novel multiprotein Dam1p complex in outer kinetochore function. *J. Cell Biol.* **155**, 1137–1145.

Cheeseman, I.M., Chappie, J.S., Wilson-Kubalek, E.M., Desai, A., (2006). The conserved KMN network constitutes the core microtubule-binding site of the kinetochore. *Cell* **127**, 983–997.

Chi, A., Huttenhower, C., Geer, L.Y., Coon, J.J., Syka, J.E.P., Bai, D.L., Shabanowitz, J., Burke, D.J., Troyanskaya, O.G., Hunt, D.F., (2007). Analysis of phosphorylation sites on proteins from Saccharomyces cerevisiae by electron transfer dissociation (ETD) mass spectrometry. *PNAS* **104**, 2193–2198.

Cho, U.-S., Harrison, S.C., (2011). Ndc10 is a platform for inner kinetochore assembly in budding yeast. *Nat. Struct. Mol. Biol* **19**, 48–55.

Cimini, D., Wan, X., Hirel, C.B., Salmon, E.D., (2006). Aurora kinase promotes turnover of kinetochore microtubules to reduce chromosome segregation errors. *Curr. Biol.* **16**, 1711–1718.

Ciosk, R., Zachariae, W., Michaelis, C., Shevchenko, A., Mann, M., Nasmyth, K., (1998). An ESP1/PDS1 complex regulates loss of sister chromatid cohesion at the metaphase to anaphase transition in yeast. *Cell* **93**, 1067–1076.

Cohen-Fix, O., Peters, J.-M., Kirschner, M.W., Koshland, D., (1996). Anaphase initiation in Saccharomyces cerevisiae is controlled by the APC-dependent degradation of the anaphase inhibitor Pds1p. *Genes Dev.* **10**, 3081–3093.

Connell, C.M., Colnaghi, R., Wheatley, S.P., (2008). Nuclear survivin has reduced stability and is not cytoprotective. *J. Biol. Chem.* **283**, 3289–3296.

Cooke, C.A., Heck, M.M., Earnshaw, W.C., (1987). The inner centromere protein (INCENP) antigens: movement from inner centromere to midbody during mitosis. *J. Cell Biol.* **105**, 2053–2067.

Crosio, C., Fimia, G.M., Loury, R., Kimura, M., Okano, Y., Zhou, H., Sen, S., Allis, C.D., Sassone-Corsi, P., (2002). Mitotic Phosphorylation of Histone H3: Spatio-Temporal Regulation by Mammalian Aurora Kinases. *Mol. Cell. Biol.* **22**, 874–885.

Cullen, P.J., Sprague, G.F., (2012). The regulation of filamentous growth in yeast. *Genetics* **190**, 23–49.

Cvrčková, F., Virgilio, C.D., Manser, E., Pringle, J.R., Nasmyth, K., (1995). Ste20-like protein kinases are required for normal localization of cell growth and for cytokinesis in budding yeast. *Genes Dev.* **9**, 1817-1830.

Cyert, M.S., (2001). Genetic analysis of calmodulin and its targets in Saccharomyces cerevisiae. *Annu. Rev. Genet.* **35**, 647-672.

Dai, J., Hyland, E.M., Yuan, D.S., Huang, H., Bader, J.S., Boeke, J.D., (2008). Probing nucleosome function: a highly versatile library of synthetic histone H3 and H4 mutants. *Cell* **134**, 1066–1078.

Dai, J., Kateneva, A. V, Higgins, J.M.G., (2009). Studies of haspin-depleted cells reveal that spindle-pole integrity in mitosis requires chromosome cohesion. *J. Cell Sci.* **122**, 4168–4176.

Dai, J., Sullivan, B.A., Higgins, J.M.G., (2006). Regulation of mitotic chromosome cohesion by Haspin and Aurora B. *Dev. Cell* **11**, 741–750.

Dai, J., Sultan, S., Taylor, S.S., Higgins, J.M.G., (2005). The kinase haspin is required for mitotic histone H3 Thr 3 phosphorylation and normal metaphase chromosome alignment. *Genes Dev.* **19**, 472–488.

De Gramont, A., Barbour, L., Ross, K.E., Cohen-Fix, O., (2007). The Spindle Midzone Microtubule-Associated Proteins Ase1p and Cin8p Affect the Number and Orientation of Astral Microtubules in Saccharomyces cerevisiae. *Cell Cycle* **6**, 1231–1241.

De Smet, I., Beeckman, T., (2011). Asymmetric cell division in land plants and algae: the driving force for differentiation. *Nat. Rev. Mol. Cell Biol.* **12**, 177–188.

DeLuca, J.G., Gall, W.E., Ciferri, C., Cimini, D., Musacchio, A., Salmon, E.D., (2006). Kinetochore microtubule dynamics and attachment stability are regulated by Hec1. *Cell* **127**, 969–982.

DeLuca, J.G., Musacchio, A., (2011). Structural organization of the kinetochore-microtubule interface. *Curr. Opin. Cell Biol.* **24**, 48–56.

DeMay, B.S., Bai, X., Howard, L., Occhipinti, P., Meseroll, R.A., Spiliotis, E.T., Oldenbourg, R., Gladfelter, A.S., (2011). Septin filaments exhibit a dynamic, paired organization that is conserved from yeast to mammals. *J. Cell Biol.* **193**, 1065–1081.

Denis, V., Cyert, M.S., (2005). Molecular Analysis Reveals Localization of Saccharomyces cerevisiae Protein Kinase C to Sites of Polarized Growth and Pkc1p Targeting to the Nucleus and Mitotic Spindle. *Euk. Cell* **4**, 36–45.

Desai, A., Mitchison, T.J., (1997). Microtubule polymerization dynamics. *Annu. Rev. Cell Dev.* Biol. **13**, 83–117.

Dickinson, J.R., (2008). Filament formation in Saccharomyces cerevisiae - a review. *Folia Microbiol.* **53**, 3–14.

Dieterich, K., Rifo, R.S., Faure, A.K., Hennebicq, S., Amar, B. Ben, Zahi, M., Perrin, J., Martinez, D., Sèle, B., Jouk, P.-S., Ohlmann, T., Rousseaux, S., Lunardi, J., Ray, P.F., (2007). Homozygous mutation of AURKC yields large-headed polyploid spermatozoa and causes male infertility. *Nature Genetics* **39**, 661–665.

Diffley, J.F.X., (2004). Regulation of early events in chromosome replication. *Curr. Biol.* **14**, R778–786.

Dirick, L., Böhm, T., Nasmyth, K., (1995). Roles and regulation of Cln-Cdc28 kinases at the start of the cell cycle of Saccharomyces cerevisiae. *EMBO* **14**, 4803–4813.

Ditchfield, C., Johnson, V.L., Tighe, A., Ellston, R., Haworth, C., Johnson, T., Mortlock, A., Keen, N., Taylor, S.S., (2003). Aurora B couples chromosome alignment with anaphase by targeting BubR1, Mad2, and Cenp-E to kinetochores. *J. Cell Biol.* **161**, 267–280.

Dobbelaere, J., Barral, Y., (2004). Spatial coordination of cytokinetic events by compartmentalization of the cell cortex. *Science* **305**, 393–396.

Dobrynin, G., Popp, O., Romer, T., Bremer, S., Schmitz, M.H.A., Gerlich, D.W., Meyer, H., (2011). Cdc48/p97-Ufd1-Npl4 antagonizes Aurora B during chromosome segregation in HeLa cells. *J. Cell Sci.* **124**, 1571–1580.

Dominguez, R., Holmes, K.C., (2011). Actin Structure and Function. *Annu. Rev. Biophys.* **40**, 169–186.

Douglas, M.E., Davies, T., Joseph, N., Mishima, M., (2010). Aurora B and 14-3-3 coordinately regulate clustering of centralspindlin during cytokinesis. *Curr. Biol.* **20**, 927–933.

Duesberg, P., Stindl, R., Li, R., Hehlmann, R., Rasnick, D., (2001). Aneuploidy versus gene mutation as cause of cancer. *Curr. Science* **81**, 490–500.

Earnshaw, W.C., Bernat, R.L., (1991). Chromosomal passengers: Toward an integrated view of mitosis. *Chromosoma* **100**, 139–146.

Eby, J.J., Holly, S.P., van Drogen, F., Grishin, A. V, Peter, M., Drubin, D.G., Blumer, K.J., (1998). Actin cytoskeleton organization regulated by the PAK family of protein kinases. *Curr. Biol.* **8**, 967–970.

Elia, N., Sougrat, R., Spurlin, T.A., Hurley, J.H., Lippincott-Schwartz, J., (2011). Dynamics of endosomal sorting complex required for transport (ESCRT) machinery during cytokinesis and its role in abscission. *PNAS* **108**, 4846–4851.

Emanuele, M.J., Lan, W., Jwa, M., Miller, S.A., Chan, C.S.M., Stukenberg, P.T., (2008). Aurora B kinase and protein phosphatase 1 have opposing roles in modulating kinetochore assembly. *J. Cell Biol*. **181**, 241–254.

Eshel, D., Urrestarazu, L.A., Vissers, S., Jauniaux, J.C., van Vliet-Reedijk, J.C., Planta, R.J., Gibbons, I.R., (1993). Cytoplasmic dynein is required for normal nuclear segregation in yeast. *PNAS* **90**, 11172–11176.

Etienne-Manneville, S., (2004). Cdc42 - the centre of polarity. *J. Cell Sci.* **117**, 1291–1300.

Evangelista, M., Blundell, K., Longtine, M.S., Chow, C.J., Adames, N., Pringle, J.R., Peter, M., Boone, C., (1997). Bni1p, a yeast formin linking Cdc42 and the actin cytoskeleton during polarized morphogenesis. *Science* **276**, 118-122

Fernández-Miranda, G., de Castro, I.P., Carmena, M., Aguirre-Portolés, C., Ruchaud, S., Fant, X., Montoya, G., Earnshaw, W.C., Malumbres, M., (2010). SUMOylation modulates the function of Aurora-B kinase. *J. Cell Sci.* **123**, 2823–2833.

Fernius, J., Hardwick, K.G., (2007). Bub1 kinase targets Sgo1 to ensure efficient chromosome biorientation in budding yeast mitosis. *PLoS Genet.* **3**, e213.

Finley, D., (2009). Recognition and processing of ubiquitin-protein conjugates by the proteasome. *Annu. Rev. Biochem.* **78**, 477–513.

Fischle, W., Tseng, B.S., Dormann, H.L., Ueberheide, B.M., Garcia, B.A., Shabanowitz, J., Hunt, D.F., Funabiki, H., Allis, C.D., (2005). Regulation of HP1 – chromatin binding by histone H3 methylation and phosphorylation. *Nature* **438**, 1116–1122.

Foley, E.A., Maldonado, M., Kapoor, T.M., (2011). Formation of stable attachments between kinetochores and microtubules depends on the B56-PP2A phosphatase. *Nat. Cell Biol.* **13**, 1265–1271.

Francisco, L., Chan, C.S., (1994). Regulation of yeast chromosome segregation by Ipl1 protein kinase and type 1 protein phosphatase. *Cell. Mol. Biol. Res.* **40**, 207–213.

Fraschini, R., Beretta, A., Sironi, L., Musacchio, A., Lucchini, G., Piatti, S., (2001). Bub3 interaction with Mad2, Mad3 and Cdc20 is mediated by WD40 repeats and does not require intact kinetochores. *EMBO* **20**, 6648–6659.

Gardner, K.E., Zhou, L., Parra, M.A., Chen, X., Strahl, B.D., (2011). Identification of lysine 37 of histone H2B as a novel site of methylation. PloS one **6**, e16244.

Gassmann, R., Carvalho, A., Henzing, A.J., Ruchaud, S., Hudson, D.F., Honda, R., Nigg, E.A., Gerloff, D.L., Earnshaw, W.C., (2004). Borealin: a novel chromosomal passenger required for stability of the bipolar mitotic spindle. *J. Cell Biol.* **166**, 179–191.

Gestaut, D.R., Graczyk, B., Cooper, J., Widlund, P.O., Zelter, A., Wordeman, L., Asbury, C.L., Davis, T.N., (2008). Phosphoregulation and depolymerization-driven movement of the Dam1 complex do not require ring formation. *Nat. Cell Biol.* **10**, 407–414.

Giaever, G., Chu, A.M., Ni, L., Connelly, C., Riles, L., *et al*., (2002). Functional profiling of the Saccharomyces cerevisiae genome. *Nature* **418**, 387–391.

Giet, R., Glover, D.M., (2001). Drosophila Aurora B Kinase Is Required for Histone H3 Phosphorylation and Condensin Recruitment during Chromosome Condensation and to Organize the Central Spindle during Cytokinesis. *J. Cell Biol.* **152**, 669–681.

Gietz, R.D., Sugino, A., (1988) New yeast-*Escherichia coli* shuttle vectors constructed with in vitro mutagenized yeast genes lacking six-base pair restriction sites. *Gene* **74**, 527-534

Gietz, R.D., Woods, R.A., (2002). Transformation of yeast by the LiAc/ss carrier DNA/PEG method. *Methods In Enzymology* **350**, 87–96.

Gillis, A.N., Thomas, S., Hansen, S.D., Kaplan, K.B., (2005). A novel role for the CBF3 kinetochore-scaffold complex in regulating septin dynamics and cytokinesis. *J. Cell Biol.* **171**, 773–784.

Gilmore, J.M., Sardiu, M.E., Venkatesh, S., Stutzman, B., Peak, A., Seidel, C.W., Workman, J.L., Florens, L., Washburn, M.P., (2012). Characterization of a highly conserved histone related protein, Ydl156w, and its functional associations using quantitative proteomic analyses. *Mol. Cell. Prot.* **11**, 1–4.

Gladfelter, A.S., Pringle, J.R., Lew, D.J., (2001). The septin cortex at the yeast mother-bud neck. *Curr. Opin. Microbiol.* **4**, 681–689.

Glotzer, M., Murray, A.W., Kirschner, M.W., (1991). Cyclin is degraded by the ubiquitin pathway. *Nature* **349**, 132–138.

Glover, D.M., Leibowitz, M.H., McLean, D.A., Parry, H., (1995). Mutations in aurora prevent centrosome separation leading to the formation of monopolar spindles. *Cell* **81**, 95–105.

Gnad, F., de Godoy, L.M.F., Cox, J., Neuhauser, N., Ren, S., Olsen, J. V, Mann, M., (2009). High-accuracy identification and bioinformatic analysis of in vivo protein phosphorylation sites in yeast. *Proteomics* **9**, 4642–4652.

Goffeau, A., Barrell, B.G., Bussey, H., Davis, R.W., Dujon, B., Feldmann, H., Galibert, F., Hoheisel, J.D., Jacq, C., Johnston, M., Louis, E.J., Mewes, H.W., Murakami, Y., Philippsen, P., Tettelin, H., Oliver, S.G., (1996). Life with 6000 Genes. *Science* **274**, 546–567.

Gordon, D.J., Resio, B., Pellman, D., (2012). Causes and consequences of aneuploidy in cancer. *Nat. Rev. Genetics* **13**, 189–203.

Grava, S., Schaerer, F., Faty, M., Philippsen, P., Barral, Y., (2006). Asymmetric recruitment of dynein to spindle poles and microtubules promotes proper spindle orientation in yeast. *Dev. Cell* **10**, 425–439.

Grötsch, H., Giblin, J.P., Idrissi, F-Z., Fernandez-Golbano, I-M., Collette, J.R., Newpher, T.M., Robles, V., Lemmon, S.K., Geli, M-I., (2010). Calmodulin dissociation regulates Myo5 recruitment and function at endocytic sites. *EMBO* **29**, 2899-2914.

Gruneberg, U., Neef, R., Honda, R., Nigg, E.A., Barr, F.A., (2004). Relocation of Aurora B from centromeres to the central spindle at the metaphase to anaphase transition requires MKlp2. *J. Cell Biol.* **166**, 167–172.

Guizetti, J., Schermelleh, L., Mäntler, J., Maar, S., Poser, I., Leonhardt, H., Müller-Reichert, T., Gerlich, D.W., (2011). Cortical constriction during abscission involves helices of ESCRT-III-dependent filaments. *Science* **331**, 1616–1620.

Gupta, M.L., Carvalho, P., Roof, D.M., Pellman, D., (2006). Plus end-specific depolymerase activity of Kip3, a kinesin-8 protein, explains its role in positioning the yeast mitotic spindle. *Nat. Cell Biol.* **8**, 913–923.

Gutiérrez-Caballero, C., Cebollero, L.R., Pendás, A.M., (2012). Shugoshins: from protectors of cohesion to versatile adaptors at the centromere. *TRENDS Genet.* **28**, 351–360.

Hailey, D.W., Davis, T.N., Muller, E.G.D., (2001). Cover photo, in: Palazzo, R.E., Davis, T.N. (Eds.), *Methods in Cell Biology* Vol. 67 - Centrosomes and Spindle Pole Bodies. Academic Press, San Diego.

Hardwick, K.G., Johnston, R.C., Smith, D.L., Murray, A.W., (2000). MAD3 encodes a novel component of the spindle checkpoint which interacts with Bub3p, Cdc20p, and Mad2p. *J. Cell Biol*. **148**, 871–882.

Hartman, M.A., Spudich, J.A., (2012). The myosin superfamily at a glance. *J. Cell Sci.* **125**, 1627–1632.

Hartwell, L.H., (1971). Genetic control of the cell division cycle in yeast. IV. Genes controlling bud emergence and cytokinesis. *Exp. Cell Res.* **69**, 265–276.

Hauf, S., Cole, R.W., LaTerra, S., Zimmer, C., Schnapp, G., Walter, R., Heckel, A., van Meel, J., Rieder, C.L., Peters, J.-M., (2003). The small molecule Hesperadin reveals a role for Aurora B in correcting kinetochore-microtubule attachment and in maintaining the spindle assembly checkpoint. *J. Cell Biol.* **161**, 281–294.

Heil-Chapdelaine, R.A., Oberle, J.R., Cooper, J.A., (2000). The cortical protein Num1p is essential for dynein-dependent interactions of microtubules with the cortex. *J. Cell Biol.* **151**, 1337–1344.

Heng, Y.-W., Koh, C.-G., (2010). Actin cytoskeleton dynamics and the cell division cycle. *Int. J. Biochem. Cell Biol.* **42**, 1622–1633.

Higgins, J.M.G., (2001). The Haspin gene: location in an intron of the integrin alphaE gene, associated transcription of an integrin alphaE-derived RNA and expression in diploid as well as haploid cells. *Gene* **267**, 55–69.

Higgins, J.M.G., (2001). Haspin-like proteins: A new family of evolutionarily conserved putative eukaryotic protein kinases. *Pro. Sci.* **10**, 1677–1684.

Higgins, J.M.G., (2003). Structure, function and evolution of haspin and haspin-related proteins, a distinctive group of eukaryotic protein kinases. *Cell. Mol. Life Sci*. **60**, 446–462.

Higgins, J.M.G., (2010). Haspin: a newly discovered regulator of mitotic chromosome behavior. *Chromosoma* **119**, 137–147.

Hildebrandt, E.R., Hoyt, M.A., (2001). Cell cycle-dependent degradation of the Saccharomyces cerevisiae spindle motor Cin8p requires APC(Cdh1) and a bipartite destruction sequence. *Mol. Biol. Cell* **12**, 3402–3416.

Hirota, T., Lipp, J.J., Toh, B.-H., Peters, J.-M., (2005). Histone H3 serine10 phosphorylation by Aurora B causes HP1 dissociation from heterochromatin. *Nature* **438**, 1176–1180.

Holt, L.J., Tuch, B.B., Villen, J., Johnson, A.D., Gygi, S.P., Morgan, D.O., (2009). Global Analysis of Cdk1 Substrate Phosphorylation Sites Provides Insights into Evolution. *Science* **325**, 1682–1686.

Honda, R., Ko, R., Nigg, E.A., (2003). Exploring the Functional Interactions between Aurora B, INCENP, and Survivin in Mitosis. *Mol. Biol. Cell* **14**, 3325–3341.

Honnappa, S., Gouveia, S.M., Weisbrich, A., Damberger, F.F., Bhavesh, N.S., Jawhari, H., Grigoriev, I., van Rijssel, F.J.A., Buey, R.M., Lawera, A., Jelesarov, I., Winkler, F.K., Wüthrich, K., Akhmanova, A., Steinmetz, M.O., (2009). An EB1-binding motif acts as a microtubule tip localization signal. *Cell* **138**, 366–376.

Howell, B.J., McEwen, B.F., Canman, J.C., Hoffman, D.B., Farrar, E.M., Rieder, C.L., Salmon, E.D., (2001). Cytoplasmic dynein/dynactin drives kinetochore protein transport to the spindle poles and has a role in mitotic spindle checkpoint inactivation. *J. Cell Biol.* **155**, 1159–1172.

Hoyt, M.A., Totis, L., Roberts, B.T., (1991). S. cerevisiae genes required for cell cycle arrest in response to loss of microtubule function. *Cell* **66**, 507–517.

Hsu, J.Y., Sun, Z.-W., Li, X., Reuben, M., Tatchell, K., Bishop, D.K., Grushcow, J.M., Brame, C.J., Caldwell, J.A., Hunt, D.F., Lin, R., Smith, M.M., Allis, C.D., (2000). Mitotic phosphorylation of histone H3 is governed by Ipl1/aurora kinase and Glc7/PP1 phosphatase in budding yeast and nematodes. *Cell* **102**, 279–291.

Hsu, S-C., TerBush, D., Abraham, M., Guo, W., (2004). The exocyst complex in polarized exocytosis. *Int. Rev. Cytol.* **233**, 243-265.

Huang, J.N., Park, I., Ellingson, E., Littlepage, L.E., Pellman, D., (2001). Activity of the APCCdh1 form of the anaphase-promoting complex persists until S phase and prevents the premature expression of Cdc20p. *J. Cell Biol.* **154**, 85–94.

Huber, A., Bodenmiller, B., Uotila, A., Stahl, M., Wanka, S., Gerrits, B., Aebersold, R., Loewith, R., (2009). Characterization of the rapamycin-sensitive phosphoproteome reveals that Sch9 is a central coordinator of protein synthesis. *Genes Dev.* **23**, 1929–1943.

Huh, W.-K., Falvo, J. V, Gerke, L.C., Carroll, A.S., Howson, R.W., Weissman, J.S., O'Shea, E.K., (2003). Global analysis of protein localization in budding yeast. *Nature* **425**, 686–691.

Huisman, S.M., Segal, M., (2005). Cortical capture of microtubules and spindle polarity in budding yeast – where's the catch? *J. Cell Sci.* **118**, 463–471.

Hümmer, S., Mayer, T.U., (2009). Cdk1 negatively regulates midzone localization of the mitotic kinesin Mklp2 and the chromosomal passenger complex. *Curr. Biol.* **19**, 607–612.

Hwang, E., Kusch, J., Barral, Y., Huffaker, T.C., (2003). Spindle orientation in Saccharomyces cerevisiae depends on the transport of microtubule ends along polarized actin cables. *J. Cell Biol.* **161**, 483–488.

Indjeian, V.B., Stern, B.M., Murray, A.W., (2005). The Centromeric Protein Sgo1 Is Required to Sense Lack of Tension on Mitotic Chromosomes. *Science* **307**, 130–133.

Irazoqui, J.E., Gladfelter, A.S., Lew, D.J., (2003). Scaffold-mediated symmetry breaking by Cdc42p. *Nat. Cell Biol.* **5**, 1062-1070.

Irazoqui, J.E., Howell, A.S., Theesfeld, C.L., Lew, D.J., (2005). Opposing Roles for Actin in Cdc42p Polarization. *Mol. Biol. Cell* **16**, 1296–1304.

Janke, C., Ortiz, J., Lechner, J., Shevchenko, A., Magiera, M.M., Schramm, C., Schiebel, E., (2001). The budding yeast proteins Spc24p and Spc25p interact with Ndc80p and Nuf2p at the kinetochore and are important for kinetochore clustering and checkpoint control. *EMBO* **20**, 777–791.

Janke, C., Ortíz, J., Tanaka, T.U., Lechner, J., Schiebel, E., (2002). Four new subunits of the Dam1-Duo1 complex reveal novel functions in sister kinetochore biorientation. *EMBO* **21**, 181–193.

Jaspersen, S.L., Winey, M., (2004). The budding yeast spindle pole body: structure, duplication, and function. *Annu. Rev. Cell Dev. Biol.* **20**, 1–28.

Jelluma, N., Brenkman, A.B., van den Broek, N.J.F., Cruijsen, C.W.A., van Osch, M.H.J., Lens, S.M.A., Medema, R.H., Kops, G.J.P.L., (2008). Mps1 phosphorylates Borealin to control Aurora B activity and chromosome alignment. *Cell* **132**, 233–246.

Jelluma, N., Dansen, T.B., Sliedrecht, T., Kwiatkowski, N.P., Kops, G.J.P.L., (2010). Release of Mps1 from kinetochores is crucial for timely anaphase onset. *J. Cell Biol.* **191**, 281–90.

Jeyaprakash, A.A., Santamaria, A., Jayachandran, U., Chan, Y.W., Benda, C., Nigg, E.A., Conti, E., (2012). Structural and Functional Organization of the Ska Complex, a Key Component of the Kinetochore-Microtubule Interface. *Mol. Cell* **46**, 1–13.

Jin, T., (2013). Gradient sensing during chemotaxis. *Curr. Opin. Cell Biol.* **25**, 1–6.

Joglekar, A.P., Bloom, K., Salmon, E.D., (2009). In Vivo Protein Architecture of the Eukaryotic Kinetochore with Nanometer Scale Accuracy. *Curr. Biol.* **19**, 694–699.

Juang, Y.-L., Huang, J., Peters, J.-M., McLaughlin, M.E., Tai, C.-Y., Pellman, D., (1997). APC-Mediated Proteolysis of Ase1 and the Morphogenesis of the Mitotic Spindle. *Science* **275**, 1311–1314.

Kallio, M.J., McCleland, M.L., Stukenberg, P.T., Gorbsky, G.J., (2002). Inhibition of aurora B kinase blocks chromosome segregation, overrides the spindle checkpoint, and perturbs microtubule dynamics in mitosis. *Curr. Biol.* **12**, 900–905.

Kang, J., Cheeseman, I.M., Kallstrom, G., Velmurugan, S., Barnes, G., Chan, C.S., (2001). Functional cooperation of Dam1, Ipl1, and the inner centromere protein (INCENP)-related protein Sli15 during chromosome segregation. *J. Cell Biol.* **155**, 763–774.

Kardon, J.R., Reck-Peterson, S.L., Vale, R.D., (2009). Regulation of the processivity and intracellular localization of Saccharomyces cerevisiae dynein by dynactin. *PNAS* **106**, 5669–5674.

Karimi-Ashtiyani, R., Houben, A., (2013). In vitro phosphorylation of histone h3 at threonine 3 by Arabidopsis haspin is strongly influenced by posttranslational modifications of adjacent amino acids. *Mol. Plant* **6**, 574–576.

Katinka, M.D., Duprat, S., Cornillot, E., Méténier, G., Thomarat, F., Prensier, G., Barbe, V., Peyretaillade, E., Brottier, P., Wincker, P., Delbac, F., El Alaoui, H., Peyret, P., Saurin, W., Gouy, M., Weissenbach, J., Vivarès, C.P., (2001). Genome sequence and gene compaction of the eukaryote parasite Encephalitozoon cuniculi. *Nature* **414**, 450–453.

Kawashima, S.A., Tsukahara, T., Langegger, M., Hauf, S., Kitajima, T.S., Watanabe, Y., (2007). Shugoshin enables tension-generating attachment of kinetochores by loading Aurora to centromeres. *Genes Dev.* **21**, 420–435.

Kawashima, S.A., Yamagishi, Y., Honda, T., Ishiguro, K., Watanabe, Y., (2010). Phosphorylation of H2A by Bub1 Prevents Chromosomal Instability Through Localizing Shugoshin. *Science* **327**, 172–177.

Keating, P., Rachidi, N., Tanaka, T.U., Stark, M.J.R., (2009). Ipl1-dependent phosphorylation of Dam1 is reduced by tension applied on kinetochores. *J. Cell Sci.* **122**, 4375–4382.

Kelly, A.E., Ghenoiu, C., Xue, J.Z., Zierhut, C., Kimura, H., Funabiki, H., (2010). Survivin Reads Phosphorylated Histone H3 Threonine 3 to Activate the Mitotic Kinase Aurora B. *Science* **330**, 235–239.

Kim, J., Kang, J., Chan, C.S.M., (1999). Chromosome Segregation in Saccharomyces cerevisiae. *J. Cell Biol.* **145**, 1381–1394.

Kim, Y., Holland, A.J., Lan, W., Cleveland, D.W., (2010). Aurora Kinases and Protein Phosphatase 1 Mediate Chromosome Congression through Regulation of CENP-E. *Cell* **142**, 444–455.

King, E.M.J., Rachidi, N., Morrice, N., Hardwick, K.G., Stark, M.J., (2007a). Ipl1p-dependent phosphorylation of Mad3p is required for the spindle checkpoint response to lack of tension at kinetochores. *Genes Dev*. **21**, 1163–1168.

King, E.M.J., van der Sar, S.J.A., Hardwick, K.G., (2007b). Mad3 KEN boxes mediate both Cdc20 and Mad3 turnover, and are critical for the spindle checkpoint. *PloS one* **2**, e342.

Kinoshita, M., Kumar, S., Mizoguchi, A., Ide, C., Kinoshita, A., Haraguchi, T., Hiraoka, Y., Noda, M., (1997). Nedd5, a mammalian septin, is a novel cytoskeletal component interacting with actin-based structures. *Genes Dev.* **11**, 1535–1547.

Kitagawa, M., Fung, S.Y.S., Onishi, N., Saya, H., Lee, S.H., (2013). Targeting Aurora B to the Equatorial Cortex by MKlp2 Is Required for Cytokinesis. *PloS one* **8**, e64826.

Kitajima, T.S., Kawashima, S.A., Watanabe, Y., (2004). The conserved kinetochore protein shugoshin protects centromeric cohesion during meiosis. *Nature* **427**, 510–517.

Kitamura, E., Tanaka, K., Kitamura, Y., Tanaka, T.U., (2007). Kinetochore microtubule interaction during S phase in Saccharomyces cerevisiae. *Genes Dev.* **21**, 3319–3330.

Kline-Smith, S.L., Khodjakov, A., Hergert, P., Walczak, C.E., (2004). Depletion of Centromeric MCAK Leads to Chromosome Congression and Segregation Defects Due to Improper Kinetochore Attachments. *Mol. Biol. Cell* **15**, 1146–1159.

Kline-Smith, S.L., Sandall, S., Desai, A., (2005). Kinetochore-spindle microtubule interactions during mitosis. *Curr. Opin. Cell Biol.* **17**, 35–46.

Knoblich, J.A., (2010). Asymmetric cell division: recent developments and their implications for tumour biology. *Nat. Rev. Mol. Cell Biol.* **11**, 849–860.

Kollman, J.M., Merdes, A., Mourey, L., Agard, D.A., (2011). Microtubule nucleation by gamma-tubulin complexes. *Nat. Rev. Mol. Cell Biol.* **12**, 709–721.

Korinek, W.S., Copeland, M.J., Chaudhuri, A., Chant, J., (2000). Molecular Linkage Underlying Microtubule Orientation Toward Cortical Sites in Yeast. *Science* **287**, 2257–2259.

Kotwaliwale, C. V., Buvelot Frei, S., Stern, B.M., Biggins, S., (2007). A pathway containing the Ipl1/Aurora protein kinase and the spindle midzone protein Ase1 regulates yeast spindle assembly. *Dev. Cell* **13**, 433–445.

Kozubowski, L., Saito, K., Johnson, J. M., Howell, A. S., Zyla, T. R., Lew, D. J., (2008). Symmetry-breaking polarization driven by a Cdc42p GEF-PAK complex. *Curr. Biol.* **18**, 1719-1726.

Kurasawa, Y., Earnshaw, W.C., Mochizuki, Y., Dohmae, N., Todokoro, K., (2004). Essential roles of KIF4 and its binding partner PRC1 in organized central spindle midzone formation. *EMBO* **23**, 3237–3248.

Kurihara, D., Matsunaga, S., Omura, T., Higashiyama, T., Fukui, K., (2011). Identification and characterization of plant Haspin kinase as a histone H3 threonine kinase. *BMC Plant Biol.* **11**, 73.

Lampert, F., Hornung, P., Westermann, S., (2010). The Dam1 complex confers microtubule plus end-tracking activity to the Ndc80 kinetochore complex. *J. Cell Biol.* **189**, 641–649.

Lampert, F., Mieck, C., Alushin, G.M., Nogales, E., Westermann, S., (2013). Molecular requirements for the formation of a kinetochore-microtubule interface by Dam1 and Ndc80 complexes. *J. Cell Biol.* **200**, 21–30.

Lampson, M.A., Cheeseman, I.M., (2011). Sensing centromere tension: Aurora B and the regulation of kinetochore function. *TRENDS Cell Biol.* **21**, 133–140.

Lampson, M.A., Renduchitala, K., Khodjakov, A., Kapoor, T.M., (2004). Correcting improper chromosome-spindle attachments during cell division. *Nat. Cell Biol.* **6**, 232–237.

Lara-Gonzalez, P., Westhorpe, F.G., Taylor, S.S., (2012). The spindle assembly checkpoint. *Curr. Biol.* **22**, R966–R980.

Lavoie, B.D., Hogan, E., Koshland, D., (2004). In vivo requirements for rDNA chromosome condensation reveal two cell-cycle-regulated pathways for mitotic chromosome folding. *Genes Dev.* **18**, 76–87.

Lawless, C., Wilkinson, D.J., Young, A., Addinall, S.G., Lydall, D.A., (2010). Colonyzer: automated quantification of micro-organism growth characteristics on solid agar. *BMC bioinformatics* **11**, 1–12.

Lee, J.S., Wang, S., Sritubtim, S., Chen, J.-G., Ellis, B.E., (2009). Arabidopsis mitogen-activated protein kinase MPK12 interacts with the MAPK phosphatase IBR5 and regulates auxin signaling. *The Plant Journal* **57**, 975–985.

Lee, L., Tirnauer, J.S., Li, J., Schuyler, S.C., Liu, J.Y., Pellman, D., (2000). Positioning of the Mitotic Spindle by a Cortical-Microtubule Capture Mechanism. *Science* **287**, 2260–2262.

Lesage, B., Qian, J., Bollen, M., (2011). Spindle checkpoint silencing: PP1 tips the balance. *Curr. Biol*. **21**, R898–903.

Lew, D.J., Reed, S.I., (1993). Morphogenesis in the yeast cell cycle: regulation by Cdc28 and cyclins. *J. Cell Biol*. **120**, 1305–1320.

Lewellyn, L., Carvalho, A., Desai, A., Maddox, A.S., Oegema, K., (2011). The chromosomal passenger complex and centralspindlin independently contribute to contractile ring assembly. *J. Cell Biol.* **193**, 155–169.

Li, J., Li, Y., Elledge, S.J., (2005). Genetic Analysis of the Kinetochore DASH Complex Reveals an Antagonistic Relationship with the Ras/Protein Kinase A Pathway and a Novel Subunit Required for Ask1 Association. *Mol. Cell. Biol* **25**, 767–778.

Li, R., Murray, A.W., (1991). Feedback control of mitosis in budding yeast. *Cell* **66**, 519–531.

Li, X., Sakashita, G., Matsuzaki, H., Sugimoto, K., Kimura, K., Hanaoka, F., Taniguchi, H., Furukawa, K., Urano, T., (2004). Direct association with inner centromere protein (INCENP) activates the novel chromosomal passenger protein, Aurora-C. *J. Biol. Chem.* **279**, 47201–47211.

Li, Y., Kao, G.D., Garcia, B.A., Shabanowitz, J., Hunt, D.F., Qin, J., Phelan, C., Lazar, M.A., (2006). A novel histone deacetylase pathway regulates mitosis by modulating Aurora B kinase activity. *Genes Dev.* **20**, 2566–2579.

Liakopoulos, D., Kusch, J., Grava, S., Vogel, J., Barral, Y., (2003). Asymmetric loading of Kar9 onto spindle poles and microtubules ensures proper spindle alignment. *Cell* **112**, 561–574.

Lipp, J.J., Hirota, T., Poser, I., Peters, J.-M., (2007). Aurora B controls the association of condensin I but not condensin II with mitotic chromosomes. *J. Cell Sci.* **120**, 1245–1255.

Liu, D., Vader, G., Vromans, M.J., Lampson, M.A., Lens, S.M., (2009). Sensing chromosome bi-orientation by spatial separation of Aurora B kinase from kinetochore substrates. *Science* **323**, 1350–1353.

Liu, D., Vleugel, M., Backer, C.B., Hori, T., Fukagawa, T., Cheeseman, I.M., Lampson, M.A., (2010). Regulated targeting of protein phosphatase 1 to the outer kinetochore by KNL1 opposes Aurora B kinase. J. Cell Biol. **188**, 809–820.

Lodish, H., Berk, A., Matsudaira, P., Kaiser, C.A., Scott, M.P., Zipursky, S.L., Darnell, J., (2004). *Molecular Cell Biology*, 5th ed. W. H. Freeman & Company, New York.

Loewith, R., Jacinto, E., Wullschleger, S., Lorberg, A., Crespo, J.L., Bonenfant, D., Oppliger, W., Jenoe, P., Hall, M.N., (2002). Two TOR complexes, only one of which is rapamycin sensitive, have distinct roles in cell growth control. *Mol. Cell* **10**, 457-468.

London, N., Ceto, S., Ranish, J.A., Biggins, S., (2012). Phosphoregulation of Spc105 by Mps1 and PP1 regulates Bub1 localization to kinetochores. *Curr. Biol.* **22**, 900–906.

Loomis, R.J., Naoe, Y., Parker, J.B., Savic, V., Bozovsky, M.R., Macfarlan, T., Manley, J.L., Chakravarti, D., (2009). Chromatin binding of SRp20 and ASF/SF2 and dissociation from mitotic chromosomes is modulated by histone H3 serine 10 phosphorylation. *Mol. Cell* **33**, 450–461.

Luo, G., Zhang, J., Luca, F.C., Guo, W., (2013). Mitotic phosphorylation of Exo84 disrupts exocyst assembly and arrests cell growth. *J. Cell Biol.* **202**, 97-111.

Maccallum, D.E., Losada, A., Kobayashi, R., Hirano, T., (2002). ISWI Remodeling Complexes in Xenopus Egg Extracts : Identification as Major Chromosomal Components that Are Regulated by INCENP-aurora B. *Mol. Biol. Cell* **13**, 25–39.

Madden, K., Snyder, M., (1992). Specification of sites for polarised growth in Saccharomyces cerevisiae and the influence of external factors on site selection. *Mol. Biol. Cell* **3**, 1025-1035.

Maddox, P.S., Stemple, J.K., Satterwhite, L., Salmon, E.D., Bloom, K., (2003). The Minus End-Directed Motor Kar3 Is Required for Coupling Dynamic Microtubule Plus Ends to the Cortical Shmoo Tip in Budding Yeast. *Curr. Biol.* **13**, 1423–1428.

Maere, S., Heymans, K., Kuiper, M., (2005). BiNGO: a Cytoscape plugin to assess overrepresentation of gene ontology categories in biological networks. *Bioinformatics* **21**, 3448–3449.

Maerki, S., Olma, M.H., Staubli, T., Steigemann, P., Gerlich, D.W., Quadroni, M., Sumara, I., Peter, M., (2009). The Cul3-KLHL21 E3 ubiquitin ligase targets aurora B to midzone microtubules in anaphase and is required for cytokinesis. *J. Cell Biol.* **187**, 791–800.

Makrantoni, V., Stark, M.J.R., (2009). Efficient Chromosome Biorientation and the Tension Checkpoint in Saccharomyces cerevisiae both Require Bir1. *Mol. Cell. Biol.* **29**, 4552–4562.

Malumbres, M., Barbacid, M., (2005). Mammalian cyclin-dependent kinases. *TRENDS Biochem. Sci.* **30**, 630–641.

Marco, E., Wedlich-Soldner, R., Li, R., Altschuler, S.J., Wu, L.F., (2007). Endocytosis optimizes the dynamic localization of membrane proteins that regulate cortical polarity. *Cell* **129**, 411-422

Maresca, T.J., Salmon, E.D., (2010). Welcome to a new kind of tension: translating kinetochore mechanics into a wait-anaphase signal. *J. Cell Sci.* **123**, 825–835.

Markus, S.M., Kalutkiewicz, K.A., Lee, W.-L., (2012a). Astral microtubule asymmetry provides directional cues for spindle positioning in budding yeast. *Exp. Cell Res.* **318**, 1400–1406.

Markus, S.M., Kalutkiewicz, K.A., Lee, W.-L., (2012b). She1-mediated inhibition of dynein motility along astral microtubules promotes polarized spindle movements. *Curr. Biol.* **22**, 2221–2230.

Markus, S.M., Lee, W.-L., (2011). Regulated offloading of cytoplasmic dynein from microtubule plus ends to the cortex. *Dev. Cell* **20**, 639–651.

Martín, H., Mendoza, A., Rodriguez-Pachón, J.M., Molina, M., Nombela, C., (1997). Characterization of SKM1, a Saccharomyces cerevisiae gene encoding a novel Ste20/PAK-like protein kinase. *Mol. Microbiol.* **23**, 431-444.

Maure, J.-F., Komoto, S., Oku, Y., Mino, A., Pasqualato, S., Natsume, K., Clayton, L., Musacchio, A., Tanaka, T.U., (2011). The Ndc80 loop region facilitates formation of kinetochore attachment to the dynamic microtubule plus end. *Curr. Biol.* **21**, 207–213.

McCaffrey, L.M., Macara, I.G., (2009). Widely conserved signaling pathways in the establishment of cell polarity. *Cold Spring Harb. Perspect. Biol.* **1**, a001370.

McNally, F.J., (2013). Mechanisms of spindle positioning. *J. Cell Biol.* **200**, 131–140.

Meadows, J.C., Shepperd, L.A., Vanoosthuyse, V., Lancaster, T.C., Sochaj, A.M., Buttrick, G.J., Hardwick, K.G., Millar, J.B.A., (2011). Spindle Checkpoint Silencing Requires Association of PP1 to Both Spc7 and Kinesin-8 Motors. *Dev. Cell* **20**, 739–750.

Mendoza, M., Norden, C., Durrer, K., Rauter, H., Uhlmann, F., Barral, Y., (2009). A mechanism for chromosome segregation sensing by the NoCut checkpoint. *Nat. Cell Biol.* **11**, 477–483.

Michaelis, C., Ciosk, R., Nasmyth, K., (1997). Cohesins: Chromosomal proteins that prevent premature separation of sister chromatids. *Cell* **91**, 35–45.

Miller, R.K., Cheng, S.C., Rose, M.D., (2000). Bim1p/Yeb1p mediates the Kar9p-dependent cortical attachment of cytoplasmic microtubules. *Mol. Biol. Cell* **11**, 2949–2959.

Miller, R.K., Rose, M.D., (1998). Kar9p is a novel cortical protein required for cytoplasmic microtubule orientation in yeast. *J. Cell Biol.* **140**, 377–390.

Minoshima, Y., Kawashima, T., Hirose, K., Tonozuka, Y., Kawajiri, A., Bao, Y.C., Deng, X., Tatsuka, M., Narumiya, S., May, W.S., Nosaka, T., Semba, K., Inoue, T., Satoh, T., Inagaki, M., Kitamura, T., (2003). Phosphorylation by aurora B converts MgcRacGAP to a RhoGAP during cytokinesis. *Dev. Cell* **4**, 549–560.

Miranda, J.J.L., De Wulf, P., Sorger, P.K., Harrison, S.C., (2005). The yeast DASH complex forms closed rings on microtubules. *Nat. Struc. Mol. Biol.* **12**, 138–143.

Mirchenko, L., Uhlmann, F., (2010). Sli15(INCENP) Dephosphorylation Prevents Mitotic Checkpoint Reengagement Due to Loss of Tension at Anaphase Onset. *Curr. Biol.* **20**, 1–6.

Mishima, M., Kaitna, S., Glotzer, M., (2002). Central spindle assembly and cytokinesis require a kinesin-like protein/RhoGAP complex with microtubule bundling activity. *Dev. Cell* **2**, 41–54.

Mochida, J., Yamamoto, T., Fujimura-Kamada, K., Tanaka, K., (2002). The Novel Adaptor Protein, Mti1p, and Vrp1p, a Homolog of Wiskott-Aldrich Syndrome

Protein-Interacting Protein (WIP), May Antagonistically Regulate Type I Myosins in Saccharomyces cerevisiae. *Genetics* **160**, 923–934.

Mollinari, C., Kleman, J.-P., Jiang, W., Schoehn, G., Hunter, T., Margolis, R.L., (2002). PRC1 is a microtubule binding and bundling protein essential to maintain the mitotic spindle midzone. *J. Cell Biol.* **157**, 1175–1186.

Mollinari, C., Reynaud, C., Martineau-Thuillier, S., Monier, S., Kieffer, S., Garin, J., Andreassen, P.R., Boulet, A., Goud, B., Kleman, J.-P., Margolis, R.L., (2003). The mammalian passenger protein TD-60 is an RCC1 family member with an essential role in prometaphase to metaphase progression. *Dev. Cell* **5**, 295–307.

Moore, A., Wordeman, L., (2004). The mechanism, function and regulation of depolymerizing kinesins during mitosis. *TRENDS Cell Biol.* **14**, 537–546.

Morgan, D.O., (2007). *The Cell Cycle: Principles of Control.* New Science Press, London.

Morin, X., Bellaïche, Y., (2011). Mitotic spindle orientation in asymmetric and symmetric cell divisions during animal development. *Dev. Cell* **21**, 102–119.

Morishita, J., Matsusaka, T., Goshima, G., Nakamura, T., Tatebe, H., Yanagida, M., (2001). Bir1/Cut17 moving from chromosome to spindle upon the loss of cohesion is required for condensation, spindle elongation and repair. *Genes to Cells* **6**, 743–763.

Morrow, C.J., Tighe, A., Johnson, V.L., Scott, M.I.F., Ditchfield, C., Taylor, S.S., (2005). Bub1 and aurora B cooperate to maintain BubR1-mediated inhibition of APC/C-Cdc20. *J. Cell Sci.* **118**, 3639–3652.

Moseley, J.B., Goode, B.L., (2006). The yeast actin cytoskeleton: from cellular function to biochemical mechanism. *Microbiol. Mol. Biol. Rev.* **70**, 605–645.

Muller, E.G.D., Snydsman, B.E., Novik, I., Hailey, D.W., Gestaut, D.R., Niemann, C.A., O'Toole, E.T., Giddings, T.H., Sundin, B.A., Davis, T.N., (2005). The organization of the core proteins of the yeast spindle pole body. *Mol. Biol. Cell* **16**, 3341-3352.

Murata-Hori, M., Fumoto, K., Fukuta, Y., Iwasaki, T., Kikuchi, A., Tatsuka, M., Hosoya, H., (2000). Myosin II Regulatory Light Chain as a Novel SUbstrate for AIM-1, an Aurora / Ipllp-related Kinase from Rat. *J. Biochem.* **128**, 903–907.

Murata-Hori, M., Tatsuka, M., Wang, Y., (2002). Probing the Dynamics and Functions of Aurora B Kinase in Living Cells during Mitosis and Cytokinesis. *Mol. Biol. Cell* **13**, 1099–1108.

Musacchio, A., (2011). Spindle assembly checkpoint: the third decade. *Phil. Trans. R. Soc. B* **366**, 3595–3604.

Musacchio, A., Salmon, E.D., (2007). The spindle-assembly checkpoint in space and time. *Nat. Rev. Mol. Cell Biol.* **8**, 379–393.

Nakajima, Y., Cormier, A., Tyers, R.G., Pigula, A., Peng, Y., Drubin, D.G., Barnes, G., (2011). Ipl1/Aurora-dependent phosphorylation of Sli15/INCENP regulates CPC-spindle interaction to ensure proper microtubule dynamics. *J. Cell Biol.* **194**, 137–153.

Nakajima, Y., Tyers, R.G., Wong, C.C., Yates, J.R., Drubin, D.G., Barnes, G., (2009). Nbl1p: a Borealin/Dasra/CSC-1-like protein essential for Aurora/Ipl1 complex function and integrity in Saccharomyces cerevisiae. *Mol. Biol. Cell* **20**, 1772–1784.

Nakazawa, N., Mehrotra, R., Ebe, M., Yanagida, M., (2011). Condensin phosphorylated by the Aurora-B-like kinase Ark1 is continuously required until telophase in a mode distinct from Top2. *J. Cell Sci.* **124**, 1795–1807.

Nasmyth, K., (1993). Control of the yeast cell cycle by the Cdc28 protein kinase. *Curr. Opin. Cell Biol*. **5**, 166–179.

Nasmyth, K., Haering, C.H., (2009). Cohesin: its roles and mechanisms. *Annu. Rev. Genet*. **43**, 525–558.

Nespoli, A., Vercillo, R., Nola, L., Plevani, P., Muzi-Falconi, M., (2006). Alk1 and Alk2 are Two New Cell Cycle-Regulated Haspin-Like Proteins in Budding Yeast. *Cell Cycle* **5**, 1464–1471.

Neurohr, G., Naegeli, A., Titos, I., Theler, D., Greber, B., Díez, J., Gabaldón, T., Mendoza, M., Barral, Y., (2011). A midzone-based ruler adjusts chromosome compaction to anaphase spindle length. *Science* **332**, 465–468.

Nguyen, H.G., Chinnappan, D., Urano, T., Ravid, K., (2005). Mechanism of Aurora-B Degradation and Its Dependency on Intact KEN and A-Boxes : Identification of an Aneuploidy-Promoting Property. *Mol. Cell. Biol*. **25**, 4977–4992.

Nguyen, T.S.L., Kohno, K., Kimata, Y., (2013). Zinc Depletion Activates the Endoplasmic Reticulum-Stress Sensor Ire1 via Pleiotropic Mechanisms. *Biosci. Biotechnol. Biochem.* **77**, 1337–1339.

Nicklas, R.B., Koch, C.A., (1969). Chromosome micromanipulation. III. Spindle fiber tension and the reorientation of mal-oriented chromosomes. *J. Cell Biol.* **43**, 40–50.

Nishimura, Y., Yonemura, S., (2006). Centralspindlin regulates ECT2 and RhoA accumulation at the equatorial cortex during cytokinesis. *J. Cell Sci.* **119**, 104–114.

Nogales, E., Ramey, V.H., (2009). Structure-function insights into the yeast Dam1 kinetochore complex. *J. Cell Sci*. **122**, 3831–3836.

Norden, C., Mendoza, M., Dobbelaere, J., Kotwaliwale, C. V, Biggins, S., Barral, Y., (2006). The NoCut pathway links completion of cytokinesis to spindle midzone function to prevent chromosome breakage. *Cell* **125**, 85–98.

North, M., Steffen, J., Loguinov, A. V, Zimmerman, G.R., Vulpe, C.D., Eide, D.J., (2012). Genome-wide functional profiling identifies genes and processes important for zinc-limited growth of Saccharomyces cerevisiae. *PLoS genetics* **8**, e1002699.

Novick, P., Medkova, M., Dong, G., Hutagalung, A., Reinisch, K., Grosshans, B., (2006). Interactions between Rabs, tethers, SNAREs and their regulators in exocytosis. *Biochem. Soc. Trans.* **34**, 683–686.

Oh, Y., Bi, E., (2011). Septin structure and function in yeast and beyond. *TRENDS Cell Biol.* **21**, 141–148.

Okada, S., Leda, M., Hanna, J., Savage, N.S., Bi, E., Goryachev, A.B., (2013). Daughter cell identity emerges from the interplay of Cdc42, septins, and exocytosis. D*ev. Cell* **26**, 148-161.

Okano, H., Ohya, Y., (2003). Binding of calmodulin to Nuf1p is required for karyogamy in Saccharomyces cerevisiae. *Mol. Gen. Genomics*. **269**, 649-657.

Oliver, S.S., Denu, J.M., (2010). Dynamic Interplay between Histone H3 Modifications and Protein Interpreters: Emerging Evidence for a "Histone Language". *ChemBioChem* **12**, 299–307.

Olson, K.A., Nelson, C., Tai, G., Hung, W., Yong, C., Astell, C., Sadowski, I., (2000). Two regulators of Ste12p inhibit pheromone-responsive transcription by separate mechanisms. *Mol. Cell. Biol.* **20**, 4199–4209.

Ozlü, N., Monigatti, F., Renard, B.Y., Field, C.M., Steen, H., Mitchison, T.J., Steen, J.J., (2010). Binding partner switching on microtubules and aurora-B in the mitosis to cytokinesis transition. *Mol. Cell. Prot.* **9**, 336–350.

Pan, F., Malmberg, R.L., Momany, M., (2007). Analysis of septins across kingdoms reveals orthology and new motifs. *BMC Evo. Biol*. **7**, 1–17.

Panigada, D., Grianti, P., Nespoli, A., Rotondo, G., Gallo Castro, D., Quadri, R., Piatti, S., Plevani, P., Muzi-Falconi, M., (2013). Yeast Haspin Kinase Regulates Polarity Cues Necessary for Mitotic Spindle Positioning and Is Required to Tolerate Mitotic Arrest. *Dev. Cell* 10.1016/j.devcel.2013.07.013.

Parry, D.H., Hickson, G.R.X., Farrell, P.H.O., (2003). Cyclin B Destruction Triggers Changes in Kinetochore Behavior Essential for Successful Anaphase. *Curr. Biol.* **13**, 647–653.

Parsons, A.B., Brost, R.L., Ding, H., Li, Z., Zhang, C., Sheikh, B., Brown, G.W., Kane, P.M., Hughes, T.R., Boone, C., (2004). Integration of chemical-genetic and genetic interaction data links bioactive compounds to cellular target pathways. *Nat. Biotech.* **22**, 62–69.

Pereira, G., Schiebel, E., (2003). Separase regulates INCENP-Aurora B anaphase spindle function through Cdc14. *Science* **302**, 2120–2124.

Peters, J.-M., (2006). The anaphase promoting complex/cyclosome: a machine designed to destroy. *Nat. Rev. Mol. Cell Biol* **7**, 644–656.

Petersen, J., Hagan, I.M., (2003). S . pombe Aurora Kinase / Survivin Is Required for Chromosome Condensation and the Spindle Checkpoint Attachment Response. *Curr. Biol*. **13**, 590–597.

Petsalaki, E., Akoumianaki, T., Black, E.J., Gillespie, D.A.F., Zachos, G., (2011). Phosphorylation at serine 331 is required for Aurora B activation. *J. Cell Biol.* **195**, 449–466.

Pfleger, C.M., Kirschner, M.W., (2000). The KEN box: an APC recognition signal distinct from the D box targeted by Cdh1. *Genes Dev*. **14**, 655–665.

Piekny, A., Werner, M., Glotzer, M., (2005). Cytokinesis: welcome to the Rho zone. *TRENDS Cell Biol.* **15**, 651–658.

Pinsky, B.A., Biggins, S., (2005). The spindle checkpoint: tension versus attachment. *TRENDS Cell Biol.* **15**, 486–493.

Pinsky, B.A., Kotwaliwale, C. V, Tatsutani, S.Y., Breed, C.A., Biggins, S., (2006a). Glc7/protein phosphatase 1 regulatory subunits can oppose the Ipl1/Aurora protein kinase by redistributing Glc7. *Mol. Cell. Biol.* **26**, 2648–2660.

Pinsky, B.A., Kung, C., Shokat, K.M., Biggins, S., (2006b). The Ipl1-Aurora protein kinase activates the spindle checkpoint by creating unattached kinetochores. *Nat. Cell Biol.* **8**, 78–83.

Posch, M., Khoudoli, G.A., Swift, S., King, E.M., Deluca, J.G., Swedlow, J.R., (2010). Sds22 regulates aurora B activity and microtubule-kinetochore interactions at mitosis. *J. Cell Biol.* **191**, 61–74.

Pruyne, D., Bretscher, A., (2000). Polarization of cell growth in yeast. I. Establishment and maintenance of polarity states. *J. Cell Sci*. **113**, 365–375.

Pruyne, D., Bretscher, A., (2000). Polarization of cell growth in yeast II . The role of the cortical actin cytoskeleton. *J. Cell Sci.* **113**, 571–585.

Pruyne, D.W., Schott, D.H., Bretscher, A., (1998). Tropomyosin-containing actin cables direct the myo2p-dependent polarized delivery of secretory vesicles in budding yeast. *J. Cell Biol.* **143**, 1931-1945

Qi, M., Yu, W., Liu, S., Jia, H., Tang, L., Shen, M., Yan, X., Saiyin, H., Lang, Q., Wan, B., Zhao, S., Yu, L., (2005). Septin1, a new interaction partner for human serine/threonine kinase aurora-B. *Biochem. Biophys. Res. Comm.* **336**, 994–1000.

Qian, J., Lesage, B., Beullens, M., Van Eynde, A., Bollen, M., (2011). PP1/Repo-Man Dephosphorylates Mitotic Histone H3 at T3 and Regulates Chromosomal Aurora B Targeting. *Curr. Biol.* **21**, 1–8.

Ramadan, K., Bruderer, R., Spiga, F.M., Popp, O., Baur, T., Gotta, M., Meyer, H.H., (2007). Cdc48/p97 promotes reformation of the nucleus by extracting the kinase Aurora B from chromatin. *Nature* **450**, 1258–1262.

Ranjitkar, P., Press, M.O., Yi, X., Baker, R., MacCoss, M.J., Biggins, S., (2010). An E3 Ubiquitin Ligase Prevents Ectopic Localization of the Centromeric Histone H3 Variant via the Centromere Targeting Domain. *Mol. Cell* **40**, 455–464.

Raychaudhuri, S., Young, B.P., Espenshade, P.J., Loewen, C., (2012). Regulation of lipid metabolism: a tale of two yeasts. *Curr. Opin. Cell Biol.* **24**, 502–508.

Richardson, H., Lew, D.J., Henze, M., Sugimoto, K., Reed, S.I., (1992). Cyclin-B homologs in Saccharomyces cerevisiae function in S phase and in G2. *Genes Dev.* **6**, 2021–2034.

Rock, J.M., Amon, A., (2009). The FEAR network. *Curr. Biol.* **19**, R1063–1068.

Romano, A., Guse, A., Krascenicova, I., Schnabel, H., Schnabel, R., Glotzer, M., (2003). CSC-1: a subunit of the Aurora B kinase complex that binds to the survivin-like protein BIR-1 and the incenp-like protein ICP-1. *J. Cell Biol.* **161**, 229–236.

Ron, D., Walter, P., (2007). Signal integration in the endoplasmic reticulum unfolded protein response. *Nat. Rev. Mol. Cell Biol.* **8**, 519–529.

Rosasco-Nitcher, S.E., Lan, W., Khorasanizadeh, S., Stukenberg, P.T., (2008). Centromeric Aurora-B activation requires TD-60, microtubules, and substrate priming phosphorylation. *Science* **319**, 469–472.

Rosenberg, J.S., Cross, F.R., Funabiki, H., (2011). KNL1/Spc105 Recruits PP1 to Silence the Spindle Assembly Checkpoint. *Curr. Biol*. **21**, 942–947.

Ruchaud, S., Carmena, M., Earnshaw, W.C., (2007). Chromosomal passengers: conducting cell division. *Nat. Rev. Mol. Cell Biol.* **8**, 798–812.

Sampath, S.C., Ohi, R., Leismann, O., Salic, A., Pozniakovski, A., Funabiki, H., (2004). The chromosomal passenger complex is required for chromatin-induced microtubule stabilization and spindle assembly. *Cell* **118**, 187–202.

Sanchez-Diaz, A., Nkosi, P.J., Murray, S., Labib, K., (2012). The mitotic exit network and Cdc14 phosphatase initiate cytokinesis by counteracting CDK phosphorylations and blocking polarised growth. *EMBO* **31**, 3620–3634.

Santaguida, S., Tighe, A., D'Alise, A.M., Taylor, S.S., Musacchio, A., (2010). Dissecting the role of MPS1 in chromosome biorientation and the spindle checkpoint through the small molecule inhibitor reversine. *J. Cell Biol.* **190**, 73–87.

Santaguida, S., Vernieri, C., Villa, F., Ciliberto, A., Musacchio, A., (2011). Evidence that Aurora B is implicated in spindle checkpoint signalling independently of error correction. *EMBO* **30**, 1508–1519.

Schaerer-Brodbeck, C., Riezman, H., (2003). Genetic and biochemical interactions between the Arp2/3 complex, Cmd1p, casein kinase II, and Tub4p in yeast. *FEMS Yeast Res.* **4**, 37-49.

Schöner, D., Kalisch, M., Leisner, C., Meier, L., Sohrmann, M., Faty, M., Barral, Y., Peter, M., Gruissem, W., Bühlmann, P., (2008). Annotating novel genes by integrating synthetic lethals and genomic information. *BMC Sys. Biol.* **2**.

Schvartzman, J.-M., Sotillo, R., Benezra, R., (2010). Mitotic chromosomal instability and cancer: mouse modelling of the human disease. *Nat. Rev. Cancer* **10**, 102–115.

Schwob, E., Böhm, T., Mendenhall, M.D., Nasmyth, K., (1994). The B-type cyclin kinase inhibitor p40SIC1 controls the G1 to S transition in S. cerevisiae. *Cell* **79**, 233–244.

Sessa, F., Mapelli, M., Ciferri, C., Tarricone, C., Areces, L.B., Schneider, T.R., Stukenberg, P.T., Musacchio, A., (2005). Mechanism of Aurora B activation by INCENP and inhibition by hesperadin. *Mol. Cell* **18**, 379–391.

Sheeman, B., Carvalho, P., Sagot, I., Geiser, J., Kho, D., Hoyt, M.A., Pellman, D., (2003). Determinants of S. cerevisiae dynein localization and activation: implications for the mechanism of spindle positioning. *Curr. Biol*. **13**, 364–372.

Sheu, Y.-J., Santos, B., Fortin, N., Costigan, C., Snyder, M., (1998). Spa2p Interacts with Cell Polarity Proteins and Signaling Components Involved in Yeast Cell Morphogenesis. *Mol. Cell. Biol.* **18**, 4053–4069.

Shirk, K., Jin, H., Giddings, T.H., Winey, M., Yu, H.-G., (2011). The Aurora kinase Ipl1 is necessary for spindle pole body cohesion during budding yeast meiosis. *J. Cell Sci*. **124**, 2891–2896.

Simon, M-N., Virgilio, C.D., Souza, B., Pringle, J.R., Abo, A., Reed, S.I., (1995). Role for the Rho-family GTPase Cdc42 in yeast mating-pheromone signal pathway. *Nature* **376**, 702-705.

Slattery, S.D., Mancini, M.A., Brinkley, B.R., Hall, R.M., (2009). Aurora-C kinase supports mitotic progression in the absence of Aurora-B. *Cell Cycle* **8**, 2986–2997.

Slaughter, B.D., Das, A., Schwartz, J.W., Rubinstein, B., Li, R., (2009). Dual modes of cdc42 recycling fine-tune polarized morphogenesis. *Dev. Cell* **17**, 823–835.

Smart, K., Chambers, K., Lambert, I., Jenkins, C., (1999). Use of methylene violet staining procedures to determine yeast viability and vitality. *J. Am. Soc. Brew. Chem.* **57**, 18-23

Smith, S.E., Rubinstein, B., Pinto, I.M., Slaughter, B.D., Unruh, J.R., Li, R., (2013) Independence of symmetry breaking on Bem1-mediated autocatalytic activation of Cdc42. *J. Cell Biol.* **202**, 1091-1106

Smolka, M.B., Albuquerque, C.P., Chen, S., Zhou, H., (2007). Proteome-wide identification of in vivo targets of DNA damage checkpoint kinases. *PNAS* **104**, 10364–10369.

Smoot, M.E., Ono, K., Ruscheinski, J., Wang, P.-L., Ideker, T., (2011). Cytoscape 2.8: new features for data integration and network visualization. *Bioinformatics* **27**, 431–432.

Soufi, B., Kelstrup, C.D., Stoehr, G., Fröhlich, F., Walther, T.C., Olsen, J. V, (2009). Global analysis of the yeast osmotic stress response by quantitative proteomics. *Mol. BioSyst.* **5**, 1337–1346.

Soulard, A., Cremonesi, A., Moes, S., Hall, M.N., (2010). The Rapamycin-sensitive Phosphoproteome Reveals That TOR Controls Protein Kinase A Toward Some But Not All Substrates. *Mol. Biol. Cell* **21**, 3475–3486.

Spencer, F., Hieter, P., (1992). Centromere DNA mutations induce a mitotic delay in Saccharomyces cerevisiae. *PNAS* **89**, 8908–8912.

Stansfield, I., Stark, M.J.R., (2007). Yeast Genetics and Strain Construction, in: Stansfield, I., Stark, M.J.R. (Eds.), *Methods in Microbiology* Vol. 36 - Yeast Gene Analysis. Elsevier, pp. 23–43.

Stegmeier, F., Amon, A., (2004). Closing mitosis: the functions of the Cdc14 phosphatase and its regulation. *Annu. Rev. Genet.* **38**, 203–232.

Steigemann, P., Wurzenberger, C., Schmitz, M.H.A., Held, M., Guizetti, J., Maar, S., Gerlich, D.W., (2009). Aurora B-mediated abscission checkpoint protects against tetraploidization. *Cell* **136**, 473–484.

Stewart, S., Fang, G., (2005). Destruction box-dependent degradation of aurora B is mediated by the anaphase-promoting complex/cyclosome and Cdh1. *Cancer Res.* **65**, 8730–8735.

Storchová, Z., Becker, J.S., Talarek, N., Kögelsberger, S., Pellman, D., (2011). Bub1, Sgo1, and Mps1 mediate a distinct pathway for chromosome biorientation in budding yeast. *Mol. Biol. Cell* **22**, 1473–1485.

Straight, A.F., Belmont, A.S., Robinett, C.C., Murray, A.W., (1996). GFP tagging of budding yeast chromosomes reveals that protein-protein interactions can mediate sister chromatid cohesion. *Curr. Biol.* **6**, 1599–1608.

Sudakin, V., Chan, G.K., Yen, T.J., (2001). Checkpoint inhibition of the APC/C in HeLa cells is mediated by a complex of BUBR1, BUB3, CDC20, and MAD2. *J. Cell Biol.* **154**, 925–936.

Sugiyama, K., Sugiura, K., Hara, T., Sugimoto, K., Shima, H., Honda, K., Furukawa, K., Yamashita, S., Urano, T., (2002). Aurora-B associated protein phosphatases as negative regulators of kinase activation. *Oncogene* **21**, 3103–3111.

Sullivan, M., Hornig, N.C.D., Porstmann, T., Uhlmann, F., (2004). Studies on substrate recognition by the budding yeast separase. J. Biol. Chem. **279**, 1191–1196.

Sumara, I., Quadroni, M., Frei, C., Olma, M.H., Sumara, G., Ricci, R., Peter, M., (2007). A Cul3-based E3 ligase removes Aurora B from mitotic chromosomes,

regulating mitotic progression and completion of cytokinesis in human cells. *Dev. Cell* **12**, 887–900.

Sun, L., Gao, J., Dong, X., Liu, M., Shi, X., Dong, J.-T., Lu, X., Liu, C., Zhou, J., (2008). EB1 promotes Aurora-B kinase activity through blocking its inactivation by protein phosphatase 2A. *PNAS* **105**, 7153–7158.

Tada, K., Susumu, H., Sakuno, T., Watanabe, Y., (2011). Condensin association with histone H2A shapes mitotic chromosomes. *Nature* **474**, 477–483.

Takai, H., Tominaga, K., Motoyama, N., Minamishima, Y.A., Nagahama, H., Tsukiyama, T., Ikeda, K., Nakayama, K., Nakanishi, M., Nakayama, K.-I., (2000). Aberrant cell cycle checkpoint function and early embryonic death in Chk1 − / − mice. *Genes Dev.* **14**, 1439–1447.

Tanaka, H., Yoshimura, Y., Nishina, Y., Nozaki, M., Nojima, H., Nishimune, Y., (1994). Isolation and characterization of cDNA clones specifically expressed in testicular germ cells. *FEBS letters* **355**, 4–10.

Tanaka, H., Yoshimura, Y., Nozaki, M., Yomogida, K., Tsuchida, J., Tosaka, Y., Habu, T., Nakanishi, T., Okada, M., Nojima, H., Nishimune, Y., (1999). Identification and characterization of a haploid germ cell-specific nuclear protein kinase (Haspin) in spermatid nuclei and its effects on somatic cells. *J. Biol. Chem.* **274**, 17049–17057.

Tanaka, K., Kitamura, E., Kitamura, Y., Tanaka, T.U., (2007). Molecular mechanisms of microtubule-dependent kinetochore transport toward spindle poles. *J. Cell Biol.* **178**, 269–281.

Tanaka, K., Kitamura, E., Tanaka, T.U., (2010). Live-cell analysis of kinetochore – microtubule interaction in budding yeast. *METHODS* **51**, 206–213.

Tanaka, T., Fuchs, J., Loidl, J., Nasmyth, K., (2000). Cohesin ensures bipolar attachment of microtubules to sister centromeres and resists their precocious separation. *Nat. Cell Biol.* **2**, 492–499.

Tanaka, T.U., Rachidi, N., Janke, C., Pereira, G., Galova, M., Schiebel, E., Stark, M.J., Nasmyth, K., (2002a). Evidence that the Ipl1-Sli15 (Aurora kinase-INCENP) complex promotes chromosome bi-orientation by altering kinetochore-spindle pole connections. *Cell* **108**, 317–329.

Tanaka, T.U., Rachidi, N., Janke, C., Pereira, G., Galova, M., Schiebel, E., Stark, M.J., Nasmyth, K., (2002b). Evidence that the Ipl1-Sli15 (Aurora kinase-INCENP) complex promotes chromosome bi-orientation by altering kinetochore-spindle pole connections. *Cell* **108**, 317–329.

Tanaka, T.U., Stark, M.J.R., Tanaka, K., (2005). Kinetochore capture and bi-orientation on the mitotic spindle. *Nat. Rev. Mol. Cell Biol.* **6**, 929–942.

Tanenbaum, M.E., Macurek, L., van der Vaart, B., Galli, M., Akhmanova, A., Medema, R.H., (2011). A complex of Kif18b and MCAK promotes microtubule

depolymerization and is negatively regulated by Aurora kinases. *Curr. Biol.* **21**, 1356–1365.

Tanno, Y., Kitajima, T.S., Honda, T., Ando, Y., Ishiguro, K.-I., Watanabe, Y., (2010). Phosphorylation of mammalian Sgo2 by Aurora B recruits PP2A and MCAK to centromeres. *Genes Dev.* **24**, 2169–2179.

Ten Hoopen, R., Cepeda-García, C., Fernández-Arruti, R., Juanes, M.A., Delgehyr, N., Segal, M., (2012). Mechanism for astral microtubule capture by cortical Bud6p priming spindle polarity in S. cerevisiae. *Curr. Biol.* **22**, 1075–1083.

Terada, Y., (2006). Aurora-B / AIM-1 Regulates the Dynamic Behavior of HP1alpha at the G 2 – M Transition. *Mol. Biol. Cell* **17**, 3232–3241.

Thadani, R., Uhlmann, F., Heeger, S., (2012). Condensin , Chromatin Crossbarring and Chromosome Condensation. *Curr. Biol.* **22**, R1012–R1021.

Theesfeld, C.L., Irazoqui, J.E., Bloom, K., Lew, D.J., (1999). The role of actin in spindle orientation changes during the Saccharomyces cerevisiae cell cycle. *J. Cell Biol.* **146**, 1019–1032.

Thomas, S., Kaplan, K.B., (2007). A Bir1p-Sli15p kinetochore passenger complex regulates septin organization during anaphase. *Mol. Biol. Cell* **18**, 3820–3824.

Tkach, J.M., Yimit, A., Lee, A., Riffle, M., Costanzo, M., Jaschob, D., Hendry, J.A., Ou, J., Moffat, J., Boone, C., Davis, T.N., Nislow, C., Brown, G.W., (2012). Dissecting DNA damage response pathways by analysing protein localization and abundance changes during DNA replication stress. *Nat. Cell Biol.* **14**, 966–976.

Tkacz, J.S., Lampen, J.O., (1973) Surface distribution of invertase on growing Saccharomyces cells. *J. Bacteriology* **113**, 1073-1075

Tong, A.H.Y., Boone, C., (2006). Synthetic Genetic Array (SGA) Analysis in Saccharomyces cerevisiae. *Methods Mol. Biol* **313**, 171–192.

Toone, W.M., Aerne, B.L., Morgan, B. A, Johnston, L.H., (1997). Getting started: regulating the initiation of DNA replication in yeast. *Ann. Rev. Microbiol.* **51**, 125–149.

Toulmay, A., Schneiter, R., (2006). A two-step method for the introduction of single or multiple defined point mutations into the genome of Saccharomyces cerevisiae. *Yeast* **23**, 825–831.

Tseng, B.S., Tan, L., Kapoor, T.M., Funabiki, H., (2010). Dual Detection of Chromosomes and Microtubules by the Chromosomal Passenger Complex Drives Spindle Assembly. *Dev. Cell* **18**, 903–912.

Tsukahara, T., Tanno, Y., Watanabe, Y., (2010). Phosphorylation of the CPC by Cdk1 promotes chromosome bi-orientation. *Nature* **467**, 719–723.

Tu, Z., He, G., Li, K.X., Chen, M.J., Chang, J., Chen, L., Yao, Q., Liu, D.P., Ye, H., Shi, J., Wu, X., (2005). An improved system for competent cell preparation and high efficiency plasmid transformation using different Escherichia coli strains. *Elec. J. Biochem.* **8**, 113–120.

Tully, G.H., Nishihama, R., Pringle, J.R., Morgan, D.O., (2009). The Anaphase-promoting Complex Promotes Actomyosin- Ring Disassembly during Cytokinesis in Yeast. *Mol. Biol. Cell* **20**, 1201–1212.

Uhlmann, F., Wernic, D., Poupart, M.-A., Koonin, E. V, Nasmyth, K., (2000). Cleavage of cohesin by the CD clan protease separin triggers anaphase in yeast. *Cell* **103**, 375–386.

Uren, A.G., Beilharz, T., O'Connell, M.J., Bugg, S.J., van Driel, R., Vaux, D.L., Lithgow, T., (1999). Role for yeast inhibitor of apoptosis (IAP)-like proteins in cell division. *PNAS* **96**, 10170–10175.

Uren, A.G., Wong, L., Pakusch, M., Fowler, K.J., Burrows, F.J., Vaux, D.L., Choo, K.H., (2000). Survivin and the inner centromere protein INCENP show similar cell-cycle localization and gene knockout phenotype. *Curr. Biol.* **10**, 1319–1328.

Vader, G., Cruijsen, C.W., van Harn, T., Vromans, M.J.M., Medema, R.H., Lens, S.M., (2007). The chromosomal passenger complex controls spindle checkpoint function independent from its role in correcting microtubule kinetochore interactions. *Mol. Biol. Cell* **18**, 4553–4564.

Vader, G., Lens, S.M.A., (2010). Chromosome segregation: taking the passenger seat. *Curr. Biol.* **20**, R879–881.

Van der Waal, M.S., Hengeveld, R.C.C., van der Horst, A., Lens, S.M.A., (2012). Cell division control by the Chromosomal Passenger Complex. *Exp. Cell Res.* **318**, 1407–1420.

Van Pel, D.M., Stirling, P.C., Minaker, S.W., Sipahimalani, P., Hieter, P., (2013). Saccharomyces cerevisiae genetics predicts candidate therapeutic genetic interactions at the mammalian replication fork. *G3* **3**, 273-282.

Vanoosthuyse, V., Prykhozhij, S., Hardwick, K.G., (2007). Shugoshin 2 regulates localization of the chromosomal passenger proteins in fission yeast mitosis. *Mol. Biol. Cell* **18**, 1657–1669.

Vázquez-Novelle, M.D., Mirchenko, L., Uhlmann, F., Petronczki, M., (2010). The "anaphase problem": how to disable the mitotic checkpoint when sisters split. *Biochem. Soc. Trans.* **38**, 1660–1666.

Vázquez-Novelle, M.D., Petronczki, M., (2010). Relocation of the Chromosomal Passenger Complex Prevents Mitotic Checkpoint Engagement at Anaphase. *Curr. Biol.* **20**, 1–6.

Verma, R., Annan, R.S., Huddleston, M.J., Carr, S.A., Reynard, G., Deshaies, R.J., (1997). Phosphorylation of Sic1p by G1 Cdk Required for Its Degradation and Entry into S Phase. *Science* **278**, 455–460.

VerPlank, L., Li, R., (2005) Cell cycle-regulated trafficking of Chs2 controls actomyosin ring stability during cytokinesis. *Mol. Biol. Cell* **16**, 2529-2543

Vong, Q.P., Cao, K., Li, H.Y., Iglesias, P.A., Zheng, Y., (2005). Chromosome alignment and segregation regulated by ubiquitination of survivin. *Science* **310**, 1499–1504.

Walczak, C.E., Heald, R., (2008). Mechanisms of mitotic spindle assembly and function. *Int. Rev. Cyt.* **265**, 111–158.

Wan, X., O'Quinn, R.P., Pierce, H.L., Joglekar, A.P., Gall, W.E., Deluca, J.G., Carroll, C.W., Liu, S.T., Yen, T.J., Mcewen, B.F., (2009). Protein architecture of the human kinetochore microtubule attachment site. *Cell* **137**, 672–684.

Wang, F., Dai, J., Daum, J.R., Niedzialkowska, E., Banerjee, B., Stukenberg, P.T., Gorbsky, G.J., Higgins, J.M.G., (2010). Histone H3 Thr-3 Phosphorylation by Haspin Positions Aurora B at Centromeres in Mitosis. *Science* **330**, 231–235.

Wang, F., Ulyanova, N.P., van der Waal, M.S., Patnaik, D., Lens, S.M.A., Higgins, J.M.G., (2011). A Positive Feedback Loop Involving Haspin and Aurora B Promotes CPC Accumulation at Centromeres in Mitosis. *Curr. Biol.* **21**, 1–9.

Wang, H., Liu, D., Wang, Y., Qin, J., Elledge, S.J., (2001). Pds1 phosphorylation in response to DNA damage is essential for its DNA damage checkpoint function. *Genes Dev.* **15**, 1361–1372.

Wargacki, M., Tay, J., Muller, E., Asbury, C., Davis, T., (2010). Kip3, the yeast kinesin-8, is required for clustering of kinetochores at metaphase. *Cell Cycle* **9**, 76–75.

Watanabe, M., Watanabe, D., Nogami, S., Morishita, S., Ohya, Y., (2009). Comprehensive and quantitative analysis of yeast deletion mutants defective in apical and isotropic bud growth. *Curr. Genet.* **55**, 365–380.

Weaver, B.A.A., Cleveland, D.W., (2006). Does aneuploidy cause cancer? *Curr. Opin. Cell Biol.* **18**, 658–667.

Wedlich-Soldner, R., Wai, S.C., Schmidt, T., Li, R., (2004). Robust cell polarity is a dynamic state established by coupling transport and GTPase signaling. J. Cell Biol. **166**, 889–900.

Wei, Y., Mizzen, C.A., Cook, R.G., Gorovsky, M.A., Allis, C.D., (1998). Phosphorylation of histone H3 at serine 10 is correlated with chromosome condensation during mitosis and meiosis in Tetrahymena. *PNAS* **95**, 7480–7484.

Weiss, E., Winey, M., (1996). The Saccharomyces cerevisiae spindle pole body duplication gene MPS1 is part of a mitotic checkpoint. *J. Cell Biol.* **132**, 111–123.

Welburn, J.P.I., Grishchuk, E.L., Backer, C.B., Wilson-Kubalek, E.M., Yates III, J.R., Cheeseman, I.M., (2009). The human kinetochore Ska1 complex facilitates microtubule depolymerization-coupled motility. *Dev. Cell* **16**, 374–385.

Welburn, J.P.I., Vleugel, M., Liu, D., Yates, J.R., Lampson, M.A., Fukagawa, T., Cheeseman, I.M., (2010). Aurora B Phosphorylates Spatially Distinct Targets to Differentially Regulate the Kinetochore-Microtubule Interface. Mol. Cell **38**, 383–392.

Welihinda, A.A., Tirasophon, W., Kaufman, R.J., (2000). The Transcriptional Co-activator ADA5 Is Required for HAC1 mRNA Processing in Vivo. *J. Biol. Chem.* **275**, 3377–3381.

Westermann, S., Avila-Sakar, A., Wang, H.-W., Niederstrasser, H., Wong, J., Drubin, D.G., Nogales, E., Barnes, G., (2005). Formation of a dynamic kinetochore-microtubule interface through assembly of the Dam1 ring complex. *Mol. Cell* **17**, 277–290.

Westermann, S., Wang, H.-W., Avila-Sakar, A., Drubin, D.G., Nogales, E., Barnes, G., (2006). The Dam1 kinetochore ring complex moves processively on depolymerizing microtubule ends. *Nature* **440**, 565–569.

Wheatley, S.P., Carvalho, A., Vagnarelli, P., Earnshaw, W.C., (2001). INCENP is required for proper targeting of Survivin to the centromeres and the anaphase spindle during mitosis. *Curr. Biol.* **11**, 886–890.

Widlund, P.O., Lyssand, J.S., Anderson, S., Niessen, S., Yates, J.R., Davis, T.N., (2006). Phosphorylation of the Chromosomal Passenger Protein Bir1 Is Required for Localization of Ndc10 to the Spindle during Anaphase and Full Spindle Elongation. *Mol. Biol. Cell* **17**, 1065–1074.

Winey, M., Bloom, K., (2012). Mitotic spindle form and function. *Genetics* **190**, 1197–1224.

Winzeler, E.A., Shoemaker, D.D., Astromoff, A., Liang, H., Anderson, K., *et al*., (1999). Functional Characterization of the S. cerevisiae Genome by Gene Deletion and Parallel Analysis. *Science* **285**, 901–906.

Woodruff, J.B., Drubin, D.G., Barnes, G., (2009). Dynein-Driven Mitotic Spindle Positioning Restricted to Anaphase by She1p Inhibition of Dynactin Recruitment. *Mol. Biol. Cell* **20**, 3003–3011.

Woodruff, J.B., Drubin, D.G., Barnes, G., (2010). Mitotic spindle disassembly occurs via distinct subprocesses driven by the anaphase-promoting complex, Aurora B kinase, and kinesin-8. *J. Cell Biol.* **191**, 795–808.

Xu, Z., Ogawa, H., Vagnarelli, P., Bergmann, J.H., Hudson, D.F., Ruchaud, S., Fukagawa, T., Earnshaw, W.C., Samejima, K., (2009). INCENP–aurora B interactions modulate kinase activity and chromosome passenger complex localization. *J. Cell Biol.* **187**, 637–653.

Yamagishi, Y., Honda, T., Tanno, Y., Watanabe, Y., (2010). Two Histone Marks Establish the Inner Centromere and Chromosome Bi-Orientation. *Science* **330**, 239–243.

Yamagishi, Y., Yang, C.-H., Tanno, Y., Watanabe, Y., (2012). MPS1/Mph1 phosphorylates the kinetochore protein KNL1/Spc7 to recruit SAC components. *Nat. Cell Biol*. **14**, 746–752.

Yan, X., Cao, L., Li, Q., Wu, Y., Zhang, H., Saiyin, H., Liu, X., Zhang, X., Shi, Q., Yu, L., (2005). Aurora C is directly associated with Survivin and required for cytokinesis. *Genes to Cells* **10**, 617–626.

Yang, Y., Wu, F., Ward, T., Yan, F., Wu, Q., Wang, Z., McGlothen, T., Peng, W., You, T., Sun, M., Cui, T., Hu, R., Dou, Z., Zhu, J., Xie, W., Rao, Z., Ding, X., Yao, X., (2008). Phosphorylation of HsMis13 by Aurora B kinase is essential for assembly of functional kinetochore. *J. Biol. Chem*. **283**, 26726–26736.

Yasui, Y., Urano, T., Kawajiri, A., Nagata, K., Tatsuka, M., Saya, H., Furukawa, K., Takahashi, T., Izawa, I., Inagaki, M., (2004). Autophosphorylation of a newly identified site of Aurora-B is indispensable for cytokinesis. *J. Biol. Chem.* **279**, 12997–13003.

Yin, H., Pruyne, D., Huffaker, T.C., Bretscher, A., (2000). Myosin V orientates the mitotic spindle in yeast. *Nature* **406**, 1013–1015.

Yoon, H.-J., Carbon, J., (1999). Participation of Bir1p, a member of the inhibitor of apoptosis family, in yeast chromosome segregation events. *PNAS* **96**, 13208–13213.

Yoshida, S., Saiga, S., Weijers, D., (2013). Auxin regulation of embryonic root formation. *Plant Cell Physiol.* **54**, 325–332.

Yu, H.-G., Koshland, D., (2007). The Aurora kinase Ipl1 maintains the centromeric localization of PP2A to protect cohesin during meiosis. *J. Cell Biol*. **176**, 911–918.

Yue, Z., Carvalho, A., Xu, Z., Yuan, X., Cardinale, S., Ribeiro, S., Lai, F., Ogawa, H., Gudmundsdottir, E., Gassmann, R., Morrison, C.G., Ruchaud, S., Earnshaw, W.C., (2008). Deconstructing Survivin: comprehensive genetic analysis of Survivin function by conditional knockout in a vertebrate cell line. *J. Cell Biol.* **183**, 279–296.

Zachos, G., Black, E.J., Walker, M., Scott, M.T., Vagnarelli, P., Earnshaw, W.C., Gillespie, D.A.F., (2007). Chk1 is required for spindle checkpoint function. *Dev. Cell* **12**, 247–260.

Zhang, X., Bi, E., Novick, P., Du, L., Kozminski, K.G., Lipschutz, J.H., Guo, W., (2001). Cdc42 interacts with the exocyst and regulates polarized secretion. *J. Biol. Chem.* **276**, 46745-46750.

Zhang, K., Lin, W., Latham, J.A., Riefler, G.M., Schumacher, J.M., Chan, C., Tatchell, K., Hawke, D.H., Kobayashi, R., Dent, S.Y.R., (2005). The Set1 methyltransferase

opposes Ipl1 aurora kinase functions in chromosome segregation. *Cell* **122**, 723–734.

Zhang, X., Lan, W., Ems-McClung, S.C., Stukenberg, P.T., Walczak, C.E., (2007). Aurora B Phosphorylates Multiple Sites on Mitotic Centromere-associated Kinesin to Spatially and Temporally Regulate Its Function. *Mol. Biol. Cell* **18**, 3264 –3276.

Zhang, Z., Laux, T., (2011). The asymmetric division of the Arabidopsis zygote: from cell polarity to an embryo axis. *Sex. Plant Reprod.* **24**, 161–169.

Zhao, F.Y., Hu, F., Zhang, S.Y., Wang, K., Zhang, C.R., Liu, T., (2013). MAPKs regulate root growth by influencing auxin signaling and cell cycle-related gene expression in cadmium-stressed rice. *Environ. Sci. Pollut. Res* **20**, 5449–5460.

Zhao, H., Eide, D., (1996). The yeast ZRT1 gene encodes the zinc transporter protein of a high-affinity uptake system induced by zinc limitation. *PNAS* **93**, 2454–2458.

Zhao, Z.S., Leung, T., Manser, E., Lim, L., (1995). Pheromone signalling in Saccharomyces cerevisiae requires the small GTP-binding protein Cdc42p and its activator CDC24. *Mol. Cell. Biol.* **15**, 5246-5257

Zheng, Y., Cerione, R., Bender, A., (1994). Control of the yeast bud-site assembly GTPase Cdc42. *J. Biol. Chem.* **269**, 2369-2372.

Zimniak, T., Fitz, V., Zhou, H., Lampert, F., Opravil, S., Mechtler, K., Stolt-Bergner, P., Westermann, S., (2012). Spatiotemporal regulation of Ipl1/Aurora activity by direct Cdk1 phosphorylation. *Curr. Biol*. **22**, 787–793.

Zimniak, T., Stengl, K., Mechtler, K., Westermann, S., (2009). Phosphoregulation of the budding yeast EB1 homologue Bim1p by Aurora/Ipl1p. *J. Cell Biol.* **186**, 379–391.

APPENDIX

Table A1. SGA screen results for *alk1*Δ query strain

ORF	Gene	*P*	*Q*	GIS	Query Fitness	Control Fitness	Query SE	Control SE
YBR144C	*YBR144C*	3.88E-04	4.30E-03	-60063	3634	93327	767	3621
YDR319C	*YFT2*	6.80E-12	6.87E-09	-57474	78	84323	1007	61
YDR213W	*UPC2*	3.81E-16	1.93E-12	-53560	77	78586	309	45
YDR107C	*TMN2*	9.88E-03	3.90E-02	-48168	9185	84031	972	8289
YGL255W	*ZRT1*	6.02E-05	1.22E-03	-48112	6619	80190	814	1986
YDR111C	*ALT2*	1.85E-02	5.94E-02	-46183	9895	82164	667	9895
YBR076W	*ECM8*	3.16E-02	8.73E-02	-41341	16357	84537	280	10829
YBR171W	*SEC66*	5.38E-06	2.42E-04	-40667	11156	75928	504	997
YPR133C	*SPN1*	1.63E-02	5.47E-02	-38735	12398	74919	5438	9045
YMR168C	*CEP3*	2.21E-06	1.30E-04	-38539	13448	76169	214	573
YMR205C	*PFK2*	2.79E-02	7.98E-02	-38491	15154	78599	681	9634
YDR150W	*NUM1*	7.36E-04	6.95E-03	-38307	4396	62567	339	2731
YDR477W	*SNF1*	2.50E-04	3.25E-03	-35295	23559	86230	830	2149
YLL039C	*UBI4*	7.81E-06	3.04E-04	-35023	17892	77530	514	981
YBL094C	*YBL094C*	2.55E-03	1.58E-02	-34983	0	51255	11196	0
YDR132C	*YDR132C*	6.80E-11	4.91E-08	-34217	22387	82935	547	446
YPR173C	*VPS4*	1.42E-13	2.39E-10	-32774	15979	71432	597	154
YOR340C	*RPA43*	1.08E-05	3.70E-04	-32327	14760	68990	389	867
YOL081W	*IRA2*	1.75E-03	1.22E-02	-31006	20614	75632	1382	3413
YDL143W	*CCT4*	7.37E-04	6.95E-03	-30844	4813	52243	8237	2987
YCR071C	*IMG2*	1.09E-04	1.82E-03	-30835	23387	79444	1850	2352
YNR006W	*VPS27*	9.36E-06	3.41E-04	-30609	32760	92846	631	1039
YOR149C	*SMP3*	2.13E-02	6.55E-02	-30093	22046	76391	290	6795
YBR189W	*RPS9B*	4.16E-05	9.52E-04	-29906	12464	62079	679	1301
YGL001C	*ERG26*	1.55E-03	1.13E-02	-29766	27612	84068	1013	3019
YHR189W	*PTH1*	1.92E-06	1.27E-04	-28517	25373	78958	472	721
YPR035W	*GLN1*	2.39E-02	7.11E-02	-28241	22967	75028	467	6663
YOR148C	*SPP2*	5.32E-03	2.60E-02	-27153	21625	71468	267	3739
YKL173W	*SNU114*	3.92E-02	1.02E-01	-26808	25084	76031	1084	7693
YGR032W	*GSC2*	2.28E-03	1.47E-02	-26567	26558	77838	593	2846
YGL006W	*PMC1*	7.27E-03	3.21E-02	-26261	30447	83087	570	4077
YGR097W	*ASK10*	2.58E-03	1.60E-02	-25938	16137	61647	4537	4328
YHL025W	*SNF6*	9.41E-13	1.19E-09	-25919	5383	45862	560	135
YBR200W	*BEM1*	1.00E-02	3.94E-02	-25749	7130	48173	10549	3582
YPR141C	*KAR3*	3.42E-02	9.19E-02	-25673	20782	68064	425	6943
YHR198C	*FMP22*	6.34E-07	5.61E-05	-25368	45084	103223	1893	1333
YML028W	*TSA1*	5.61E-10	2.83E-07	-24793	27634	76813	442	2659
YNL315C	*ATP11*	3.34E-05	8.40E-04	-24700	11815	53500	798	1225
YIL076W	*SEC28*	4.23E-04	4.62E-03	-24610	4384	42481	5848	2605
YNL284C	*MRPL10*	5.38E-03	2.61E-02	-24585	19182	64126	1961	3974
YGL005C	*COG7*	7.90E-07	6.33E-05	-24217	41588	96414	2184	1361
YNL297C	*MON2*	6.53E-04	6.39E-03	-23803	28499	76631	806	1965
YKL144C	*RPC25*	1.03E-03	8.74E-03	-23588	32917	82788	2346	2952

(*Table continues*)

Table A1. Continued…

ORF	Gene	*P*	*Q*	GIS	Query Fitness	Control Fitness	Query SE	Control SE
YGR027C	*RPS25A*	4.10E-08	7.13E-06	-23493	34188	84511	725	652
YPL143W	*RPL33A*	3.61E-04	4.10E-03	-23295	31152	79773	2027	2401
YGL063W	*PUS2*	1.95E-02	6.16E-02	-23069	14337	54806	4826	5920
YLR066W	*SPC3*	3.37E-02	9.09E-02	-22915	9930	48122	3011	6541
YKR035C	*YKR035C*	3.64E-05	8.89E-04	-22912	35373	85396	1050	1360
YKL041W	*VPS24*	3.36E-02	9.09E-02	-22811	24217	68903	1132	6196
YGL115W	*SNF4*	2.84E-05	7.66E-04	-22694	30274	77606	620	1018
YAL010C	*MDM10*	9.15E-05	1.59E-03	-22629	12880	52026	1368	1696
YKL195W	*MIA40*	9.72E-03	3.84E-02	-22482	32432	80458	1158	4017
YLR317W	*YLR317W*	1.29E-02	4.68E-02	-22188	35131	83981	550	4202
YGL047W	*ALG13*	2.29E-02	6.91E-02	-22096	35027	83694	2065	5424
YBR036C	*CSG2*	1.11E-03	9.17E-03	-21907	25444	69376	227	1792
YOR065W	*CYT1*	6.40E-03	2.92E-02	-21764	30039	75899	1133	3440
YCL032W	*STE50*	1.03E-04	1.75E-03	-21668	32441	79278	1275	1628
YGL042C	*YGL042C*	6.00E-04	5.99E-03	-21649	32698	79627	5421	2371
YGR017W	*YGR017W*	3.71E-04	4.18E-03	-21485	39476	89318	1269	1920
YGL219C	*MDM34*	2.83E-03	1.70E-02	-21400	42645	93836	634	2511
YOL002C	*IZH2*	4.76E-02	1.16E-01	-21311	36050	84043	411	6570
YFR010W	*UBP6*	4.60E-05	1.02E-03	-21072	23313	65030	239	726
YGL035C	*MIG1*	4.66E-04	4.91E-03	-20757	46923	99162	512	1470
YNL003C	*PET8*	2.74E-04	3.42E-03	-20649	14908	52096	1369	1848
YCR009C	*RVS161*	2.92E-02	8.25E-02	-20643	38052	85997	1939	5485
YOR360C	*PDE2*	6.22E-04	6.16E-03	-20257	37010	83904	1096	1908
YFL031W	*HAC1*	4.65E-03	2.37E-02	-20198	27771	70281	258	2665
YPR144C	*NOC4*	4.01E-03	2.14E-02	-20171	34031	79415	497	2593
YGR013W	*SNU71*	7.58E-03	3.30E-02	-20063	38102	85221	532	3179
YKL213C	*DOA1*	7.69E-05	1.44E-03	-19700	31783	75430	239	775
YOR256C	*TRE2*	2.81E-02	8.00E-02	-19616	26873	68115	4390	5564
YJR120W	*YJR120W*	4.99E-04	5.21E-03	-19552	28597	70546	151	1225
YOR243C	*PUS7*	4.96E-02	1.19E-01	-19426	34459	78950	888	6121
YOR106W	*VAM3*	6.25E-04	6.18E-03	-19309	33943	78022	329	1381
YCL044C	*MGR1*	3.52E-05	8.70E-04	-19226	35971	80872	1778	1562
YOR139C	*YOR139C*	2.39E-08	5.49E-06	-19145	38967	85143	1262	237
YDL013W	*HEX3*	1.15E-04	1.88E-03	-19098	15022	49993	554	1079
YGL004C	*RPN14*	1.10E-02	4.23E-02	-18877	35061	79027	867	3480
YPR024W	*YME1*	6.92E-04	6.66E-03	-18818	10398	42805	1575	2096
YPL057C	*SUR1*	4.69E-03	2.38E-02	-18786	33578	76721	474	2541
YPR164W	*MMS1*	2.58E-06	1.40E-04	-18542	29166	69899	722	786
YGL237C	*HAP2*	4.23E-03	2.22E-02	-18454	45588	93831	1594	2873
YGR031W	*YGR031W*	2.48E-02	7.28E-02	-18437	41313	87544	1120	4519
YOR043W	*WHI2*	7.79E-05	1.45E-03	-18415	43145	90195	1409	1503
YGL010W	*YGL010W*	1.56E-02	5.32E-02	-18357	32130	73972	7865	3311
YDL083C	*RPS16B*	4.30E-02	1.08E-01	-18129	31823	73187	868	5402

(*Table continues*)

Table A1. Continued…

ORF	Gene	*P*	*Q*	GIS	Query Fitness	Control Fitness	Query SE	Control SE
YKL212W	*SAC1*	6.44E-03	2.94E-02	-18099	23087	60344	3309	3585
YBR289W	*SNF5*	2.35E-03	1.49E-02	-18058	1503	28661	5847	1503
YMR021C	*MAC1*	6.30E-03	2.89E-02	-17934	25914	64244	635	2720
YBR267W	*REI1*	3.20E-03	1.85E-02	-17862	26099	64410	612	2205
YKL083W	*YKL083W*	8.08E-04	7.43E-03	-17841	34276	76360	1021	1792
YGR022C	*YGR022C*	4.01E-03	2.14E-02	-17804	45309	92470	1180	2589
YDL006W	*PTC1*	1.77E-04	2.51E-03	-17647	22227	58421	3189	1933
YPL270W	*MDL2*	4.10E-05	9.46E-04	-17626	31806	72426	1514	1413
YHR012W	*VPS29*	1.50E-07	1.94E-05	-17616	44945	91662	1633	782
YDR532C	*KRE28*	1.27E-05	4.16E-04	-17572	18157	52348	1896	1355
YGR010W	*NMA2*	5.22E-03	2.57E-02	-17558	35296	77439	821	2585
YLR214W	*FRE1*	4.26E-02	1.07E-01	-17486	42965	88571	900	5199
YKL073W	*LHS1*	1.26E-02	4.64E-02	-17483	48129	96132	1583	3590
YGL127C	*SOH1*	2.18E-04	2.95E-03	-17482	38477	81989	496	1097
YLL043W	*FPS1*	2.88E-05	7.70E-04	-17444	36916	79646	420	738
YBR266C	*YBR266C*	8.16E-03	3.47E-02	-17305	27536	65699	548	2831
YGR008C	*STF2*	8.73E-03	3.61E-02	-17115	46158	92705	193	2802
YLL009C	*COX17*	5.22E-06	2.37E-04	-16974	33494	73944	807	851
YJL082W	*IML2*	8.46E-10	3.56E-07	-16916	40355	83911	928	306
YOR247W	*SRL1*	6.31E-05	1.27E-03	-16898	46634	93084	838	1108
YML047C	*PRM6*	2.00E-02	6.27E-02	-16782	55059	105259	985	3814
YJL029C	*VPS53*	6.19E-03	2.87E-02	-16692	22591	57557	244	2432
YLR229C	*CDC42*	3.92E-03	2.12E-02	-16521	32544	71888	1069	2377
YGL151W	*NUT1*	5.25E-05	1.10E-03	-16521	35478	76186	571	896
YGR007W	*MUQ1*	6.96E-03	3.11E-02	-16489	34079	74090	266	2506
YEL013W	*VAC8*	1.69E-03	1.18E-02	-16429	39326	81691	550	1697
YPR062W	*FCY1*	1.65E-07	2.02E-05	-16377	36457	77410	843	663
YBR025C	*YBR025C*	4.90E-03	2.46E-02	-16357	41993	85492	464	2259
YOL095C	*HMI1*	2.53E-04	3.27E-03	-16340	27460	64174	551	1117
YGR085C	*RPL11B*	1.29E-04	2.00E-03	-16147	40296	82698	688	1085
YMR229C	*RRP5*	1.17E-04	1.90E-03	-16084	54947	104070	2708	1674
YNL306W	*MRPS18*	7.44E-03	3.26E-02	-16059	44555	88809	1789	2987
YDL188C	*PPH22*	1.39E-05	4.45E-04	-16049	47750	93476	503	708
YDL186W	*YDL186W*	9.38E-06	3.41E-04	-16016	43980	87903	740	833
YNR020C	*YNR020C*	1.46E-03	1.10E-02	-16002	32810	71517	1335	2007
YKL208W	*CBT1*	1.32E-03	1.03E-02	-15992	31694	69867	33	1362
YOR244W	*ESA1*	2.52E-02	7.35E-02	-15965	35176	74930	251	3841
YHR008C	*SOD2*	9.23E-04	8.09E-03	-15960	36057	76214	854	1609
YGL049C	*TIF4632*	2.45E-04	3.22E-03	-15872	49443	95697	955	1346
YLR455W	*YLR455W*	8.63E-05	1.54E-03	-15738	40219	81986	1818	2319
YGR055W	*MUP1*	4.54E-06	2.13E-04	-15694	46108	90550	1103	945
YAL013W	*DEP1*	1.36E-02	4.84E-02	-15656	34607	73643	507	3041
YGR038W	*ORM1*	9.42E-04	8.22E-03	-15615	42083	84536	550	1413

(*Table continues*)

Table A1. Continued…

ORF	Gene	*P*	*Q*	GIS	Query Fitness	Control Fitness	Query SE	Control SE
YGR018C	*YGR018C*	6.72E-03	3.02E-02	-15613	40714	82528	1793	2857
YGR011W	*YGR011W*	2.82E-02	8.02E-02	-15521	43995	87201	1968	4178
YPL183C	*YPL183C*	1.04E-04	1.77E-03	-15450	51892	98667	747	1066
YJL122W	*ALB1*	3.64E-03	2.02E-02	-15326	52239	98994	1171	2245
YPR185W	*ATG13*	5.09E-06	2.34E-04	-15269	42742	84996	1182	968
YCL046W	*YCL046W*	8.76E-03	3.62E-02	-15266	41739	83521	1784	2975
YGR028W	*MSP1*	8.51E-05	1.52E-03	-15222	53319	100424	3008	1234
YOR293W	*RPS10A*	9.35E-08	1.44E-05	-15172	28666	64230	1395	482
YPR191W	*QCR2*	1.95E-06	1.27E-04	-15011	32009	68892	262	392

Table A2. SGA screen results for *alk2*Δ query strain

ORF	Gene	*P*	*Q*	GIS	Query Fitness	Control Fitness	Query SE	Control SE
YGL255W	*ZRT1*	8.04E-06	1.85E-04	-63583	3125	80190	814	1842
YFL032W	*YFL032W*	6.50E-05	8.33E-04	-59359	7149	79950	320	1989
YHR079C	*IRE1*	6.45E-04	4.12E-03	-57433	19456	92427	1813	4896
YDR388W	*RVS167*	7.60E-04	4.65E-03	-57371	11079	82284	1632	4926
YBR036C	*CSG2*	1.54E-05	2.97E-04	-56487	1226	69376	227	1226
YMR205C	*PFK2*	8.67E-05	1.04E-03	-56394	8991	78599	681	2398
YKL212W	*SAC1*	3.32E-07	2.15E-05	-49952	247	60344	3309	247
YCR009C	*RVS161*	1.53E-03	7.64E-03	-49940	21599	85997	1939	5405
YGL237C	*HAP2*	1.11E-03	6.12E-03	-45168	32887	93831	1594	4446
YGL219C	*MDM34*	2.72E-04	2.30E-03	-44894	33166	93836	634	2583
YML028W	*TSA1*	1.32E-15	6.67E-12	-43551	20348	76813	442	2700
YML013C-A	*YML013C-A*	1.54E-03	7.66E-03	-42402	18350	73029	622	3962
YBR189W	*RPS9B*	3.71E-04	2.87E-03	-40862	10780	62079	679	2624
YFL031W	*HAC1*	5.67E-05	7.59E-04	-40365	18100	70281	258	1339
YBL021C	*HAP3*	9.05E-03	2.79E-02	-39346	31923	85672	5293	8208
YGL115W	*SNF4*	4.05E-03	1.57E-02	-39112	25447	77606	620	4980
YDR359C	*VID21*	9.02E-11	9.11E-08	-37838	12004	59915	1344	779
YBR025C	*YBR025C*	7.85E-04	4.75E-03	-37701	33418	85492	464	2837
YHR198C	*FMP22*	3.30E-09	8.34E-07	-36968	48901	103223	1893	720
YNR006W	*VPS27*	3.11E-10	2.24E-07	-35863	41373	92846	631	609
YNL315C	*ATP11*	3.80E-05	5.84E-04	-35633	8872	53500	798	1660
YLR338W	*YLR338W*	4.35E-04	3.19E-03	-35545	24388	72046	496	2301
YDR071C	*PAA1*	1.08E-08	1.74E-06	-35351	40566	91260	1865	531
YML013W	*SEL1*	7.08E-04	4.40E-03	-34699	20522	66382	4080	4577
YNL284C	*MRPL10*	8.93E-03	2.76E-02	-34642	18703	64126	1961	6232
YHR189W	*PTH1*	2.57E-03	1.12E-02	-34593	31090	78958	472	3781
YCR028C-A	*RIM1*	2.14E-06	7.36E-05	-33586	18343	62423	410	809
YDR392W	*SPT3*	9.52E-03	2.87E-02	-32643	34380	80569	141	5495
YHL020C	*OPI1*	4.13E-02	8.29E-02	-32496	28869	73767	817	9483

(*Table continues*)

Table A2. Continued…

ORF	Gene	*P*	*Q*	GIS	Query Fitness	Control Fitness	Query SE	Control SE
YLL039C	*UBI4*	7.45E-04	4.58E-03	-31912	32583	77530	514	2441
YFL036W	*RPO41*	9.23E-03	2.82E-02	-31891	16724	58440	1100	5519
YPR066W	*UBA3*	2.16E-07	1.61E-05	-31646	25328	68488	2166	1542
YDR207C	*UME6*	4.85E-06	1.33E-04	-31566	18517	60204	3406	2105
YMR282C	*AEP2*	2.69E-04	2.29E-03	-31434	15191	56048	465	1820
YGR101W	*PCP1*	2.28E-02	5.33E-02	-30915	17228	57873	1714	7404
YJL175W	*YJL175W*	1.46E-03	7.39E-03	-30779	28105	70785	628	2928
YDR477W	*SNF1*	1.64E-04	1.68E-03	-30759	40974	86230	830	1934
YJL091C	*GWT1*	1.24E-03	6.59E-03	-30142	26728	68364	4217	4457
YKL213C	*DOA1*	1.82E-05	3.37E-04	-30045	32704	75430	239	813
YJR073C	*OPI3*	1.96E-03	9.11E-03	-29740	10350	48191	1469	3601
YGL127C	*SOH1*	1.98E-03	9.17E-03	-29389	38816	81989	496	2999
YGL092W	*NUP145*	7.32E-03	2.40E-02	-29129	4960	40978	8608	4908
YAL010C	*MDM10*	2.37E-04	2.08E-03	-29056	14223	52026	1368	2405
YIL076W	*SEC28*	5.62E-04	3.78E-03	-28896	6443	42481	5848	365
YLR061W	*RPL22A*	7.70E-03	2.49E-02	-28790	24719	64323	248	4509
YPR144C	*NOC4*	1.13E-03	6.18E-03	-28618	37445	79415	497	2480
YLR218C	*YLR218C*	1.14E-08	1.74E-06	-27747	38702	79879	755	746
YKL041W	*VPS24*	6.80E-09	1.37E-06	-27684	29634	68903	1132	886
YDR080W	*VPS41*	2.28E-08	2.83E-06	-27438	34366	74295	439	549
YLR038C	*COX12*	1.05E-03	5.85E-03	-27295	33061	72555	765	2515
YDR375C	*BCS1*	1.16E-03	6.27E-03	-27200	30733	69641	283	2279
YOR065W	*CYT1*	1.52E-05	2.96E-04	-26812	36327	75899	1133	1543
YMR304W	*UBP15*	2.99E-05	4.86E-04	-25984	60120	103505	3046	2266
YHL023C	*RMD11*	4.67E-04	3.36E-03	-25905	41351	80849	451	1777
YFR010W	*UBP6*	4.74E-04	3.38E-03	-25888	28209	65030	239	1634
YLR192C	*HCR1*	4.05E-06	1.16E-04	-25699	19366	54173	1281	1431
YBL091C-A	*SCS22*	5.17E-04	3.57E-03	-25611	52068	93378	494	1839
YJL204C	*RCY1*	5.19E-04	3.57E-03	-25588	33737	71315	620	1940
YLR056W	*ERG3*	1.53E-07	1.22E-05	-25179	36591	74253	1955	1090
YNL297C	*MON2*	7.37E-09	1.43E-06	-24961	38786	76631	806	720
YPR024W	*YME1*	6.47E-08	6.40E-06	-24689	10920	42805	1575	412
YLR285W	*NNT1*	8.68E-07	4.14E-05	-24611	46652	85666	944	1062
YDR512C	*EMI1*	6.23E-04	4.02E-03	-24337	34387	70593	530	1876
YJR120W	*YJR120W*	3.21E-05	5.10E-04	-24167	34519	70546	151	692
YLR062C	*BUD28*	1.80E-03	8.56E-03	-23982	46663	84923	379	2363
YNR020C	*YNR020C*	2.29E-08	2.83E-06	-23941	35552	71517	1335	911
YNL003C	*PET8*	8.23E-04	4.92E-03	-23567	19770	52096	1369	2547
YDR005C	*MAF1*	6.08E-07	3.20E-05	-23529	20397	52804	1192	1140
YBR131W	*CCZ1*	9.67E-03	2.90E-02	-23495	40681	77147	956	4177
YBR006W	*UGA2*	1.95E-02	4.75E-02	-23381	48902	86892	1165	5279
YBR289W	*SNF5*	1.94E-03	9.05E-03	-23285	557	28661	5847	519
YIL027C	*KRE27*	3.47E-04	2.77E-03	-23240	51191	89473	1920	2513

(*Table continues*)

Table A2. Continued…

ORF	Gene	*P*	*Q*	GIS	Query Fitness	Control Fitness	Query SE	Control SE
YPR173C	*VPS4*	9.99E-04	5.66E-03	-23147	36276	71432	597	2072
YCL044C	*MGR1*	5.75E-03	2.00E-02	-23058	44217	80872	1778	3913
YMR115W	*FMP24*	1.92E-10	1.61E-07	-23008	37786	73081	609	483
YNL021W	*HDA1*	4.14E-07	2.39E-05	-22958	54249	92810	1849	1181
YKR035C	*YKR035C*	1.57E-09	5.48E-07	-22911	48128	85396	1050	369
YLR393W	*ATP10*	4.90E-10	2.75E-07	-22808	35286	69835	958	560
YGL236C	*MTO1*	5.53E-03	1.94E-02	-22806	57807	96906	1446	3688
YGR250C	*YGR250C*	1.91E-06	6.66E-05	-22806	56592	95445	2402	1131
YLR390W-A	*CCW14*	4.41E-06	1.23E-04	-22736	61118	100800	1439	1422
YDL142C	*CRD1*	1.94E-03	9.05E-03	-22691	54959	93343	1202	2792
YFR039C	*YFR039C*	2.08E-03	9.51E-03	-22625	67951	108883	2105	3298
YBR267W	*REI1*	4.69E-04	3.36E-03	-22589	30993	64410	612	1727
YER153C	*PET122*	8.76E-09	1.64E-06	-22584	32873	66666	1206	379
YOR106W	*VAM3*	1.19E-04	1.32E-03	-21984	42921	78022	329	1065
YBL031W	*SHE1*	4.50E-03	1.69E-02	-21954	44890	80354	316	2885
YHL041W	*YHL041W*	2.22E-04	2.01E-03	-21757	43828	78840	1992	2306
YKL137W	*YKL137W*	2.74E-05	4.51E-04	-21720	49570	85698	795	1233
YLR317W	*YLR317W*	2.04E-04	1.89E-03	-21243	48618	83981	550	1365
YPR191W	*QCR2*	1.33E-03	6.96E-03	-21242	36067	68892	262	1876
YMR086C-A	*YMR086C-A*	1.96E-03	9.11E-03	-21226	50767	86543	1019	2554
YHR178W	*STB5*	3.15E-02	6.74E-02	-21182	35480	68114	1190	5674
YMR256C	*COX7*	5.80E-05	7.73E-04	-21022	35571	68031	676	1223
YDL232W	*OST4*	1.64E-03	8.05E-03	-20974	29851	61097	357	2024
YBL102W	*SFT2*	1.66E-03	8.11E-03	-20925	54626	90821	2046	2979
YIL002C	*INP51*	3.43E-04	2.75E-03	-20829	65836	104180	1805	2286
YDR173C	*ARG82*	1.16E-05	2.48E-04	-20789	29767	60773	2531	1496
YGR183C	*QCR9*	1.48E-03	7.45E-03	-20785	42279	75809	737	2187
YLL049W	*LDB18*	3.88E-03	1.52E-02	-20767	33775	65565	470	2661
YOL095C	*HMI1*	9.82E-12	1.24E-08	-20612	32773	64174	551	347
YDR386W	*MUS81*	1.37E-03	7.07E-03	-20591	51938	87187	794	2171
YPL183C	*YPL183C*	4.63E-09	1.02E-06	-20557	61521	98667	747	610
YBR171W	*SEC66*	2.10E-03	9.56E-03	-20519	42644	75928	504	2211
YDL100C	*GET3*	2.33E-04	2.07E-03	-20405	59976	96626	2098	2253
YGL256W	*ADH4*	1.03E-02	3.04E-02	-20240	41679	74433	1264	3839
YBR170C	*NPL4*	2.18E-04	1.98E-03	-20175	37175	68940	610	1387
YFR024C	*YFR024C*	1.60E-02	4.13E-02	-20017	73477	112389	2598	4732
YBR007C	*DSF2*	1.81E-02	4.50E-02	-19839	49158	82941	4087	5055
YBR001C	*NTH2*	4.38E-05	6.38E-04	-19838	54298	89119	563	1052
YMR316C-A	*YMR316C-A*	2.57E-06	8.44E-05	-19793	55004	89913	1567	1267
YPR179C	*HDA3*	1.57E-04	1.62E-03	-19723	59880	95691	3494	1028
YMR280C	*CAT8*	3.32E-03	1.35E-02	-19698	51068	85069	243	2330
YGL212W	*VAM7*	2.84E-05	4.64E-04	-19688	40416	72252	710	1114
YDR532C	*KRE28*	1.69E-03	8.20E-03	-19610	23937	52348	1896	2791

(*Table continues*)

Table A2. Continued…

ORF	Gene	*P*	*Q*	GIS	Query Fitness	Control Fitness	Query SE	Control SE
YHR012W	*VPS29*	6.47E-04	4.12E-03	-19598	56653	91662	1633	2309
YBR084W	*MIS1*	8.04E-03	2.56E-02	-19506	47366	80387	578	3198
YBL001C	*ECM15*	3.83E-02	7.87E-02	-19023	47368	79809	791	5430
YMR087W	*YMR087W*	1.07E-04	1.23E-03	-18995	51659	84933	795	1346
YLR126C	*YLR126C*	1.61E-07	1.25E-05	-18779	46935	78995	1074	861
YGL173C	*KEM1*	6.41E-03	2.17E-02	-18688	29573	58015	756	2936
YLR199C	*YLR199C*	1.10E-04	1.25E-03	-18649	55158	88723	1471	1731
YNR041C	*COQ2*	1.68E-04	1.70E-03	-18624	42931	73995	526	1196
YDR334W	*SWR1*	4.26E-02	8.48E-02	-18591	53123	86207	1306	5608
YBL079W	*NUP170*	1.95E-05	3.54E-04	-18551	49909	82297	1099	1285
YLR443W	*ECM7*	6.03E-05	7.90E-04	-18545	53081	86102	766	1218
YGR027C	*RPS25A*	2.54E-06	8.40E-05	-18544	51759	84511	725	878
YNL223W	*ATG4*	9.56E-03	2.88E-02	-18500	52844	85763	435	3177
YKL139W	*CTK1*	5.11E-05	7.06E-04	-18479	36048	65547	404	888
YBR073W	*RDH54*	1.51E-04	1.57E-03	-18423	56629	90220	1957	1947
YIL128W	*MET18*	6.12E-06	1.54E-04	-18418	30039	58250	1264	1223
YDL013W	*HEX3*	1.68E-02	4.27E-02	-18265	23322	49993	554	3835
YDL163W	*YDL163W*	6.36E-07	3.28E-05	-18223	36255	65489	334	1212
YPR134W	*MSS18*	8.93E-04	5.23E-03	-18207	41395	71649	676	1736
YLL043W	*FPS1*	3.92E-04	2.97E-03	-18142	48114	79646	420	1278
YCR034W	*FEN1*	8.75E-07	4.14E-05	-18108	58854	92517	753	817
YLR394W	*CST9*	3.28E-04	2.67E-03	-18101	66259	101409	3464	1776
YMR021C	*MAC1*	6.03E-10	2.77E-07	-18093	35350	64244	635	459
YNL170W	*YNL170W*	3.78E-04	2.89E-03	-18079	34296	62960	1480	1970
YLR460C	*YLR460C*	5.18E-04	3.57E-03	-18054	52874	85262	758	1616
YMR186W	*HSC82*	4.93E-03	1.80E-02	-17945	71466	107481	1690	3077
YDR526C	*YDR526C*	2.39E-02	5.50E-02	-17913	37943	67144	3296	4870
YNL192W	*CHS1*	1.32E-02	3.61E-02	-17701	59819	93186	3447	4178
YNL333W	*SNZ2*	5.22E-03	1.87E-02	-17682	63374	97438	2398	3309
YLR265C	*NEJ1*	9.91E-09	1.68E-06	-17678	64341	98596	743	587
YPR070W	*MED1*	1.29E-02	3.57E-02	-17620	46054	76543	1133	3578
YCR063W	*BUD31*	4.82E-02	9.34E-02	-17575	40000	69210	757	5484
YLR401C	*DUS3*	2.39E-05	4.17E-04	-17566	60138	93409	972	1202
YDL076C	*RXT3*	5.44E-03	1.93E-02	-17514	69168	104201	3441	3421
YLR090W	*XDJ1*	3.44E-07	2.20E-05	-17512	63243	97076	584	655
YOR267C	*HRK1*	7.29E-07	3.68E-05	-17495	54048	86002	1022	914
YPL159C	*PET20*	3.04E-02	6.56E-02	-17491	47356	77952	658	4565
YOR252W	*TMA16*	1.04E-02	3.05E-02	-17382	64709	98681	1807	3580
YLR395C	*COX8*	9.12E-04	5.30E-03	-17242	49313	80007	618	1636
YBR185C	*MBA1*	5.27E-06	1.42E-04	-17179	47364	77587	1294	1163
YKR035W-A	*DID2*	5.60E-07	2.98E-05	-17134	49941	80631	996	875
YKL208W	*CBT1*	5.50E-04	3.73E-03	-17050	41070	69867	33	1081
YPL111W	*CAR1*	2.60E-02	5.85E-02	-17038	58720	91068	459	4170

(*Table continues*)

Table A2. Continued…

ORF	Gene	*P*	*Q*	GIS	Query Fitness	Control Fitness	Query SE	Control SE
YDR125C	*ECM18*	7.04E-06	1.71E-04	-17016	53168	84368	543	787
YNL239W	*LAP3*	2.88E-03	1.22E-02	-17015	60497	93178	863	2257
YGR203W	*YGR203W*	9.44E-03	2.86E-02	-16988	70196	104804	2110	3528
YKR008W	*RSC4*	2.86E-03	1.22E-02	-16966	54465	85867	821	2225
YGR080W	*TWF1*	2.70E-03	1.16E-02	-16960	67853	101954	901	2240
YPL183W-A	*RTC6*	2.80E-07	1.91E-05	-16899	50372	80866	403	511
YBR042C	*YBR042C*	1.86E-02	4.59E-02	-16786	55417	86796	642	3678
YBR206W	*YBR206W*	2.79E-05	4.57E-04	-16766	59039	91125	923	1162
YDL077C	*VAM6*	1.23E-02	3.44E-02	-16743	35920	63307	778	3241
YIL005W	*EPS1*	9.93E-04	5.64E-03	-16489	59752	91650	3265	2241
YLR452C	*SST2*	1.13E-02	3.24E-02	-16443	58584	90191	1125	3239
YMR209C	*YMR209C*	9.54E-03	2.88E-02	-16386	53262	83725	1216	3121
YOR263C	*YOR263C*	5.96E-05	7.83E-04	-16330	63804	96330	298	746
YOR247W	*SRL1*	1.22E-06	4.96E-05	-16293	61141	93084	838	838
YNL089C	*YNL089C*	2.16E-03	9.79E-03	-16280	64895	97581	1305	2292
YDR316W	*OMS1*	1.76E-03	8.42E-03	-16276	46632	75622	678	1847
YPL143W	*RPL33A*	1.34E-04	1.43E-03	-16249	50112	79773	2027	1735
YGL162W	*SUT1*	5.46E-06	1.44E-04	-16193	61159	92985	1359	1132
YGR085C	*RPL11B*	8.94E-07	4.14E-05	-16189	52606	82698	688	740
YAL055W	*PEX22*	2.82E-02	6.21E-02	-16162	56810	87720	1433	4291
YDR042C	*YDR042C*	1.48E-05	2.90E-04	-16125	54635	85060	804	1005
YNL169C	*PSD1*	2.17E-03	9.79E-03	-16123	41565	69347	553	1846
YBL071C	*YBL071C*	1.76E-02	4.40E-02	-16110	54286	84623	381	3417
YGR268C	*HUA1*	1.43E-02	3.81E-02	-16109	72280	106253	2345	3765
YLR309C	*IMH1*	8.43E-05	1.02E-03	-16104	66903	99782	869	1241
YBL104C	*YBL104C*	1.19E-05	2.51E-04	-16103	55182	85692	1676	1253
YLR034C	*SMF3*	1.78E-04	1.74E-03	-16098	58615	89813	597	1162
YLR450W	*HMG2*	3.65E-07	2.25E-05	-16032	64485	96790	675	684
YKR065C	*PAM17*	1.63E-05	3.15E-04	-15943	52806	82643	795	1002
YBR022W	*POA1*	4.02E-03	1.56E-02	-15914	52879	82697	4145	2523
YCL032W	*STE50*	9.73E-03	2.92E-02	-15895	50054	79278	1275	3080
YHR111W	*UBA4*	4.16E-03	1.59E-02	-15883	52188	81829	392	2092
YIL077C	*YIL077C*	2.78E-03	1.19E-02	-15882	53631	83562	661	2005
YGL151W	*NUT1*	4.88E-05	6.81E-04	-15872	47505	76186	571	953
YDR077W	*SED1*	2.27E-02	5.31E-02	-15806	53610	83445	1256	3880
YMR318C	*ADH6*	2.38E-04	2.08E-03	-15796	57331	87906	940	1438
YHR203C	*RPS4B*	1.59E-02	4.10E-02	-15753	47150	75616	407	3227
YNL100W	*YNL100W*	1.04E-02	3.05E-02	-15734	57130	87590	382	2785
YPL213W	*LEA1*	4.74E-04	3.38E-03	-15710	31911	57245	1836	1960
YMR130W	*YMR130W*	2.22E-02	5.23E-02	-15624	61126	92261	1461	3871
YLR063W	*YLR063W*	5.34E-06	1.43E-04	-15609	67588	100012	1201	1065
YCR088W	*ABP1*	4.00E-02	8.14E-02	-15561	72440	105786	3008	4897
YER020W	*GPA2*	8.87E-03	2.75E-02	-15534	53387	82850	936	2813

(*Table continues*)

Table A2. Continued…

ORF	Gene	*P*	*Q*	GIS	Query Fitness	Control Fitness	Query SE	Control SE
YEL049W	*PAU2*	6.23E-04	4.02E-03	-15528	52985	82360	847	1570
YGR275W	*RTT102*	1.51E-02	3.97E-02	-15458	70933	103851	1454	3440
YLR015W	*BRE2*	2.69E-05	4.48E-04	-15447	53230	82557	766	1016
YOR139C	*YOR139C*	3.01E-06	9.32E-05	-15443	55386	85143	1262	1010
YBR011C	*IPP1*	1.58E-02	4.09E-02	-15432	48123	76400	1222	3400
YLR171W	*YLR171W*	8.81E-03	2.73E-02	-15410	51185	80055	481	2611
YMR092C	*AIP1*	5.35E-04	3.65E-03	-15405	53732	83109	565	1326
YLR346C	*YLR346C*	4.15E-03	1.59E-02	-15344	69047	101446	3835	2580
YBR023C	*CHS3*	2.91E-03	1.23E-02	-15306	54184	83534	434	1841
YPR020W	*ATP20*	1.03E-03	5.80E-03	-15294	52456	81443	3569	1212
YLR079W	*SIC1*	1.73E-03	8.32E-03	-15244	34250	59496	1352	2125
YPR061C	*JID1*	6.34E-09	1.33E-06	-15197	60018	90417	819	491
YDR382W	*RPP2B*	2.75E-02	6.09E-02	-15089	35958	61364	207	3754
YOR360C	*PDE2*	4.26E-07	2.41E-05	-15054	54744	83904	1096	791

Table A3. SGA screen results for *alk1*Δ *alk2*Δ query strain

ORF	Gene	*P*	*Q*	GIS	Query Fitness	Control Fitness	Query SE	Control SE
YGL116W	*CDC20*	3.42E-16	8.63E-13	-62826	46	88386	290	30
YGL255W	*ZRT1*	2.55E-14	4.29E-11	-56623	418	80190	814	219
YLR166C	*SEC10*	3.59E-13	4.53E-10	-55975	0	78691	592	0
YBR011C	*IPP1*	7.05E-11	5.93E-08	-54345	0	76400	1222	0
YLR339C	*YLR339C*	9.42E-07	7.55E-05	-51609	0	72553	4562	0
YFL032W	*YFL032W*	1.98E-04	3.54E-03	-45992	10878	79950	320	2153
YML031W	*NDC1*	6.39E-05	1.63E-03	-41486	2264	61504	7466	1576
YPR133C	*SPN1*	6.70E-03	3.80E-02	-41480	11811	74919	5438	7858
YFL031W	*HAC1*	4.51E-08	7.59E-06	-41210	8783	70281	258	418
YPL063W	*TIM50*	4.49E-03	2.98E-02	-40320	6859	66325	4313	6739
YDR392W	*SPT3*	1.38E-06	9.82E-05	-37357	19954	80569	141	445
YJL204C	*RCY1*	4.68E-04	6.49E-03	-36186	14542	71315	620	2407
YBR001C	*NTH2*	5.72E-04	7.49E-03	-34843	28550	89119	563	2427
YBL021C	*HAP3*	3.11E-05	1.02E-03	-33182	27759	85672	5293	925
YBR036C	*CSG2*	7.46E-05	1.77E-03	-32987	16362	69376	227	1163
YBR009C	*HHF1*	4.95E-05	1.40E-03	-32381	38479	99616	3413	2889
YGL127C	*SOH1*	4.16E-02	1.21E-01	-31830	26492	81989	496	9294
YOR256C	*TRE2*	6.21E-03	3.64E-02	-30195	18257	68115	4390	5748
YDR173C	*ARG82*	1.44E-07	1.82E-05	-28463	14767	60773	2531	1253
YNL297C	*MON2*	8.01E-07	6.85E-05	-28184	26326	76631	806	934
YOR224C	*RPB8*	1.15E-02	5.34E-02	-28038	154	39633	11597	153
YBR189W	*RPS9B*	2.36E-03	2.00E-02	-26248	17911	62079	679	2892
YDR207C	*UME6*	7.13E-06	3.53E-04	-26111	16714	60204	3406	604
YBR005W	*RCR1*	7.63E-03	4.13E-02	-25559	32915	82204	2960	4857

(*Table continues*)

Table A3. Continued…

ORF	Gene	*P*	*Q*	GIS	Query Fitness	Control Fitness	Query SE	Control SE
YDR359C	*VID21*	1.66E-08	3.99E-06	-25454	17164	59915	1344	141
YLR198C	*YLR198C*	6.14E-03	3.61E-02	-25411	2303	38961	9335	1976
YML028W	*TSA1*	1.26E-16	6.36E-13	-25107	29532	76813	442	1464
YBL020W	*RFT1*	3.13E-03	2.35E-02	-24694	38679	89091	1245	3232
YOL078W	*AVO1*	2.58E-03	2.08E-02	-24476	0	34409	7532	0
YLR066W	*SPC3*	4.54E-02	1.28E-01	-24362	9869	48122	3011	7673
YCR071C	*IMG2*	2.38E-08	4.62E-06	-24186	32324	79444	1850	804
YBR012C	*YBR012C*	1.26E-02	5.62E-02	-24160	32451	79585	880	4603
YBL003C	*HTA2*	3.35E-03	2.46E-02	-23906	38934	88343	1407	3280
YBR004C	*GPI18*	5.72E-09	2.18E-06	-23593	42740	93253	1183	757
YML013W	*SEL1*	7.29E-05	1.74E-03	-23236	23984	66382	4080	513
YMR224C	*MRE11*	3.44E-10	2.17E-07	-22955	20721	61402	842	2445
YBL079W	*NUP170*	9.59E-03	4.80E-02	-22841	35699	82297	1099	4055
YIL040W	*APQ12*	4.39E-03	2.94E-02	-22802	34017	79878	1663	3482
YLR061W	*RPL22A*	4.17E-04	5.99E-03	-22234	23520	64323	248	1356
YBR025C	*YBR025C*	7.80E-03	4.19E-02	-22036	38777	85492	464	3503
YGL219C	*MDM34*	1.28E-03	1.34E-02	-21690	45057	93836	634	2051
YMR304W	*UBP15*	2.70E-04	4.34E-03	-21452	52174	103505	3046	2504
YJR074W	*MOG1*	1.83E-02	7.10E-02	-20933	31103	73154	1447	4685
YER095W	*RAD51*	1.27E-04	2.60E-03	-20396	38957	83441	339	987
YDR123C	*INO2*	5.02E-03	3.21E-02	-20315	7471	39062	441	2793
YNL226W	*YNL226W*	1.24E-02	5.57E-02	-20143	32465	73959	593	3788
YDR071C	*PAA1*	2.18E-04	3.76E-03	-20126	44790	91260	1865	2024
YDR080W	*VPS41*	1.78E-03	1.65E-02	-19878	32970	74295	439	1985
YNL299W	*TRF5*	1.99E-04	3.54E-03	-19851	42785	88055	641	1300
YJR073C	*OPI3*	2.93E-06	1.74E-04	-19675	14605	48191	1469	1193
YNL284C	*MRPL10*	2.57E-02	8.77E-02	-19612	26003	64126	1961	5037
YHR189W	*PTH1*	3.36E-05	1.07E-03	-19558	36607	78958	472	863
YIL076W	*SEC28*	2.20E-03	1.89E-02	-19485	10732	42481	5848	415
YCR034W	*FEN1*	3.28E-07	3.52E-05	-19422	46388	92517	753	722
YKL137W	*YKL137W*	1.05E-07	1.43E-05	-19226	41733	85698	795	687
YNL227C	*JJJ1*	5.39E-03	3.35E-02	-19076	31773	71485	462	2697
YER083C	*GET2*	7.70E-03	4.16E-02	-19038	22456	58333	109	2975
YLL039C	*UBI4*	2.43E-03	2.02E-02	-19013	36135	77530	514	2121
YPL076W	*GPI2*	1.91E-02	7.31E-02	-19006	49634	96496	2454	4604
YBR109C	*CMD1*	4.53E-02	1.28E-01	-18689	6857	35914	2862	5966
YBR006W	*UGA2*	3.45E-03	2.51E-02	-18527	43281	86892	1165	2594
YBL023C	*MCM2*	2.41E-05	8.39E-04	-18509	42272	85447	2031	1546
YNL296W	*YNL296W*	3.79E-06	2.08E-04	-18336	35826	76142	939	951
YJL175W	*YJL175W*	1.27E-02	5.64E-02	-18335	32016	70785	628	3490
YHR178W	*STB5*	1.74E-03	1.62E-02	-18285	30166	68114	1190	2229
YBR289W	*SNF5*	3.38E-03	2.47E-02	-18161	2227	28661	5847	2227
YLR089C	*ALT1*	7.97E-06	3.83E-04	-18109	38204	79166	463	691

(*Table continues*)

Table A3. Continued…

ORF	Gene	*P*	*Q*	GIS	Query Fitness	Control Fitness	Query SE	Control SE
YBL031W	*SHE1*	4.29E-02	1.23E-01	-18013	39145	80354	316	5327
YLR143W	*YLR143W*	5.75E-07	5.45E-05	-17189	49901	94317	1858	712
YIL084C	*SDS3*	9.04E-06	4.12E-04	-17104	34085	71963	495	707
YGR085C	*RPL11B*	1.47E-03	1.48E-02	-16925	41900	82698	688	1770
YLR320W	*MMS22*	2.17E-04	3.76E-03	-16834	31674	68194	549	1123
YPR191W	*QCR2*	1.04E-02	5.05E-02	-16754	32251	68892	262	2928
YLR214W	*FRE1*	3.36E-03	2.46E-02	-16654	46348	88571	900	2248
YDR335W	*MSN5*	6.27E-05	1.61E-03	-16535	47478	89991	707	1031
YDL020C	*RPN4*	2.30E-09	1.16E-06	-16516	36800	74954	543	413
YLR140W	*YLR140W*	2.23E-02	8.03E-02	-16513	18066	48611	3673	4416
YML013C-A	*YML013C-A*	1.29E-07	1.72E-05	-16512	35436	73029	622	567
YBL004W	*UTP20*	3.46E-04	5.32E-03	-16511	40340	79923	413	1109
YOL064C	*MET22*	1.36E-03	1.40E-02	-16488	34070	71075	937	1844
YLR410W	*VIP1*	4.35E-03	2.92E-02	-16429	49219	92291	1490	2625
YBR024W	*SCO2*	1.42E-04	2.76E-03	-16293	42694	82925	501	990
YHR198C	*FMP22*	5.46E-04	7.24E-03	-16282	57144	103223	1893	1983
YKL073W	*LHS1*	4.39E-04	6.21E-03	-16145	52236	96132	1583	1809
YDL163W	*YDL163W*	7.29E-06	3.58E-04	-15973	30611	65489	334	1424
YPL172C	*COX10*	3.25E-03	2.40E-02	-15970	36469	73720	1020	2212
YLR212C	*TUB4*	5.22E-04	7.01E-03	-15937	52832	96677	2403	2053
YDR245W	*MNN10*	4.70E-07	4.74E-05	-15915	28595	62574	1680	682
YBL019W	*APN2*	2.38E-06	1.52E-04	-15909	42039	81465	1547	1018
YNL153C	*GIM3*	1.83E-07	2.26E-05	-15715	39779	78015	1383	733
YGL256W	*ADH4*	1.11E-05	4.77E-04	-15529	37418	74433	1264	1094
YBR010W	*HHT1*	4.89E-04	6.70E-03	-15484	41917	80697	1540	1768
YLR287C-A	*RPS30A*	1.31E-04	2.63E-03	-15436	37935	75031	760	1126
YIL027C	*KRE27*	5.53E-06	2.82E-04	-15435	48210	89473	1920	1066
YBR023C	*CHS3*	1.62E-03	1.57E-02	-15404	44016	83534	434	1544
YDL232W	*OST4*	9.34E-03	4.70E-02	-15391	28069	61097	357	2608
YLR079W	*SIC1*	9.95E-08	1.40E-05	-15290	27031	59496	1352	603
YOR360C	*PDE2*	4.73E-05	1.36E-03	-15230	44453	83904	1096	1169
YOR333C	*YOR333C*	1.42E-02	6.04E-02	-15184	39144	76375	530	3004
YJL206C-A	*YJL206C-A*	6.60E-05	1.66E-03	-15135	57664	102342	1908	1455
YDL150W	*RPC53*	1.12E-02	5.25E-02	-15061	47255	87605	1438	3031
YNL306W	*MRPS18*	6.41E-03	3.71E-02	-15058	48114	88809	1789	2770
YBR008C	*FLR1*	1.88E-02	7.24E-02	-15010	39430	76533	1036	3389

Table A4. SGA screen GO term enrichment analysis for negative genetic interactors

Screen	GO-ID	Description	*P*-value	corr *P*-value	Enrichment	x	n	X	N
alk1Δ	7005	mitochondrion organization	1.55E-05	1.93E-02	3.38	16	172	127	4609
	16197	endosomal transport	1.08E-04	6.77E-02	4.67	9	70	127	4609
	7034	vacuolar transport	2.60E-04	1.08E-01	3.50	11	114	127	4609
	46907	intracellular transport	5.64E-04	1.34E-01	1.89	28	539	127	4609
	9991	response to extracellular stimulus	6.45E-04	1.34E-01	3.39	10	107	127	4609
	1902582	single-organism intracellular transport	7.13E-04	1.34E-01	1.92	26	492	127	4609
	70676	intralumenal vesicle formation	7.53E-04	1.34E-01	36.29	2	2	127	4609
	9605	response to external stimulus	8.62E-04	1.35E-01	3.27	10	111	127	4609
	45324	late endosome to vacuole transport	1.20E-03	1.67E-01	6.05	5	30	127	4609
	51649	establishment of localization in cell	1.94E-03	1.76E-01	1.74	28	583	127	4609
	71496	cellular response to external stimulus	1.94E-03	1.76E-01	3.17	9	103	127	4609
	31668	cellular response to extracellular stimulus	1.94E-03	1.76E-01	3.17	9	103	127	4609
	6900	membrane budding	2.13E-03	1.76E-01	10.89	3	10	127	4609
	6688	glycosphingolipid biosynthetic process	2.22E-03	1.76E-01	24.19	2	3	127	4609
	7005	mitochondrion organization	1.55E-05	1.93E-02	3.38	16	172	127	4609
	42221	response to chemical	2.24E-03	1.76E-01	2.02	19	341	127	4609
	44765	single-organism transport	2.25E-03	1.76E-01	1.58	36	826	127	4609
	32106	positive regulation of response to extracellular stimulus	2.87E-03	1.88E-01	9.90	3	11	127	4609
	32109	positive regulation of response to nutrient levels	2.87E-03	1.88E-01	9.90	3	11	127	4609
	32103	positive regulation of response to external stimulus	2.87E-03	1.88E-01	9.90	3	11	127	4609
	6950	response to stress	3.12E-03	1.95E-01	1.69	28	602	127	4609
	6810	transport	3.36E-03	1.98E-01	1.49	41	1001	127	4609
	45913	positive regulation of carbohydrate metabolic process	3.75E-03	1.98E-01	9.07	3	12	127	4609
	10676	positive regulation of cellular carbohydrate metabolic process	3.75E-03	1.98E-01	9.07	3	12	127	4609
	70887	cellular response to chemical stimulus	3.87E-03	1.98E-01	2.14	15	254	127	4609

(Table continues)

Table A4. continued…

Screen	GO-ID	Description	*P*-value	corr *P*-value	Enrichment	x	n	X	N
alk1Δ	16482	cytoplasmic transport	4.09E-03	1.98E-01	1.84	21	414	127	4609
	1900436	positive regulation of filamentous growth of a population of unicellular organisms in response to starvation	4.36E-03	1.98E-01	18.15	2	4	127	4609
	6687	glycosphingolipid metabolic process	4.36E-03	1.98E-01	18.15	2	4	127	4609
	32543	mitochondrial translation	4.44E-03	1.98E-01	5.81	4	25	127	4609
	72594	establishment of protein localization to organelle	5.19E-03	2.03E-01	2.23	13	212	127	4609
	10467	gene expression	5.23E-03	2.03E-01	1.39	48	1252	127	4609
	51234	establishment of localization	5.34E-03	2.03E-01	1.45	41	1026	127	4609
	6605	protein targeting	5.40E-03	2.03E-01	2.21	13	213	127	4609
	16050	vesicle organization	6.11E-03	2.03E-01	4.22	5	43	127	4609
	31667	response to nutrient levels	6.30E-03	2.03E-01	2.87	8	101	127	4609
	44764	multi-organism cellular process	6.30E-03	2.03E-01	2.87	8	101	127	4609
	51641	cellular localization	6.38E-03	2.03E-01	1.57	30	693	127	4609
	33554	cellular response to stress	6.72E-03	2.03E-01	1.71	23	489	127	4609
	1900434	regulation of filamentous growth of a population of unicellular organisms in response to starvation	7.13E-03	2.03E-01	14.52	2	5	127	4609
	10907	positive regulation of glucose metabolic process	7.13E-03	2.03E-01	14.52	2	5	127	4609
	45722	positive regulation of gluconeogenesis	7.13E-03	2.03E-01	14.52	2	5	127	4609
	70272	proton-transporting ATP synthase complex biogenesis	7.13E-03	2.03E-01	14.52	2	5	127	4609
	43461	proton-transporting ATP synthase complex assembly	7.13E-03	2.03E-01	14.52	2	5	127	4609
	33615	mitochondrial proton-transporting ATP synthase complex assembly	7.13E-03	2.03E-01	14.52	2	5	127	4609
	45041	protein import into mitochondrial intermembrane space	7.13E-03	2.03E-01	14.52	2	5	127	4609
	7154	cell communication	8.18E-03	2.24E-01	1.92	16	302	127	4609
	32107	regulation of response to nutrient levels	8.80E-03	2.24E-01	6.80	3	16	127	4609
	32104	regulation of response to extracellular stimulus	8.80E-03	2.24E-01	6.80	3	16	127	4609
	32101	regulation of response to external stimulus	8.80E-03	2.24E-01	6.80	3	16	127	4609

(Table continues)

Table A4. continued…

Screen	GO-ID	Description	*P*-value	corr *P*-value	Enrichment	x	n	X	N
alk1Δ	34614	cellular response to reactive oxygen species	8.80E-03	2.24E-01	6.80	3	16	127	4609
	33365	protein localization to organelle	9.20E-03	2.30E-01	2.01	14	253	127	4609
alk2Δ	7005	mitochondrion organization	2.09E-09	3.03E-06	3.67	27	172	197	4609
	6996	organelle organization	1.84E-06	1.33E-03	1.65	72	1021	197	4609
	16043	cellular component organization	2.55E-05	1.23E-02	1.45	87	1407	197	4609
	2	mitochondrial genome maintenance	1.79E-04	4.63E-02	6.68	6	21	197	4609
	10821	regulation of mitochondrion organization	1.98E-04	4.63E-02	11.70	4	8	197	4609
	97034	mitochondrial respiratory chain complex IV biogenesis	1.98E-04	4.63E-02	8.36	5	14	197	4609
	61024	membrane organization	2.79E-04	4.63E-02	2.29	21	215	197	4609
	71840	cellular component organization or biogenesis	3.30E-04	4.63E-02	1.34	92	1610	197	4609
	70271	protein complex biogenesis	3.83E-04	4.63E-02	2.35	19	189	197	4609
	43623	cellular protein complex assembly	4.39E-04	4.63E-02	2.78	14	118	197	4609
	33108	mitochondrial respiratory chain complex assembly	5.51E-04	4.63E-02	6.88	5	17	197	4609
	44802	single-organism membrane organization	5.81E-04	4.63E-02	2.22	20	211	197	4609
	16197	endosomal transport	6.82E-04	4.63E-02	3.34	10	70	197	4609
	10907	positive regulation of glucose metabolic process	7.22E-04	4.63E-02	14.04	3	5	197	4609
	10822	positive regulation of mitochondrion organization	7.22E-04	4.63E-02	14.04	3	5	197	4609
	45722	positive regulation of gluconeogenesis	7.22E-04	4.63E-02	14.04	3	5	197	4609
	70272	proton-transporting ATP synthase complex biogenesis	7.22E-04	4.63E-02	14.04	3	5	197	4609
	43461	proton-transporting ATP synthase complex assembly	7.22E-04	4.63E-02	14.04	3	5	197	4609
	33615	mitochondrial proton-transporting ATP synthase complex assembly	7.22E-04	4.63E-02	14.04	3	5	197	4609
	42773	ATP synthesis coupled electron transport	7.37E-04	4.63E-02	6.50	5	18	197	4609
	42775	mitochondrial ATP synthesis coupled electron transport	7.37E-04	4.63E-02	6.50	5	18	197	4609
	22904	respiratory electron transport chain	7.37E-04	4.63E-02	6.50	5	18	197	4609

(Table continues)

Table A4. continued…

Screen	GO-ID	Description	*P*-value	corr *P*-value	Enrichment	x	n	X	N
alk2Δ	17004	cytochrome complex assembly	7.37E-04	4.63E-02	6.50	5	18	197	4609
	22900	electron transport chain	9.65E-04	5.59E-02	6.16	5	19	197	4609
	6119	oxidative phosphorylation	9.65E-04	5.59E-02	6.16	5	19	197	4609
	70071	proton-transporting two-sector ATPase complex assembly	1.40E-03	7.78E-02	11.70	3	6	197	4609
	51668	localization within membrane	1.71E-03	8.09E-02	7.20	4	13	197	4609
	10978	gene silencing involved in chronological cell aging	1.82E-03	8.09E-02	23.40	2	2	197	4609
	46	autophagic vacuole fusion	1.82E-03	8.09E-02	23.40	2	2	197	4609
	32042	mitochondrial DNA metabolic process	1.82E-03	8.09E-02	23.40	2	2	197	4609
	31047	gene silencing by RNA	1.82E-03	8.09E-02	23.40	2	2	197	4609
	70676	intralumenal vesicle formation	1.82E-03	8.09E-02	23.40	2	2	197	4609
	9991	response to extracellular stimulus	1.85E-03	8.09E-02	2.62	12	107	197	4609
	10467	gene expression	2.04E-03	8.52E-02	1.35	72	1252	197	4609
	71822	protein complex subunit organization	2.08E-03	8.52E-02	1.86	24	302	197	4609
	6461	protein complex assembly	2.12E-03	8.52E-02	2.15	17	185	197	4609
	6122	mitochondrial electron transport, ubiquinol to cytochrome c	2.37E-03	9.27E-02	10.03	3	7	197	4609
	9605	response to external stimulus	2.53E-03	9.62E-02	2.53	12	111	197	4609
	7006	mitochondrial membrane organization	2.79E-03	1.03E-01	4.13	6	34	197	4609
	10468	regulation of gene expression	3.32E-03	1.14E-01	1.50	43	672	197	4609
	9891	positive regulation of biosynthetic process	3.43E-03	1.14E-01	1.88	21	261	197	4609
	31328	positive regulation of cellular biosynthetic process	3.43E-03	1.14E-01	1.88	21	261	197	4609
	44237	cellular metabolic process	3.45E-03	1.14E-01	1.16	132	2652	197	4609
	31667	response to nutrient levels	3.58E-03	1.14E-01	2.55	11	101	197	4609
	44088	regulation of vacuole organization	3.67E-03	1.14E-01	8.77	3	8	197	4609
	6515	misfolded or incompletely synthesized protein catabolic process	3.93E-03	1.14E-01	5.85	4	16	197	4609
	436	carbon catabolite activation of transcription from RNA polymerase II promoter	3.93E-03	1.14E-01	5.85	4	16	197	4609

(Table continues)

Table A4. continued…

Screen	GO-ID	Description	*P*-value	corr *P*-value	Enrichment	x	n	X	N
alk2Δ	32107	regulation of response to nutrient levels	3.93E-03	1.14E-01	5.85	4	16	197	4609
	32104	regulation of response to extracellular stimulus	3.93E-03	1.14E-01	5.85	4	16	197	4609
	32101	regulation of response to external stimulus	3.93E-03	1.14E-01	5.85	4	16	197	4609
	71496	cellular response to external stimulus	4.17E-03	1.16E-01	2.50	11	103	197	4609
	31668	cellular response to extracellular stimulus	4.17E-03	1.16E-01	2.50	11	103	197	4609
	10565	regulation of cellular ketone metabolic process	4.97E-03	1.25E-01	3.69	6	38	197	4609
	60988	lipid tube assembly	5.30E-03	1.25E-01	15.60	2	3	197	4609
	32978	protein insertion into membrane from inner side	5.30E-03	1.25E-01	15.60	2	3	197	4609
	32979	protein insertion into mitochondrial membrane from inner side	5.30E-03	1.25E-01	15.60	2	3	197	4609
	30042	actin filament depolymerization	5.30E-03	1.25E-01	15.60	2	3	197	4609
	71825	protein-lipid complex subunit organization	5.30E-03	1.25E-01	15.60	2	3	197	4609
	65005	protein-lipid complex assembly	5.30E-03	1.25E-01	15.60	2	3	197	4609
	34389	lipid particle organization	5.30E-03	1.25E-01	15.60	2	3	197	4609
	51205	protein insertion into membrane	5.34E-03	1.25E-01	7.80	3	9	197	4609
	30837	negative regulation of actin filament polymerization	5.34E-03	1.25E-01	7.80	3	9	197	4609
	1902589	single-organism organelle organization	5.42E-03	1.25E-01	1.49	40	630	197	4609
	8104	protein localization	5.94E-03	1.34E-01	1.53	35	535	197	4609
	9893	positive regulation of metabolic process	6.09E-03	1.36E-01	1.74	23	310	197	4609
	32272	negative regulation of protein polymerization	7.39E-03	1.56E-01	7.02	3	10	197	4609
	33617	mitochondrial respiratory chain complex IV assembly	7.39E-03	1.56E-01	7.02	3	10	197	4609
	6900	membrane budding	7.39E-03	1.56E-01	7.02	3	10	197	4609
	45184	establishment of protein localization	7.45E-03	1.56E-01	1.57	30	446	197	4609
	45991	carbon catabolite activation of transcription	7.57E-03	1.56E-01	4.93	4	19	197	4609
	31669	cellular response to nutrient levels	7.95E-03	1.60E-01	2.41	10	97	197	4609
	45324	late endosome to vacuole transport	8.07E-03	1.60E-01	3.90	5	30	197	4609

(Table continues)

Table A4. continued…

Screen	GO-ID	Description	*P*-value	corr *P*-value	Enrichment	x	n	X	N
alk2Δ	34727	piecemeal microautophagy of nucleus	8.07E-03	1.60E-01	3.90	5	30	197	4609
	90150	establishment of protein localization to membrane	8.41E-03	1.64E-01	2.54	9	83	197	4609
	72657	protein localization to membrane	9.08E-03	1.71E-01	2.51	9	84	197	4609
	44804	nucleophagy	9.30E-03	1.71E-01	3.77	5	31	197	4609
	6351	transcription, DNA-templated	9.59E-03	1.71E-01	1.56	29	435	197	4609
	8535	respiratory chain complex IV assembly	9.84E-03	1.71E-01	6.38	3	11	197	4609
alk1Δ	9987	cellular process	4.49E-05	2.97E-02	1.19	90	3630	96	4609
alk2Δ	34645	cellular macromolecule biosynthetic process	9.39E-05	2.97E-02	1.87	34	875	96	4609
	9058	biosynthetic process	1.04E-04	2.97E-02	1.65	44	1281	96	4609
	9059	macromolecule biosynthetic process	1.06E-04	2.97E-02	1.85	34	880	96	4609
	1901576	organic substance biosynthetic process	1.40E-04	2.97E-02	1.65	43	1254	96	4609
	44249	cellular biosynthetic process	1.57E-04	2.97E-02	1.66	42	1218	96	4609
	16043	cellular component organization	2.28E-04	3.69E-02	1.57	46	1407	96	4609
	6996	organelle organization	4.09E-04	4.30E-02	1.69	36	1021	96	4609
	45862	positive regulation of proteolysis	4.29E-04	4.30E-02	48.01	2	2	96	4609
	32436	positive regulation of proteasomal ubiquitin-dependent protein catabolic process	4.29E-04	4.30E-02	48.01	2	2	96	4609
	1901800	positive regulation of proteasomal protein catabolic process	4.29E-04	4.30E-02	48.01	2	2	96	4609
	51037	regulation of transcription during meiosis	4.55E-04	4.30E-02	18.00	3	8	96	4609
	44237	cellular metabolic process	5.55E-04	4.85E-02	1.29	71	2652	96	4609
	71840	cellular component organization or biogenesis	7.66E-04	5.89E-02	1.46	49	1610	96	4609
	44699	single-organism process	7.79E-04	5.89E-02	1.25	74	2834	96	4609
	43170	macromolecule metabolic process	8.47E-04	6.01E-02	1.38	57	1985	96	4609
	44260	cellular macromolecule metabolic process	9.27E-04	6.19E-02	1.39	55	1897	96	4609
	10954	positive regulation of protein processing	1.27E-03	6.87E-02	32.01	2	3	96	4609

(Table continues)

Table A4. continued…

Screen	GO-ID	Description	*P*-value	corr *P*-value	Enrichment	x	n	X	N
alk1Δ alk2Δ	32434	regulation of proteasomal ubiquitin-dependent protein catabolic process	1.27E-03	6.87E-02	32.01	2	3	96	4609
	32958	inositol phosphate biosynthetic process	1.27E-03	6.87E-02	32.01	2	3	96	4609
	34389	lipid particle organization	1.27E-03	6.87E-02	32.01	2	3	96	4609
	71704	organic substance metabolic process	1.36E-03	7.01E-02	1.26	70	2662	96	4609
	44238	primary metabolic process	1.42E-03	7.01E-02	1.27	68	2562	96	4609
	32543	mitochondrial translation	1.60E-03	7.56E-02	7.68	4	25	96	4609
	6325	chromatin organization	2.30E-03	9.81E-02	2.69	11	196	96	4609
	43457	regulation of cellular respiration	2.51E-03	9.81E-02	24.01	2	4	96	4609
	10674	negative regulation of transcription from RNA polymerase II promoter during meiosis	2.51E-03	9.81E-02	24.01	2	4	96	4609
	10672	regulation of transcription from RNA polymerase II promoter during meiosis	2.51E-03	9.81E-02	24.01	2	4	96	4609
	51785	positive regulation of nuclear division	2.51E-03	9.81E-02	24.01	2	4	96	4609
	6913	nucleocytoplasmic transport	2.95E-03	1.11E-01	3.25	8	118	96	4609
	51169	nuclear transport	3.10E-03	1.14E-01	3.23	8	119	96	4609
	8152	metabolic process	3.22E-03	1.14E-01	1.22	73	2883	96	4609
	44710	single-organism metabolic process	3.41E-03	1.17E-01	1.42	44	1486	96	4609
	46488	phosphatidylinositol metabolic process	3.57E-03	1.19E-01	4.80	5	50	96	4609
	436	carbon catabolite activation of transcription from RNA polymerase II promoter	4.03E-03	1.28E-01	9.00	3	16	96	4609
	31497	chromatin assembly	4.06E-03	1.28E-01	6.00	4	32	96	4609
	6461	protein complex assembly	4.77E-03	1.46E-01	2.60	10	185	96	4609
	10467	gene expression	5.11E-03	1.52E-01	1.46	38	1252	96	4609
	6974	cellular response to DNA damage stimulus	5.29E-03	1.52E-01	2.30	12	250	96	4609
	6281	DNA repair	5.40E-03	1.52E-01	2.41	11	219	96	4609
	70271	protein complex biogenesis	5.55E-03	1.52E-01	2.54	10	189	96	4609
	44763	single-organism cellular process	5.64E-03	1.52E-01	1.25	64	2466	96	4609

(Table continues)

Table A4. continued…

Screen	GO-ID	Description	*P*-value	corr *P*-value	Enrichment	x	n	X	N
alk1Δ alk2Δ	6650	glycerophospholipid metabolic process	6.07E-03	1.54E-01	3.60	6	80	96	4609
	45732	positive regulation of protein catabolic process	6.10E-03	1.54E-01	16.00	2	6	96	4609
	43647	inositol phosphate metabolic process	6.10E-03	1.54E-01	16.00	2	6	96	4609
	45991	carbon catabolite activation of transcription	6.66E-03	1.64E-01	7.58	3	19	96	4609
	31670	cellular response to nutrient	6.90E-03	1.67E-01	5.19	4	37	96	4609
	7584	response to nutrient	7.59E-03	1.71E-01	5.05	4	38	96	4609
	6351	transcription, DNA-templated	7.60E-03	1.71E-01	1.88	17	435	96	4609
	50658	RNA transport	7.68E-03	1.71E-01	3.43	6	84	96	4609
	51236	establishment of RNA localization	7.68E-03	1.71E-01	3.43	6	84	96	4609
	32774	RNA biosynthetic process	8.12E-03	1.71E-01	1.86	17	438	96	4609
	50657	nucleic acid transport	8.13E-03	1.71E-01	3.39	6	85	96	4609
	6644	phospholipid metabolic process	8.34E-03	1.71E-01	3.00	7	112	96	4609
	61136	regulation of proteasomal protein catabolic process	8.42E-03	1.71E-01	13.72	2	7	96	4609
	51038	negative regulation of transcription during meiosis	8.42E-03	1.71E-01	13.72	2	7	96	4609
	22402	cell cycle process	8.71E-03	1.72E-01	1.77	19	515	96	4609
	6334	nucleosome assembly	8.87E-03	1.72E-01	6.86	3	21	96	4609
	51028	mRNA transport	8.95E-03	1.72E-01	3.87	5	62	96	4609
	46486	glycerolipid metabolic process	9.08E-03	1.72E-01	3.31	6	87	96	4609
	44711	single-organism biosynthetic process	9.63E-03	1.76E-01	1.75	19	520	96	4609
	44255	cellular lipid metabolic process	9.69E-03	1.76E-01	2.34	10	205	96	4609

Cytoscape v2.82 (Smoot *et al*., 2011); BiNGO v2.44 (Maere *et al*., 2005); Ontology file: OBO v1.2; Annotation file: gene_association.sgd; Reference set: All mutants in array; Statistical test: Hypergeometric test; Correction: Benjamini & Hochberg False Discovery Rate (FDR) correction. N = total number of genes, n = total number of genes associated with specific go term, X = number of genes input for analysis from screen, x = number of genes in the intersection. Enrichment = (x/X) / (n/N)

Ipl1 (YPL209C)

```
1    MQRNSLVNIK LNANSPSKKT TTRPNTSRIN KPWRISHSPQ QRNPNSKIPS
51   PVREKLNRLP VNNKKFLDME SSKIPSPIRK ATSSKMIHEN KKLPKFKSLS
101  LDDFELGKKL GKGKFGKVYC VRHRSTGYIC ALKVMEKEEI IKYNLQKQFR
151  REVEIQTSLN HPNLTKSYGY FHDEKRVYLL MEYLVNGEMY KLLRLHGPFN
201  DILASDYIYQ IANALDYMHK KNIIHRDIKP ENILIGFNNV IKLTDFGWSI
251  INPPENRRKT VCGTIDYLSP EMVESREYDH TIDAWALGVL AFELLTGAPP
301  FEEEMKDTTY KRIAALDIKM PSNISQDAQD LILKLLKYDP KDRMRLGDVK
351  MHPWILRNKP FWENKRL
```

Sli15 (YBR156C)

```
1    MDWAIKAARK KTQRKPGSTR SIIETLDDLN NLTTDAHSEI NQRLYESSEW
51   LRNNVYMNTL KYEDKKMEES LISPENTHNK MDVEFPKMKG EYELSNSQND
101  AAKDVTKTPR NGLHNDKSIT PKSLRRKEVT EGMNRFSIHD TNKSPVEPLN
151  SVKVDANESE KSSPWSPYKV EKVLRESSKT SESPINTKRF DNQTWAAKEE
201  MENEPILQAL KKAESVKVKP PPNSGIARSQ RRSNMFVPLP NKDPLIIQHI
251  PPTKSSGSIP KVRTVKESPI AFKKKSTINS PAIRAVENSD TAGSTKASSV
301  FDRLSSIPTK SFENKISRGN VGHKYSSSSI DLTGSPMKKV SQKFKSINST
351  DTDMQEALRD IFSVKNKITK NNSPKGKNSR KSSIPRFDKT SLKLTTHKKL
401  AIIAEQKKKS KHSSDVHKTG SRPHSISPTK ISVDSSSPSK EVKNYYQSPV
451  RGYLRPTKAS ISPNKNKNLT TSQIPHRLKI KEKTLRKLSP NIADISKPES
501  RKSKNYRLTN LQLLPPAEAE RDDLKKKFDK RLSGIMRSQQ EHHRRKQEKQ
551  KRMSHLEQDL KKQTSFSNDY KDIRLKESLA PFDNHVRDTI NKNTAFSTDN
601  ILATINTVDH REIIGNVIPK IASVNDSLPE INTDSEDEAS VTLAAWAKSP
651  YLQEQLIRQQ DINPQTIFGP IPPLHTDEIF PNPRLNRLKP RQIVPKRS
```

Bir1 (YJR089W)

```
1    MDGQIDKMEK RYSMTKLENR LRTFQDGVAL EKKKLKWSFK VIPYQAMAKL
51   GFYFDPVIDP KTSKLKKDSV RCCYCHRQTY NVRDCRSKRK DVLETLSNIM
101  RQHLTVTDNK QVCLLIYLRN KLLTDYSFHM GVSDWKNDKY FSNPDDENVI
151  NLRKFTFQDN WPHSGSQNEH PLGIEKMVNA GLMRYDSSIE GLGDPSMDKT
201  LMNDTCYCIY CKQLLQGWSI NDDPMSRHYK VSQNGNCYFF QTRNRFERIK
251  NDNDSITKNC EVSPTLGENG KREVINTKTA SQRQCPLFES PPSSTGPQLD
301  DYNEKTDISV IQHNISVLDG AQGENVKRNS VEEKEQINME NGSTTLEEGN
351  INRDVLADKK EVISTPTAKE IKRPNVQLTQ SSSPIKKKRK FKRISPRKIF
401  DEEDSEHSLN NNSANGDNKD KDLVIDFTSH IIKNRDVGRK NAILDDSTDE
451  FSFSNQGHNT FDIPIPTSSH LLKGIDSDND NVIREDDTGI NTDTKGASSK
501  HEKFSVNSEE DLNFSEVKLT GRDSSTNILI RTQIVDQNLG DIDRDKVPNG
551  GSPEVPKTHE LIRDNSEKRE AQNGEFRHQK DSTVRQSPDI LHSNKSGDNS
601  SNITAIPKEE QRRGNSKTSS IPADIHPKPR KNLQEPRSLS ISGKVVPTER
651  KLDNINIDLN FSASDFSPSS QSEQSSKSSS VISTPVASPK INLTRSLHAV
701  KELSGLKKET DDGKYFTNKQ ETIKILEDVS VKNEIPNNEM LLFETGTPIA
751  SQENKSRKLF DEEFSGKELD IPIDSSTVEI KKVIKPEFEP VPSVARNLVS
801  GTSSYPRNSR LEEQRKETST SLADNSKKGS SFNEGNNEKE PNAAEWFKID
851  ENRHLVKNYF HDLLKYINNN DATLANDKDG DLAFLIKQMP AEELDMTFNN
901  WVNLKVQSIK REFIDDCDKK LDILRRDYYT ATNFIETLED DNQLIDIAKK
951  MGIL
```

Nbl1 (YHR199C-A)

```
1    MIPALTPEER QKLRSAILHR MQLELETTEK LIENIKEETL KKLNLLQQPD
51   ATSAPQSKEL IREVLEQEGR RIE
```

Figure A1. Phosphorylation sites in components of the *S. cerevisiae* CPC. Sites of phosphorylation identified by mass spectrometry are highlighted in red (phosphoGRID, Zimniak *et al*. 2012). CDK phosphorylation motifs are underlined.

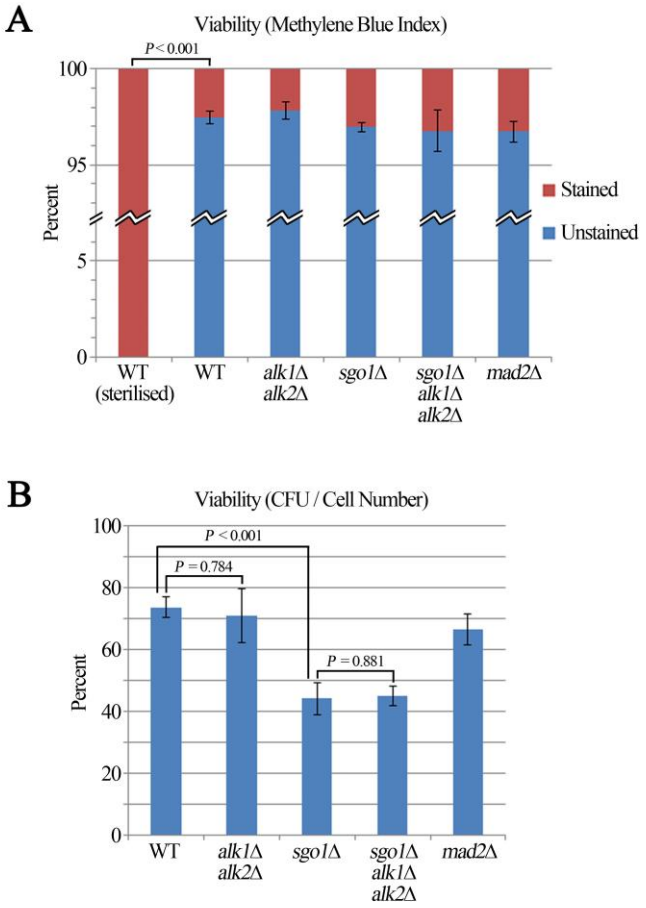

Figure A2. Viability of *alk1*Δ *alk2*Δ and *sgo1*Δ mutant cells. Viability of cells of the indicated genotypes was assessed using two independent methods: methylene blue vital staining and by determining the number of colony forming units relative to the total cell count. (A) Methylene blue is metabolised by viable cells leaving them unstained while dead cells are unable to do this and become stained. The experiment was performed in triplicate. Averages of over 900 cells were scored for each strain during each replicate. Data passed normality and equal variance tests and were subjected to a one way ANOVA test [$F(5, 12) = 15412.8$, $P < 0.001$]. Subsequent pairwise comparisons were performed using the Holm-Sidak method. WT (sterilised) vs. all other genotypes $P < 0.001$; all other pairwise comparisons are not significant. (B) Viability in terms of the ability of cells to reproduce was calculated by counting the number of colonies formed on a plate and comparing this against the total number of cells plated. The experiment was performed in triplicate. Averages of over 700 cells between 300 and 1000 colonies were counted for each strain in each replicate. Data passed normality and equal variance tests and were subjected to a one way ANOVA test [$F(4, 10) = 20.7$, $P < 0.001$]. Subsequent pairwise comparisons were performed using the Holm-Sidak method. Key *P*-values are indicated.

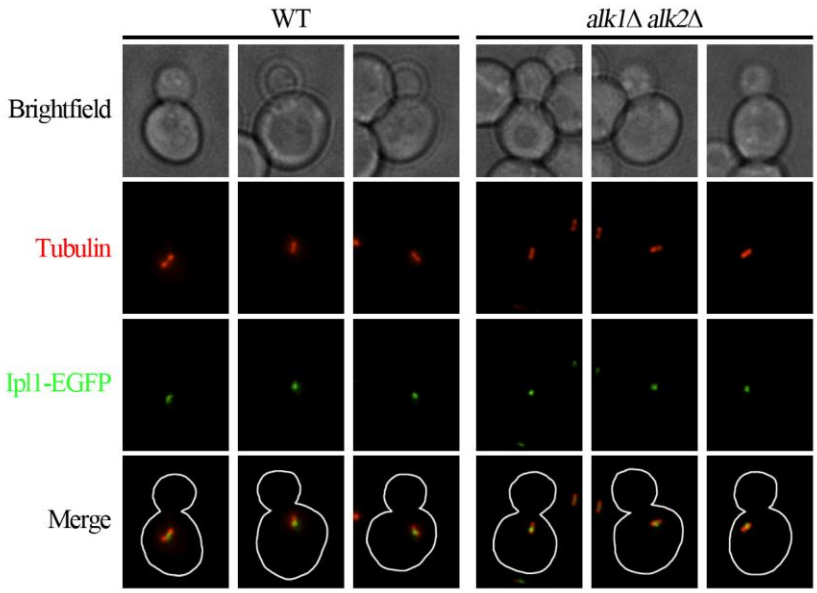

Figure A3. Preliminary experiment to assess Ipl1 localisation in *alk1*Δ *alk2*Δ cells. Examples of wild-type (WT) and *alk1*Δ *alk2*Δ cells expressing Ipl1-EGFP and mCherry-Tub1 with short bipolar spindles.

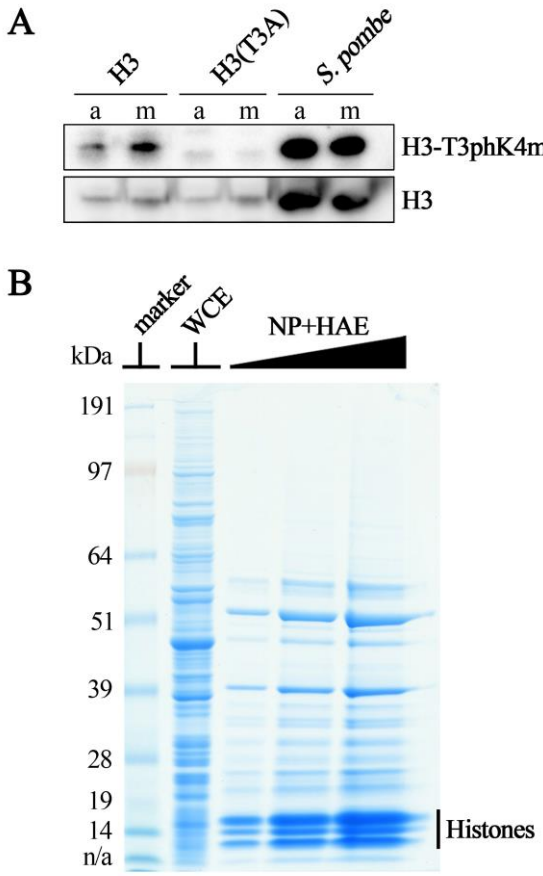

Figure A4. Preliminary experiments to detect H3-T3ph. (A) Whole cell extracts were prepared from *S. cerevisiae* strains expressing either wild-type (H3) or mutant [H3(T3A)] histone H3 and an *S. pombe* strain. Histone H3 and H3-T3phK4me3 were detected by western blot. a; asynchronous culture, m; metaphase-arrested culture. (B) Coomassie stained protein gel highlights how histones are enriched when the nuclei preparation and histone acid extraction (NP+HAE) method is used compared with a whole cell extract (WCE).